The Analysis of Symmetric Structures using Group Representation Theory

University of Cambridge
Department of Engineering

Dissertation submitted to the University of Cambridge
for the degree of Doctor of Philosophy

by

Riki Dale Kangwai

Clare College

December, 1997

To my Parents

Acknowledgements

The work described in this dissertation has been carried out at the Department of Engineering, University of Cambridge, between October 1994 and December 1997.

First and foremost, I would like to thank my supervisor Dr. S.D. Guest for his help, guidance and friendship throughout the course of my research. His insight and enthusiasm have been inspiring and have helped to make my work a valuable and fulfilling experience. I would also like to thank Dr. S. Pellegrino for his support and invaluable advice.

I would like to thank all of the Structures Research Group and the members of the Deployable Structures Laboratory for their constructive suggestions and helpful discussions on the work carried out in this dissertation. I have also had the pleasure of making some firm friendship during the course of my research and in particular, I would like to thank Simon King, David Miles, Keith Seffen, Thorsten Hack, Tim Ibell and Gopal Srinivasan, who have all experienced the highs and lows of working for a PhD degree, and with whom I have shared many lively and enjoyable occasions.

I would also like thank my St. Regis House flatmates Ann Summersgill, Jo Shotton, Rich Varcoe, John Woolmore, Alex Hacking, Chris Withers and Steve Newman, who have often helped to distract me from my work and contributed to an enjoyable three years at Clare College. Thanks also goes to all the members of Clare Rugby Football Club for the memorable victories on the rugby field and the many memorable occasions off the rugby field.

My research was made possible with financial support from both the Cambridge Commonwealth Trust in the form of a Tate & Lyle Cambridge Scholarship, and the Engineering and Physical Sciences Research Council in the form of a research studentship and travel grants for attending conferences. A W.G. Collins travel grant to attend an overseas conference was also received from the Department of Engineering. All financial contributions were greatly appreciated.

Declaration

The author wishes to declare that, except for commonly understood ideas and concepts, or where specific reference is made to the work of other authors, the contents of this dissertation are original and include nothing that is the outcome of work done in collaboration. This dissertation has not been previously submitted, in part or whole, to any other University or institution for any degree, diploma or other qualification. This dissertation is 162 pages long and contains approximately 37000 words including appendices and bibliography.

Riki Kangwai

Riki Kangwai

Abstract

Group Representation Theory is the mathematical language best suited to describing the symmetry properties of a structure, and a structural analysis can utilises Group Representation Theory to provide the most efficient and systematic method of exploiting the full symmetry properties of any symmetric structure.

Group Representation Theory methods currently exist for the Stiffness Method of structural analysis, where the stiffness matrix of a structure is block-diagonalised into a number of independent submatrices, each of which relates applied loads and displacements with a particular type of symmetry. This dissertation extends the application of Group Representation Theory to the equilibrium and compatibility matrices which are commonly used in the Force Method of structural analysis.

Group Representation Theory is used to find symmetry-adapted coordinate systems for both the external vector space which is suitable for representing the loads applied to a structure, and the internal vector space which is suitable for representing the internal forces. Using these symmetry-adapted coordinate systems the equilibrium matrix is block-diagonalised into a number of independent submatrix blocks, thus decomposing the analysis into a number of subproblems which require less computational effort.

Each independent equilibrium submatrix block relates applied loads and internal forces with particular symmetry properties, and hence any states of self-stress or inextensional mechanisms in one of these equilibrium submatrix blocks will necessarily have corresponding symmetry properties. Thus, a symmetry analysis provides valuable insight into the behaviour of symmetric structures by helping to identify and classify any states of self-stress or inextensional mechanisms present in a structure.

In certain cases it is also possible for a symmetry analysis to identify when a structure contains a finite rather than infinitesimal mechanism. To do this a symmetry analysis must be carried out using the symmetry properties of the inextensional mechanism of interest. If the analysis shows that any states of self-stress which exist in the structure have "lesser" symmetry properties, then the states of self-stress exist independently from the mechanism and cannot prevent its finite motion.

Keywords: Group Representation Theory, symmetric structure, symmetry group, symmetry operation, irreducible matrix representation, symmetry-adapted coordinate system, symmetry subspace, stiffness matrix, equilibrium matrix, block-diagonalised matrix, state of self-stress, infinitesimal mechanism, finite mechanism, Great Orthogonality Theorem, projection operator matrix, descent of symmetry.

Contents

Acknowledgements i
Declaration ii
Abstract iii

1 Introduction **1**

2 Previous Work on the Use of Symmetry in Structural Analysis **7**
2.1 Introduction 7
2.2 The Analysis of Rotationally Symmetric Structures using the Fourier Method 10
2.3 The Analysis of Symmetric Structures using Group Representation Theory 13

3 Symmetric Structures and Group Representation Theory **17**
3.1 Introduction 17
3.1.1 Stiffness Matrix 18
3.2 Pin-Jointed Structure with $\mathbf{C_{3v}}$ Symmetry 18
3.2.1 Matrix Representations of Symmetry Operations 20
3.3 Group Representation Theory 23
3.3.1 Great Orthogonality Theorem and the Projection Operator Matrix 26
3.4 External Symmetry-Adapted Coordinate System 30
3.5 Block-Diagonalised Stiffness Matrix 33
3.6 The Fourier Method as a Special Case of the Group Representation Theory Method 35
3.7 Analysis of the Symmetry Sub-Structure 37
3.7.1 Example Sub-Structure Analysis 39

4 Symmetry Analysis of the Equilibrium Matrix **42**
4.1 Introduction 42
4.2 Equilibrium, Compatibility and Flexibility Matrices 43
4.3 Block-Diagonal Form of the Equilibrium, Compatibility and Flexibility Matrices 45
4.4 Pin-jointed Structure with $\mathbf{C_{3v}}$ Symmetry 46

4.4.1 Internal Symmetry-Adapted Coordinate System 47
4.4.2 Block-Diagonalised Equilibrium Matrix 51
4.4.3 Analysis of the Block-Diagonalised Equilibrium Matrix . . . 54
4.5 Simplification of the Force Method 57
4.6 Analysis of the Symmetry Sub-Structure 60
4.6.1 Example Sub-Structure Analysis 62
4.7 Geiger Dome Example 63
4.7.1 States of Self-Stress in the Geiger Dome 66
4.7.2 Mechanisms in the Geiger Dome 67

5 Detection of Finite Mechanisms 73
5.1 Introduction 73
5.1.1 Statically and Kinematically Indeterminate Structures . . . 74
5.2 Hexagonal Ring with Rotation and Reflection Symmetry 75
5.2.1 Symmetry-Adapted Coordinate Systems 77
5.2.2 Block-Diagonalised Equilibrium Matrix using $\mathbf{C_{6v}}$ Symmetry 82
5.2.3 Block-Diagonalised Equilibrium Matrix using $\mathbf{C_{3v}}$ Symmetry 85
5.3 Bifurcation Point of the Hexagonal Ring 87
5.4 Comments on the Identification of Finite Mechanisms 91

6 Cubic or Higher Symmetry Groups 93
6.1 Introduction 93
6.2 Pin-Jointed Cube with $\mathbf{O_h}$ Symmetry 94
6.2.1 Block-Diagonalised Equilibrium Matrix using $\mathbf{O_h}$ Symmetry 98
6.3 Analysis of the Internal Mechanisms 105
6.3.1 Block-Diagonalised Equilibrium Matrix using $\mathbf{T_d}$ Symmetry 105
6.3.2 Block-Diagonalised Equilibrium Matrix using $\mathbf{D_2}$ Symmetry 108

7 Frame Structures 111
7.1 Introduction 111
7.2 Simple Frame with $\mathbf{C_{3v}}$ Symmetry 114
7.3 Frames with Finite Mechanisms 120
7.3.1 Frame with $\mathbf{C_{2v}}$ Symmetry 120
7.3.2 Frame with $\mathbf{C_{3v}}$ Symmetry 128

8 Conclusions and Future Work 133
8.1 Conclusions 133
8.2 Future Work 134

A Group Representation Theory 137
A.1 Symmetry Operations 137
A.2 Symmetry Groups 138
A.2.1 Classes of Conjugate Elements 140
A.2.2 Point Groups 141

A.3 Reducible and Irreducible Matrix Representations 143
A.3.1 Equivalent Representations 144
A.3.2 Character of a Representation 144
A.3.3 Reducible and Irreducible Matrix Representations 145
A.3.4 Properties of Irreducible Matrix Representations 146
A.3.5 Notation for Irreducible Representations 148
A.4 Great Orthogonality Theorem 148
A.5 Projection Operator Theory 150

B Calculating Irreducible Matrix Representations **153**
B.1 Calculating the Initial Irreducible Matrix Representations 154
B.2 Calculating the Remaining Irreducible Matrix Representations . . . 156

Bibliography **158**

Chapter 1

Introduction

The purpose of this dissertation is to show how the utilisation of symmetry can simplify the analysis of any symmetric structure. Of course, all the examples used in this dissertation could be analysed using standard "brute force" techniques; however with the use of symmetry the analysis is not only more efficient but also provides valuable insight into the behaviour of the structure.

It is *Group Theory* that provides a systematic method of describing the symmetry of a structure and analysing its implications. The mathematical theory of groups is a highly developed and abstract subject; however the actual mathematical techniques required to apply the theory are quite simple.

For the purpose of structural analysis, the main outcome of applying Group Theory is the systematic method of finding symmetry-adapted coordinate systems for a structure and classifying the different symmetry subspaces. This dissertation will show that it is this information, derived from studying the symmetry of the structure, that simplifies the analysis into a number of independent sub-problems with particular symmetry properties. Hence, the usefulness of Group Theory in structural analysis is that it provides the detailed connection between the physical properties of the structure and its symmetry.

In order to apply Group Theory, two mathematical concepts are required. The first is the study of the geometrical symmetry of a structure, which leads to the introduction of symmetry groups. The second is the representation of the physical properties of the structure using a coordinate system in vector space. This gives rise to *Group Representation Theory* which is described in Chapter 3 and applied extensively throughout the rest of this dissertation.

The occurrence of symmetry in everyday life ranges through a wide spectrum of objects, activities and theorems; for example, the theory of groups, the structure of space, equilibrium positions in crystals, the theory of relativity and quantum physics, flower petals, Romanesque cathedrals, snowflakes and music. Of interest in this dissertation are man-made structures which have symmetry, and because of its basic aesthetic appeal (regularity, even proportions, periodicity and harmonious arrangement), symmetry has always been used extensively in art, design and architecture (Hargittai & Hargittai 1994). Symmetry is also commonly used in engineering and industry, in order to simplify design and production. A good example of the use of symmetry in architecture is the octagonal ceiling in Ely Cathedral, shown in Figure 1.1.

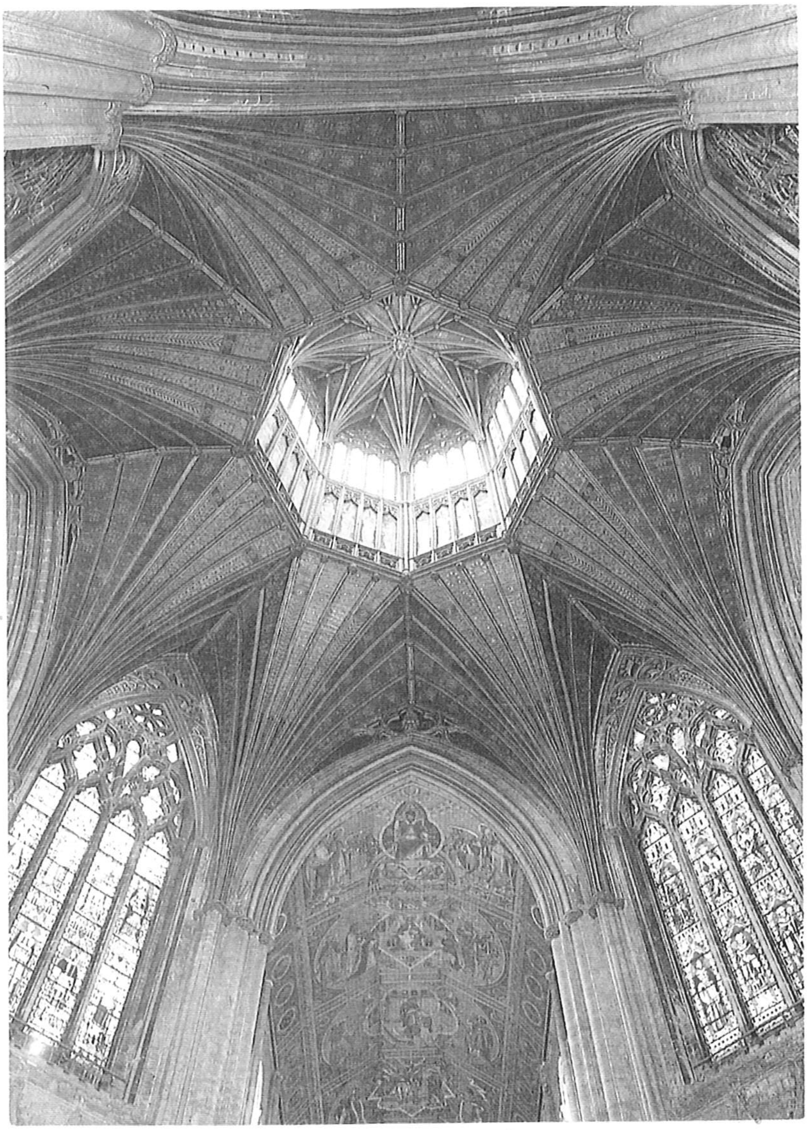

Figure 1.1: The octagonal ceiling in Ely Cathedral.

The word *symmetry* is also commonly used in everyday language and the Collins Concise English Dictionary gives the following definitions:

- *An exact correspondence in position or form about a given point, line or plane.*
- *Beauty or harmony of form based on a proportionate arrangement of parts.*

For the purpose of structural analysis, a symmetric structure is a structure that is left unaltered, geometrically and mechanically, by a *symmetry operation.* These operations may be reflections, rotations, improper rotations (an improper rotation is a reflection in a plane followed by a rotation about an axis perpendicular to that plane), translations or magnifications. Translations and magnifications only leave infinite structures unaltered, and so these two symmetry operations are not covered in this dissertation. Note however, that apart from regions near their boundaries, some *repetitive* structures will also have translation or magnification symmetry, and hence it is likely that similar techniques to the ones described in this dissertation can be used to simplify their analysis. Symmetry operations are described in more detail in Chapter 3.

This dissertation aims to review and explain the techniques used to analyse symmetric structures subject to any general, i.e. unsymmetric loading. After an extensive review of previous work in this field, this dissertation introduces the most general way of describing the full symmetry properties of a structure, based on Group Theory, and shows how this approach can be used to systematically simplify the analysis of a symmetric structure. A technique which is better known to structural engineers, known as the *Fourier Method*, is also presented, but it is shown that this method is a special case of the Group Theory method. For both methods the techniques that are used to block-diagonalise the full stiffness matrix of a structure are presented. It is also shown that sub-structure techniques can be used so that the full stiffness matrix never needs to be generated.

As it is an introduction to the subject, this dissertation makes a number of restrictions and simplifications. Firstly it deals only with discrete matrix analysis of structures; but as structures are generally discretised for computational analysis, this is really no restriction. Secondly, it mainly considers pin-jointed structure examples. This is to simplify the matrices involved in the calculation, and hence the complexity of the analysis. However, these techniques are equally suited to more advanced elements, as shown in Chapter 7 for rigid frame examples. Thirdly, it only considers the static analysis of structures. It shows how the *stiffness matrix* or *equilibrium matrix* of a structure can be block-diagonalised by choosing coordinate systems based on the symmetry of the structure, and hence the analysis is decomposed into a number of independent subproblems. Chapter 2 reviews work where similar Group Theory techniques have been used for dynamic or bifurcation analysis of symmetric structures.

It is commonly understood that, if a structure with a certain type of symmetry is subjected to a loading with identical symmetry, considerable time and computational effort can be saved by analysing only the *symmetry sub-structure.* It is less commonly understood that this is also true if the structure is subjected to any general loading; and it is this concept that forms the basis of this dissertation.

In order to help introduce the analysis of symmetric structures, a simple example that *is* well understood is a structure that has simple bilateral symmetry, i.e. it is left in an identical position by a reflection in a central plane. For such a structure it is well known that simple symmetry arguments can be used to split any general loading into what are commonly called symmetric and antisymmetric components, and the structure analysed for each of these separately. An example is shown in Figure 1.2, where a 2-dimensional rigid frame is subject to a general loading. Using the principle of superposition, the general load on the left can be divided into

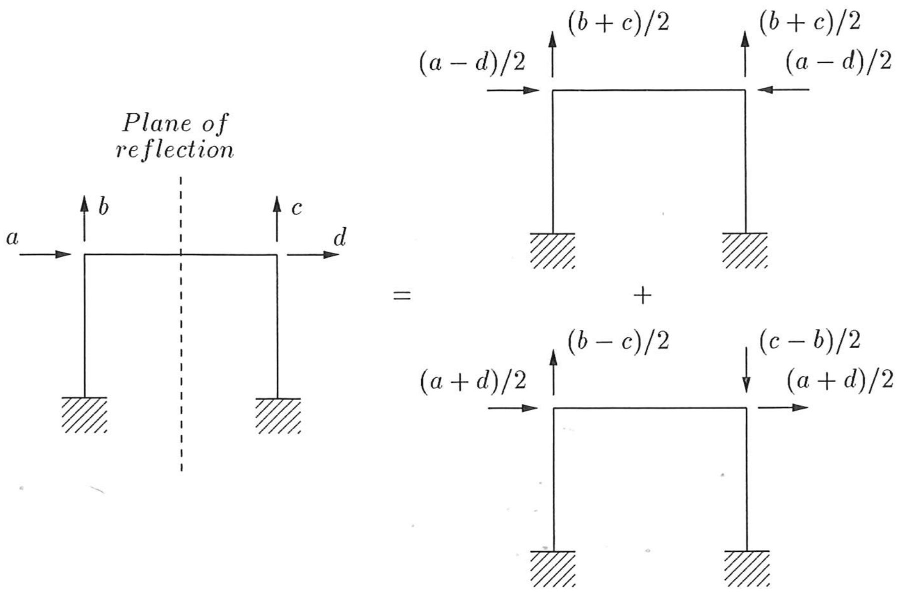

Figure 1.2: 2-dimensional rigid frame. Decomposition of a general load into symmetric and anti-symmetric components.

the symmetric and anti-symmetric load components on the right. The symmetric load component causes symmetric displacements and the anti-symmetric load component causes anti-symmetric displacements. The analysis of each of these components requires only half the number of simultaneous equations compared with the analysis of a general load, and solving a smaller number of simultaneous equations (albeit, more than once) reduces both the complexity of the analysis and the computational effort required.

This dissertation will show how, using Group Representation Theory techniques, the use of symmetry arguments can be extended to structures with *any* type of symmetry subject to *any* general loading.

The layout of this dissertation is as follows. Chapter 2 gives a review of previous work that has been carried out on the analysis of symmetric structures. There have been two differing approaches, first the Fourier Method which can only exploit rotational symmetry and second, the application of Group Theory which is a more general and systematic method of exploiting any type of symmetry.

Chapter 3 gives an introduction to the analysis of symmetric structures and explains how the application of Group Representation Theory can be used to provide a systematic method to fully describe the symmetry properties of a structure. An introduction to Group Theory is given, in particular the theory required to find a symmetry-adapted coordinate system for the load and displacement vector space of the structure. Using a symmetry-adapted coordinate system, the stiffness matrix is block-diagonalised, thus considerably simplifying the analysis of any symmetric structure. Chapter 3 also shows that the Fourier Method described in Chapter 2 is simply a special case of the Group Theory method. Techniques are also presented to show that only a symmetry sub-structure is required in order to block-diagonalise the stiffness matrix of a symmetric structure, thus further simplifying the analysis.

Chapter 4 goes on to show how Group Representation Theory can also be applied to find a symmetry-adapted coordinate system for the internal force and elongation vector space, and hence to block-diagonalise the equilibrium matrix of a symmetric structure, thus relating internal forces to the applied external loads with particular symmetry properties. This symmetry analysis provides valuable insight into the static and kinematic response of the structure and considerably reduces the computational effort required for a Force Method analysis. In a similar way to that presented for the stiffness matrix, this chapter shows that a block-diagonalised equilibrium matrix can be calculated using only a symmetry sub-structure.

Chapter 5 shows how a symmetry analysis can provide valuable insight into the nature of structures which are both statically and kinematically indeterminate. In particular, a symmetry analysis helps identify and classify any states of self-stress and inextensional mechanisms present in a structure and in some cases it can identify when such a structure admits a finite mechanism. Utilising the same techniques as Chapter 4, an analysis is carried out on a hexagonal ring structure which satisfies Maxwell's rule but is statically and kinematically indeterminate. Using only symmetry arguments the hexagonal ring is shown to contain a finite mechanism. A summary is also given for the general case where a symmetry analysis can identify a finite mechanism.

Chapter 6 shows that the Group Representation Theory method can also easily be applied to structures with highly complex symmetry, i.e. structures which have more than one main axis of symmetry. A pin-jointed cube is analysed and the techniques introduced in Chapter 5 are used to investigate its internal mechanisms.

Chapter 7 extends the analysis to include more general symmetric structures such as frames with rigid joints, and shows that the Group Representation Theory method used to analyse pin-jointed structures is equally suited to the analysis of these rigid frames. Two interesting frames are analysed and symmetry arguments are used to show that both frames contain finite mechanisms.

Chapter 8 concludes the dissertation and discusses ideas for future research in the field of symmetric structures.

Appendices A and B gives a general introduction to Group Representation Theory, and provide some key concepts that are required in this dissertation for the analysis of symmetric structures.

Chapter 2

Previous Work on the Use of Symmetry in Structural Analysis

2.1 Introduction

This chapter gives a review of the literature relevant to the analysis of symmetric structures. In particular it describes the methods employed to exploit symmetry in structures in order to reduce both the complexity of the analysis and the computational effort required.

The development of methods to exploit the symmetry properties of a structure does not have a clearly defined origin nor a continuous historical path. In common with other areas of structural analysis, there has been an increase in the work done in this area since the advent of the electronic computer, and especially since the development of finite element structural analysis packages. However the underlying ideas of symmetry are generally not well known in the structural engineering community, and the currently available commercial structural analysis packages are unable to exploit symmetry properties beyond purely rotational symmetry. For example, the analysis of large radio telescope or space dome structures, which can possess high degrees of rotational and reflective symmetry, as shown in Figures 2.1 and 2.2, would be considerably simplified by such a facility.

The use of symmetry in structural analysis is commonly limited to *simple* symmetry arguments, where a structure is termed symmetric if it has an *axis* of rotation symmetry or a *bilateral plane* of reflection symmetry. Then any symmetric load on the structure will result in a similarly symmetric displacements.

For the particular case of a structure with bilateral symmetry, it is well known that symmetry arguments can be used to simplify the analysis for any general load applied to the structure, as demonstrated in Chapter 1 for the 2-dimensional rigid frame shown in Figure 1.2. Some interesting applications of symmetric and anti-

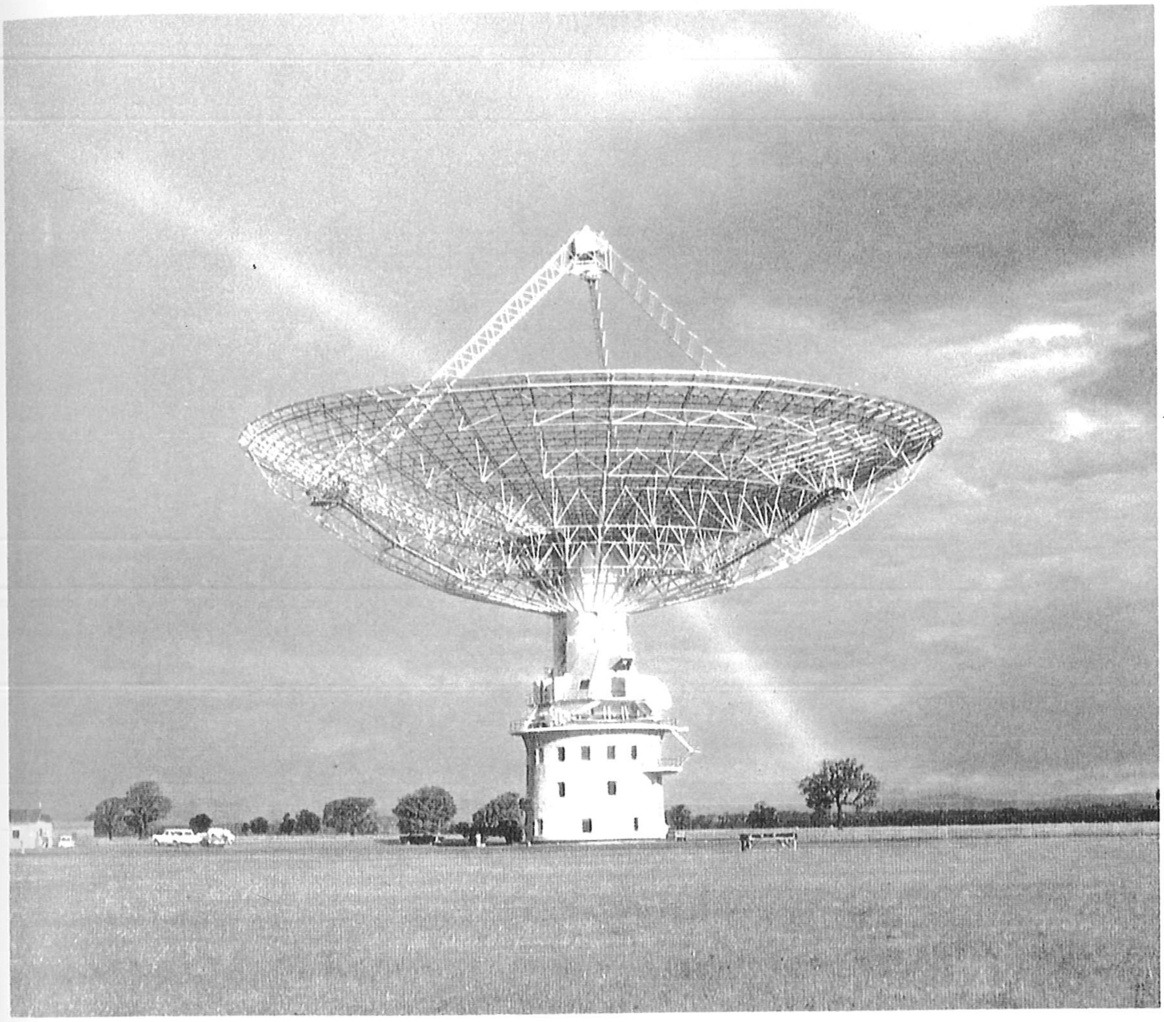

Figure 2.1: Parks radio telescope, Australia. Wire mesh reflector, 64m diameter.

symmetric loadings and deformation patterns in bilaterally symmetric structures are given by Charlton (1969). Crandall, Dahl & Landner (1978) also gives a useful description of symmetry principles required to determine symmetric force and deformation components or patterns.

For structures with bilateral symmetry, using the principle of superposition, any general load can be divided into symmetric and anti-symmetric load components. The symmetric load component causes symmetric displacements and the anti-symmetric load component causes anti-symmetric displacements. The analysis of each of these components requires only half the number of simultaneous equations compared with the analysis of a general load, and solving a smaller number of simultaneous equations (albeit, more than once) reduces both the complexity of the analysis and the computational effort required.

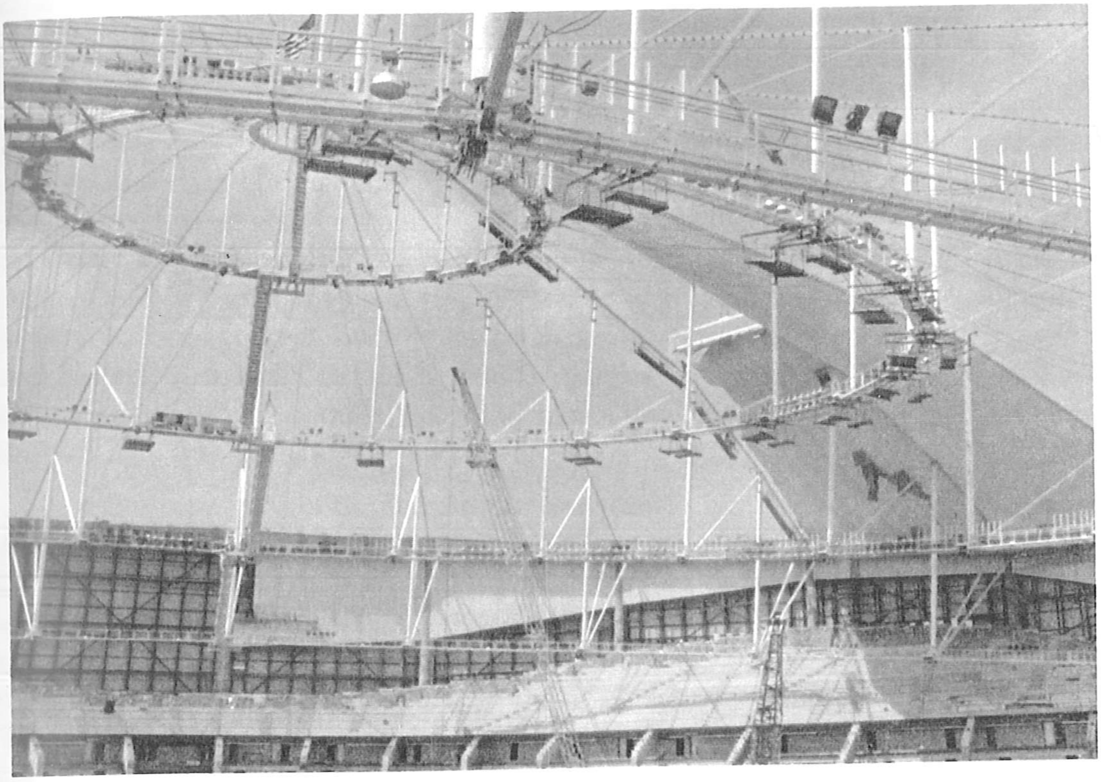

Figure 2.2: Sun coast dome, Florida USA. Cable and strut prestressed tensegrity dome, 210m diameter.

However for structures with more complex symmetry, the use of these simple symmetry arguments does not fully exploit the symmetry of the structure, and hence the application of symmetry to the field of structural analysis is commonly under utilised. It is only in isolated cases and in specialised areas that symmetry arguments and Group Theory have begun to be fully utilised.

The main advances in the analysis of symmetric structures have come through two differing approaches. The first approach exploits only the *rotational* symmetry of a structure with a method based on the discrete Fourier transformation. This Fourier Method is described in the next section. The second, more recent development, is a method which can exploit any type of symmetry, based on the application of Group Representation Theory to structural analysis. This is a more general and systematic method of exploiting symmetry and is the main theme of this dissertation.

2.2 The Analysis of Rotationally Symmetric Structures using the Fourier Method

The Fourier approach was first developed by Fortescue (1918), for the analysis of polyphase electrical circuits. Fortescue used a tensor analysis approach to find a new *symmetry-adapted* coordinate system, which reduces the governing system of equations into a number of independent sub-systems of equations. Another electrical engineer (Kron 1935) presented Fortescue's method of symmetric components in matrix form and set up a transformation matrix (the Fourier matrix, which will be introduced in Chapter 3) which reduces the governing matrix to a *block-diagonalised* form. A detailed description of symmetric components in matrix form is given by Pipes (1966).

The first application of discrete Fourier transformation methods to structural analysis was made by Renton (1964), who was concerned with the stability analysis of rotationally symmetric frameworks. Further development has been carried out by several authors. Hussey (1967) applied the discrete Fourier transformation method in order to decouple the stiffness equations of rotationally symmetric frameworks and investigated the buckling under cyclically symmetric loading. Thomas (1979) and Williams (1986*a*, 1986*b*) have provided exact methods for solving eigenvalue problems for rotationally periodic structures purely from the stiffness equations of the repeating symmetry sub-structure. Williams showed that this sub-structuring technique allows the analysis to be carried out with considerable savings in computational effort. Thomas also analysed the dynamics of rotationally periodic structures to show that any forced vibrations can be decomposed into independent rotating components. Renton (1964) and Samartin (1988) have also shown how the Fourier approach can be extended to structures with translational and magnification symmetry properties.

The first, general purpose finite element (FE) package to become available which was able to simplify the analysis of a rotationally symmetric structure using a Fourier transformation method was NASTRAN in 1974 (MacNeal, Harder & Mason 1977). NASTRAN uses methods based on the theoretical work published by Fortescue in order to transform general loads into sets of rotationally symmetric load components. This is now a common feature of FE packages, e.g. ANSYS (Swanson Analysis Systems, Inc. 1992) and ABAQUS (Hibbitt, Karlsson and Sorensen, Inc. 1993). However, considering that many structures with high degrees of rotational symmetry will also have other types of symmetry, for example Figures 2.1 and 2.2 show rotational structures which also have planes of reflection, it is surprising that the development of FE packages has not been extended to include non-rotational symmetry.

The rest of this section gives a brief overview of the analysis of structures with purely rotational symmetry, based on the discrete Fourier transformation method.

The analysis of a rotationally symmetric structure under an arbitrary load system can be modelled as a repeated analysis of the *symmetry sub-structure* subject to rotationally periodic components of the load, which are computed using a discrete Fourier transformation. This section shows that the stiffness matrix $\mathbf{K}$ for any structure with rotational symmetry, will have a known special form such that there exists a Fourier matrix which transforms the stiffness matrix into a block-diagonalised form.

The *Fourier Method* is described with the use of the 2-dimensional pin-jointed structure shown in Figure 2.3. A pre-requisite of the Fourier Method is that the

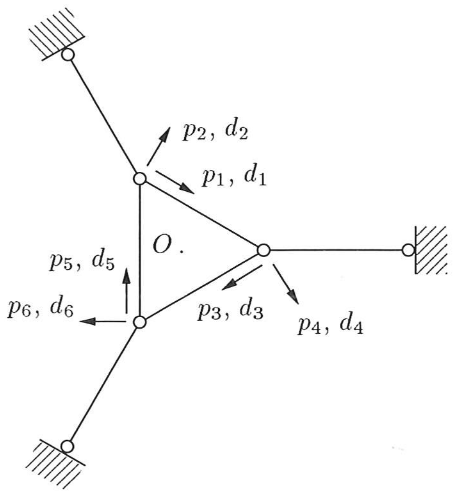

Figure 2.3: 2-dimensional pin-jointed structure with a polar coordinate system for the load and displacement vectors $\mathbf{p}$ and $\mathbf{d}$.

coordinate system for the load and displacement vectors $\mathbf{p}$ and $\mathbf{d}$ must have the same rotational symmetry as the structure, and such a coordinate system is shown in Figure 2.3. Using this polar coordinate system, the stiffness matrix $\mathbf{K}$ for the whole structure has the following explicit form:

$$\mathbf{K} = \frac{EA}{l}\left[\begin{array}{cc|cc|cc} 2 & -\sqrt{3}/2 & 1/2 & -\sqrt{3}/2 & 1/2 & 0 \\ -\sqrt{3}/2 & 1 & 0 & 0 & -\sqrt{3}/2 & 0 \\ \hline 1/2 & 0 & 2 & -\sqrt{3}/2 & 1/2 & -\sqrt{3}/2 \\ -\sqrt{3}/2 & 0 & -\sqrt{3}/2 & 1 & 0 & 0 \\ \hline 1/2 & -\sqrt{3}/2 & 1/2 & 0 & 2 & -\sqrt{3}/2 \\ 0 & 0 & -\sqrt{3}/2 & 0 & -\sqrt{3}/2 & 1 \end{array}\right] \tag{2.1}$$

Equation 2.1 shows that the stiffness matrix $\mathbf{K}$ has the special form:

$$\mathbf{K} = \left[\begin{array}{c|c|c} \mathbf{K}_1 & \mathbf{K}_2 & \mathbf{K}_3 \\ \hline \mathbf{K}_3 & \mathbf{K}_1 & \mathbf{K}_2 \\ \hline \mathbf{K}_2 & \mathbf{K}_3 & \mathbf{K}_1 \end{array}\right] \tag{2.2}$$

where the blocks $\mathbf{K}_i$ are the submatrices in Equation 2.1. The stiffness matrix $\mathbf{K}$ is formed by simple permutations of the submatrices in the first row. This special form of a matrix is called a *blockcirculant* matrix (referred to as a *quasicirculant* matrix by Samartin 1988). In general, any rotationally periodic structure with a polar coordinate system will have a stiffness matrix with this blockcirculant form. It is this special form that enables us to easily understand how the Fourier Method will block-diagonalise the stiffness matrix $\mathbf{K}$.

Before solving this blockcirculant stiffness matrix, it is helpful to look at the simplest form of a blockcirculant matrix, that is a *circulant* matrix where the submatrices are (1×1) blocks. An example of a circulant matrix is:

$$\mathbf{C} = \begin{bmatrix} 1 & 2 & 3 & 4 \\ 4 & 1 & 2 & 3 \\ 3 & 4 & 1 & 2 \\ 2 & 3 & 4 & 1 \end{bmatrix} \tag{2.3}$$

Every $(n \times n)$ circulant matrix has the same eigenvectors, and these are given by the columns of the Fourier matrix $\mathbf{F}$ (Strang 1986):

$$\mathbf{F} = \frac{1}{\sqrt{n}} \begin{bmatrix} 1 & 1 & 1 & \cdot & 1 \\ 1 & w & w^2 & \cdot & w^{n-1} \\ 1 & w^2 & w^4 & \cdot & w^{2(n-1)} \\ \cdot & \cdot & \cdot & \cdot & \cdot \\ 1 & w^{n-1} & w^{2(n-1)} & \cdot & w^{(n-1)^2} \end{bmatrix} \quad \text{where } w = e^{2\pi i/n} = \sqrt[n]{1} \tag{2.4}$$

In order to apply this solution to the stiffness matrix of a rotationally periodic structure it must be extended to blockcirculant matrices. It is not possible to find the eigenvectors of a blockcirculant stiffness matrix $\mathbf{K}$ from the symmetry of the structure alone, and hence the stiffness matrix cannot be fully diagonalised without further calculation. However, it is possible to block-diagonalise the stiffness matrix using the following block form of the Fourier matrix:

$$\mathbf{F} = \frac{1}{\sqrt{n}} \begin{bmatrix} \mathbf{I} & \mathbf{I} & \mathbf{I} & \cdot & \mathbf{I} \\ \mathbf{I} & w\mathbf{I} & w^2\mathbf{I} & \cdot & w^{n-1}\mathbf{I} \\ \mathbf{I} & w^2\mathbf{I} & w^4\mathbf{I} & \cdot & w^{2(n-1)}\mathbf{I} \\ \cdot & \cdot & \cdot & \cdot & \cdot \\ \mathbf{I} & w^{n-1}\mathbf{I} & w^{2(n-1)}\mathbf{I} & \cdot & w^{(n-1)^2}\mathbf{I} \end{bmatrix} \tag{2.5}$$

where $\mathbf{I}$ is an identity matrix of the same size as the permuting matrix blocks $\mathbf{K}_i$, in the blockcirculant matrix.

For the blockcirculant stiffness matrix $\mathbf{K}$ of Equation 2.1, where $n = 3$ and the identity matrix $\mathbf{I}$ is (2×2), a vector basis for the block Fourier matrix is:

$$\mathbf{F} = \frac{1}{\sqrt{3}} \left[\begin{array}{cc|cc|cc} 1 & 0 & 1 & 0 & 1 & 0 \\ 0 & -1 & 0 & -1 & 0 & -1 \\ 1 & 0 & -1/2+i\sqrt{3}/2 & 0 & -1/2-i\sqrt{3}/2 & 0 \\ 0 & -1 & 0 & 1/2-i\sqrt{3}/2 & 0 & 1/2+i\sqrt{3}/2 \\ 1 & 0 & -1/2-i\sqrt{3}/2 & 0 & -1/2+i\sqrt{3}/2 & 0 \\ 0 & -1 & 0 & 1/2+i\sqrt{3}/2 & 0 & 1/2-i\sqrt{3}/2 \end{array} \right] \tag{2.6}$$

The stiffness matrix $\mathbf{K}$ is then block-diagonalised as follows:

$$\tilde{\mathbf{K}} = \mathbf{F}^{-1}\mathbf{K}\mathbf{F} \tag{2.7}$$

As the Fourier matrix $\mathbf{F}$ is a unitary matrix, the inverse Fourier matrix $\mathbf{F}^{-1}$, is $\mathbf{F}^{-1} = \bar{\mathbf{F}}$, where $\bar{\mathbf{F}}$ is the conjugate transpose of $\mathbf{F}$, and so:

$$\tilde{\mathbf{K}} = \bar{\mathbf{F}}\mathbf{K}\mathbf{F} \tag{2.8}$$

$$\tilde{\mathbf{K}} = \frac{EA}{l} \left[\begin{array}{cccccc} 3 & \sqrt{3} & 0 & 0 & 0 & 0 \\ \sqrt{3} & 1 & 0 & 0 & 0 & 0 \\ 0 & 0 & 3/2 & \sqrt{3}/4+i3/4 & 0 & 0 \\ 0 & 0 & \sqrt{3}/4-i3/4 & 1 & 0 & 0 \\ 0 & 0 & 0 & 0 & 3/2 & \sqrt{3}/4-i3/4 \\ 0 & 0 & 0 & 0 & \sqrt{3}/4+i3/4 & 1 \end{array} \right] \tag{2.9}$$

Thus the (6×6) stiffness matrix $\mathbf{K}$ is block-diagonalised into three (2×2) complex stiffness blocks $\tilde{\mathbf{K}}^{(i)}$. Each stiffness block $\tilde{\mathbf{K}}^{(i)}$ acts on an independent subspace of the load and displacement vectors and any general load or displacement vector may be decomposed into these subspaces using the *block-columns* of the Fourier matrix $\mathbf{F}$.

2.3 The Analysis of Symmetric Structures using Group Representation Theory

Although the Fourier approach has been shown to be useful for structures with rotational symmetry and some other simple types of symmetry, it is not easily extended to structures with more complex symmetry properties. In such cases, an alternative approach, based on Group Representation Theory, is more suitable. Group Representation Theory provides a systematic way to describe the full symmetry properties of any structure and allows for the maximum utilisation of these symmetry properties in an analysis.

Group Theory is generally regarded as having been founded by Évariste Galois. The concept of a group was introduced by Galois in his work on the theory of equations and this was followed up by Baron Augustin Louis Cauchy who originated the theory of permutation groups. Another important figure involved in early Group Theory is Arthur Cayley who defined the general abstract group (as it is known today) and also developed the theory of matrices. The theoretical basis of abstract Group Theory has since been extensively developed and an introduction to the subject is given by numerous authors (for example Weyl 1946, Leech & Newman 1969, Serre 1977). Mackay (1980) also provides a detailed review of the history and applications of Group Theory.

Although Group Theory has been widely applied in physics and chemistry (e.g. Hammermesh 1962, Schonland 1965, Cotton 1971, Bishop 1973), for example to simplify calculations concerning the vibration of molecules or crystals, the literature applying Group Theory to structural analysis is more scarce. The application of Group Theory in physics and chemistry dates back to the turn of the century when George Ferdinand Frobenius developed *Group Representation Theory*. This is the most important part of Group Theory in terms of application to the fields of chemistry, physics or indeed structural analysis. One of the earliest applications of Group Representation Theory in chemistry was in the study of crystal structure and with the development of X-ray analysis. However, more important work was done by Herman Weyl who developed the relationship between Group Theory and quantum mechanics and created a general theory of matrix representation of continuous groups. Another author worth mentioning is Eugene Paul Wigner who applied Group Theory to atomic and nuclear problems. It is these developments which also allow the application of Group Theory to the field of structural mechanics and provide the basis for understanding the effects symmetry has on the behaviour of a structure.

Although symmetry is studied in structural engineering it is nearly always done without recourse to Group Representation Theory. Glockner (1973) carried out a detailed review of symmetry in applied and structural mechanics and was surprised at the lack of literature dealing with Group Representation Theory or even symmetry principles. This neglect of the theoretical aspects of symmetry has meant that only simple bilateral symmetry and purely rotational symmetry, as discussed in the previous section, have regularly been exploited in structural analysis. Since Glockner's (1973) paper the situation has improved and the rest of this section reviews the relevant authors in this field.

The first application of Group Theory to structural analysis appears to have been made by Zlokovic (1973, 1989), who formulated a *G-vector analysis* based on Group Theory, and applied it to problems in statics, vibration and stability. From studying applications of Group Theory to physical problems in quantum mechanics and mathematical crystallography, Zlokovic understood that symmetry governs and simplifies the analysis of a symmetric system. Zlokovic applies

Group Theory to find what he termed "G-vector spaces", which are composed of "G-invariant subspaces" that have independent systems of equations. The method of G-vector analysis is mostly equivalent to the symmetry analysis of the stiffness matrix, described in Chapter 3 of this dissertation. However, G-vector analysis only calculates G-invariant subspaces corresponding to different *irreducible representations*; additional calculations are required to split the G-invariant subspaces corresponding to higher-dimensional irreducible representations, into the smaller *symmetry subspaces* introduced in Chapter 3. Zlokovic uses the *idempotents* of the group algebra to find G-invariant subspaces; these idempotents correspond to the *projection operator matrices* described in Chapter 3.

Other authors have since applied Group Representation Theory to different areas of structural analysis, of which the following papers are either relevant to this dissertation, or may be of interest to the reader. Bossavit (1986) introduces the Group Representation Theory required to utilise symmetry in structural analysis and shows how it can be implemented in finite element codes. Bossavit considers continuous and discrete systems, using Group Theory to find reduced linear systems of equations with boundary value problems. Bossavit has also shown that the Fourier Method is a special case of Group Theory, a point which will be expanded in Chapter 3.

Healey & Treacy (1991) have investigated eigenvalue problems associated with statics and vibrations of symmetric structures. Group Representation Theory is used to find symmetry-adapted modes which decouple the original eigenvalue problem into several smaller, independent eigenvalue problems. Healey & Treacy also provide an exact and efficient procedure requiring only the structural equations of the repeating sub-structure in order to decouple the full system of equations into symmetry-adapted sub-systems of equations. The sub-structure methods described in Chapters 3 and 4 follow from this work.

Sattinger (1979) and Golubitsky, Stewart & Schaeffer (1988) have carried out extensive work to show how Group Theory techniques aid the understanding of bifurcation problems with symmetry. Further work has since been carried out by Healey (1988), Ikeda & Murota (1991) and Wohlever (1993), who apply Group Representation Theory to bifurcation problems in non-linear mechanics, and consider symmetry-breaking solutions. The exploitation of symmetry enables the accurate computation of singular points and a considerable reduction in the numerical effort required for the determination of global solution branches.

The following authors, Miller (1981), Zhong & Qiu (1983), Dinkevich (1984, 1991), Chang & Healey (1988) and Ikeda, Ario & Torii (1992), have also applied Group Representation Theory to various problems in structural analysis.

In general, these authors all apply Group Representation Theory to the analysis of the stiffness relationship between the external loads and displacements of a symmetric structure. Bossavit (1993) however, shows that Group Representation

Theory can be equally applied to the equilibrium and compatibility relationships of a symmetric structure, which require both the external loads and displacements and the internal forces and elongations of the structure. Chapters 4 to 7 of this dissertation apply Group Representation Theory to the analysis of the equilibrium and compatibility equations of symmetric structures, but take a more concrete approach than Bossavit to provide a practical computational method. The emphasis is placed on the application of Group Theory methods to the analysis of symmetric structures, using interesting example structures in order to illustrate how symmetry governs the behaviour of a structure, and what the implications of symmetry are for symmetric structures.

Of particular interest with the equilibrium and compatibility relationships is the introduction of a coordinate system for the internal forces and elongations of a structure. The application of Group Representation Theory using internal symmetry coordinate systems was first applied to the field of chemistry, where an internal coordinate system is used to describe the internal configuration of a molecule without regard for its position in the external space.

Wilson, Decius & Cross (1955) showed that the interatomic distances and angles between chemical bonds can be used to define an internal coordinate system for a molecule. Such an internal coordinate system will have the same symmetry properties as the molecule and hence is suitable for calculating the potential energy of a molecule. In contrast, the kinetic energy is best described using an external Cartesian coordinate system for the displacements of the atoms.

A number of authors (Wilson et al. 1955, Schonland 1965, Bishop 1973) have investigated the vibrational spectra of molecules and have shown that when calculating normal modes and frequencies of vibrations, symmetric considerations helped reduce the required calculations considerably. This is due to the normal modes of vibration of symmetrical molecules having special symmetry properties. Group Representation Theory can then be used to find a symmetry-adapted internal coordinate system where the normal nodes with particular symmetry properties are obtained.

In a similar way, a coordinate system can be defined for the internal forces and elongations of a symmetric structure, and using Group Representation Theory a symmetry-adapted vector basis can be found for this internal vector space. These internal coordinate systems are introduced in Chapter 4.

Chapter 3

Symmetric Structures and Group Representation Theory

3.1 Introduction

This chapter provides an introduction to the analysis of symmetric structures, and aims to show how the application of Group Representation Theory to symmetric structures can be used to simplify the analysis and provide considerable reductions in the computational effort required. Group Representation Theory is applied to the *Stiffness Method* of structural analysis throughout this chapter; the *Force Method* is described in Chapter 4.

Chapter 2 provided an extensive review of the work done in the field of symmetry structures. This chapter shows that Group Representation Theory provides a general and systematic method to fully describe the symmetry properties of a structure and to analyse the implications of symmetry on the physical response of a structure.

Group Representation Theory can be used to find *symmetry-adapted coordinate systems* for any symmetric structure. These symmetry-adapted coordinate systems are made up of vector *symmetry subspaces*, each of which have particular symmetry properties corresponding to the structure. The analysis of any symmetric structure can then be considerably simplified by using these symmetry-adapted coordinate systems to block-diagonalise the stiffness matrix.

The layout of this chapter is as follows. The rest of this section outlines the Stiffness Method commonly used in structural analysis. Section 3.2 introduces an example structure and defines its symmetry properties. Section 3.3 introduces Group Representation Theory, in particular the Great Orthogonality Theorem and the projection operator matrix, which are required to fully exploit the symmetry of any symmetric structure. Section 3.4 shows how, using the projection operator matrix, a symmetry-adapted coordinate system can be found for the external load and displacement vector space of the example structure. Section 3.5 block-diagonalises the stiffness matrix of the example structure into stiffness blocks which define the relationship between load and displacement vectors that have a particular type of symmetry.

In Chapter 2 the analysis of rotationally periodic structures using the *Fourier Method* was described; Section 3.6 goes on to show that the Fourier Method is simply a special case of the Group Representation Theory method. Finally, Section 3.7 shows how techniques, utilising only the the repeating symmetry sub-structure, can be used to further simplify the analysis of the stiffness matrix.

3.1.1 Stiffness Matrix

The Stiffness Method of structural analysis relates the applied external loads to the resulting external deflections at the joints of a structure (Livesley 1975). For small perturbations about the initial configuration of a structure, these stiffness equations can be linearised as a matrix relationship.

The system of stiffness equations for a general structure is given by:

$$\mathbf{K}\mathbf{d} = \mathbf{p} \tag{3.1}$$

where: $\mathbf{K}$ is the stiffness matrix.
$\mathbf{d}$ is the external displacement vector.
$\mathbf{p}$ is the external load vector.

The above stiffness equations are equally suited to the analysis of pin-jointed structures, rigid body frames or finite element discretisation of continuous structures. However, the examples used in this chapter are limited to pin-jointed structures, in order to simplify the matrix calculations.

3.2 Pin-Jointed Structure with C_{3v} Symmetry

Shown in Figure 3.1 is a pin-jointed structure in 2-dimensional space which will be used to demonstrate how the symmetry properties of a structure can be defined in terms of *symmetry operations*. This pin-jointed structure is used throughout this chapter and will be referred to as the "example structure".

In order to exploit these symmetry properties, vector coordinate systems can be attached to the structure, allowing the symmetry operations to be written down as *matrix representations*. Group Representation Theory uses these matrix representations to find symmetry-adapted coordinate systems for the structure,

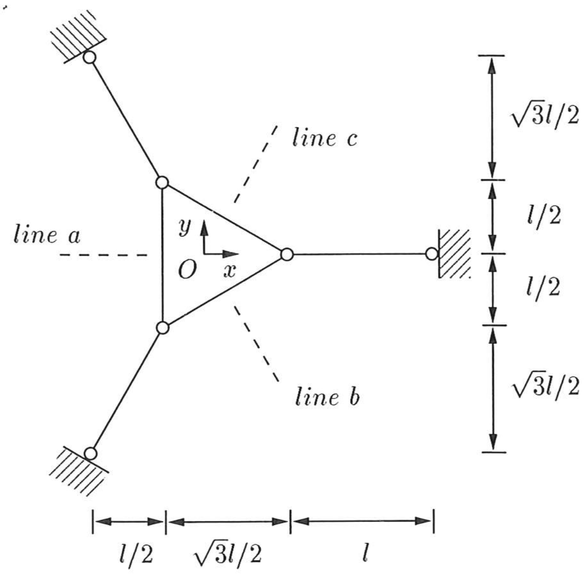

Figure 3.1: Pin-jointed structure in 2-dimensional space. All joints are pinned.

and hence it is possible to show that a stiffness matrix can be block-diagonalised using a symmetry-adapted coordinate system for the load and displacement vector space.

A symmetry operation is an operation, such as a rotation about an axis or a reflection in a plane, that brings a structure into a new position which coincides exactly with the original position, such that the structure is left in a geometrically and mechanically identical configuration. This is called an *equivalent configuration.* A full description of all the different possible symmetry operations is given in Appendix A.1.

The example structure has 3-fold rotational symmetry in its plane and reflection symmetry in the three lines a, b and c. Hence, it is transformed into an *equivalent configuration* by the following set of symmetry operations:

1. The identity, symmetry operation E.
2. Rotation by 120° about the origin O, symmetry operation C_3.
3. Rotation by 240° about the origin O, symmetry operation C_3^2.
4. Reflection in line a, symmetry operation σ_a.
5. Reflection in line b, symmetry operation σ_b.
6. Reflection in line c, symmetry operation σ_c.

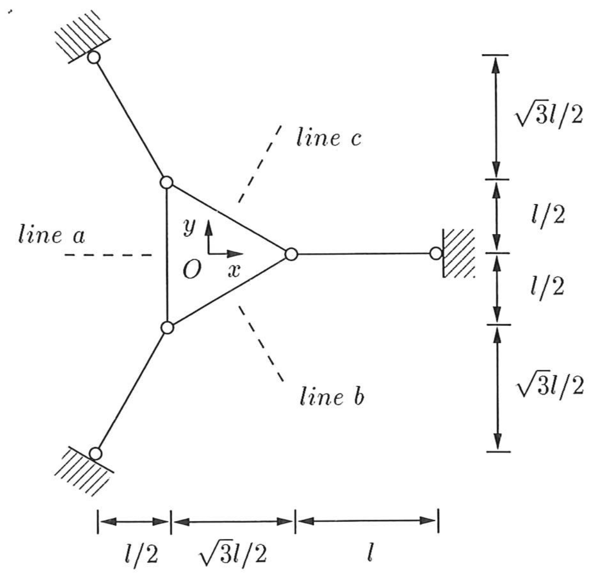

Figure 3.1: Pin-jointed structure in 2-dimensional space. All joints are pinned.

and hence it is possible to show that a stiffness matrix can be block-diagonalised using a symmetry-adapted coordinate system for the load and displacement vector space.

A symmetry operation is an operation, such as a rotation about an axis or a reflection in a plane, that brings a structure into a new position which coincides exactly with the original position, such that the structure is left in a geometrically and mechanically identical configuration. This is called an *equivalent configuration*. A full description of all the different possible symmetry operations is given in Appendix A.1.

The example structure has 3-fold rotational symmetry in its plane and reflection symmetry in the three lines a, b and c. Hence, it is transformed into an *equivalent configuration* by the following set of symmetry operations:

1. The identity, symmetry operation E.
2. Rotation by 120° about the origin O, symmetry operation C_3.
3. Rotation by 240° about the origin O, symmetry operation C_3^2.
4. Reflection in line a, symmetry operation σ_a.
5. Reflection in line b, symmetry operation σ_b.
6. Reflection in line c, symmetry operation σ_c.

Notice the terminology introduced here. The symbol E is used for an identity operation. C_3 for a rotation by an angle 120° about the origin O, and C_3^2 for *two* operations C_3, i.e., a rotation by an angle 240° about the origin O. σ_a for a reflection in line a, σ_b for a reflection in line b, and σ_c for a reflection in line c. Also note that rotations are defined as positive in the anti-clockwise direction. The terminology used for symmetry operations is described in more detail in Appendix A.1.

For any structure it is possible to write down the distinct symmetry operations that can be performed on the structure to bring it into an equivalent configuration. This set of symmetry operations forms the *symmetry group* of the structure. For example, the six symmetry operations $\{E, C_3, C_3^2, \sigma_a, \sigma_b, \sigma_c\}$ of the example structure in Figure 3.1, constitute the symmetry group $\mathbf{C_{3v}}$.

The total number of possible symmetry groups is restricted, and hence many structures will share the same symmetry group. The restriction that translations or magnifications are not allowed, limits the symmetry groups that are consider in this dissertation to a set known as *point groups*. Symmetry groups are discussed in more detail in Appendix A.2.

Each symmetry group is defined by a *multiplication table* of its symmetry operations. For the example structure with symmetry group $\mathbf{C_{3v}}$, a rotation by 120° about the origin O, symmetry operation C_3, followed by a reflection in line a, symmetry operation σ_a, is exactly the same as a reflection in line b, symmetry operation σ_b. The complete multiplication table for group $\mathbf{C_{3v}}$ is shown in Table 3.1.

		1st Operation					
		E	C_3	C_3^2	σ_a	σ_b	σ_c
2nd Operation	E	E	C_3	C_3^2	σ_a	σ_b	σ_c
	C_3	C_3	C_3^2	E	σ_c	σ_a	σ_b
	C_3^2	C_3^2	E	C_3	σ_b	σ_c	σ_a
	σ_a	σ_a	σ_b	σ_c	E	C_3	C_3^2
	σ_b	σ_b	σ_c	σ_a	C_3^2	E	C_3
	σ_c	σ_c	σ_a	σ_b	C_3	C_3^2	E

Table 3.1: Multiplication table for symmetry group $\mathbf{C_{3v}}$.

3.2.1 Matrix Representations of Symmetry Operations

Once a coordinate system is attached to a structure, it enables the symmetry operations acting on the structure to be written down as matrix operations acting on the vectors defined by the coordinate system. These matrices will of course change depending on the coördinate system that is used, but for a particular coordinate system, each symmetry operation will be represented by a unique matrix. The complete set of matrices that represent every symmetry operation in a symmetry group are then said to form a *matrix representation* of the group. These matrices will, obviously, also follow the group multiplication table.

Section 3.1.1 shows that a coordinate system is required to define the external load and displacement vectors which act on a structure. In Figure 3.2 a coordinate system that is suitable for representing both the load vectors **p** and the displacement vectors **d**, is attached to the example structure.

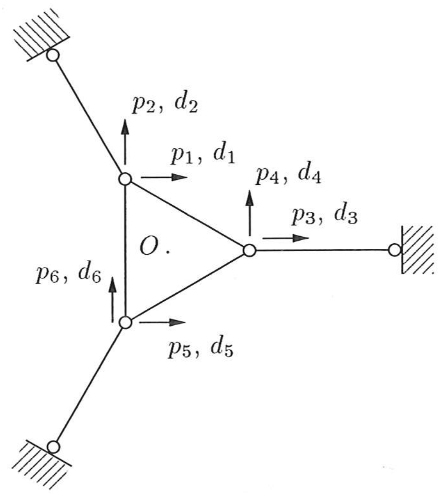

Figure 3.2: A Cartesian coordinate system for the external load and displacement vector space $\mathbb{V}_{\mathbf{p}}$.

Unit vectors in the direction of p_1-p_6 or d_1-d_6 form a vector basis for this 6-dimensional space in which the loads or displacements are represented, and the symbol $\mathbb{V}_{\mathbf{p}}$ is used to denote this vector space. It is then possible, using Group Representation Theory, to show how this vector space can be split into independent *symmetry subspaces*, each of which will show different aspects of the symmetry of the structure.

Using the particular vector basis shown in Figure 3.2, i.e. a Cartesian coordinate system, a matrix representation of the group can be written down. For example, following a rotation by 120° about the origin O, the new component of load in the 1 direction, p_1' will be a combination of the components of load that were formerly in the 3 and 4 directions, p_3 and p_4, specifically:

$$p_1' = -\frac{1}{2}p_3 - \frac{\sqrt{3}}{2}p_4 \tag{3.2}$$

Similar expressions can be written for every other vector component to define the matrix operation $\mathbf{P}(C_3)$:

$$\mathbf{P}(C_3) = \begin{bmatrix} 0 & 0 & -1/2 & -\sqrt{3}/2 & 0 & 0 \\ 0 & 0 & \sqrt{3}/2 & -1/2 & 0 & 0 \\ 0 & 0 & 0 & 0 & -1/2 & -\sqrt{3}/2 \\ 0 & 0 & 0 & 0 & \sqrt{3}/2 & -1/2 \\ -1/2 & -\sqrt{3}/2 & 0 & 0 & 0 & 0 \\ \sqrt{3}/2 & -1/2 & 0 & 0 & 0 & 0 \end{bmatrix} \tag{3.3}$$

The complete set of matrices representing the effects of the symmetry operations on either the load or displacement vectors $\mathbf{p}$ or $\mathbf{d}$, in the Cartesian coordinate system of Figure 3.2, are shown in Table 3.2.

$$\mathbf{P}(E)=\mathbf{D}(E)= \begin{bmatrix} 1 & 0 & 0 & 0 & 0 & 0 \\ 0 & 1 & 0 & 0 & 0 & 0 \\ 0 & 0 & 1 & 0 & 0 & 0 \\ 0 & 0 & 0 & 1 & 0 & 0 \\ 0 & 0 & 0 & 0 & 1 & 0 \\ 0 & 0 & 0 & 0 & 0 & 1 \end{bmatrix}$$

$$\mathbf{P}(\sigma_a)=\mathbf{D}(\sigma_a)= \begin{bmatrix} 0 & 0 & 0 & 0 & 1 & 0 \\ 0 & 0 & 0 & 0 & 0 & -1 \\ 0 & 0 & 1 & 0 & 0 & 0 \\ 0 & 0 & 0 & -1 & 0 & 0 \\ 1 & 0 & 0 & 0 & 0 & 0 \\ 0 & -1 & 0 & 0 & 0 & 0 \end{bmatrix}$$

$$\mathbf{P}(C_3)=\mathbf{D}(C_3)= \begin{bmatrix} 0 & 0 & -1/2 & -\sqrt{3}/2 & 0 & 0 \\ 0 & 0 & \sqrt{3}/2 & -1/2 & 0 & 0 \\ 0 & 0 & 0 & 0 & -1/2 & -\sqrt{3}/2 \\ 0 & 0 & 0 & 0 & \sqrt{3}/2 & -1/2 \\ -1/2 & -\sqrt{3}/2 & 0 & 0 & 0 & 0 \\ \sqrt{3}/2 & -1/2 & 0 & 0 & 0 & 0 \end{bmatrix}$$

$$\mathbf{P}(\sigma_b)=\mathbf{D}(\sigma_b)= \begin{bmatrix} -1/2 & -\sqrt{3}/2 & 0 & 0 & 0 & 0 \\ -\sqrt{3}/2 & 1/2 & 0 & 0 & 0 & 0 \\ 0 & 0 & 0 & 0 & -1/2 & -\sqrt{3}/2 \\ 0 & 0 & 0 & 0 & -\sqrt{3}/2 & 1/2 \\ 0 & 0 & -1/2 & -\sqrt{3}/2 & 0 & 0 \\ 0 & 0 & -\sqrt{3}/2 & 1/2 & 0 & 0 \end{bmatrix}$$

$$\mathbf{P}(C_3^2)=\mathbf{D}(C_3^2)= \begin{bmatrix} 0 & 0 & 0 & 0 & -1/2 & \sqrt{3}/2 \\ 0 & 0 & 0 & 0 & -\sqrt{3}/2 & -1/2 \\ -1/2 & \sqrt{3}/2 & 0 & 0 & 0 & 0 \\ -\sqrt{3}/2 & -1/2 & 0 & 0 & 0 & 0 \\ 0 & 0 & -1/2 & \sqrt{3}/2 & 0 & 0 \\ 0 & 0 & -\sqrt{3}/2 & -1/2 & 0 & 0 \end{bmatrix}$$

$$\mathbf{P}(\sigma_c)=\mathbf{D}(\sigma_c)= \begin{bmatrix} 0 & 0 & -1/2 & \sqrt{3}/2 & 0 & 0 \\ 0 & 0 & \sqrt{3}/2 & 1/2 & 0 & 0 \\ -1/2 & \sqrt{3}/2 & 0 & 0 & 0 & 0 \\ \sqrt{3}/2 & 1/2 & 0 & 0 & 0 & 0 \\ 0 & 0 & 0 & 0 & -1/2 & \sqrt{3}/2 \\ 0 & 0 & 0 & 0 & \sqrt{3}/2 & 1/2 \end{bmatrix}$$

Table 3.2: Load and displacement vector matrix representation $\mathbf{P}$ and $\mathbf{D}$, of symmetry group $\mathbf{C_{3v}}$.

These matrices constitute the *reducible matrix representation* $\mathbf{P}$ and $\mathbf{D}$ of the symmetry group $\mathbf{C_{3v}}$. The reader may wish to check that these matrices do indeed follow the multiplication table for group $\mathbf{C_{3v}}$, shown in Table 3.1. The term *reducible* will be explained in Section 3.3.

3.3 Group Representation Theory

This section introduces the Group Representation Theory required to find the symmetry-adapted coordinate systems of any symmetric structure. In particular the Great Orthogonality Theorem and the projection operator matrix are described in terms of structural analysis. Appendix A gives a more general and detailed description of Group Representation Theory required for the analysis of symmetric structures. This dissertation aims only to introduce the reader to the relevant Group Representation Theory. No proofs are given for any of the theoretical properties described. If the reader is interested in the mathematical background to these ideas, the following standard textbooks on Group Representation Theory are recommended, Schonland (1965) or Bishop (1973).

In Figure 3.2, a Cartesian coordinate system was defined for the load and displacement vector space $\mathbb{V}_\mathbf{p}$ of the example structure. This Cartesian coordinate system resulted in the reducible matrix representation shown in Table 3.2.

Group Representation Theory shows that, had a particular choice of coordinate system been used, the equivalent matrix representation would be in a block-diagonal form, with the blocks being as small as possible. These blocks are called the *irreducible matrix representations* $\Gamma^{(\mu)}$ of a symmetry group (a more detailed description of irreducible matrix representations is given in Appendix A.3).

For a general vector space $\mathbb{V}$, a block-diagonalised matrix representation $\tilde{\mathbf{R}}$ will have the following form, irrespective of the particular structure:

$$\tilde{\mathbf{R}} = \begin{bmatrix} \boxed{\Gamma^{(1)}_1} & & & & & \\ & \boxed{\Gamma^{(1)}_{a_1}} & & & \mathbf{0} & \\ & & \boxed{\Gamma^{(\mu)}_1} & & & \\ & & & \boxed{\Gamma^{(\mu)}_{a_\mu}} & & \\ & \mathbf{0} & & & \boxed{\Gamma^{(\alpha)}_1} & \\ & & & & & \boxed{\Gamma^{(\alpha)}_{a_\alpha}} \end{bmatrix} \tag{3.4}$$

where: $\Gamma^{(\mu)}_m = \Gamma^{(\nu)}_n$ for all m and n, if $\mu = \nu$.
$\Gamma^{(\mu)}_m \neq \Gamma^{(\nu)}_n$ for all m and n, if $\mu \neq \nu$.
α is the number of different $\Gamma^{(\mu)}$.
a_μ is the multiplicity of each different $\Gamma^{(\mu)}$.
$\sim$ denotes a block-diagonalised matrix.

Equation 3.4 shows that each irreducible matrix representation $\Gamma_i^{(\mu)}$ operates on an *irreducible invariant subspace* $\mathbb{V}_i^{(\mu)}$, such that the vector space $\mathbb{V}$ is now given by:

$$\mathbb{V} = \left(\mathbb{V}_1^{(1)}, \cdots, \mathbb{V}_{a_1}^{(1)}, \cdots, \mathbb{V}_1^{(\mu)}, \cdots, \mathbb{V}_{a_\mu}^{(\mu)}, \cdots, \mathbb{V}_1^{(\alpha)}, \cdots, \mathbb{V}_{a_\alpha}^{(\alpha)}\right) \tag{3.5}$$

The multiplicity a_μ of each different $\Gamma^{(\mu)}$ can change depending on the particular structure under analysis, but the contents of a particular $\Gamma^{(\mu)}$ depend only on the symmetry group. For all symmetry groups with only one main n-fold axis of symmetry these irreducible matrix representations $\Gamma^{(\mu)}$ are either (1×1) or (2×2), while for other symmetry groups they may also be (3×3). For a particular μ, if $\Gamma^{(\mu)}$ is (1×1), then its vector basis will be unique. However, if $\Gamma^{(\mu)}$ is of higher dimension there will be a choice of vector basis, although $\Gamma^{(\mu)}$ will always have the same *trace* and *determinant* for each symmetry operation, irrespective of the choice of vector basis.

The irreducible matrix representations $\Gamma^{(\mu)}$ for the symmetry group $\mathbf{C_{3v}}$, are shown in Table 3.3. $\Gamma^{(A_1)}$ and $\Gamma^{(A_2)}$ are (1×1) representations, and hence are unique. $\Gamma^{(E)}$ is a (2×2) representation, and so there is a choice of vector basis for this representation. Shown in Table 3.3 is one particular choice of vector basis for $\Gamma^{(E)}$ that will be used to find the load and displacement vector symmetry subspaces later in this chapter. A different choice of vector basis gives an equivalent $\Gamma^{(E)}$, and the effect this has on the symmetry subspaces is discussed later. Obviously, the irreducible matrix representations in Table 3.3 will also follow the multiplication table for the group, shown in Table 3.1.

For the example structure, shown in Figure 3.1, the block-diagonalised matrix representation $\tilde{\mathbf{P}}$ (and $\tilde{\mathbf{D}}$), actually has the following form:

$$\tilde{\mathbf{P}} = \begin{bmatrix} \boxed{\Gamma_1^{(A_1)}} & & & \mathbf{0} \\ & \boxed{\Gamma_1^{(A_2)}} & & \\ & & \boxed{\Gamma_1^{(E)}} & \\ \mathbf{0} & & & \boxed{\Gamma_2^{(E)}} \end{bmatrix} \tag{3.6}$$

Inserting the irreducible representations from Table 3.3 into Equation 3.6, a complete set of block-diagonalised matrices are obtained, as shown in Table 3.4.

$\mathbf{C_{3v}}$	E	C_3	C_3^2	σ_a	σ_b	σ_c
$\Gamma^{(A_1)}$	1	1	1	1	1	1
$\Gamma^{(A_2)}$	1	1	1	−1	−1	−1
$\Gamma^{(E)}$	$\begin{bmatrix}1 & 0\\0 & 1\end{bmatrix}$	$\begin{bmatrix}-1/2 & -\sqrt{3}/2\\\sqrt{3}/2 & -1/2\end{bmatrix}$	$\begin{bmatrix}-1/2 & \sqrt{3}/2\\-\sqrt{3}/2 & -1/2\end{bmatrix}$	$\begin{bmatrix}1 & 0\\0 & -1\end{bmatrix}$	$\begin{bmatrix}-1/2 & -\sqrt{3}/2\\-\sqrt{3}/2 & 1/2\end{bmatrix}$	$\begin{bmatrix}-1/2 & \sqrt{3}/2\\\sqrt{3}/2 & 1/2\end{bmatrix}$

Table 3.3: Irreducible matrix representations of symmetry group $\mathbf{C_{3v}}$.

$$\tilde{\mathbf{P}}(E)=\tilde{\mathbf{D}}(E)=\begin{bmatrix}1&0&0&0&0&0\\0&1&0&0&0&0\\0&0&1&0&0&0\\0&0&0&1&0&0\\0&0&0&0&1&0\\0&0&0&0&0&1\end{bmatrix}$$

$$\tilde{\mathbf{P}}(\sigma_a)=\tilde{\mathbf{D}}(\sigma_a)=\begin{bmatrix}1&0&0&0&0&0\\0&-1&0&0&0&0\\0&0&1&0&0&0\\0&0&0&-1&0&0\\0&0&0&0&1&0\\0&0&0&0&0&-1\end{bmatrix}$$

$$\tilde{\mathbf{P}}(C_3)=\tilde{\mathbf{D}}(C_3)=\begin{bmatrix}1&0&0&0&0&0\\0&1&0&0&0&0\\0&0&-1/2&-\sqrt{3}/2&0&0\\0&0&\sqrt{3}/2&-1/2&0&0\\0&0&0&0&-1/2&-\sqrt{3}/2\\0&0&0&0&\sqrt{3}/2&-1/2\end{bmatrix}$$

$$\tilde{\mathbf{P}}(\sigma_b)=\tilde{\mathbf{D}}(\sigma_b)=\begin{bmatrix}1&0&0&0&0&0\\0&-1&0&0&0&0\\0&0&-1/2&-\sqrt{3}/2&0&0\\0&0&-\sqrt{3}/2&1/2&0&0\\0&0&0&0&-1/2&-\sqrt{3}/2\\0&0&0&0&-\sqrt{3}/2&1/2\end{bmatrix}$$

$$\tilde{\mathbf{P}}(C_3^2)=\tilde{\mathbf{D}}(C_3^2)=\begin{bmatrix}1&0&0&0&0&0\\0&1&0&0&0&0\\0&0&-1/2&\sqrt{3}/2&0&0\\0&0&-\sqrt{3}/2&-1/2&0&0\\0&0&0&0&-1/2&\sqrt{3}/2\\0&0&0&0&-\sqrt{3}/2&-1/2\end{bmatrix}$$

$$\tilde{\mathbf{P}}(\sigma_c)=\tilde{\mathbf{D}}(\sigma_c)=\begin{bmatrix}1&0&0&0&0&0\\0&-1&0&0&0&0\\0&0&-1/2&\sqrt{3}/2&0&0\\0&0&\sqrt{3}/2&1/2&0&0\\0&0&0&0&-1/2&\sqrt{3}/2\\0&0&0&0&\sqrt{3}/2&1/2\end{bmatrix}$$

Table 3.4: Block-diagonalised load and displacement vector matrix representation $\tilde{\mathbf{P}}$ and $\tilde{\mathbf{D}}$, of symmetry group $\mathbf{C_{3v}}$.

It is clear from the block-diagonalised matrix representation $\tilde{\mathbf{P}}$, that the vector space $\mathbb{V}_{\mathbf{p}}$ (in this case a 6-dimensional space of loads or displacements) has been decomposed into a number of irreducible invariant subspaces $\mathbb{V}_{\mathbf{p}i}^{(\mu)}$, each operated on by a particular irreducible representation $\Gamma_i^{(\mu)}$. Because of the block-diagonalised nature of the matrix representation $\tilde{\mathbf{P}}$, any vector in an irreducible invariant subspace $\mathbb{V}_{\mathbf{p}i}^{(\mu)}$, will remain within that subspace following any symmetry operation of symmetry group $\mathbf{C_{3v}}$.

Although the block-diagonalised matrix representation $\tilde{\mathbf{P}}$ is an important concept, finding the coordinate system that is required to generate it will not be pursued. Instead, it is possible to generate the required *symmetry subspaces* directly from the irredúcible matrix representations $\Gamma_i^{(\mu)}$, which leads to the block-diagonalisation of the stiffness matrix, the ultimate aim of this chapter.

From the irreducible invariant subspaces, these symmetry subspaces can be defined in two steps. First, the summation of the irreducible invariant subspaces $\mathbb{V}_{\mathrm{p}i}^{(\mu)}$ corresponding to each $\Gamma^{(\mu)}$, is required:

$$\mathbb{V}_{\mathrm{p}}^{(\mu)} = \left(\mathbb{V}_{\mathrm{p}1}^{(\mu)}, \mathbb{V}_{\mathrm{p}2}^{(\mu)}, \cdots, \mathbb{V}_{\mathrm{p}a_\mu}^{(\mu)}\right) \tag{3.7}$$

Each of these invariant subspaces $\mathbb{V}_{\mathrm{p}}^{(\mu)}$ represents a particular type of symmetry.

Second, for any subspace $\mathbb{V}_{\mathrm{p}}^{(\mu)}$ that correspond to $\Gamma^{(\mu)}$ bigger than (1×1), this subspace can be further decomposed into subspaces corresponding to the different rows of $\Gamma^{(\mu)}$, each of which will represent a further refinement on the type of symmetry. It is these subspaces that are called *symmetry subspaces*, $\mathbb{V}_{\mathrm{p}}^{(\mu)i}$. Hence, for the example structure:

1. $\mathbb{V}_{\mathrm{p}}^{(A_1)} = \mathbb{V}_{\mathrm{p}1}^{(A_1)}$ is a 1-dimensional symmetry subspace.

2. $\mathbb{V}_{\mathrm{p}}^{(A_2)} = \mathbb{V}_{\mathrm{p}1}^{(A_2)}$ is a 1-dimensional symmetry subspace.

3. $\mathbb{V}_{\mathrm{p}}^{(E)} = \left(\mathbb{V}_{\mathrm{p}1}^{(E)}, \mathbb{V}_{\mathrm{p}2}^{(E)}\right)$ is a 4-dimensional subspace which can be decomposed into two 2-dimensional symmetry subspaces $\mathbb{V}_{\mathrm{p}}^{(E)1}$ and $\mathbb{V}_{\mathrm{p}}^{(E)2}$.

To find these symmetry subspaces $\mathbb{V}_{\mathrm{p}}^{(\mu)i}$, requires the Great Orthogonality Theorem and the projection operator matrix.

3.3.1 Great Orthogonality Theorem and the Projection Operator Matrix

The *Great Orthogonality Theorem* is a remarkable relationship between the different irreducible representations of a symmetry group and may be put into words as follows:

Each irreducible representation (if 1-dimensional), or particular component of an irreducible representation (if higher-dimensional) is orthogonal to every other 1-dimensional irreducible representation or component of a higher-dimensional irreducible representation.

This property also holds for the cases where the irreducible representations are complex, but of course orthogonality then requires the complex conjugate of one of the two terms. The Great Orthogonality Theorem is stated in Appendix A.4 and a proof is given by Bishop(1973). Its validity however, can be easily verified for the symmetry group $\mathbf{C_{3v}}$. For example, from Table 3.3, $\Gamma^{(A_2)}$ is orthogonal to the (1,2) component of $\Gamma^{(E)}$:

$$(1\times 0)+(1\times -\frac{\sqrt{3}}{2})+(1\times \frac{\sqrt{3}}{2})+(-1\times 0)+(-1\times -\frac{\sqrt{3}}{2})+(-1\times \frac{\sqrt{3}}{2})=0 \quad (3.8)$$

The same orthogonality would be found for any choice of different component of any $\Gamma^{(\mu)}$ in the symmetry group.

Hence, the Great Orthogonality Theorem enables the symmetry subspaces to be found using the following procedure:

1. A linear combination of the matrices of a general reducible matrix representation $\mathbf{R}$, where each matrix is multiplied by the i,j component of the corresponding irreducible matrix representation $\Gamma^{(\mu)}$, will give the *projection operator matrix* $\mathbf{O}_{ij}^{(\mu)}$.

2. The column space of $\mathbf{O}_{ij}^{(\mu)}$ defines the symmetry subspace $\mathbb{V}^{(\mu)i}$.

This is particularly easy to show if the block-diagonalised matrix representation $\tilde{\mathbf{R}}$ of a symmetry group is being used; however similar arguments can then be extended to any reducible matrix representation $\mathbf{R}$. A heuristic proof follows for the example structure with $\mathbf{C_{3v}}$ symmetry, to find a vector basis for symmetry subspace $\mathbb{V}_{\mathbf{P}}^{(E)1}$ (the symmetry subspace corresponding to the first row of irreducible representation $\Gamma^{(E)}$). Appendix A.5 contains a rigorous proof of the projection operator matrix.

Using the procedure described above to find the projection operator matrix $\tilde{\mathbf{O}}_{11}^{(E)}$, the matrices of the block-diagonalised matrix representation $\tilde{\mathbf{P}}$ given in Table 3.4, are multiplied by the corresponding (1,1) component of irreducible matrix representation $\Gamma^{(E)}$ and summed over all the operations in symmetry group $\mathbf{C_{3v}}$. By the Great Orthogonality Theorem, this summation will reduce to zero every component except the (1,1) component of $\Gamma^{(E)}$:

$$\tilde{\mathbf{O}}_{11}^{(E)} = \sum_{\tilde{P}} \Gamma_{11}^{(E)} \tilde{\mathbf{P}} = \left[\begin{array}{cccccc} 0 & & & & & \\ & 0 & & & & \\ & & 3 & 0 & & \\ & & 0 & 0 & & \\ & & & & 3 & 0 \\ & & & & 0 & 0 \end{array}\right] \quad (3.9)$$

Note that in general, the complex conjugate of $\Gamma_{11}^{(E)}$ must be used, but in this example all numbers are real.

The column space of the projection operator matrix $\tilde{\mathbf{O}}_{11}^{(E)}$ defines the symmetry subspace $\mathbb{V}_{\mathrm{p}}^{(E)1}$ in the symmetry-adapted coordinate system, and an orthonormal vector basis, $\tilde{\mathbf{V}}_{\mathrm{p}}^{(E)1}$ is:

$$\tilde{\mathbf{V}}_{\mathrm{p}}^{(E)1} = \text{column space of } \tilde{\mathbf{O}}_{11}^{(E)} = \begin{bmatrix} 0 & 0 \\ 0 & 0 \\ 1 & 0 \\ 0 & 0 \\ 0 & 1 \\ 0 & 0 \end{bmatrix} \tag{3.10}$$

where $\sim$ denotes that this symmetry-adapted vector basis is written in the symmetry-adapted coordinate system and hence is denoted $\tilde{\mathbf{V}}_{\mathrm{p}}^{(E)1}$.

Note that the (1,2) component of the third irreducible matrix representation $\Gamma_{12}^{(E)}$, will give the same symmetry subspace $\mathbb{V}_{\mathrm{p}}^{(E)1}$.

The same procedure also works for the case where the original problem was not defined in the symmetry-adapted coordinate system, but in a more common coordinate system such as a Cartesian or polar coordinate system. In general, any reducible matrix representation $\mathbf{R}$ can be transformed into a block-diagonalised representation $\tilde{\mathbf{R}}$ by a similarity transformation. For example, the block-diagonalised representation $\tilde{\mathbf{P}}$ that operates on the symmetry-adapted load and displacement vector space $\mathbb{V}_{\mathrm{p}}$ of the example structure, is given by:

$$\tilde{\mathbf{P}} = \mathbf{V}_{\mathrm{p}}^{\mathbf{T}}\mathbf{P}\mathbf{V}_{\mathrm{p}} \tag{3.11}$$

where the orthogonal matrix $\mathbf{V}_{\mathrm{p}}$ is as yet unknown.
Equation 3.11 can be rearranged as:

$$\mathbf{P} = \mathbf{V}_{\mathrm{p}}\tilde{\mathbf{P}}\mathbf{V}_{\mathrm{p}}^{\mathbf{T}} \tag{3.12}$$

Hence, following the same procedure described above, but now using the reducible matrix representation $\mathbf{P}$ to find a basis for $\mathbb{V}_{\mathrm{p}}^{(E)1}$ in the original coordinate system, the matrices $\mathbf{P}$ given by Table 3.2, are now multiplied by the (1,1) component of the third irreducible representation $\Gamma_{11}^{(E)}$ and summed over all the symmetry operations in the symmetry group $\mathbf{C_{3v}}$:

$$\sum_{P}\Gamma_{11}^{(E)}\mathbf{P} = \sum_{\tilde{P}}\Gamma_{11}^{(E)}(\mathbf{V}_{\mathrm{p}}\tilde{\mathbf{P}}\mathbf{V}_{\mathrm{p}}^{\mathbf{T}}) \tag{3.13}$$

Since matrix multiplication is distributive, the right hand side of Equation 3.13 can be rewritten as:

$$\sum_{P}\Gamma_{11}^{(E)}\mathbf{P} = \mathbf{V}_{\mathrm{p}}(\sum_{\tilde{P}}\Gamma_{11}^{(E)}\tilde{\mathbf{P}})\mathbf{V}_{\mathrm{p}}^{\mathbf{T}} \tag{3.14}$$

Then, substituting Equation 3.9 into the right hand side of Equation 3.14 gives:

$$\sum_P \Gamma_{11}^{(E)}\mathbf{P} = \mathbf{V_P}\begin{bmatrix} \boxed{0} & & & & & \\ & \boxed{0} & & & & \\ & & 3 & 0 & & \\ & & 0 & 0 & & \\ & & & & 3 & 0 \\ & & & & 0 & 0 \end{bmatrix}\mathbf{V_P^T} \tag{3.15}$$

Equation 3.10 shows that the column space of $\sum_{\tilde{P}} \Gamma_{11}^{(E)}\tilde{\mathbf{P}}$ defines the symmetry subspace $\mathbb{V}_{\mathbf{P}}^{(E)1}$ in the symmetry-adapted coordinate system. Now, Equation 3.15 shows that $\sum_P \Gamma_{11}^{(E)}\mathbf{P}$ is a similar matrix to $\sum_{\tilde{P}} \Gamma_{11}^{(E)}\tilde{\mathbf{P}}$ and hence, its column space also defines the symmetry subspace $\mathbb{V}_{\mathbf{P}}^{(E)1}$, but in the original Cartesian coordinate system of Figure 3.1. Hence:

$$\mathbb{V}_{\mathbf{P}}^{(E)1} = \text{column space of} \sum_P \Gamma_{11}^{(E)}\mathbf{P} \tag{3.16}$$

Similar expressions can be written for each of the matrix components $\Gamma_{ij}^{(\mu)}$ of any irreducible matrix representation in symmetry group $\mathbf{C_{3v}}$, to find the orthonormal basis vector for all the symmetry subspaces $\mathbb{V}_{\mathbf{P}}^{(\mu)i}$.

Thus, for a general matrix representation $\mathbf{R}$, which operates on some given vector space $\mathbb{V}$ of a structure, a vector basis for each of the symmetry subspaces $\mathbb{V}^{(\mu)i}$ is given by the column space of the projection operator matrix $\mathbf{O}_{ij}^{(\mu)}$:

$$\mathbf{V}^{(\mu)i} = \text{column space of } \mathbf{O}_{ij}^{(\mu)} = \sum_R \Gamma_{ij}^{(\mu)}\mathbf{R} \tag{3.17}$$

Hence, the irreducible matrix representations define the different symmetry subspaces $\mathbb{V}^{(\mu)i}$ that make up the full space $\mathbb{V}$. Each symmetry subspace $\mathbb{V}^{(\mu)i}$ corresponds to row i of irreducible matrix representation $\Gamma^{(\mu)}$ and as the next section will show, has particular symmetry properties.

Note that strictly speaking, symmetry subspace $\mathbb{V}^{(\mu)i}$ is given by the column space of the projection operator matrix in Equation A.29, where the complex conjugate term $\Gamma_{ij}^{(\mu)*}$ is used. However, for real irreducible representations $\Gamma^{(\mu)*} = \Gamma^{(\mu)}$. Furthermore, Appendix A.3 shows that any symmetry group with a complex irreducible representation $\Gamma^{(c)}$ will also have its complex conjugate pair $\Gamma^{(c)*}$. Thus, the projection operator matrix in Equation 3.17 is "equivalent" to that in Equation A.29.

3.4 External Symmetry-Adapted Coordinate System

The example structure in Figure 3.1 has $\mathbf{C_{3v}}$ symmetry properties defined by the three irreducible matrix representations $\Gamma^{(\mu)}$, shown in Table 3.3. Hence, using these irreducible matrix representations and the projection operator matrix, the external vector space $\mathbb{V}_\mathbf{p}$ can be decomposed into four symmetry subspaces:

$$\mathbb{V}_\mathbf{p} = \left(\mathbb{V}_\mathbf{p}^{(A_1)}, \mathbb{V}_\mathbf{p}^{(A_2)}, \mathbb{V}_\mathbf{p}^{(E)1}, \mathbb{V}_\mathbf{p}^{(E)2}\right) \tag{3.18}$$

A vector basis for each of the symmetry subspaces $\mathbb{V}_\mathbf{p}^{(\mu)i}$ is given by the column space of the projection operator matrix:

$$\mathbf{O}_{ij}^{(\mu)} = \sum_P \Gamma_{ij}^{(\mu)} \mathbf{P} \tag{3.19}$$

Hence, to find a vector basis for the symmetry subspace $\mathbb{V}_\mathbf{p}^{(A_1)}$ that corresponds to the first irreducible representation $\Gamma^{(A_1)}$, the reducible representation $\mathbf{P}$ from Table 3.2 are used, and the first irreducible representation $\Gamma^{(A_1)}$ from Table 3.3 to give:

$$\begin{aligned}
\mathbf{O}_{11}^{(A_1)} &= \sum_P \Gamma_{11}^{(A_1)} \mathbf{P} \\
&= \left[1\times\mathbf{P}(E)+1\times\mathbf{P}(C_3)+1\times\mathbf{P}(C_3^2)+1\times\mathbf{P}(\sigma_a)+1\times\mathbf{P}(\sigma_b)+1\times\mathbf{P}(\sigma_c)\right] \\
&= \begin{bmatrix}
1/\sqrt{144} & -1/\sqrt{48} & -1/\sqrt{36} & 0 & 1/\sqrt{144} & 1/\sqrt{48} \\
-1/\sqrt{48} & 1/4 & 1/\sqrt{12} & 0 & -1/\sqrt{48} & -1/4 \\
-1/\sqrt{36} & 1/\sqrt{12} & 1/3 & 0 & -1/\sqrt{36} & -1/\sqrt{12} \\
0 & 0 & 0 & 0 & 0 & 0 \\
1/\sqrt{144} & -1/\sqrt{48} & -1/\sqrt{36} & 0 & 1/\sqrt{144} & 1/\sqrt{48} \\
1/\sqrt{48} & -1/4 & -1/\sqrt{12} & 0 & 1/\sqrt{48} & 1/4
\end{bmatrix}
\end{aligned} \tag{3.20}$$

A suitable vector basis $\mathbf{V_p}^{(A_1)}$ for the symmetry subspace $\mathbb{V}_\mathbf{p}^{(A_1)}$ can then be chosen:

$$\mathbf{V_p}^{(A_1)} = \text{column space of } \mathbf{O}_{11}^{(A_1)} = \begin{bmatrix} 1/\sqrt{12} \\ -1/2 \\ -1/\sqrt{3} \\ 0 \\ 1/\sqrt{12} \\ 1/2 \end{bmatrix} \tag{3.21}$$

A similar calculation is carried out to find a vector basis $\mathbf{V_p}^{(A_2)}$ for the symmetry subspace $\mathbb{V}_{\mathbf{p}}^{(A_2)}$:

$$\mathbf{V_p}^{(A_2)} = \begin{bmatrix} 1/2 \\ 1/\sqrt{12} \\ 0 \\ -1/\sqrt{3} \\ -1/2 \\ 1/\sqrt{12} \end{bmatrix} \tag{3.22}$$

To find a vector basis $\mathbf{V_p}^{(E)1}$ for the symmetry subspace $\mathbb{V}_{\mathbf{p}}^{(E)1}$, either of the two components of the first row of the third irreducible representation $\Gamma^{(E)}$ will give an identical vector basis:

$$\mathbf{V_p}^{(E)1} = \begin{bmatrix} \sqrt{5/12} & 0 \\ 1/\sqrt{20} & 1/\sqrt{5} \\ 1/\sqrt{15} & -\sqrt{3/5} \\ 0 & 0 \\ \sqrt{5/12} & 0 \\ -1/\sqrt{20} & -1/\sqrt{5} \end{bmatrix} \tag{3.23}$$

Similarly, a vector basis $\mathbf{V_p}^{(E)2}$ for the symmetry subspace $\mathbb{V}_{\mathbf{p}}^{(E)2}$ can be found by using either of the two components of the second row of the third irreducible representation $\Gamma^{(E)}$:

$$\mathbf{V_p}^{(E)2} = \begin{bmatrix} -1/\sqrt{20} & -1/\sqrt{5} \\ -\sqrt{3/20} & \sqrt{4/15} \\ 0 & 0 \\ -\sqrt{3/5} & -1/\sqrt{15} \\ 1/\sqrt{20} & 1/\sqrt{5} \\ -\sqrt{3/20} & \sqrt{4/15} \end{bmatrix} \tag{3.24}$$

These basis vectors define a new *symmetry-adapted coordinate system* for the 6-dimensional load and displacement vector space $\mathbb{V}_{\mathbf{p}}$. To transforms load and displacement vectors from the symmetry adapted coordinate system to the original Cartesian coordinate system shown in Figure 3.2, requires the orthonormal matrix $\mathbf{V_p}$, which has the above basis vectors written side by side:

$$\mathbf{V_p} = \left[\begin{array}{c|c|cc|cc} 1/\sqrt{12} & 1/2 & \sqrt{5/12} & 0 & -1/\sqrt{20} & -1/\sqrt{5} \\ -1/2 & 1/\sqrt{12} & 1/\sqrt{20} & 1/\sqrt{5} & -\sqrt{3/20} & \sqrt{4/15} \\ -1/\sqrt{3} & 0 & 1/\sqrt{15} & -\sqrt{3/5} & 0 & 0 \\ 0 & -1/\sqrt{3} & 0 & 0 & -\sqrt{3/5} & -1/\sqrt{15} \\ 1/\sqrt{12} & -1/2 & \sqrt{5/12} & 0 & 1/\sqrt{20} & 1/\sqrt{5} \\ 1/2 & 1/\sqrt{12} & -1/\sqrt{20} & -1/\sqrt{5} & -\sqrt{3/20} & \sqrt{4/15} \end{array}\right] \tag{3.25}$$

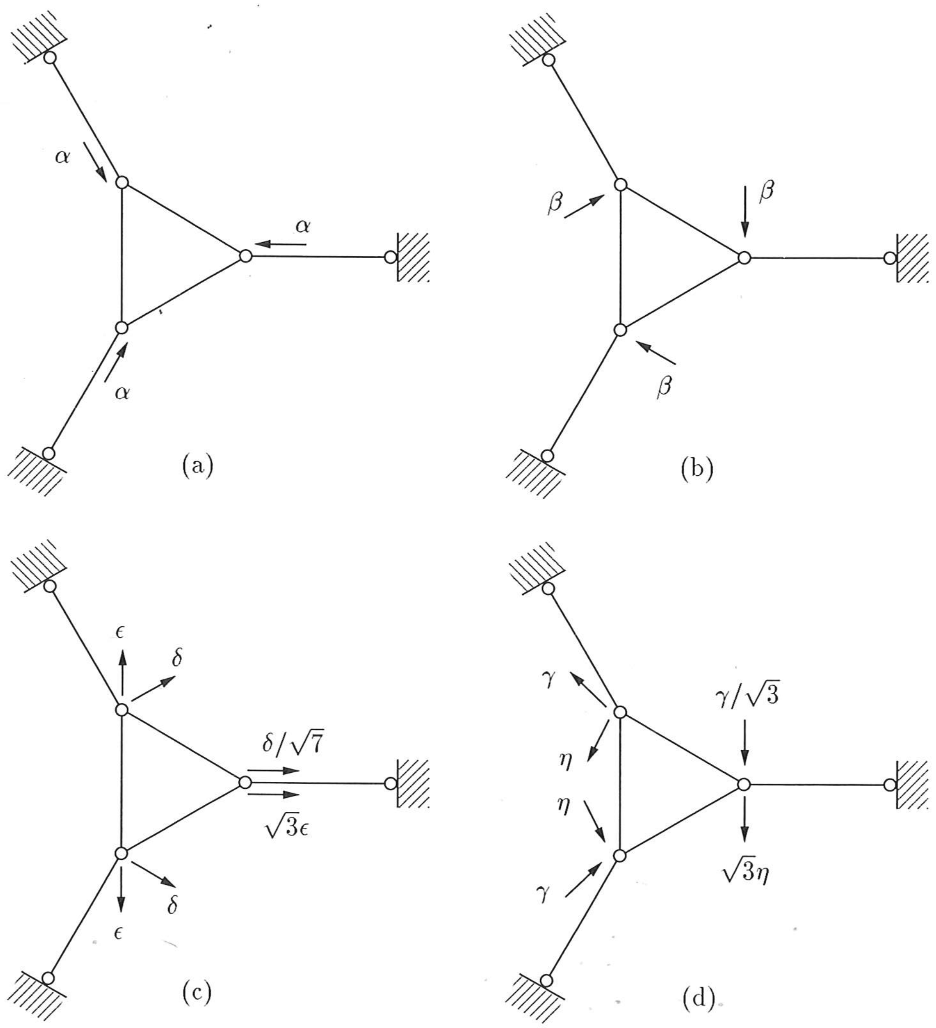

Figure 3.3: External load and displacement vector symmetry subspaces: (a) $\mathbb{V}_{\mathbf{P}}^{(A_1)}$; (b) $\mathbb{V}_{\mathbf{P}}^{(A_2)}$; (c) $\mathbb{V}_{\mathbf{P}}^{(E)1}$; (d) $\mathbb{V}_{\mathbf{P}}^{(E)2}$. $\alpha - \eta$ are arbitrary constants.

To understand these new basis vectors, it is best to look at them drawn out in Figure 3.3. Each of the symmetry subspaces corresponds to a particular type of symmetry. Any vector in the symmetry subspace $\mathbb{V}_{\mathbf{P}}^{(A_1)}$ is left unchanged by any symmetry operation of the symmetry group $\mathbf{C_{3v}}$, which explains why the irreducible representation $\Gamma^{(A_1)}$ is [1] for any symmetry operation. Any vector in the symmetry subspace $\mathbb{V}_{\mathbf{P}}^{(A_2)}$ is left unchanged by any rotation, but is reversed by any reflection, and so the irreducible representation $\Gamma^{(A_2)}$ is [1] for a rotation, but [-1] for a reflection. Any vector in $\mathbb{V}_{\mathbf{P}}^{(E)1}$ has only reflection symmetry in line a, while any vector in $\mathbb{V}_{\mathbf{P}}^{(E)2}$ has only reflection anti-symmetry in line a. It can be seen why $\Gamma^{(E)}$ is a 2-dimensional irreducible representation, as the effect of symmetry operations on these symmetry subspaces is more complex, with a coupling between the basis vectors.

It should be noted that, $\mathbb{V}_{\mathrm{p}}^{(E)1}$ and $\mathbb{V}_{\mathrm{p}}^{(E)2}$ contain vectors which are symmetric and anti-symmetric in line a because of the particular choice of vector basis that was made for the 2-dimensional irreducible representation $\Gamma^{(E)}$. A different choice would have given an equivalent $\Gamma^{(E)}$, and made vectors in $\mathbb{V}_{\mathrm{p}}^{(E)1}$ and $\mathbb{V}_{\mathrm{p}}^{(E)2}$ symmetric and anti-symmetric in another line.

3.5 Block-Diagonalised Stiffness Matrix

Using Group Theory to exploit the full symmetry of the example structure, it has been possible to decompose the load and displacement vector space $\mathbb{V}_{\mathrm{p}}$ into symmetry subspaces $\mathbb{V}_{\mathrm{p}}^{(\mu)i}$. Each of these symmetry subspaces corresponds to different symmetry properties of the example structure.

If the response of the example structure is linear, a load vector $\mathbf{p}$ from any of the symmetry subspaces $\mathbb{V}_{\mathrm{p}}^{(\mu)i}$ shown in Figure 3.3, will induce a displacement vector $\mathbf{d}$ from the same symmetry subspace. Hence, the stiffness matrix $\mathbf{K}$ will block-diagonalise into four submatrix blocks, each corresponding to a particular symmetry subspace $\mathbb{V}_{\mathrm{p}}^{(\mu)i}$.

The key to the block-diagonalisation is to define load and displacement vectors $\tilde{\mathbf{p}}$ and $\tilde{\mathbf{d}}$ in the symmetry-adapted vector basis $\mathbf{V}_{\mathrm{p}}$ given by Equation 3.25. These can be transformed into equivalent load and displacement vectors $\mathbf{p}$ and $\mathbf{d}$ in the original Cartesian vector basis shown in Figure 3.1, by the following transformations:

$$\mathbf{p} = \mathbf{V}_{\mathrm{p}}\tilde{\mathbf{p}} \tag{3.26}$$

$$\mathbf{d} = \mathbf{V}_{\mathrm{p}}\tilde{\mathbf{d}} \tag{3.27}$$

Substituting Equations 3.26 and 3.27 into the stiffness equation $\mathbf{Kd} = \mathbf{p}$ gives:

$$\mathbf{K}\mathbf{V}_{\mathrm{p}}\tilde{\mathbf{d}} = \mathbf{V}_{\mathrm{p}}\tilde{\mathbf{p}} \tag{3.28}$$

Multiplying both sides of Equation 3.28 by $\mathbf{V}_{\mathrm{p}}^{\mathbf{T}}$:

$$(\mathbf{V}_{\mathrm{p}}^{\mathbf{T}}\mathbf{K}\mathbf{V}_{\mathrm{p}})\tilde{\mathbf{d}} = \tilde{\mathbf{p}} \tag{3.29}$$

The block-diagonalised stiffness matrix $\tilde{\mathbf{K}}$ is therefore:

$$\tilde{\mathbf{K}} = (\mathbf{V}_{\mathrm{p}}^{\mathbf{T}}\mathbf{K}\mathbf{V}_{\mathrm{p}}) \tag{3.30}$$

and the symmetry-adapted stiffness equation is now:

$$\tilde{\mathbf{K}}\tilde{\mathbf{d}} = \tilde{\mathbf{p}} \tag{3.31}$$

The (6×6) stiffness matrix $\mathbf{K}$ for the example structure, written in the original Cartesian coordinate system, can be found using standard methods:

$$\mathbf{K} = \frac{EA}{l}\begin{bmatrix} 1 & -\sqrt{3}/2 & -3/4 & \sqrt{3}/4 & 0 & 0 \\ -\sqrt{3}/2 & 2 & \sqrt{3}/4 & -1/4 & 0 & -1 \\ -3/4 & \sqrt{3}/4 & 5/2 & 0 & -3/4 & -\sqrt{3}/4 \\ \sqrt{3}/4 & -1/4 & 0 & 1/2 & -\sqrt{3}/4 & -1/4 \\ 0 & 0 & -3/4 & -\sqrt{3}/4 & 1 & \sqrt{3}/2 \\ 0 & -1 & -\sqrt{3}/4 & -1/4 & \sqrt{3}/2 & 2 \end{bmatrix} \tag{3.32}$$

where E is Young's Modulus, A is the cross-sectional area and all bar-elements are of length l.

Hence substituting Equation 3.25 and Equation 3.32 into Equation 3.30, the block-diagonalised stiffness matrix $\tilde{\mathbf{K}}$ is:

$$\tilde{\mathbf{K}} = \frac{EA}{l}\left[\begin{array}{c|c|cc|cc} \boxed{4} & 0 & 0 & 0 & 0 & 0 \\ 0 & \boxed{0} & 0 & 0 & 0 & 0 \\ 0 & 0 & 0.4 & 0.3 & 0 & 0 \\ 0 & 0 & 0.3 & 2.1 & 0 & 0 \\ 0 & 0 & 0 & 0 & 0.4 & 0.3 \\ 0 & 0 & 0 & 0 & 0.3 & 2.1 \end{array}\right] \tag{3.33}$$

Equation 3.33 shows that the block-diagonalised stiffness matrix $\tilde{\mathbf{K}}$ consists of a number of independent stiffness blocks $\tilde{\mathbf{K}}^{(\mu)i}$ along the diagonal. Each of these blocks operates on the symmetry-adapted load and displacement vectors $\tilde{\mathbf{p}}^{(\mu)i}$ and $\tilde{\mathbf{d}}^{(\mu)i}$ that belong to the symmetry subspace $\mathbb{V}_{\mathrm{p}}^{(\mu)i}$. Each stiffness block $\tilde{\mathbf{K}}^{(\mu)i}$ can be solved separately to give the induced displacement vectors in equilibrium with the applied load vectors.

Hence, the full stiffness equation $\mathbf{Kd} = \mathbf{p}$, defined in the original Cartesian coordinate system of Figure 3.1, has been decomposed into four independent sub-equations which consider the relationship between load and displacement vectors that have a particular type of symmetry:

$$\tilde{\mathbf{K}}^{(\mu)i}\tilde{\mathbf{d}}^{(\mu)i} = \tilde{\mathbf{p}}^{(\mu)i} \tag{3.34}$$

The independent stiffness blocks in these four independent sub-equations can be calculated separately and are given by the following transformation:

$$\tilde{\mathbf{K}}^{(\mu)i} = \mathbf{V_p}^{(\mu)i\mathbf{T}}\mathbf{K}\mathbf{V_p}^{(\mu)i} \tag{3.35}$$

The independent stiffness blocks $\tilde{\mathbf{K}}^{(\mu)i}$ are given by a transformation to a symmetry-adapted coordinate system for the load and displacement vector space. This symmetry-adapted coordinate system is found using symmetry arguments alone, and hence Equations 3.30 and 3.35 are valid for any general symmetric structure.

3.6 The Fourier Method as a Special Case of the Group Representation Theory Method

In Chapter 2 a review was carried out on the analysis of rotationally periodic structures using the Fourier method. This section goes on to show that the Group Representation Theory method will give identical results if it uses the same polar coordinate system, and only the rotational symmetry properties of the structure.

Now the calculations done in Sections 3.2-3.4 using the Group Representation Theory method are repeated, but with only the rotational symmetry properties of the example structure, i.e. using the symmetry group $\mathbf{C_3}$ instead of $\mathbf{C_{3v}}$. By doing this it is possible to show that the Fourier Method described in Chapter 2, is actually a special case of the more general Group Representation Theory method.

The irreducible representations $\Gamma^{(\mu)}$ of symmetry group $\mathbf{C_3}$ are shown in Table 3.5, and include a complex conjugate pair of irreducible representations $\Gamma^{(c)}$ and $\Gamma^{(c)*}$. In Mulliken's notation (see Appendix A.3) this complex conjugate pair of irreducible representations are bracketed together and denoted $\Gamma^{(E)}$. It is important to note that the *complex conjugate* of the irreducible representations in Table 3.5 are identical to the columns of the Fourier matrix of Equation 2.4 for $n = 3$, and it is possible to show that this is true for any symmetry group $\mathbf{C_n}$ (although some reordering of the irreducible representations may be necessary).

$\mathbf{C_3}$		E	C_3	C_3^2
	$\Gamma^{(A)}$	1	1	1
$\Gamma^{(E)} = \{$	$\Gamma^{(c)}$	1	w	w^*
	$\Gamma^{(c)*}$	1	w^*	w

where: E is the identity operation
C_3 is a rotation by $2\pi/3$ about the origin O
$w = e^{i2\pi/3} = -1/2 + i\sqrt{3}/2$
$w^* = w^2 = e^{i4\pi/3} = \sqrt[3]{1}$

Table 3.5: Irreducible representations of symmetry group $\mathbf{C_3}$.

To use the Group Representation Theory method, it is now necessary to generate a matrix representation $\mathbf{P}$ using the polar coordinate system for the load and displacement vector space of Figure 2.3. This is done using the method described in Section 3.2 but with symmetry group $\mathbf{C_3}$. If a coordinate system has the same rotational symmetry as the structure, the matrix representation corresponding to each symmetry operation will be formed by block row permutations of the identity matrix. Because of the special form of these matrix representations, and also because the complex conjugates of the irreducible representations are identical to the columns of the Fourier matrix, it is easy to show that the column space of each projection operator $\mathbf{O}^{(\mu)}$ is identical to one of the independent subspaces given by the block form of the Fourier matrix.

For the example structure with a polar coordinate system shown in Figure 2.3, the matrix representation $\mathbf{P}$ of symmetry group $\mathbf{C_3}$ is shown in Table 3.6.

$$\mathbf{P}(E) = \begin{bmatrix} \mathbf{I} & \mathbf{0} & \mathbf{0} \\ \mathbf{0} & \mathbf{I} & \mathbf{0} \\ \mathbf{0} & \mathbf{0} & \mathbf{I} \end{bmatrix} \quad \mathbf{P}(C_3) = \begin{bmatrix} \mathbf{0} & \mathbf{0} & \mathbf{I} \\ \mathbf{I} & \mathbf{0} & \mathbf{0} \\ \mathbf{0} & \mathbf{I} & \mathbf{0} \end{bmatrix} \quad \mathbf{P}(C_3^2) = \begin{bmatrix} \mathbf{0} & \mathbf{I} & \mathbf{0} \\ \mathbf{0} & \mathbf{0} & \mathbf{I} \\ \mathbf{I} & \mathbf{0} & \mathbf{0} \end{bmatrix}$$

where : $\mathbf{I}$ is an identity matrix of size (2×2)
$\mathbf{0}$ is a zero matrix of size (2×2)

Table 3.6: Matrix representation $\mathbf{P}$ of symmetry group $\mathbf{C_3}$.

Using Equation 3.19, the projection operator matrix $\mathbf{O}^{(A)}$ corresponding to the first irreducible representation $\Gamma^{(A)}$ is:

$$\mathbf{O}^{(A)} = \begin{bmatrix} \mathbf{I} & \mathbf{I} & \mathbf{I} \\ \mathbf{I} & \mathbf{I} & \mathbf{I} \\ \mathbf{I} & \mathbf{I} & \mathbf{I} \end{bmatrix} \tag{3.36}$$

where $\mathbf{I}$ is a (2×2) identity matrix.
So a vector basis for the first invariant symmetry subspace $\mathbb{V}_{\mathbf{P}}^{(A)}$ is given by:

$$\mathbf{V_P}^{(A)} = \frac{1}{\sqrt{3}} \begin{bmatrix} 1 & 0 \\ 0 & -1 \\ 1 & 0 \\ 0 & -1 \\ 1 & 0 \\ 0 & -1 \end{bmatrix} \tag{3.37}$$

It can be seen that this is identical to the first block-column of the block Fourier matrix in Equation 2.6.

The first block-column (two columns) of $\mathbf{O}^{(A)}$ is formed by multiplying the complex conjugate of each term in the first irreducible representation $\Gamma^{(A)}$ given in Table 3.5, by a (2×2) identity matrix $\mathbf{I}$. Since the Fourier matrix is symmetric, this is identical to multiplying each component of the first column of a (3×3) Fourier matrix by a (2×2) identity matrix $\mathbf{I}$, and so Group Representation Theory is reproducing the first block-column of the block Fourier matrix. This can be seen more clearly for the projection operator matrix $\mathbf{O}^{(E)1}$ corresponding to the first irreducible representation $\Gamma^{(c)}$ with complex components:

$$\mathbf{O}^{(E)1} = \begin{bmatrix} \mathbf{I} & w^2\mathbf{I} & w\mathbf{I} \\ w\mathbf{I} & \mathbf{I} & w^2\mathbf{I} \\ w^2\mathbf{I} & w\mathbf{I} & \mathbf{I} \end{bmatrix} \tag{3.38}$$

A vector basis for the second invariant symmetry subspace $\mathbb{V}_{\mathbf{p}}^{(E)1}$ is given by:

$$\mathbf{V_p}^{(E)1} = \frac{1}{\sqrt{3}} \begin{bmatrix} 1 & 0 \\ 0 & -1 \\ -1/2 + i\sqrt{3}/2 & 0 \\ 0 & 1/2 - i\sqrt{3}/2 \\ -1/2 - i\sqrt{3}/2 & 0 \\ 0 & 1/2 + i\sqrt{3}/2 \end{bmatrix} \tag{3.39}$$

Similarly a vector basis can be found for the third invariant symmetry subspace $\mathbb{V}_{\mathbf{p}}^{(E)2}$, giving the final transformation matrix:

$$\mathbf{V_p} = \frac{1}{\sqrt{3}} \left[\begin{array}{cc|cc|cc} 1 & 0 & 1 & 0 & 1 & 0 \\ 0 & -1 & 0 & -1 & 0 & -1 \\ 1 & 0 & -1/2+i\sqrt{3}/2 & 0 & -1/2-i\sqrt{3}/2 & 0 \\ 0 & -1 & 0 & 1/2-i\sqrt{3}/2 & 0 & 1/2+i\sqrt{3}/2 \\ 1 & 0 & -1/2-i\sqrt{3}/2 & 0 & -1/2+i\sqrt{3}/2 & 0 \\ 0 & -1 & 0 & 1/2+i\sqrt{3}/2 & 0 & 1/2-i\sqrt{3}/2 \end{array}\right] \tag{3.40}$$

It is clear that this is identical to the block Fourier matrix shown in Equation 2.6 and hence will give the same block-diagonalised stiffness matrix $\tilde{\mathbf{K}}$ shown in Equation 2.9.

It is interesting to compare this result with that obtained in Section 3.5. There the stiffness matrix was decomposed into two (1×1) blocks, and two (2×2) blocks, all of which were real. Here the stiffness matrix has only been decomposed into three (2×2) blocks, two of which are complex.

Hence, Group Representation Theory reproduces the Fourier Method for this particular example; however the proof could easily be extended to any structure belonging to a symmetry group $\mathbf{C_n}$. Following the above method the transformation matrix will be:

$$\mathbf{V_p} = \frac{1}{\sqrt{n}} \begin{bmatrix} \mathbf{I} & \mathbf{I} & \mathbf{I} & \cdot & \mathbf{I} \\ \mathbf{I} & w\mathbf{I} & w^2\mathbf{I} & \cdot & w^{n-1}\mathbf{I} \\ \mathbf{I} & w^2\mathbf{I} & w^4\mathbf{I} & \cdot & w^{2(n-1)}\mathbf{I} \\ \cdot & \cdot & \cdot & \cdot & \cdot \\ \mathbf{I} & w^{n-1}\mathbf{I} & w^{2(n-1)}\mathbf{I} & \cdot & w^{(n-1)^2}\mathbf{I} \end{bmatrix} \tag{3.41}$$

This matrix is identical to the block Fourier matrix given in Equation 2.5.

3.7 Analysis of the Symmetry Sub-Structure

In Section 3.5 the global stiffness matrix $\mathbf{K}$ was first assembled in full and then decomposed into a block-diagonalised stiffness matrix $\tilde{\mathbf{K}}$ by a transformation of the original load and displacement vector coordinate system into a symmetry-adapted coordinate system. However, this approach is inefficient since the block-diagonalised stiffness matrix $\tilde{\mathbf{K}}$ can be calculated directly from the stiffness matrix $\mathbf{k}$ of a repeating sub-structure, using well known direct assembly techniques (see Healey & Treacy 1991).

As shown in Section 3.5, the stiffness blocks which make up the block-diagonalised stiffness matrix $\tilde{\mathbf{K}}$, are given by the following transformation:

$$\tilde{\mathbf{K}}^{(\mu)i} = \mathbf{V_p}^{(\mu)i\mathbf{T}}\mathbf{K}\mathbf{V_p}^{(\mu)i} \tag{3.42}$$

where $\mathbf{V_p}^{(\mu)i}$ is an orthogonal basis of the symmetry subspace corresponding to row i of the irreducible matrix representation $\Gamma^{(\mu)}$. This transformation requires the global stiffness matrix $\mathbf{K}$ to be assembled first. A much more efficient analysis can be carried out by noting that a structure with symmetry properties, by definition consists of a repeating *symmetry sub-structure*, i.e. a segment that generates the entire structure by repetitions of itself. In this section a sub-structuring technique is presented that utilises only rotational symmetry. Thus, the symmetry sub-structure must be repeated n times to generate the entire structure, where n is the degree of rotational symmetry of the structure. The elements of the repeating sub-structure must not overlap when generating the full structure.

In order to generate the stiffness matrix of the entire structure, it is necessary to calculate, for the n repetitions of the symmetry sub-structure, the n stiffness matrices $\mathbf{K}_1 \cdots \mathbf{K}_n$ in the required global coordinate system, such that the full stiffness matrix $\mathbf{K}$ is the sum of these matrices:

$$\mathbf{K} = \sum_{q=1}^{n} \mathbf{K}_q \tag{3.43}$$

Each matrix $\mathbf{K}_q$ can be generated from $\mathbf{k}$ by a coordinate transformation from the local to the global coordinate system, so that the load and displacement vectors $\mathbf{p}$ and $\mathbf{d}$ in the global system, are written in terms of vectors $\mathbf{p}'$ and $\mathbf{d}'$ in the local system:

$$\mathbf{p} = \mathbf{Q}_q^{\mathbf{T}}\mathbf{p}' \tag{3.44}$$

$$\mathbf{d} = \mathbf{Q}_q^{\mathbf{T}}\mathbf{d}' \tag{3.45}$$

The transformation matrix $\mathbf{Q}_q$ has two effects. It carries the local vector coordinates into their required global positions and also rotates the local vectors coordinates if necessary, i.e. when the local vectors coordinates are not coincident with the global coordinate system after a rotation of the symmetry sub-structure. Combining Equations 3.44 and 3.45 with the stiffness equation $\mathbf{kd}' = \mathbf{p}'$ for the symmetry sub-structure, gives:

$$\mathbf{K}_q = \mathbf{Q}_q^{\mathbf{T}}\mathbf{k}\mathbf{Q}_q \tag{3.46}$$

Substituting Equations 3.43 and 3.46 back into Equation 3.42 gives:

$$\tilde{\mathbf{K}}^{(\mu)i} = \sum_{q=1}^{n} \mathbf{V_p}^{(\mu)i\mathbf{T}} \mathbf{Q}_q^{\mathbf{T}} \mathbf{k} \mathbf{Q}_q \mathbf{V_p}^{(\mu)i} \tag{3.47}$$

The matrix $\mathbf{V}_{\mathbf{p}_q}{}^{(\mu)i} = \mathbf{Q}_q \mathbf{V_p}^{(\mu)i}$ describes the transformation of load and displacement vectors from the symmetry-adapted coordinate system of symmetry subspace $\mathbb{V}_{\mathbf{p}}^{(\mu)i}$ to the local coordinate system of the symmetry sub-structure. Using this notation, Equations 3.47 can then be written as:

$$\tilde{\mathbf{K}}^{(\mu)i} = \sum_{q=1}^{n} \mathbf{V}_{\mathbf{p}_q}{}^{(\mu)i\mathbf{T}} \mathbf{k} \mathbf{V}_{\mathbf{p}_q}{}^{(\mu)i} \tag{3.48}$$

Thus, the independent blocks of the block-diagonalised stiffness matrix can be calculated directly from the stiffness matrix $\mathbf{k}$ of a sub-structure, eliminating the need to assemble the full stiffness matrix.

Alternatively the full block-diagonalised stiffness matrix is given by:

$$\tilde{\mathbf{K}} = \sum_{q=1}^{n} \mathbf{V}_{\mathbf{p}_q}{}^{\mathbf{T}} \mathbf{k} \mathbf{V}_{\mathbf{p}_q} \tag{3.49}$$

where $\mathbf{V}_{\mathbf{p}_q} = \mathbf{Q}_q \mathbf{V_p}$ describes the transformation of load and displacement vectors from the symmetry-adapted coordinate system of the full space $\mathbb{V}_{\mathbf{p}}$ to the local coordinate system of the symmetry sub-structure.

Note that this sub-structure technique utilises only the rotational symmetry of structures. Further work is required to extend it to more general symmetry cases.

3.7.1 Example Sub-Structure Analysis

For the example structure shown in Figure 3.1, the two bar elements shown in Figure 3.4 can serve as the repeating symmetry sub-structure. If this sub-structure

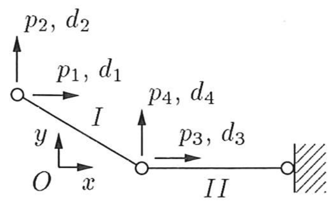

Figure 3.4: Repeating symmetry sub-structure, with a local Cartesian coordinate system for the load and displacement vectors.

is rotated by 120° anti-clockwise about the origin O, the positions of bar elements

III and IV are found. A further rotation will give the positions of bar elements V and VI and hence the full structure.

The stiffness matrix for the repeating symmetry sub-structure shown in Figure 3.4 is:

$$\mathbf{k} = \frac{EA}{l}\begin{bmatrix} 3/4 & -\sqrt{3}/4 & -3/4 & \sqrt{3}/4 \\ -\sqrt{3}/4 & 1/4 & \sqrt{3}/4 & -1/4 \\ -3/4 & \sqrt{3}/4 & 7/4 & -\sqrt{3}/4 \\ \sqrt{3}/4 & -1/4 & -\sqrt{3}/4 & 1/4 \end{bmatrix} \tag{3.50}$$

This matrix is defined using a local Cartesian coordinate system for the load and displacement vector space of the symmetry sub-structure, as shown in Figure 3.4. Transforming the local coordinate system of Figure 3.4 into the global coordinate system of Figure 3.2, requires the following transformation matrices:

$$\mathbf{Q}_1 = \begin{bmatrix} 1 & 0 & 0 & 0 & 0 & 0 \\ 0 & 1 & 0 & 0 & 0 & 0 \\ 0 & 0 & 1 & 0 & 0 & 0 \\ 0 & 0 & 0 & 1 & 0 & 0 \end{bmatrix} \tag{3.51}$$

$$\mathbf{Q}_2 = \begin{bmatrix} 0 & 0 & 0 & 0 & -1/2 & \sqrt{3}/2 \\ 0 & 0 & 0 & 0 & -\sqrt{3}/2 & -1/2 \\ -1/2 & \sqrt{3}/2 & 0 & 0 & 0 & 0 \\ -\sqrt{3}/2 & -1/2 & 0 & 0 & 0 & 0 \end{bmatrix} \tag{3.52}$$

$$\mathbf{Q}_3 = \begin{bmatrix} 0 & 0 & -1/2 & -\sqrt{3}/2 & 0 & 0 \\ 0 & 0 & \sqrt{3}/2 & -1/2 & 0 & 0 \\ 0 & 0 & 0 & 0 & -1/2 & -\sqrt{3}/2 \\ 0 & 0 & 0 & 0 & \sqrt{3}/2 & -1/2 \end{bmatrix} \tag{3.53}$$

Hence, consider generating the (2×2) stiffness block $\tilde{\mathbf{K}}^{(B)2}$:

$$\mathbf{V_{p1}}^{(B)2} = \mathbf{Q}_1\mathbf{V_p}^{(B)2} = \begin{bmatrix} -1/\sqrt{20} & -1/\sqrt{5} \\ -\sqrt{3/20} & \sqrt{4/15} \\ 0 & 0 \\ -\sqrt{3/5} & -1/\sqrt{15} \end{bmatrix} \tag{3.54}$$

$$\mathbf{V_{p2}}^{(B)2} = \mathbf{Q}_2\mathbf{V_p}^{(B)2} = \begin{bmatrix} -1/\sqrt{5} & 1/\sqrt{20} \\ 0 & -\sqrt{5/12} \\ -1/\sqrt{20} & \sqrt{9/20} \\ \sqrt{3/20} & 1/\sqrt{60} \end{bmatrix} \tag{3.55}$$

$$\mathbf{V_{p3}}^{(B)2} = \mathbf{Q}_3\mathbf{V_p}^{(B)2} = \begin{bmatrix} \sqrt{9/20} & 1/\sqrt{20} \\ \sqrt{3/20} & 1/\sqrt{60} \\ 1/\sqrt{20} & -\sqrt{9/20} \\ \sqrt{3/20} & 1/\sqrt{60} \end{bmatrix} \tag{3.56}$$

Then using Equation 3.48:

$$\tilde{\mathbf{K}}^{(B)2} = \sum_{q=1}^{3} \mathbf{V}_{\mathbf{p}_q}^{(B)2\mathbf{T}} \mathbf{k} \mathbf{V}_{\mathbf{p}_q}^{(B)2} \tag{3.57}$$

$$\begin{aligned} \tilde{\mathbf{K}}^{(B)2} &= \frac{EA}{l}\left(\begin{bmatrix} 0.15 & 0.3 \\ 0.3 & 0.6 \end{bmatrix} + \begin{bmatrix} 0.05 & -0.15 \\ -0.15 & 0.45 \end{bmatrix} + \begin{bmatrix} 0.2 & 0.15 \\ 0.15 & 1.05 \end{bmatrix} \right) \\ &= \frac{EA}{l} \begin{bmatrix} 0.4 & 0.3 \\ 0.3 & 2.1 \end{bmatrix} \end{aligned} \tag{3.58}$$

This stiffness block $\tilde{\mathbf{K}}^{(B)2}$ is identical to that calculated in Equation 3.33; however this calculation has only required the stiffness matrix $\mathbf{k}$ of the symmetry sub-structure to be assembled first. For this particular example, the computational saving generated by this method is small, as the symmetry sub-structure had a (4×4) stiffness matrix, while the full stiffness matrix was only (6×6). However, more significant savings could be obtained for structures with a greater degree of rotational symmetry.

The stiffness blocks $\tilde{\mathbf{K}}^{(\mu)i}$ corresponding to the remaining irreducible representations $\Gamma^{(\mu)i}$ of symmetry group $\mathbf{C_{3v}}$ can be calculated in a similar way, or alternatively Equation 3.49 can be used to calculate the full block-diagonalised stiffness matrix $\tilde{\mathbf{K}}$ directly.

Chapter 4

Symmetry Analysis of the Equilibrium Matrix

4.1 Introduction

In Chapter 2 a review was carried out of the authors who have applied Group Representation Theory to the analysis of symmetric structures. This review showed that this work has usually been based on the *Stiffness Method* of structural analysis, where these methods essentially provide a way to block-diagonalise a stiffness matrix into submatrix blocks. Chapter 3 then showed how this block-diagonalisation of the stiffness matrix not only simplifies the analysis but also provides submatrix blocks which have particular symmetry properties of the structure.

This chapter describes how Group Representation Theory can instead be applied to block-diagonalise an equilibrium matrix of a symmetric structure. The equilibrium matrix, which relates the internal stress resultants to the external forces applied to a structure, is commonly used in the *Force Method* of structural analysis (Livesley 1975), and is also extremely useful in identifying states of self-stress and mechanisms within a structure (Pellegrino & Calladine 1986). Block-diagonalising the equilibrium matrix into submatrix blocks, which relate internal and external forces with particular symmetry properties, can provide useful insight into the static and kinematic response of a structure. This chapter shows that with the use of Group Representation Theory, considerable simplifications can be made in an analysis of a symmetric structure, in particular helping to find and classify states of self-stress and mechanisms with particular symmetry properties, as well as reducing the computational effort required for a Force Method analysis.

The work described in this chapter builds on the mathematical foundations described by Bossavit (1993). Bossavit showed that Group Theory could be applied to equilibrium and compatibility relationships for symmetric structures. This chapter takes a quite different approach, and rather than proving the mathematical basis of the relationships used, emphasises the implications of symmetry for symmetric structures.

An important difference in terminology from Bossavit (1993) to note, is that Bossavit's compatibility matrix might be better described as an "incompatibility" matrix, whose row space corresponds to the left-nullspace of the compatibility matrix used in this chapter. The left-nullspace of the compatibility matrix used in this chapter gives all the incompatible internal deformations, i.e. all the internal deformations which are forbidden by the geometry of a structure. Hence, Bossavit's "incompatibility" matrix simply gives a measure of the incompatible internal deformations in a structure.

The layout of this chapter is as follows. Section 4.2 introduces the equilibrium, compatibility and flexibility relationships required for the analysis of structures using the Force Method. Then, using similar techniques to those introduced in Chapter 3 to find a symmetry-adapted coordinate system for the external load and displacement vector space, Section 4.4 describes how a symmetry-adapted coordinate system can be found for the internal bar-force and elongation vector space of the example structure shown in Figure 3.1.

In Section 4.3 the internal and external symmetry-adapted coordinate systems are used to block-diagonalise the equilibrium matrix of the example structure into submatrix blocks with particular symmetry properties. The analysis shows how the block-diagonalised the equilibrium matrix facilitates the identification of states of self-stress and mechanisms present in the structure. Section 4.5 then shows that an analysis of a symmetric structure using the Force Method is also considerably simplified with the use of symmetry-adapted coordinate systems.

Section 4.6 shows how similar sub-structure techniques to those introduced in Chapter 3 can be used to further simplify the analysis of the equilibrium matrix. Finally, Section 4.7 introduces a more interesting example, a tensegrity dome originally analysed by Pellegrino (1992). The equilibrium matrix of the tensegrity dome is block-diagonalised to simplify the identification of states of self-stress and mechanisms in the structure.

4.2 Equilibrium, Compatibility and Flexibility Matrices

Structural analysis requires three principles to be satisfied: that internal forces are in equilibrium with the applied load, that any internal deformation is compatible with external displacements, and that internal forces and displacements are related by a material law.

For small perturbations around an initial configuration of a structure, these relationships can be linearised as three matrix relationships:

The system of static equilibrium equations for a general structure is given by:

$$\mathbf{Hf} = \mathbf{p} \tag{4.1}$$

where: $\mathbf{H}$ is the equilibrium matrix.
$\mathbf{f}$ is the internal force vector.
$\mathbf{p}$ is the external load vector.

The system of kinematic compatibility equations is given by:

$$\mathbf{Cd} = \mathbf{e} \tag{4.2}$$

where: $\mathbf{C}$ is the compatibility matrix.
$\mathbf{d}$ is the external displacement vector.
$\mathbf{e}$ is the internal deformation vector.

The stress-strain relationship is given by:

$$\mathbf{Rf} = \mathbf{e} \tag{4.3}$$

where: $\mathbf{R}$ is the flexibility matrix.

Therefore the solution of a problem in structural analysis requires the simultaneous solutions of Equations 4.1, 4.2 and 4.3. Commonly, using the stiffness method of structural analysis, the internal forces are condensed out, and the three sets of equations are combined to form a single stiffness relationship. However, in the Force Method of structural analysis, all three equations are used explicitly.

It can easily be shown by a virtual work argument that $\mathbf{C} = \mathbf{H}^{\mathbf{T}}$ (McGuire & Gallagher 1979). Due to this static-kinematic duality, it is possible to analyse the equilibrium equation of a structure in order to identify both the states of self-stress present in a statically indeterminate structure and also the presence of inextensional mechanisms where rigid body motion is possible for all or part of a kinematically indeterminate structure (Pellegrino & Calladine 1986).

The above equations are equally suited to the static analysis of pin-jointed structures or more general structures. However, the following analysis is again restricted to the pin-jointed example structure of Chapter 3; this is to simplify the matrices involved in the calculations.

4.3 Block-Diagonal Form of the Equilibrium, Compatibility and Flexibility Matrices

Section 4.2 shows that coordinate systems are now required not only for the external load and displacement vectors, but also for the internal bar-force and elongation vectors.

In Chapter 3, symmetry arguments were used to show that load vectors with the symmetry properties of a particular symmetry subspace $\mathbb{V}_{\mathbf{p}}^{(\mu)i}$ would induce displacement vectors with the same symmetry properties, and hence from the same symmetry subspace $\mathbb{V}_{\mathbf{p}}^{(\mu)i}$. Although the induced bar-force and elongation vectors occupy a vector space $\mathbb{V}_{\mathbf{f}}$, which is different to that of the load and displacement vectors, namely $\mathbb{V}_{\mathbf{p}}$, these symmetry arguments can be extended to the analysis of the equilibrium matrix.

In a similar way to that described in Chapter 3 for the external load and displacement vector space, the internal bar-force and elongation vector space $\mathbb{V}_{\mathbf{f}}$ can also be decomposed into vector symmetry subspaces $\mathbb{V}_{\mathbf{f}}^{(\mu)i}$ with particular symmetry properties. However, the next section will show that the corresponding external and internal symmetry subspaces $\mathbb{V}_{\mathbf{p}}^{(\mu)i}$ and $\mathbb{V}_{\mathbf{f}}^{(\mu)i}$ have identical symmetry properties.

In a linear structural system, any induced bar-force and elongation vectors will have the same symmetry properties as the applied load vector. Hence, any load vector with the particular symmetry properties of symmetry subspace $\mathbb{V}_{\mathbf{p}}^{(\mu)i}$, will induce bar-force and elongation vectors from the corresponding symmetry subspace $\mathbb{V}_{\mathbf{f}}^{(\mu)i}$, which has the same symmetry properties. Therefore the equilibrium matrix $\mathbf{H}$ can be block-diagonalised into independent submatrix blocks, each operating on a pair of corresponding symmetry subspaces $\mathbb{V}_{\mathbf{p}}^{(\mu)i}$ and $\mathbb{V}_{\mathbf{f}}^{(\mu)i}$. The compatibility matrix $\mathbf{C}$ and flexibility matrix $\mathbf{R}$ can also be block-diagonalised in a similar way.

The key to the block-diagonalisation is to define the load vectors $\tilde{\mathbf{p}}$ in the symmetry-adapted vector basis $\mathbf{V}_{\mathbf{p}}$, and the bar-force vectors $\tilde{\mathbf{f}}$ in the symmetry-adapted vector basis $\mathbf{V}_{\mathbf{f}}$. These can be transformed into equivalent load and bar-force vectors $\mathbf{p}$ and $\mathbf{f}$ in the original coordinate systems, by the following transformations:

$$\mathbf{p} = \mathbf{V}_{\mathbf{p}}\tilde{\mathbf{p}} \tag{4.4}$$

$$\mathbf{f} = \mathbf{V}_{\mathbf{f}}\tilde{\mathbf{f}} \tag{4.5}$$

Substituting Equations 4.4 and 4.5 into the equilibrium equation $\mathbf{Hf} = \mathbf{p}$:

$$\mathbf{H}\mathbf{V}_{\mathbf{f}}\tilde{\mathbf{f}} = \mathbf{V}_{\mathbf{p}}\tilde{\mathbf{p}} \tag{4.6}$$

Multiplying both sides of Equation 4.3 by $\mathbf{V}_{\mathbf{p}}^{\mathbf{T}}$:

$$(\mathbf{V}_{\mathbf{p}}^{\mathbf{T}}\mathbf{H}\mathbf{V}_{\mathbf{f}})\tilde{\mathbf{f}} = \tilde{\mathbf{p}} \tag{4.7}$$

The block-diagonalised equilibrium matrix is therefore:

$$\tilde{\mathbf{H}} = (\mathbf{V}_\mathbf{p}^\mathbf{T}\mathbf{H}\mathbf{V}_\mathbf{f}) \tag{4.8}$$

and the symmetry-adapted equilibrium equation is now:

$$\tilde{\mathbf{H}}\tilde{\mathbf{f}} = \tilde{\mathbf{p}} \tag{4.9}$$

In a similar way, the block-diagonalised compatibility and flexibility matrices are given by:

$$\tilde{\mathbf{C}} = (\mathbf{V}_\mathbf{f}^\mathbf{T}\mathbf{C}\mathbf{V}_\mathbf{p}) \tag{4.10}$$

$$\tilde{\mathbf{R}} = (\mathbf{V}_\mathbf{f}^\mathbf{T}\mathbf{R}\mathbf{V}_\mathbf{f}) \tag{4.11}$$

Note that it is straightforward to show that $\tilde{\mathbf{C}} = \tilde{\mathbf{H}}^\mathbf{T}$.

4.4 Pin-jointed Structure with C_{3v} Symmetry

The 2-dimensional pin-jointed structure shown in Figure 3.1, which was analysed in the previous chapter to show how symmetry can be used to block-diagonalise the stiffness matrix, will now be used to carry out a similar analysis on the equilibrium matrix and will again be referred to as the "example structure".

Using the methods introduced in Chapter 3 to find an external symmetry-adapted coordinate system for the load and displacement vector space $\mathbb{V}_\mathbf{p}$, this section describes how Group Representation Theory can also be used to find an internal symmetry-adapted coordinate system for the bar-force and elongation vector space, which is denoted by the symbol $\mathbb{V}_\mathbf{f}$.

In Chapter 3 an external coordinate system for the load vectors $\mathbf{p}$ and the displacement vectors $\mathbf{d}$, was attached to the example structure and is shown in Figure 3.2. Using this external coordinate system, a load and displacement vector matrix representation $\mathbf{P}$ or $\mathbf{D}$, was found which represents the effects of the symmetry operations on the load and displacement vectors, and is shown in Table 3.2.

In a less obvious way, an internal coordinate system can be defined for both the bar-force and elongation vectors. A "natural" coordinate system is shown in Figure 4.1, where the force and elongation in each of the bar-elements define respectively, components of the bar-force vector $\mathbf{f}$ and components of the elongation vector $\mathbf{e}$. Vectors with only a unit component f_1-f_6 or e_1-e_6 will form a vector basis for this 6-dimensional internal bar-force and elongation vector space $\mathbb{V}_\mathbf{f}$.

The vector space $\mathbb{V}_\mathbf{f}$ can also be split into symmetry subspaces. Consider how the action of the symmetry operations on the example structure can be represented as a matrix operation acting on a bar-force vector shown in Figure 4.1. Under each

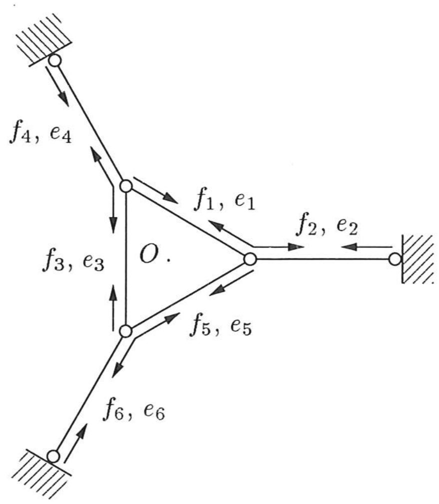

Figure 4.1: A natural coordinate system for the internal bar-force and elongation vector space $\mathbb{V}_{\mathbf{f}}$.

symmetry operation the bar-force vectors will simply transform amongst themselves, for example, following a rotation by 240° about the origin O, the force now in bar 1, f_1' will be the force that was formerly in bar 3, f_3, specifically:

$$f_1' = f_3 \tag{4.12}$$

Similar expressions can be written for every other vector component to define the matrix operation $\mathbf{F}(C_3^2)$:

$$\mathbf{F}(C_3^2) = \begin{bmatrix} 0 & 0 & 1 & 0 & 0 & 0 \\ 0 & 0 & 0 & 1 & 0 & 0 \\ 0 & 0 & 0 & 0 & 1 & 0 \\ 0 & 0 & 0 & 0 & 0 & 1 \\ 1 & 0 & 0 & 0 & 0 & 0 \\ 0 & 1 & 0 & 0 & 0 & 0 \end{bmatrix} \tag{4.13}$$

The complete set of matrices representing the effect of the symmetry operations on either the bar-force vectors $\mathbf{f}$ or the elongation vectors $\mathbf{e}$, in the natural coordinate system of Figure 4.1, are shown in Table 4.1. These matrices form a reducible matrix representation $\mathbf{F}$ or $\mathbf{E}$, of the symmetry group $\mathbf{C_{3v}}$.

4.4.1 Internal Symmetry-Adapted Coordinate System

In order to block-diagonalise the equilibrium matrix, symmetry-adapted coordinate systems are required for both the internal and external vector spaces. In Chapter 3 a symmetry-adapted coordinate system for the external load and

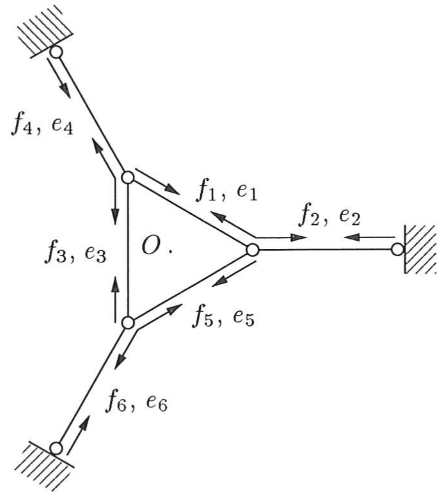

Figure 4.1: A natural coordinate system for the internal bar-force and elongation vector space $\mathbb{V}_{\mathbf{f}}$.

symmetry operation the bar-force vectors will simply transform amongst themselves, for example, following a rotation by 240° about the origin O, the force now in bar 1, f_1' will be the force that was formerly in bar 3, f_3, specifically:

$$f_1' = f_3 \tag{4.12}$$

Similar expressions can be written for every other vector component to define the matrix operation $\mathbf{F}(C_3^2)$:

$$\mathbf{F}(C_3^2) = \begin{bmatrix} 0 & 0 & 1 & 0 & 0 & 0 \\ 0 & 0 & 0 & 1 & 0 & 0 \\ 0 & 0 & 0 & 0 & 1 & 0 \\ 0 & 0 & 0 & 0 & 0 & 1 \\ 1 & 0 & 0 & 0 & 0 & 0 \\ 0 & 1 & 0 & 0 & 0 & 0 \end{bmatrix} \tag{4.13}$$

The complete set of matrices representing the effect of the symmetry operations on either the bar-force vectors $\mathbf{f}$ or the elongation vectors $\mathbf{e}$, in the natural coordinate system of Figure 4.1, are shown in Table 4.1. These matrices form a reducible matrix representation $\mathbf{F}$ or $\mathbf{E}$, of the symmetry group $\mathbf{C_{3v}}$.

4.4.1 Internal Symmetry-Adapted Coordinate System

In order to block-diagonalise the equilibrium matrix, symmetry-adapted coordinate systems are required for both the internal and external vector spaces. In Chapter 3 a symmetry-adapted coordinate system for the external load and

$$\mathbf{F}(E)=\mathbf{E}(E)=\begin{bmatrix} 1&0&0&0&0&0\\ 0&1&0&0&0&0\\ 0&0&1&0&0&0\\ 0&0&0&1&0&0\\ 0&0&0&0&1&0\\ 0&0&0&0&0&1 \end{bmatrix} \qquad \mathbf{F}(\sigma_a)=\mathbf{E}(\sigma_a)=\begin{bmatrix} 0&0&0&0&1&0\\ 0&1&0&0&0&0\\ 0&0&1&0&0&0\\ 0&0&0&0&0&1\\ 1&0&0&0&0&0\\ 0&0&0&1&0&0 \end{bmatrix}$$

$$\mathbf{F}(C_3)=\mathbf{E}(C_3)=\begin{bmatrix} 0&0&0&0&1&0\\ 0&0&0&0&0&1\\ 1&0&0&0&0&0\\ 0&1&0&0&0&0\\ 0&0&1&0&0&0\\ 0&0&0&1&0&0 \end{bmatrix} \qquad \mathbf{F}(\sigma_b)=\mathbf{E}(\sigma_b)=\begin{bmatrix} 0&0&1&0&0&0\\ 0&0&0&0&0&1\\ 1&0&0&0&0&0\\ 0&0&0&1&0&0\\ 0&0&0&0&1&0\\ 0&1&0&0&0&0 \end{bmatrix}$$

$$\mathbf{F}(C_3^2)=\mathbf{E}(C_3^2)=\begin{bmatrix} 0&0&1&0&0&0\\ 0&0&0&1&0&0\\ 0&0&0&0&1&0\\ 0&0&0&0&0&1\\ 1&0&0&0&0&0\\ 0&1&0&0&0&0 \end{bmatrix} \qquad \mathbf{F}(\sigma_c)=\mathbf{E}(\sigma_c)=\begin{bmatrix} 1&0&0&0&0&0\\ 0&0&0&1&0&0\\ 0&0&0&0&1&0\\ 0&1&0&0&0&0\\ 0&0&1&0&0&0\\ 0&0&0&0&0&1 \end{bmatrix}$$

Table 4.1: Bar-force and elongation vector matrix representation $\mathbf{F}$ and $\mathbf{E}$, of symmetry group $\mathbf{C_{3v}}$.

displacement vector space $\mathbb{V}_{\mathbf{p}}$, was found for the example structure. The external vector symmetry subspaces $\mathbb{V}_{\mathbf{p}}^{(\mu)i}$ are shown in Figure 3.3.

The internal symmetry-adapted coordinate system required for the bar-force and elongation vector space $\mathbb{V}_{\mathbf{f}}$, is also made up of vector symmetry subspaces $\mathbb{V}_{\mathbf{f}}^{(\mu)i}$, each with particular symmetry properties corresponding to those of the external vector symmetry subspaces. To find these internal vector symmetry subspaces, the Great Orthogonality Theorem and projection operator matrix are required, the relevant theory for both is described in Chapter 3 and Appendix A. In this section, only the calculations required to find the internal vector symmetry subspaces for the example structure in Figure 4.1 are shown.

Since the internal coordinate system of example structure also has $\mathbf{C_{3v}}$ symmetry, its symmetry properties are defined by three irreducible matrix representations shown in Table 3.3. Hence, the internal vector space $\mathbb{V}_{\mathbf{f}}$ is split into four symmetry subspaces; the first two correspond to the two 1-dimensional irreducible matrix representations $\Gamma^{(A_1)}$ and $\Gamma^{(A_2)}$, and the second two correspond to the two rows of the 2-dimensional irreducible matrix representation $\Gamma^{(E)}$:

$$\mathbb{V}_{\mathbf{f}} = \left(\mathbb{V}_{\mathbf{f}}^{(A_1)}, \mathbb{V}_{\mathbf{f}}^{(A_2)}, \mathbb{V}_{\mathbf{f}}^{(E)1}, \mathbb{V}_{\mathbf{f}}^{(E)2}\right) \tag{4.14}$$

A vector basis for each of the symmetry subspaces $\mathbb{V}_{\mathbf{f}}^{(\mu)i}$ is given by the column space of the projection operator matrix:

$$\mathbf{O}_{ij}^{(\mu)} = \sum_{F} \mathbf{F}\Gamma_{i,j}^{(\mu)} \tag{4.15}$$

where the irreducible matrix representations of the symmetry group $\mathbf{C_{3v}}$ are given in Table 3.3 and the summation is over the matrix representation $\mathbf{F}$ given in Table 4.1. For example, the symmetry subspace $\mathbb{V}_{\mathbf{f}}^{(A_1)}$ is given by the column space of:

$$\begin{aligned}
\mathbf{O}_{11}^{(A_1)} &= \sum_{F} \Gamma_{1,1}^{(A_1)}\mathbf{F} \\
&= \left[(1\times\mathbf{F}_E)+(1\times\mathbf{F}_{C_3})+(1\times\mathbf{F}_{C_3^2})+(1\times\mathbf{F}_{\sigma_a})+(1\times\mathbf{F}_{\sigma_b})+(1\times\mathbf{F}_{\sigma_c})\right] \\
&= \begin{bmatrix} 1/\sqrt{3} & 0 & 1/\sqrt{3} & 0 & 1/\sqrt{3} & 0 \\ 0 & 1/\sqrt{3} & 0 & 1/\sqrt{3} & 0 & 1/\sqrt{3} \\ 1/\sqrt{3} & 0 & 1/\sqrt{3} & 0 & 1/\sqrt{3} & 0 \\ 0 & 1/\sqrt{3} & 0 & 1/\sqrt{3} & 0 & 1/\sqrt{3} \\ 1/\sqrt{3} & 0 & 1/\sqrt{3} & 0 & 1/\sqrt{3} & 0 \\ 0 & 1/\sqrt{3} & 0 & 1/\sqrt{3} & 0 & 1/\sqrt{3} \end{bmatrix}
\end{aligned} \tag{4.16}$$

A suitable vector basis $\mathbf{V}_{\mathbf{f}}^{(A_1)}$ for the symmetry subspace $\mathbb{V}_{\mathbf{f}}^{(A_1)}$, can then be chosen:

$$\mathbf{V}_{\mathbf{f}}^{(A_1)} = \text{column space of } \mathbf{O}_{11}^{(A_1)} = \begin{bmatrix} 1/\sqrt{3} & 0 \\ 0 & 1/\sqrt{3} \\ 1/\sqrt{3} & 0 \\ 0 & 1/\sqrt{3} \\ 1/\sqrt{3} & 0 \\ 0 & 1/\sqrt{3} \end{bmatrix} \tag{4.17}$$

A similar calculation is carried out to find the vector basis for the symmetry subspace $\mathbb{V}_{\mathbf{f}}^{(A_2)}$:

$$\begin{aligned}
\mathbf{O}_{11}^{(A_2)} &= \sum_{F} \Gamma_{1,1}^{(A_2)}\mathbf{F} \\
&= \left[(1\times\mathbf{F}_E)+(1\times\mathbf{F}_{C_3})+(1\times\mathbf{F}_{C_3^2})+(-1\times\mathbf{F}_{\sigma_a})+(-1\times\mathbf{F}_{\sigma_b})+(-1\times\mathbf{F}_{\sigma_c})\right] \\
&= \begin{bmatrix} 0 & 0 & 0 & 0 & 0 & 0 \\ 0 & 0 & 0 & 0 & 0 & 0 \\ 0 & 0 & 0 & 0 & 0 & 0 \\ 0 & 0 & 0 & 0 & 0 & 0 \\ 0 & 0 & 0 & 0 & 0 & 0 \\ 0 & 0 & 0 & 0 & 0 & 0 \end{bmatrix}
\end{aligned} \tag{4.18}$$

The symmetry subspace $\mathbb{V}_{\mathbf{f}}^{(A_2)}$ is given by the column space of $\mathbf{O}_{11}^{(A_2)}$ and hence is a zero space, the significance of which will be explained later.

The vector bases for the two remaining symmetry subspaces $\mathbb{V}_{\mathbf{f}}^{(E)1}$ and $\mathbb{V}_{\mathbf{f}}^{(E)2}$ are found in a similar way and are shown below:

$$\mathbf{V}_{\mathbf{f}}^{(E)1} = \begin{bmatrix} 0 & 1/\sqrt{6} \\ \sqrt{2/3} & 0 \\ 0 & -\sqrt{2/3} \\ -1/\sqrt{6} & 0 \\ 0 & 1/\sqrt{6} \\ -1/\sqrt{6} & 0 \end{bmatrix} \tag{4.19}$$

$$\mathbf{V}_{\mathbf{f}}^{(E)2} = \begin{bmatrix} 0 & -1/\sqrt{2} \\ 0 & 0 \\ 0 & 0 \\ -1/\sqrt{2} & 0 \\ 0 & 1/\sqrt{2} \\ 1/\sqrt{2} & 0 \end{bmatrix} \tag{4.20}$$

Hence a new symmetry-adapted basis for the bar-force and elongation vector space $\mathbb{V}_{\mathbf{f}}$ is:

$$\mathbf{V}_{\mathbf{f}} = \left[\begin{array}{cc|cc|cc} 1/\sqrt{3} & 0 & 0 & 1/\sqrt{6} & 0 & -1/\sqrt{2} \\ 0 & 1/\sqrt{3} & \sqrt{2/3} & 0 & 0 & 0 \\ 1/\sqrt{3} & 0 & 0 & -\sqrt{2/3} & 0 & 0 \\ 0 & 1/\sqrt{3} & -1/\sqrt{6} & 0 & -1/\sqrt{2} & 0 \\ 1/\sqrt{3} & 0 & 0 & 1/\sqrt{6} & 0 & 1/\sqrt{2} \\ 0 & 1/\sqrt{3} & -1/\sqrt{6} & 0 & 1/\sqrt{2} & 0 \end{array}\right] \tag{4.21}$$

The basis vectors of the four symmetry subspaces $\mathbb{V}_{\mathbf{f}}^{(\mu)i}$ are shown in Figure 4.2. It is clear that the symmetry properties of each bar-force and elongation vector symmetry subspace $\mathbb{V}_{\mathbf{f}}^{(\mu)i}$ are identical to the corresponding load and displacement vector symmetry subspace $\mathbb{V}_{\mathbf{p}}^{(\mu)i}$, described in Section 3.4.

Of interest is the second symmetry subspace $\mathbb{V}_{\mathbf{f}}^{(A_2)}$, which is a zero space. That is, there are no bar-force or elongation vectors which have only the rotational symmetry of the example structure. In this case any bar-force or elongation vector left unchanged by the rotation operations, will also be left unchanged by the reflection operations and hence belong to the first symmetry subspace $\mathbb{V}_{\mathbf{f}}^{(A_1)}$.

Thus, it is clear that although the corresponding symmetry subspaces $\mathbb{V}_{\mathbf{p}}^{(\mu)i}$ and $\mathbb{V}_{\mathbf{f}}^{(\mu)i}$ have identical symmetry properties, the corresponding vector bases may well have different dimensions.

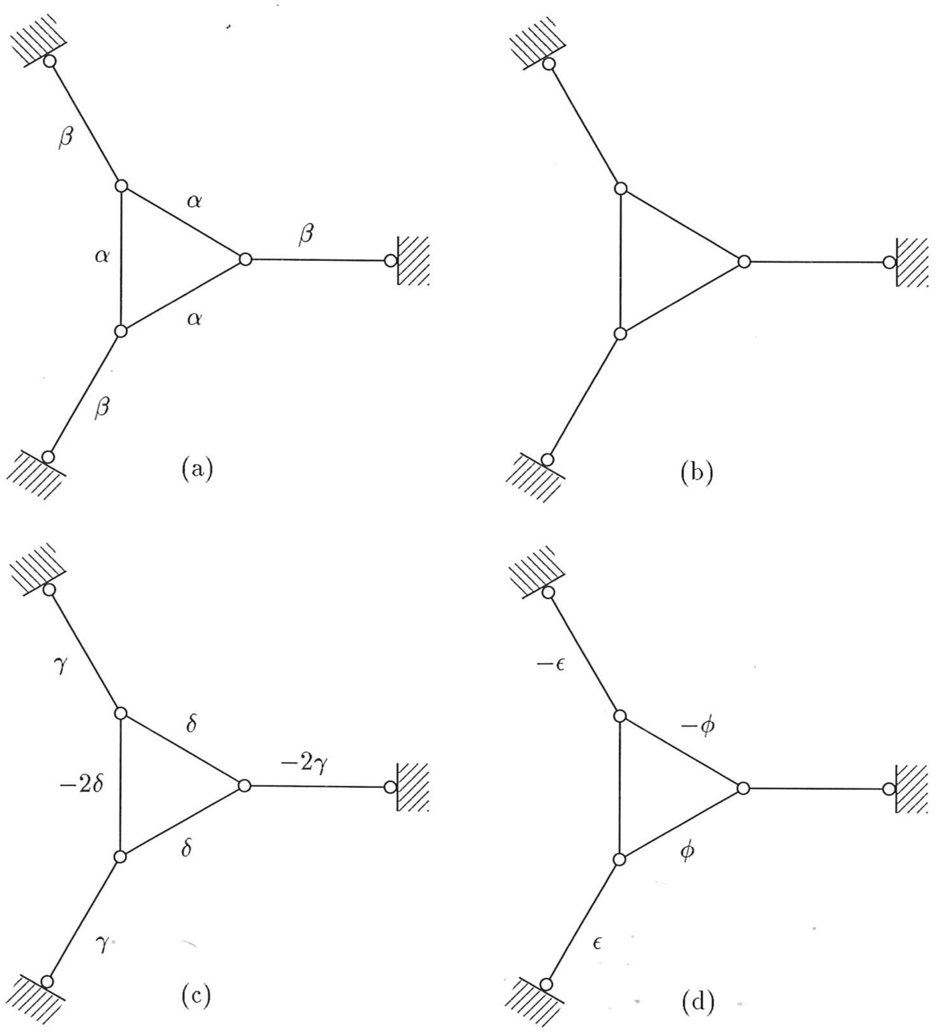

Figure 4.2: Internal bar-force and elongation vector symmetry subspaces: (a) $\mathbb{V}_{\mathbf{f}}^{(A_1)}$; (b) $\mathbb{V}_{\mathbf{f}}^{(A_2)}$; (c) $\mathbb{V}_{\mathbf{f}}^{(E)1}$; (d) $\mathbb{V}_{\mathbf{f}}^{(E)2}$. α-ϕ are arbitrary constants.

4.4.2 Block-Diagonalised Equilibrium Matrix

Using Group Representation Theory to exploit the full symmetry of the example structure, it has been possible to find symmetry-adapted coordinate systems for both the external and internal vector spaces $\mathbb{V}_{\mathbf{p}}$ and $\mathbb{V}_{\mathbf{f}}$. In these symmetry-adapted coordinate systems the external and internal vector spaces are decomposed into vector symmetry subspaces $\mathbb{V}_{\mathbf{p}}^{(\mu)i}$ and $\mathbb{V}_{\mathbf{f}}^{(\mu)i}$, and it has been shown that the corresponding internal and external symmetry subspaces have identical symmetry properties. Hence, it is now possible to show how these external and internal symmetry-adapted coordinate systems can be used to block-diagonalise the equilibrium matrix.

For the example structure shown in Figure 3.1, the (6×6) equilibrium matrix $\mathbf{H}$, written in the original load and bar-force vector coordinate systems, is given by:

$$\mathbf{H} = \begin{bmatrix} -\sqrt{3}/2 & 0 & 0 & 1/2 & 0 & 0 \\ 1/2 & 0 & 1 & -\sqrt{3}/2 & 0 & 0 \\ \sqrt{3}/2 & -1 & 0 & 0 & \sqrt{3}/2 & 0 \\ -1/2 & 0 & 0 & 0 & 1/2 & 0 \\ 0 & 0 & 0 & 0 & -\sqrt{3}/2 & 1/2 \\ 0 & 0 & -1 & 0 & -1/2 & \sqrt{3}/2 \end{bmatrix} \tag{4.22}$$

Hence, substituting Equations 3.25, 4.22 and 4.21 into Equation 4.8, gives the block-diagonalised equilibrium matrix $\tilde{\mathbf{H}}$:

$$\tilde{\mathbf{H}} = \begin{bmatrix} -\sqrt{3} & 1 & 0 & 0 & 0 & 0 \\ 0 & 0 & 0 & 0 & 0 & 0 \\ 0 & 0 & -1/\sqrt{10} & -\sqrt{3/10} & 0 & 0 \\ 0 & 0 & \sqrt{9/10} & -\sqrt{6/5} & 0 & 0 \\ 0 & 0 & 0 & 0 & -1/\sqrt{10} & -\sqrt{3/10} \\ 0 & 0 & 0 & 0 & \sqrt{9/10} & -\sqrt{6/5} \end{bmatrix} \tag{4.23}$$

Equation 4.23 shows that the block-diagonalised equilibrium matrix $\tilde{\mathbf{H}}$ consists of a number of independent submatrix blocks $\tilde{\mathbf{H}}^{(\mu)i}$ along the diagonal:

$$\tilde{\mathbf{H}} = \begin{bmatrix} \tilde{\mathbf{H}}^{(A_1)} & & & \\ & \tilde{\mathbf{H}}^{(A_2)} & & \\ & & \tilde{\mathbf{H}}^{(E)1} & \\ & & & \tilde{\mathbf{H}}^{(E)2} \end{bmatrix} \tag{4.24}$$

Each of the equilibrium submatrix blocks $\tilde{\mathbf{H}}^{(\mu)i}$ operates on symmetry-adapted load and bar-force vectors $\tilde{\mathbf{p}}^{(\mu)i}$ and $\tilde{\mathbf{f}}^{(\mu)i}$ in the corresponding symmetry subspaces $\mathbb{V}_{\mathbf{p}}^{(\mu)i}$ and $\mathbb{V}_{\mathbf{f}}^{(\mu)i}$. Each submatrix block $\tilde{\mathbf{H}}^{(\mu)i}$ can be solved separately to give the induced bar-force vectors in equilibrium with the applied load vectors. The original full problem $\mathbf{Hf} = \mathbf{p}$ defined by the original coordinate systems of Figure 3.2 and Figure 4.1, has been decomposed into four independent subproblems defined by:

$$\tilde{\mathbf{H}}^{(\mu)i}\tilde{\mathbf{f}}^{(\mu)i} = \tilde{\mathbf{p}}^{(\mu)i} \tag{4.25}$$

where each of the subproblems considers the relationship between load and bar-force vectors that have a particular type of symmetry. Similar subproblems can be written for the compatibility and flexibility relationships.

Note that, in contrast to the block-diagonalised stiffness matrix $\tilde{\mathbf{K}}$ in Chapter 3, the equilibrium submatrix blocks $\tilde{\mathbf{H}}^{(\mu)i}$ are, in general, not square. Indeed, Equation 4.23 relies on a definition of an *empty* matrix which may have rows but no columns, or alternatively columns but no rows. In this example, the submatrix block $\tilde{\mathbf{H}}^{(A_2)}$ has no columns, since the symmetry subspace $\mathbb{V}_{\mathbf{f}}^{(A_2)}$ is empty, but has one row since the symmetry subspace $\mathbb{V}_{\mathbf{p}}^{(A_2)}$ is 1-dimensional. As will be seen, this definition fits in well with the further discussion of equilibrium submatrix blocks $\tilde{\mathbf{H}}^{(\mu)i}$ in the remainder of this dissertation.

The only other description of an empty matrix known to the author is in the user manual for the MATLAB program (The MathWorks, Inc. 1996) and the definition given above is compatible to this. Indeed, the user manual states "MATLAB 5 provides for matrices where one but not all, of the dimensions is zero. The basic model for empty matrices is that any operation that is defined for $(m \times n)$ matrices, and that produces a result whose dimension is some function of m and n, should still be allowed when m or n is zero".

The block-diagonalised compatibility and flexibility matrices can also be found in a similar way. However, Equation 4.10 shows that the block-diagonalised compatibility matrix $\tilde{\mathbf{C}}$ is simply the transpose of the block-diagonalised equilibrium matrix $\tilde{\mathbf{H}}$ given in Equation 4.23:

$$\tilde{\mathbf{C}} = \tilde{\mathbf{H}}^{\mathrm{T}} = \begin{bmatrix} -\sqrt{3} & 0 & 0 & 0 & 0 & 0 \\ 1 & 0 & 0 & 0 & 0 & 0 \\ 0 & 0 & -1/\sqrt{10} & -\sqrt{3/10} & 0 & 0 \\ 0 & 0 & \sqrt{9/10} & -\sqrt{6/5} & 0 & 0 \\ 0 & 0 & 0 & 0 & -1/\sqrt{10} & -\sqrt{3/10} \\ 0 & 0 & 0 & 0 & \sqrt{9/10} & -\sqrt{6/5} \end{bmatrix} \tag{4.26}$$

The flexibility matrix $\mathbf{R}$ defined in the original internal coordinate system of Figure 4.1 is:

$$\mathbf{R} = \frac{l}{EA} \begin{bmatrix} 1 & 0 & 0 & 0 & 0 & 0 \\ 0 & 1 & 0 & 0 & 0 & 0 \\ 0 & 0 & 1 & 0 & 0 & 0 \\ 0 & 0 & 0 & 1 & 0 & 0 \\ 0 & 0 & 0 & 0 & 1 & 0 \\ 0 & 0 & 0 & 0 & 0 & 1 \end{bmatrix} \tag{4.27}$$

Notice that the flexibility matrix is necessarily in a fully diagonalised form, since the bar-forces and elongations were originally defined to occupy an identical internal coordinate system. It follows that the transformation to a symmetry-adapted internal coordinate system given by Equation 4.11 will result in a block-diagonalised flexibility matrix $\tilde{\mathbf{R}}$ which is identical to the original flexibility matrix $\mathbf{R}$ in Equation 4.27, but has the following block form:

$$\tilde{\mathbf{R}} = \frac{l}{EA}\begin{bmatrix} \boxed{\begin{matrix}\tilde{\mathbf{R}}^{(A_1)} \\ (2\times 2)\end{matrix}} & & \\ & \boxed{\begin{matrix}\tilde{\mathbf{R}}^{(E)1} \\ (2\times 2)\end{matrix}} & \\ & & \boxed{\begin{matrix}\tilde{\mathbf{R}}^{(E)2} \\ (2\times 2)\end{matrix}} \end{bmatrix} \tag{4.28}$$

The previous section showed that $\mathbb{V}_{\mathbf{f}}^{(A_2)}$ is an empty internal vector symmetry subspace, hence $\tilde{\mathbf{R}}^{(A_2)}$ is a (0×0) flexibility block and does not appear in Equation 4.28.

4.4.3 Analysis of the Block-Diagonalised Equilibrium Matrix

Using the symmetry of a structure to block-diagonalise the equilibrium matrix provides some useful results, and in particular shows how a block-diagonalised equilibrium matrix simplifies finding and classifying the states of self-stress and mechanisms in a structure.

In general, an equilibrium matrix $\mathbf{H}$ is an $(m\times n)$ matrix of rank r. From the equilibrium matrix $\mathbf{H}$ it is possible to find the states of self-stress and the inextensional mechanisms of a structure (Pellegrino & Calladine 1986).

A statically indeterminate structure will have $(m-r)$ state of self-stress. States of self-stress exist when there are bar-force vectors $\mathbf{f}$ in equilibrium with zero load vectors $\mathbf{p}$, i.e. the states of self-stress are all bar-force vectors $\mathbf{f}$ which satisfy the following equation:

$$\mathbf{Hf} = \mathbf{0} \tag{4.29}$$

Hence, any states of self-stress present in a structure are given by the nullspace of $\mathbf{H}$.

A kinematically indeterminate structure will have $(n-r)$ inextensional mechanisms. Inextensional mechanisms exist when there are displacement vectors $\mathbf{d}$ that are compatible with zero bar-elongations, i.e. the inextensional mechanisms are all displacement vectors $\mathbf{d}$ which satisfy the following equation:

$$\mathbf{Cd} = \mathbf{0} \tag{4.30}$$

Hence any inextensional mechanisms present in a structure are given by the nullspace of $\mathbf{C}$ (which corresponds to the left-nullspace of $\mathbf{H} = \mathbf{C}^{\mathbf{T}}$).

In Section 4.3, the load and bar-force vectors $\mathbf{p}$ and $\mathbf{f}$ are transformed into equivalent vectors $\tilde{\mathbf{p}}$ and $\tilde{\mathbf{f}}$ defined by the symmetry-adapted vector bases $\mathbf{V_p}$ and $\mathbf{V_f}$ respectively and hence, the equilibrium matrix $\mathbf{H}$ is block-diagonalised into a number of equilibrium submatrix blocks $\tilde{\mathbf{H}}^{(\mu)i}$ which are also $(m \times n)$ matrices of rank r. Hence, the above analysis for states of self-stress and inextensional mechanisms in the equilibrium matrix $\mathbf{H}$ is simply carried over to these independent equilibrium submatrix blocks $\tilde{\mathbf{H}}^{(\mu)i}$.

The four equilibrium submatrix blocks $\tilde{\mathbf{H}}^{(\mu)i}$ defined in Equation 4.23 for the example structure in Figure 3.1, are now examined.

State of Self-Stress in Equilibrium Block $\tilde{\mathbf{H}}^{(A_1)}$

$$\tilde{\mathbf{H}}^{(A_1)} = \begin{bmatrix} -1.7321 & 1 \end{bmatrix}$$

The (1×2) equilibrium submatrix $\tilde{\mathbf{H}}^{(A_1)}$, corresponding to the first irreducible matrix representation $\Gamma^{(A_1)}$, is of rank 1, and hence will have a state of self-stress present in the corresponding bar-force vector symmetry subspace $\mathbb{V}_{\mathbf{f}}^{(A_1)}$. The state of self-stress is a bar-force vector $\tilde{\mathbf{f}}_{\mathbf{s}}^{(A_1)}$, in equilibrium with zero load vectors:

$$\tilde{\mathbf{H}}^{(A_1)}\tilde{\mathbf{f}}_{\mathbf{s}}^{(A_1)} = \mathbf{0} \tag{4.31}$$

and is given by the nullspace of $\tilde{\mathbf{H}}^{(A_1)}$:

$$\tilde{\mathbf{f}}_{\mathbf{s}}^{(A_1)} = \begin{bmatrix} -1/2 \\ -\sqrt{3}/2 \end{bmatrix} \tag{4.32}$$

This can be transformed back to the original coordinate system:

$$\mathbf{f}_{\mathbf{s}}^{(A_1)} = \mathbf{V}_{\mathbf{f}}^{(A_1)}\tilde{\mathbf{f}}_{\mathbf{s}}^{(A_1)} \tag{4.33}$$

where $\mathbf{V}_{\mathbf{f}}^{(A_1)}$ is the bar-force vector basis for the symmetry subspace $\mathbb{V}_{\mathbf{f}}^{(A_1)}$, defined in Equation 4.17.

$$\mathbf{f}_{\mathbf{s}}^{(A_1)} = \begin{bmatrix} 1/\sqrt{3} & 0 \\ 0 & 1/\sqrt{3} \\ 1/\sqrt{3} & 0 \\ 0 & 1/\sqrt{3} \\ 1/\sqrt{3} & 0 \\ 0 & 1/\sqrt{3} \end{bmatrix} \begin{bmatrix} -1/2 \\ -\sqrt{3}/2 \end{bmatrix} = \begin{bmatrix} -1/\sqrt{12} \\ -1/2 \\ -1/\sqrt{12} \\ -1/2 \\ -1/\sqrt{12} \\ -1/2 \end{bmatrix} \tag{4.34}$$

This state of self-stress is shown in Figure 4.3. The state of self-stress has the full $\mathbf{C_{3v}}$ symmetry of the example structure, i.e. 3-fold rotation symmetry about the origin O and reflection symmetry in lines a, b and c. This must obviously be the case as it originates from the symmetry subspace which corresponds to these properties.

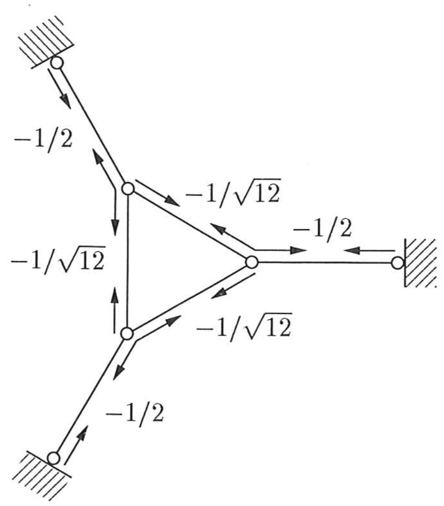

Figure 4.3: State of self-stress in the bar-force symmetry subspace $\mathbb{V}_{\mathbf{f}}^{(A_1)}$.

Mechanism in Equilibrium Block $\tilde{\mathbf{H}}^{(A_2)}$

The (1×0) equilibrium submatrix $\tilde{\mathbf{H}}^{(A_2)}$, corresponding to the second irreducible matrix representation $\Gamma^{(A_2)}$, is of rank 0, and hence there will be a load vector in the corresponding load vector symmetry subspace $\mathbb{V}_{\mathbf{p}}^{(A_2)}$ which cannot be equilibrated. The mechanism is a displacement vector $\tilde{\mathbf{d}}_{\mathbf{m}}^{(A_2)}$, which is compatible with zero bar-elongations. However, since the bar-force vector symmetry subspace $\mathbb{V}_{\mathbf{f}}^{(A_2)}$ is an empty space, any displacement vector $\tilde{\mathbf{d}}^{(A_2)}$ must be a mechanism. This mechanism is given by the symmetry subspace $\mathbb{V}_{\mathbf{p}}^{(A_2)}$ and a vector basis $\mathbf{V}_{\mathbf{p}}^{(A_2)}$ in the original Cartesian coordinate system is given by Equation 3.22:

$$\mathbf{d}_{\mathbf{m}}^{(A_2)} = \begin{bmatrix} 1/2 \\ 1/\sqrt{12} \\ 0 \\ -1/\sqrt{3} \\ -1/2 \\ 1/\sqrt{12} \end{bmatrix} \tag{4.35}$$

This mechanism is shown in Figure 4.4. The mechanism has $\mathbf{C}_3$ symmetry, i.e. only the 3-fold rotation symmetry about the origin O, and no reflection symmetry.

In general, any $(m \times 0)$ empty equilibrium submatrix $\tilde{\mathbf{H}}^{(\mu)i}$, which expresses an equilibrium relationship between an m-dimensional load vector symmetry subspace and a corresponding zero-dimensional bar-force vector symmetry subspace, implies the existence of a set of m load vectors which cannot induce any bar-force vectors in the structure. Hence these m load vectors correspond to m independent inextensional mechanisms, which have the symmetry properties of the corresponding load vector symmetry subspace $\mathbb{V}_{\mathbf{p}}^{(\mu)i}$.

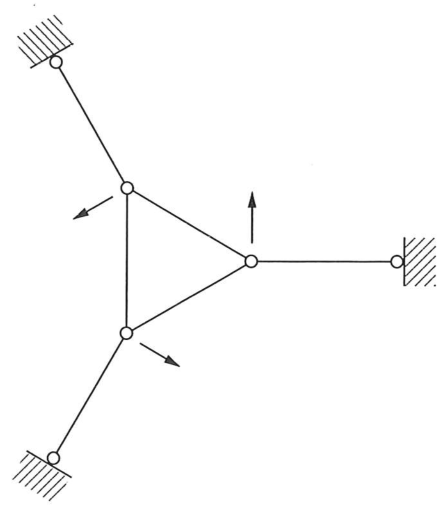

Figure 4.4: Mechanism in the displacement symmetry subspace $\mathbb{V}_{\mathbf{p}}^{(A_2)}$.

Similarly, any $(0 \times n)$ empty equilibrium submatrix $\tilde{\mathbf{H}}^{(\mu)i}$, which expresses an equilibrium relationship between a zero-dimensional load vector symmetry subspace and a corresponding n-dimensional bar-force vector symmetry subspace, implies the existence of a set of n bar-force vectors which are in equilibrium with zero applied load vectors. Hence these n bar-force vectors are n independent states of self-stress, which have the symmetry properties of the corresponding bar-force vector symmetry subspace $\mathbb{V}_{\mathbf{f}}^{(\mu)i}$.

Equilibrium Blocks $\tilde{\mathbf{H}}^{(E)1}$ and $\tilde{\mathbf{H}}^{(E)2}$

The third and fourth (2×2) equilibrium submatrices $\tilde{\mathbf{H}}^{(E)1}$ and $\tilde{\mathbf{H}}^{(E)2}$, corresponding to the third irreducible matrix representation $\Gamma^{(E)}$, are both of full rank and hence do not contain any further states of self-stress or inextensional mechanisms.

4.5 Simplification of the Force Method

This section shows how the analysis of any structure using the Force Method can now be reduced to the analysis of the independent equilibrium, compatibility and flexibility submatrix blocks, $\tilde{\mathbf{H}}^{(\mu)i}$, $\tilde{\mathbf{C}}^{(\mu)i}$ and $\tilde{\mathbf{R}}^{(\mu)i}$ respectively.

The Force Method can be used to give a complete linear analysis of the example structure, finding the bar-forces, elongations and displacements resulting from an applied loading. For a block-diagonalised equilibrium matrix $\tilde{\mathbf{H}}$, the analysis can be carried out on the independent equilibrium submatrix blocks $\tilde{\mathbf{H}}^{(\mu)i}$.

As an example, consider the example structure subject to the following loading using the original Cartesian coordinate system shown in Figure 3.2:

$$\mathbf{p}^{(A_1)} = \begin{bmatrix} 1/\sqrt{12} \\ -1/2 \\ -1/\sqrt{3} \\ 0 \\ 1/\sqrt{12} \\ 1/2 \end{bmatrix} \tag{4.36}$$

which can be transformed into:

$$\tilde{\mathbf{p}}^{(A_1)} = 1 \tag{4.37}$$

where $\tilde{\mathbf{p}}^{(A_1)}$ is a load vector described by the symmetry-adapted vector basis $\mathbf{V}_{\mathbf{p}}^{(\mathbf{A_1})}$ of the first symmetry subspace $\mathbb{V}_{\mathbf{p}}^{(A_1)}$. What is the induced bar-force vector $\tilde{\mathbf{f}}^{(A_1)}$?

In Section 4.4.3 it was shown that the first equilibrium submatrix $\tilde{\mathbf{H}}^{(A_1)}$ contains a state of self-stress, and hence the induced bar-force vector $\tilde{\mathbf{f}}^{(A_1)}$ is given by:

$$\tilde{\mathbf{f}}^{(A_1)} = \tilde{\mathbf{f}}_{\mathbf{o}}^{(A_1)} + \tilde{\mathbf{f}}_{\mathbf{s}}^{(A_1)} x \tag{4.38}$$

where: $\tilde{\mathbf{f}}_{\mathbf{o}}^{(A_1)}$ is the bar-force vector in equilibrium with the applied load vector.
$\tilde{\mathbf{f}}_{\mathbf{s}}^{(A_1)}$ is the state of self-stress.
x is the unknown magnitude of the state of self-stress.

The state of self-stress $\tilde{\mathbf{f}}_{\mathbf{s}}^{(A_1)}$ was found in Section 4.4.3. The bar-force vector $\tilde{\mathbf{f}}_{\mathbf{o}}^{(A_1)}$ is a particular solution of the equilibrium equation:

$$\tilde{\mathbf{H}}^{(A_1)}\tilde{\mathbf{f}}_{\mathbf{o}}^{(A_1)} = \tilde{\mathbf{p}}^{(A_1)} \tag{4.39}$$

for which a possible choice is:

$$\tilde{\mathbf{f}}_{\mathbf{o}}^{(A_1)} = \begin{bmatrix} 0 \\ 1 \end{bmatrix} \tag{4.40}$$

To find the magnitude of the state of self-stress x, the following equation ensures that compatibility is satisfied (Livesley 1975):

$$\tilde{\mathbf{f}}_{\mathbf{s}}^{(A_1)\mathbf{T}}\tilde{\mathbf{R}}^{(A_1)}\tilde{\mathbf{f}}_{\mathbf{s}}^{(A_1)} x = -\tilde{\mathbf{f}}_{\mathbf{s}}^{(A_1)\mathbf{T}}\tilde{\mathbf{R}}^{(A_1)}\tilde{\mathbf{f}}_{\mathbf{o}}^{(A_1)} \tag{4.41}$$

where $\tilde{\mathbf{R}}^{(A_1)}$ is the flexibility submatrix block for symmetry subspace $\mathbb{V}_{\mathbf{f}}^{(A_1)}$, given by:

$$\tilde{\mathbf{R}}^{(A_1)} = \mathbf{V_f}^{(A_1)\mathbf{T}}\mathbf{R}\mathbf{V_f}^{(A_1)} \tag{4.42}$$

The flexibility matrix $\mathbf{R}$ for the original internal vector space $\mathbb{V}_{\mathbf{f}}$ is given by Equation 4.27, and Equation 4.28 shows that $\tilde{\mathbf{R}}^{(A_1)}$ is simply:

$$\tilde{\mathbf{R}}^{(A_1)} = \frac{l}{EA}\begin{bmatrix} 1 & 0 \\ 0 & 1 \end{bmatrix} \tag{4.43}$$

Hence, solving Equation 4.41, the magnitude of the state of self-stress is:

$$x = \sqrt{3}/2 \tag{4.44}$$

Substituting Equations 4.32, 4.40 and 4.44 into Equation 4.38, the induced bar-force vector $\tilde{\mathbf{f}}^{(A_1)}$ due to the applied load is:

$$\tilde{\mathbf{f}}^{(A_1)} = \begin{bmatrix} 0 \\ 1 \end{bmatrix} + \begin{bmatrix} -1/2 \\ -\sqrt{3}/2 \end{bmatrix} \sqrt{3}/2 = \begin{bmatrix} -\sqrt{3/16} \\ 1/4 \end{bmatrix} \tag{4.45}$$

The induced bar-force vector $\mathbf{f}^{(A_1)}$ in the original bar-force coordinate system of Figure 4.1 is:

$$\mathbf{f}^{(A_1)} = \mathbf{V_f}^{(A_1)} \tilde{\mathbf{f}}^{(A_1)} \tag{4.46}$$

$$\mathbf{f}^{(A_1)} = \begin{bmatrix} 1/\sqrt{3} & 0 \\ 0 & 1/\sqrt{3} \\ 1/\sqrt{3} & 0 \\ 0 & 1/\sqrt{3} \\ 1/\sqrt{3} & 0 \\ 0 & 1/\sqrt{3} \end{bmatrix} \begin{bmatrix} -\sqrt{3/16} \\ 1/4 \end{bmatrix} = \begin{bmatrix} -1/4 \\ 1/\sqrt{48} \\ -1/4 \\ 1/\sqrt{48} \\ -1/4 \\ 1/\sqrt{48} \end{bmatrix} \tag{4.47}$$

The induced bar-elongation vector $\tilde{\mathbf{e}}^{(A_1)}$ can now be found using the stress-strain relationship of Equation 4.3:

$$\tilde{\mathbf{e}}^{(A_1)} = \tilde{\mathbf{R}}^{(A_1)} \tilde{\mathbf{f}}^{(A_1)} \tag{4.48}$$

$$\tilde{\mathbf{e}}^{(A_1)} = \frac{l}{EA} \begin{bmatrix} 1 & 0 \\ 0 & 1 \end{bmatrix} \begin{bmatrix} -\sqrt{3/16} \\ 1/4 \end{bmatrix} = \frac{l}{EA} \begin{bmatrix} -\sqrt{3/16} \\ 1/4 \end{bmatrix} \tag{4.49}$$

The induced bar-elongation vector $\mathbf{e}^{(A_1)}$ in the original bar-elongation coordinate system of Figure 4.1 is:

$$\mathbf{e}^{(A_1)} = \mathbf{V_f}^{(A_1)} \tilde{\mathbf{e}}^{(A_1)} \tag{4.50}$$

$$\mathbf{e}^{(A_1)} = \begin{bmatrix} 1/\sqrt{3} & 0 \\ 0 & 1/\sqrt{3} \\ 1/\sqrt{3} & 0 \\ 0 & 1/\sqrt{3} \\ 1/\sqrt{3} & 0 \\ 0 & 1/\sqrt{3} \end{bmatrix} \frac{l}{EA} \begin{bmatrix} -\sqrt{3/16} \\ 1/4 \end{bmatrix} = \frac{l}{EA} \begin{bmatrix} -1/4 \\ 1/\sqrt{48} \\ -1/4 \\ 1/\sqrt{48} \\ -1/4 \\ 1/\sqrt{48} \end{bmatrix} \tag{4.51}$$

The induced displacement vector $\tilde{\mathbf{d}}^{(A_1)}$ is given by the kinematic compatibility relationship of Equation 4.2:

$$\tilde{\mathbf{C}}^{(A_1)} \tilde{\mathbf{d}}^{(A_1)} = \tilde{\mathbf{H}}^{(A_1)\mathbf{T}} \tilde{\mathbf{d}}^{(A_1)} = \tilde{\mathbf{e}}^{(A_1)} \tag{4.52}$$

for which the solution is:

$$\tilde{\mathbf{d}}^{(A_1)} = \frac{l}{4EA} \tag{4.53}$$

The induced displacement vector $\mathbf{d}^{(A_1)}$ in the original coordinate system of Figure 3.2 is:

$$\mathbf{d}^{(A_1)} = \mathbf{V}_{\mathrm{p}}^{(A_1)}\tilde{\mathbf{d}}^{(A_1)} \tag{4.54}$$

$$\mathbf{d}^{(A_1)} = \begin{bmatrix} 1/\sqrt{12} \\ -1/2 \\ -1/\sqrt{3} \\ 0 \\ 1/\sqrt{12} \\ 1/2 \end{bmatrix} \frac{l}{4EA} = \frac{l}{EA} \begin{bmatrix} 1/\sqrt{192} \\ -1/8 \\ -1/\sqrt{48} \\ 0 \\ 1/\sqrt{192} \\ 1/8 \end{bmatrix} \tag{4.55}$$

Equation 4.55 gives the displacement vector $\mathbf{d}^{(A_1)}$ compatible with the bar-elongation vector $\mathbf{e}^{(A_1)}$, which is induced by the load vector $\mathbf{p}^{(A_1)}$. However a general solution displacement vector $\mathbf{d}$ may include some displacement component $\mathbf{d}_{\mathrm{m}}^{(A_2)}$ of unknown magnitude y from the second symmetry subspace $\mathbb{V}_{\mathrm{p}}^{(A_2)}$, and therefore the general solution displacement vector $\mathbf{d}$ is given by:

$$\mathbf{d} = \mathbf{d}^{(A_1)} + y\mathbf{d}_{\mathrm{m}}^{(A_2)} \tag{4.56}$$

where: $\mathbf{d}^{(A_1)}$ is the displacement vector compatible with the bar-elongation vector.
$\mathbf{d}_{\mathrm{m}}^{(A_2)}$ is the inextensional mechanism.
y is the unknown magnitude of the inextensional mechanism.

4.6 Analysis of the Symmetry Sub-Structure

In a similar way to that shown in Section 3.7 for the stiffness matrix, the block-diagonalised equilibrium matrix $\tilde{\mathbf{H}}$ can be calculated directly from the equilibrium matrix $\mathbf{h}$ of the repeating symmetry sub-structure.

Equation 4.24, shows that each of the equilibrium blocks which make up the block-diagonalised equilibrium matrix $\tilde{\mathbf{H}}$, are given by the following transformation:

$$\tilde{\mathbf{H}}^{(\mu)i} = \mathbf{V_p}^{(\mu)i\mathbf{T}}\mathbf{H}\mathbf{V_f}^{(\mu)i} \tag{4.57}$$

where $\mathbf{V_p}^{(\mu)i}$ and $\mathbf{V_f}^{(\mu)i}$ are orthogonal vector bases of the external and internal symmetry subspaces corresponding to row i of the irreducible matrix representation $\Gamma^{(\mu)}$. This transformation requires the global equilibrium matrix $\mathbf{H}$ to be assembled first. However, a more efficient analysis can be carried out which only requires the equilibrium matrix $\mathbf{h}$ of the repeating sub-structure.

For the n repetitions of the symmetry sub-structure that are required to make up the entire structure, it is necessary to calculate the corresponding n equilibrium matrices $\mathbf{H}_1 \cdots \mathbf{H}_n$ in the required global external and internal coordinate systems. Then the full equilibrium matrix $\mathbf{H}$ is given by the sum of these matrices:

$$\mathbf{H} = \sum_{q=1}^{n} \mathbf{H}_q \tag{4.58}$$

In Section 3.7 transformation matrices $\mathbf{Q}_q$ were introduced which carried the external load and displacement basis vectors $\mathbf{p}'$ and $\mathbf{d}'$ from the local external coordinate system of the sub-structure, to their positions $\mathbf{p}$ and $\mathbf{d}$ in the required global external coordinate system. Similar transformation matrices $\mathbf{S}_q$ can be found which carry bar-force and elongation vectors $\mathbf{f}'$ and $\mathbf{e}'$ from the local internal coordinate system of the sub-structure, to their positions $\mathbf{f}$ and $\mathbf{e}$ in the required global internal coordinate system:

$$\mathbf{f} = \mathbf{S}_q^{\mathbf{T}} \mathbf{f}' \tag{4.59}$$

$$\mathbf{e} = \mathbf{S}_q^{\mathbf{T}} \mathbf{e}' \tag{4.60}$$

Hence, each matrix $\mathbf{H}_q$ can be generated from $\mathbf{h}$ by a coordinate transformation from the local to the global coordinate system, for both the external load and internal bar-force basis vector. Combining Equations 3.44 and 4.59 with the equilibrium equation $\mathbf{h}\mathbf{f}' = \mathbf{p}'$ for the symmetry sub-structure, gives:

$$\mathbf{H}_q = \mathbf{Q}_q^{\mathbf{T}} \mathbf{h} \mathbf{S}_q \tag{4.61}$$

Substituting Equations 4.58 and 4.61 back into Equation 4.57 gives:

$$\tilde{\mathbf{H}}^{(\mu)i} = \sum_{q=1}^{n} \mathbf{V_p}^{(\mu)i\mathbf{T}} \mathbf{Q}_q^{\mathbf{T}} \mathbf{h} \mathbf{S}_q \mathbf{V_f}^{(\mu)i} \tag{4.62}$$

The matrices $\mathbf{V}_{\mathbf{p}_q}{}^{(\mu)i} = \mathbf{Q}_q \mathbf{V_p}^{(\mu)i}$ and $\mathbf{V}_{\mathbf{f}_q}{}^{(\mu)i} = \mathbf{S}_q \mathbf{V_f}^{(\mu)i}$ describe the transformation of load and bar-force vectors from the external and internal symmetry spaces $\mathbb{V}_{\mathbf{p}}^{(\mu)i}$ and $\mathbb{V}_{\mathbf{f}}^{(\mu)i}$ to the symmetry subspace $\mathbb{V}_{\mathbf{p}q}^{(\mu)i}$ and $\mathbb{V}_{\mathbf{f}q}^{(\mu)i}$, corresponding to symmetry sub-structure q. Using this notation, Equations 4.62 can then be written as:

$$\tilde{\mathbf{H}}^{(\mu)i} = \sum_{q=1}^{n} \mathbf{V}_{\mathbf{p}_q}{}^{(\mu)i\mathbf{T}} \mathbf{h} \mathbf{V}_{\mathbf{f}_q}{}^{(\mu)i} \tag{4.63}$$

Thus, the independent blocks of the block-diagonalised equilibrium matrix can be calculated directly from the equilibrium matrix $\mathbf{h}$ of a sub-structure, eliminating the need to assemble the full equilibrium matrix.

Alternatively the full block-diagonalised equilibrium matrix is given by:

$$\tilde{\mathbf{H}} = \sum_{q=1}^{n} \mathbf{V}_{\mathbf{p}_q}{}^{\mathbf{T}} \mathbf{h} \mathbf{V}_{\mathbf{f}_q} \tag{4.64}$$

where $\mathbf{V}_{\mathbf{p}_q} = \mathbf{Q}_q \mathbf{V_p}$ and $\mathbf{V}_{\mathbf{f}_q} = \mathbf{S}_q \mathbf{V_f}$ describe the transformation of load and bar-force vectors from the full vector spaces $\mathbb{V}_{\mathbf{p}}$ and $\mathbb{V}_{\mathbf{f}}$ to the subspaces $\mathbb{V}_{\mathbf{p}q}$ and $\mathbb{V}_{\mathbf{f}q}$, corresponding to symmetry sub-structure q.

4.6.1 Example Sub-Structure Analysis

A sub-structure analysis is now carried out in order to block-diagonalise the equilibrium matrix of the example structure shown in Figure 3.1. Attached to the repeating symmetry sub-structure, shown in Figure 4.5, is a local internal coordinate system for the bar-force and elongation vectors. The local external load and

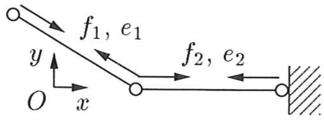

Figure 4.5: Repeating symmetry sub-structure, with a local internal coordinate system for the bar-force and elongation vectors.

displacement coordinate system is shown in Figure 3.4. The equilibrium matrix $\mathbf{h}$ for this repeating symmetry sub-structure is:

$$\mathbf{h} = \begin{bmatrix} -\sqrt{3}/2 & 0 \\ 1/2 & 0 \\ \sqrt{3}/2 & -1 \\ -1/2 & 0 \end{bmatrix} \tag{4.65}$$

In Section 3.7 the local external coordinate system of Figure 3.4 was transformed into the global external coordinate system of Figure 3.2 using the transformation matrices $\{\mathbf{Q}_1, \mathbf{Q}_2, \mathbf{Q}_3\}$ shown in Equations 3.51- 3.53. In a similar way the local internal coordinate systems of Figure 4.5 can be transformed into the global internal coordinate system of Figure 4.1 with the following transformation matrices:

$$\mathbf{S}_1 = \begin{bmatrix} 1 & 0 & 0 & 0 & 0 & 0 \\ 0 & 1 & 0 & 0 & 0 & 0 \end{bmatrix} \tag{4.66}$$

$$\mathbf{S}_2 = \begin{bmatrix} 0 & 0 & 1 & 0 & 0 & 0 \\ 0 & 0 & 0 & 1 & 0 & 0 \end{bmatrix} \tag{4.67}$$

$$\mathbf{S}_3 = \begin{bmatrix} 0 & 0 & 0 & 0 & 1 & 0 \\ 0 & 0 & 0 & 0 & 0 & 1 \end{bmatrix} \tag{4.68}$$

Hence, consider generating the (2×2) equilibrium block $\tilde{\mathbf{H}}^{(B)2}$ shown in Equation 4.23:

$$\mathbf{V_{f_1}}^{(B)2} = \mathbf{S}_1 \mathbf{V_f}^{(B)2} = \begin{bmatrix} 0 & -1/\sqrt{2} \\ 0 & 0 \end{bmatrix} \tag{4.69}$$

$$\mathbf{V_{f_2}}^{(B)2} = \mathbf{S}_2 \mathbf{V_f}^{(B)2} = \begin{bmatrix} 0 & 0 \\ -1/\sqrt{2} & 0 \end{bmatrix} \tag{4.70}$$

$$\mathbf{V_{f_3}}^{(B)2} = \mathbf{S}_3 \mathbf{V_f}^{(B)2} = \begin{bmatrix} 0 & 1/\sqrt{2} \\ 1/\sqrt{2} & 0 \end{bmatrix} \tag{4.71}$$

The matrices $\{\mathbf{V}_{\mathbf{p}1}^{(B)2}, \mathbf{V}_{\mathbf{p}2}^{(B)2}, \mathbf{V}_{\mathbf{p}3}^{(B)2}\}$ are given by Equations 3.54- 3.56. Then using Equation 4.63:

$$\tilde{\mathbf{H}}^{(B)2} = \sum_{q=1}^{3} \mathbf{V}_{\mathbf{p}_q}^{(B)2\mathbf{T}} \mathbf{h} \mathbf{V}_{\mathbf{f}_q}^{(B)2} \tag{4.72}$$

$$\begin{aligned} \tilde{\mathbf{H}}^{(B)2} &= \begin{bmatrix} 0 & -\sqrt{3/40} \\ 0 & -\sqrt{3/10} \end{bmatrix} + \begin{bmatrix} -1/\sqrt{40} & 0 \\ \sqrt{9/40} & 0 \end{bmatrix} + \begin{bmatrix} -1/\sqrt{40} & -\sqrt{3/40} \\ \sqrt{9/40} & -\sqrt{3/10} \end{bmatrix} \\ &= \begin{bmatrix} -1/\sqrt{10} & -\sqrt{3/10} \\ \sqrt{9/10} & -\sqrt{6/5} \end{bmatrix} \end{aligned} \tag{4.73}$$

This equilibrium block $\tilde{\mathbf{H}}^{(B)2}$ is identical to that calculated in Equation 4.23; however this calculation has only required the equilibrium matrix $\mathbf{h}$ of the symmetry sub-structure to be assembled first.

The equilibrium blocks $\tilde{\mathbf{H}}^{(\mu)i}$ corresponding to the remaining irreducible representations $\Gamma^{(\mu)i}$ of symmetry group $\mathbf{C_{3v}}$ can be calculated in a similar way, or alternatively Equation 4.64 can be used to calculate the full block-diagonalised stiffness matrix $\tilde{\mathbf{H}}$ directly.

4.7 Geiger Dome Example

The previous sections of this chapter have introduced the method of block-diagonalising the equilibrium matrix, and shown a simple example.

The aim of this section is to show how the methods described so far can be useful for the analysis of more complex structures. In particular, it looks at the states of self-stress and mechanisms of a Geiger dome.

A Geiger dome is a class of cable-and-strut prestressed tensegrity dome which have been proposed by D.H. Geiger. Large domes of this type have been built, an example being the Sun Coast Dome in Florida which has a diameter of 210m (Geiger, Cambell, Chen, Gossen, Hamilton & Houg 1988). There have been a number of studies of the structural behaviour of a Geiger dome under general loading conditions. For example, Pellegrino (1992) has investigated how the single state of self-stress stiffens all the inextensional mechanisms within a simplified version of a Geiger dome with only 4-fold rotation and reflection symmetry, shown in Figure 4.6. A 3-dimensional view of this simplified Geiger dome is also shown in Figure 4.7.

In this section, an analysis of this simplified Geiger dome is carried out to show how the methods described in this chapter considerably simplify finding and classifying states of self-stress and mechanisms in a structure. In the original work

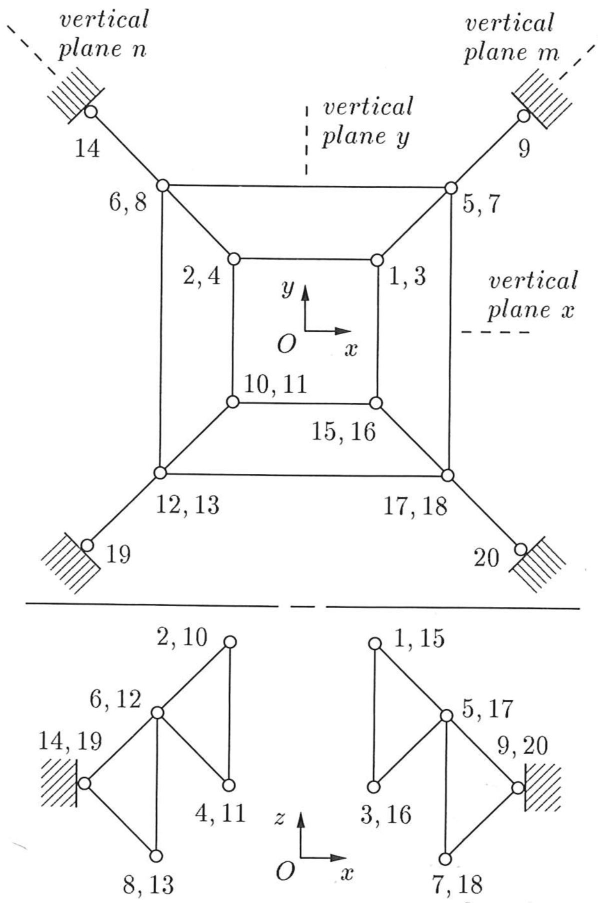

Figure 4.6: Simplified Geiger dome, with $\mathbf{C_{4v}}$ symmetry.

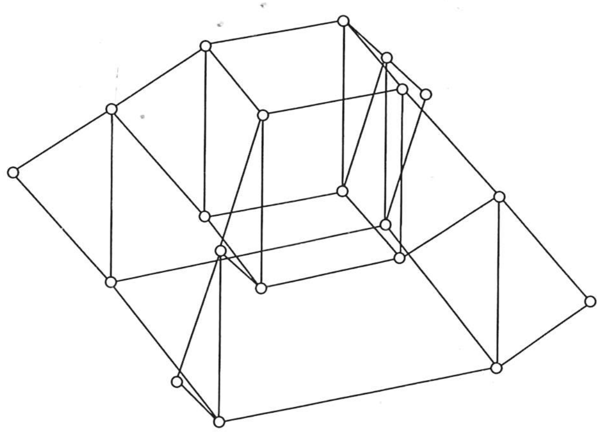

Figure 4.7: 3-dimensional view of the Simplified Geiger dome.

by Pellegrino, finding "simple" mechanisms was not an easy task, whereas in this example a sensible symmetry classification is automatically found.

The Geiger dome is transformed into an equivalent structure by the following set of symmetry operations:

1. The identity, symmetry operation E.
2. Rotation by 90° about the vertical z-axis, symmetry operation C_4.
3. Rotation by 180° about the vertical z-axis, symmetry operation C_4^2.
4. Rotation by 270° about the vertical z-axis, symmetry operation C_4^3.
5. Reflection in the vertical plane x, symmetry operation σ_x.
6. Reflection in the vertical plane y, symmetry operation σ_y.
7. Reflection in the vertical plane m, symmetry operation σ_m.
8. Reflection in the vertical plane n, symmetry operation σ_n.

These eight symmetry operations constitute the symmetry group $\mathbf{C_{4v}}$. The irreducible matrix representations $\Gamma^{(\mu)}$ for this symmetry group are shown in Table 4.2.

$\mathbf{C_{4v}}$	E	C_4	C_4^2	C_4^3	σ_x	σ_y	σ_m	σ_n
$\Gamma^{(A_1)}$	1	1	1	1	1	1	1	1
$\Gamma^{(A_2)}$	1	1	1	1	−1	−1	−1	−1
$\Gamma^{(B_1)}$	1	−1	1	−1	1	1	−1	−1
$\Gamma^{(B_2)}$	1	−1	1	−1	−1	−1	1	1
$\Gamma^{(E)}$	$\begin{bmatrix} 1 & 0 \\ 0 & 1 \end{bmatrix}$	$\begin{bmatrix} 0 & 1 \\ -1 & 0 \end{bmatrix}$	$\begin{bmatrix} -1 & 0 \\ 0 & -1 \end{bmatrix}$	$\begin{bmatrix} 0 & -1 \\ 1 & 0 \end{bmatrix}$	$\begin{bmatrix} 1 & 0 \\ 0 & -1 \end{bmatrix}$	$\begin{bmatrix} -1 & 0 \\ 0 & 1 \end{bmatrix}$	$\begin{bmatrix} 0 & 1 \\ 1 & 0 \end{bmatrix}$	$\begin{bmatrix} 0 & -1 \\ -1 & 0 \end{bmatrix}$

Table 4.2: Irreducible representations of symmetry group $\mathbf{C_{4v}}$.

Using the methods described in Sections 3.4 and 4.4.1, symmetry-adapted coordinate systems can be found for both the load and bar-force vector spaces $\mathbb{V}_\mathbf{p}$ and $\mathbb{V}_\mathbf{f}$. Both vector spaces are decomposed into six symmetry subspaces, since there are four 1-dimensional and one 2-dimensional irreducible matrix representations for the symmetry group $\mathbf{C_{4v}}$, as shown in Table 4.2.

$$\mathbb{V}_\mathbf{p} = \left(\mathbb{V}_\mathbf{p}^{(A_1)}, \mathbb{V}_\mathbf{p}^{(A_2)}, \mathbb{V}_\mathbf{p}^{(B_1)}, \mathbb{V}_\mathbf{p}^{(B_2)}, \mathbb{V}_\mathbf{p}^{(E)1}, \mathbb{V}_\mathbf{p}^{(E)2}\right) \tag{4.74}$$

$$\mathbb{V}_\mathbf{f} = \left(\mathbb{V}_\mathbf{f}^{(A_1)}, \mathbb{V}_\mathbf{f}^{(A_2)}, \mathbb{V}_\mathbf{f}^{(B_1)}, \mathbb{V}_\mathbf{f}^{(B_2)}, \mathbb{V}_\mathbf{f}^{(E)1}, \mathbb{V}_\mathbf{f}^{(E)2}\right) \tag{4.75}$$

by Pellegrino, finding "simple" mechanisms was not an easy task, whereas in this example a sensible symmetry classification is automatically found.

The Geiger dome is transformed into an equivalent structure by the following set of symmetry operations:

1. The identity, symmetry operation E.
2. Rotation by 90° about the vertical z-axis, symmetry operation C_4.
3. Rotation by 180° about the vertical z-axis, symmetry operation C_4^2.
4. Rotation by 270° about the vertical z-axis, symmetry operation C_4^3.
5. Reflection in the vertical plane x, symmetry operation σ_x.
6. Reflection in the vertical plane y, symmetry operation σ_y.
7. Reflection in the vertical plane m, symmetry operation σ_m.
8. Reflection in the vertical plane n, symmetry operation σ_n.

These eight symmetry operations constitute the symmetry group $\mathbf{C_{4v}}$. The irreducible matrix representations $\Gamma^{(\mu)}$ for this symmetry group are shown in Table 4.2.

$\mathbf{C_{4v}}$	E	C_4	C_4^2	C_4^3	σ_x	σ_y	σ_m	σ_n
$\Gamma^{(A_1)}$	1	1	1	1	1	1	1	1
$\Gamma^{(A_2)}$	1	1	1	1	−1	−1	−1	−1
$\Gamma^{(B_1)}$	1	−1	1	−1	1	1	−1	−1
$\Gamma^{(B_2)}$	1	−1	1	−1	−1	−1	1	1
$\Gamma^{(E)}$	$\begin{bmatrix} 1 & 0 \\ 0 & 1 \end{bmatrix}$	$\begin{bmatrix} 0 & 1 \\ -1 & 0 \end{bmatrix}$	$\begin{bmatrix} -1 & 0 \\ 0 & -1 \end{bmatrix}$	$\begin{bmatrix} 0 & -1 \\ 1 & 0 \end{bmatrix}$	$\begin{bmatrix} 1 & 0 \\ 0 & -1 \end{bmatrix}$	$\begin{bmatrix} -1 & 0 \\ 0 & 1 \end{bmatrix}$	$\begin{bmatrix} 0 & 1 \\ 1 & 0 \end{bmatrix}$	$\begin{bmatrix} 0 & -1 \\ -1 & 0 \end{bmatrix}$

Table 4.2: Irreducible representations of symmetry group $\mathbf{C_{4v}}$.

Using the methods described in Sections 3.4 and 4.4.1, symmetry-adapted coordinate systems can be found for both the load and bar-force vector spaces $\mathbb{V}_\mathbf{p}$ and $\mathbb{V}_\mathbf{f}$. Both vector spaces are decomposed into six symmetry subspaces, since there are four 1-dimensional and one 2-dimensional irreducible matrix representations for the symmetry group $\mathbf{C_{4v}}$, as shown in Table 4.2.

$$\mathbb{V}_\mathbf{p} = \left(\mathbb{V}_\mathbf{p}^{(A_1)}, \mathbb{V}_\mathbf{p}^{(A_2)}, \mathbb{V}_\mathbf{p}^{(B_1)}, \mathbb{V}_\mathbf{p}^{(B_2)}, \mathbb{V}_\mathbf{p}^{(E)1}, \mathbb{V}_\mathbf{p}^{(E)2}\right) \tag{4.74}$$

$$\mathbb{V}_\mathbf{f} = \left(\mathbb{V}_\mathbf{f}^{(A_1)}, \mathbb{V}_\mathbf{f}^{(A_2)}, \mathbb{V}_\mathbf{f}^{(B_1)}, \mathbb{V}_\mathbf{f}^{(B_2)}, \mathbb{V}_\mathbf{f}^{(E)1}, \mathbb{V}_\mathbf{f}^{(E)2}\right) \tag{4.75}$$

A structural analysis shows that the full equilibrium matrix $\mathbf{H}$ of the Geiger dome is a (48×36) matrix of rank 35, hence there must exist 13 inextensional mechanisms and a single state of self-stress in the Geiger dome (Pellegrino 1992). In order to block-diagonalise this equilibrium matrix the loads and bar-forces must be transformed into their symmetry-adapted coordinate systems, which gives a block-diagonalised equilibrium matrix $\tilde{\mathbf{H}}$ with the following form:

$$\tilde{\mathbf{H}} = \begin{bmatrix} \boxed{\begin{matrix}\tilde{\mathbf{H}}^{(A_1)} \\ (8\times 9)\end{matrix}} & & & & & \\ & \tilde{\mathbf{H}}^{(A_2)}\ (4\times 0) & & & & \\ & & \tilde{\mathbf{H}}^{(B_1)}\ (4\times 3) & & & \\ & & & \tilde{\mathbf{H}}^{(B_2)}\ (8\times 6) & & \\ & & & & \boxed{\begin{matrix}\tilde{\mathbf{H}}^{(E)1} \\ (12\times 9)\end{matrix}} & \\ & & & & & \boxed{\begin{matrix}\tilde{\mathbf{H}}^{(E)2} \\ (12\times 9)\end{matrix}} \end{bmatrix} \tag{4.76}$$

Due to the size of the matrices, $\tilde{\mathbf{H}}$, $\mathbf{V_p}$ and $\mathbf{V_f}$ are not shown in full. However, the next two sections will examine the states of self-stress and mechanisms found in the different submatrix blocks $\tilde{\mathbf{H}}^{(\mu)i}$.

4.7.1 States of Self-Stress in the Geiger Dome

Equilibrium Block $\tilde{\mathbf{H}}^{(A_1)}$

The first equilibrium submatrix block $\tilde{\mathbf{H}}^{(A_1)}$ is an (8×9) matrix of rank 8. Hence a single state of self-stress exists in the bar-force symmetry subspace $\mathbb{V}_{\mathbf{f}}^{(A_1)}$ and is shown in Figure 4.8.

The bar-force vector symmetry subspace $\mathbb{V}_{\mathbf{f}}^{(A_1)}$ has the full symmetry of the Geiger dome, i.e. bar-force vectors in this symmetry subspace are left unchanged by all the operations of the symmetry group $\mathbf{C_{4v}}$.

Remaining Equilibrium Blocks

The remaining five bar-force vector symmetry subspaces of the Geiger dome do not contain any states of self-stress.

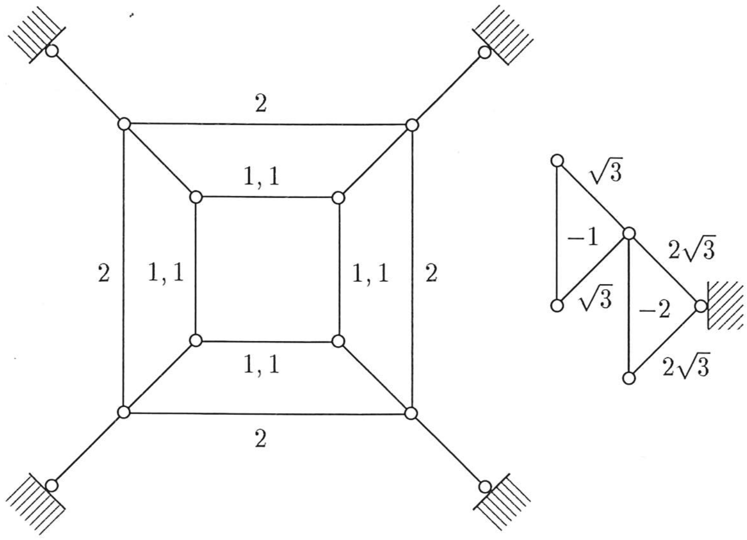

Figure 4.8: Bar-forces of the state of self-stress in the bar-force symmetry subspace $\mathbb{V}_{\mathbf{f}}^{(A_1)}$, with $\mathbf{C_{4v}}$ symmetry properties. [1,1] indicates there is a unit magnitude tensile force in both the upper and lower inner rings.

4.7.2 Mechanisms in the Geiger Dome

Equilibrium Block $\tilde{\mathbf{H}}^{(A_2)}$

The second equilibrium submatrix block $\tilde{\mathbf{H}}^{(A_2)}$, which operates on the symmetry subspaces $\mathbb{V}_{\mathbf{p}}^{(A_2)}$ and $\mathbb{V}_{\mathbf{f}}^{(A_2)}$, is a (4×0) matrix of rank 0. The bar-force symmetry subspace $\mathbb{V}_{\mathbf{f}}^{(A_2)}$ is therefore an empty subspace and hence the four displacement vectors in the symmetry subspace $\mathbb{V}_{\mathbf{p}}^{(A_2)}$ must be inextensional mechanisms. An example of this 4-dimensional vector space of mechanisms is given by the four basis vectors of $\mathbf{V}_{\mathbf{p}}^{(A_2)}$, which are shown in Figure 4.9. Each of these mechanisms has the full rotation symmetry but none of the reflection symmetry of the Geiger dome, i.e. $\mathbf{C_4}$ symmetry properties.

Equilibrium Block $\tilde{\mathbf{H}}^{(B_1)}$

The third equilibrium submatrix block $\tilde{\mathbf{H}}^{(B_1)}$ is a (4×3) matrix of rank 3. Hence, an inextensional mechanism exists in the symmetry subspace $\mathbb{V}_{\mathbf{p}}^{(B_1)}$, and is shown in Figure 4.10. This mechanism has only $\mathbf{C_{2v}}$ symmetry properties, with reflection symmetry in the x and y planes.

Equilibrium Block $\tilde{\mathbf{H}}^{(B_2)}$

The fourth equilibrium submatrix block $\tilde{\mathbf{H}}^{(B_2)}$ is an (8×6) matrix of rank 6. Hence, two inextensional mechanism exist in the symmetry subspace $\mathbb{V}_{\mathbf{p}}^{(B_2)}$ and are shown in Figure 4.11. They also have only $\mathbf{C_{2v}}$ symmetry properties, but now with reflection symmetry in the m and n planes.

Equilibrium Block $\tilde{\mathbf{H}}^{(E)1}$

The fifth equilibrium submatrix block $\tilde{\mathbf{H}}^{(E)1}$ is a (12×9) matrix of rank 9. Hence, three inextensional mechanisms exists in the symmetry subspace $\mathbb{V}_{\mathbf{p}}^{(E)1}$ and are shown in Figure 4.12. These mechanisms have only reflection symmetry in the x plane, i.e. $\mathbf{C_s}$ symmetry properties.

Equilibrium Block $\tilde{\mathbf{H}}^{(E)2}$

The sixth equilibrium submatrix block $\tilde{\mathbf{H}}^{(E)2}$ is a (12×9) matrix of rank 9. Hence, three inextensional mechanisms exists in the symmetry subspace $\mathbb{V}_{\mathbf{p}}^{(E)2}$ and are shown in Figure 4.13. These mechanisms have only reflection symmetry in the y plane, i.e $\mathbf{C_s}$ symmetry properties.

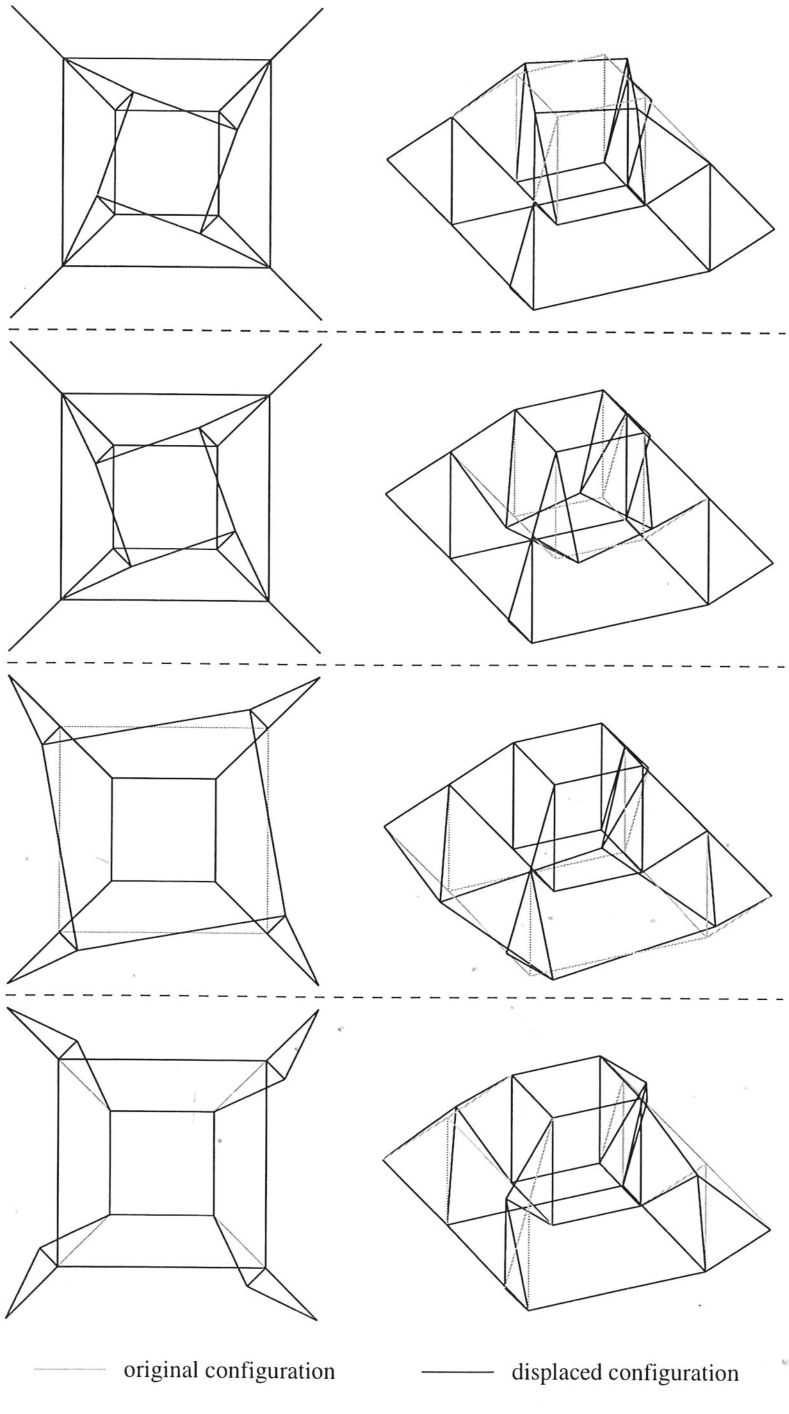

Figure 4.9: Four mechanisms in the displacement symmetry subspace $\mathbb{V}_{\mathbf{d}}^{(A_2)}$, with $\mathbf{C_4}$ symmetry properties.

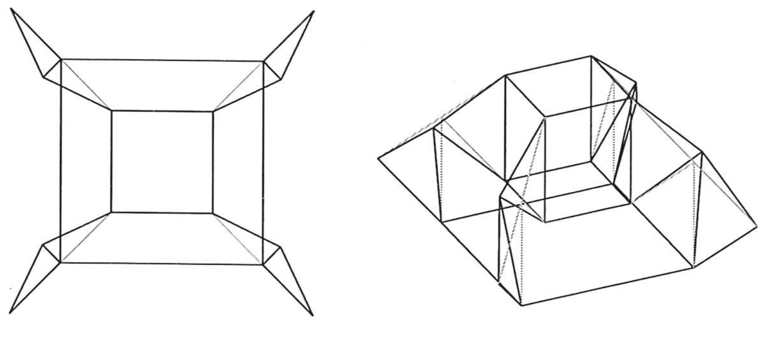

Figure 4.10: Mechanism in the displacement symmetry subspace $\mathbb{V}_{\mathbf{d}}^{(B_1)}$, with $\mathbf{C_{2v}}$ symmetry properties (reflection in planes x and y).

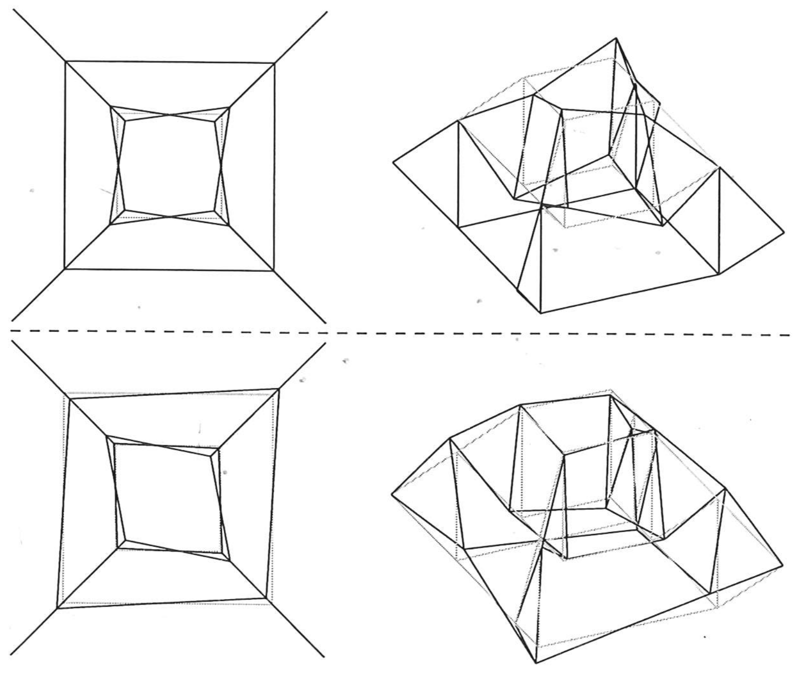

Figure 4.11: Two mechanisms in the displacement symmetry subspace $\mathbb{V}_{\mathbf{d}}^{(B_2)}$, with $\mathbf{C_{2v}}$ symmetry properties (reflection in planes m and n).

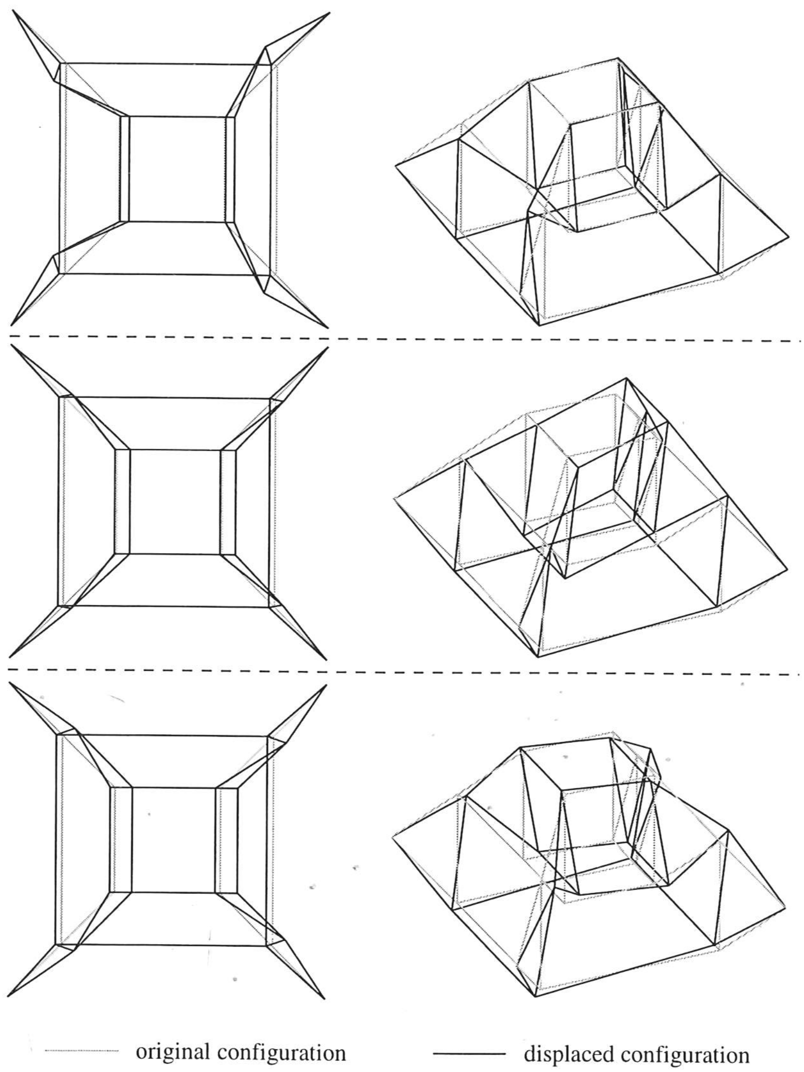

Figure 4.12: Three mechanisms in the displacement symmetry subspace $\mathbb{V}_{\mathbf{d}}^{(E)1}$, with $\mathbf{C_s}$ symmetry properties (reflection in plane x).

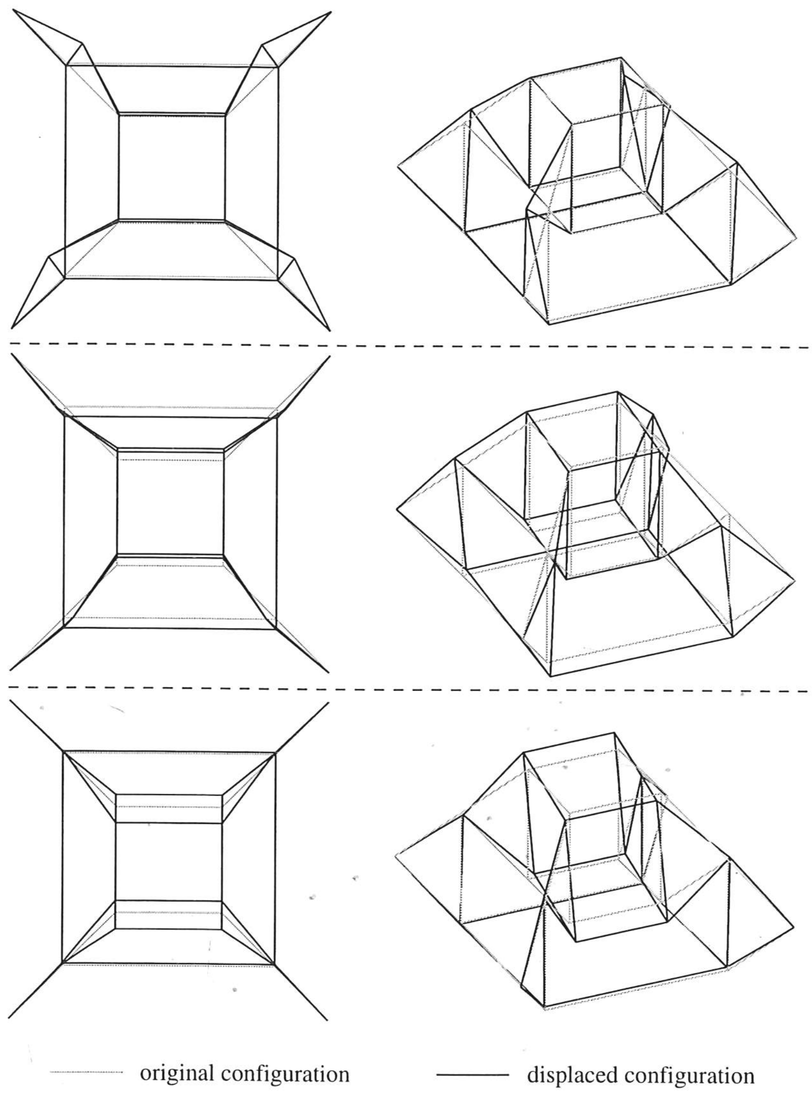

Figure 4.13: Three mechanisms in the displacement symmetry subspace $\mathbb{V}_{\mathbf{d}}^{(E)2}$, with $\mathbf{C_s}$ symmetry properties (reflection in plane y).

Chapter 5

Detection of Finite Mechanisms

5.1 Introduction

This chapter will show how a linear analysis based on symmetry can provide considerable insight into the nature of symmetric structures which are both statically and kinematically indeterminate. In particular, this chapter will show that in some circumstances, it is possible to identify when a structure admits a mechanism which is *finite* rather than *infinitesimal*.

In Chapter 4, Group Representation Theory was applied to block-diagonalise the equilibrium matrix of a symmetric structure, and this provided useful insight into the structural response of such structures. In particular, it provides a useful classification of any states of self-stress or inextensional mechanisms present in the structure.

Using the same techniques as the previous chapter, an additional step is taken to investigate statically and kinematically indeterminate symmetric structures that admit finite mechanisms. In particular, an analysis is carried out on a ring structure originally investigated by Tarnai (1980) which belongs to a class of structures that satisfy Maxwell's rule, but is both statically and kinematically indeterminate. Using only symmetry arguments, a linear analysis of the equilibrium matrix will show that this ring structure contains a finite mechanism.

The layout of this chapter is as follows. The rest of this section gives some background on statically and kinematically indeterminate structures. Section 5.2 analyses a hexagonal ring with rotational and reflection symmetry properties, to show that it admits a finite mechanism. Section 5.3 analyses the same hexagonal ring at another configuration where there exists a kinematic bifurcation with four possible finite paths, of which only one can be identified using symmetry arguments. Finally, Section 5.4 gives a summary of when in general, a symmetry analysis can identify finite mechanisms.

Chapter 5

Detection of Finite Mechanisms

5.1 Introduction

This chapter will show how a linear analysis based on symmetry can provide considerable insight into the nature of symmetric structures which are both statically and kinematically indeterminate. In particular, this chapter will show that in some circumstances, it is possible to identify when a structure admits a mechanism which is *finite* rather than *infinitesimal.*

In Chapter 4, Group Representation Theory was applied to block-diagonalise the equilibrium matrix of a symmetric structure, and this provided useful insight into the structural response of such structures. In particular, it provides a useful classification of any states of self-stress or inextensional mechanisms present in the structure.

Using the same techniques as the previous chapter, an additional step is taken to investigate statically and kinematically indeterminate symmetric structures that admit finite mechanisms. In particular, an analysis is carried out on a ring structure originally investigated by Tarnai (1980) which belongs to a class of structures that satisfy Maxwell's rule, but is both statically and kinematically indeterminate. Using only symmetry arguments, a linear analysis of the equilibrium matrix will show that this ring structure contains a finite mechanism.

The layout of this chapter is as follows. The rest of this section gives some background on statically and kinematically indeterminate structures. Section 5.2 analyses a hexagonal ring with rotational and reflection symmetry properties, to show that it admits a finite mechanism. Section 5.3 analyses the same hexagonal ring at another configuration where there exists a kinematic bifurcation with four possible finite paths, of which only one can be identified using symmetry arguments. Finally, Section 5.4 gives a summary of when in general, a symmetry analysis can identify finite mechanisms.

5.1.1 Statically and Kinematically Indeterminate Structures

A *statically determinate* structure is a structure whose internal forces can be uniquely found by an equilibrium analysis, i.e. it does not admit a state of self-stress. Similarly, a *kinematically determinate* structure's position can be uniquely found from a kinematic analysis, i.e. there is no mechanism. Maxwell's rule is a well known formula which provides a necessary condition for *both* static and kinematic determinacy. For a 3-dimensional pin-jointed structure rigidly connected to a foundation, Maxwell's rule states:

$$b = 3j \tag{5.1}$$

where b is the total number of bars and j is the number of non-foundation joints. In this case, the equilibrium matrix of a structure is square.

However, Maxwell (1864) anticipated exceptions to his rule and these special cases have been investigated by a number of authors. These special cases include structures which satisfy Maxwell's rule but are statically and kinematically indeterminate and hence, contain states of self-stress and either *infinitesimal* or *finite* mechanisms (Mohr 1885, Föppl 1912, Tarnai 1980). A finite mechanism will allow the joints to move freely for a finite distance without any change in bar-lengths, while an infinitesimal mechanism will cause second-order or higher changes in bar-lengths when the joints move.

Tarnai (1980) pointed out that the *topological* condition expressed by Maxwell's rule is not sufficient to determine whether a structure is stiff or not. The stiffness can only be determined by the *geometry* of the structure. A more complete analysis of the equilibrium and compatibility matrices is required to provide the following expressions:

$$\begin{aligned} s &= b - r \\ m &= 3j - r \end{aligned} \tag{5.2}$$

where: r is the *rank* of either the equilibrium matrix or its transpose, the compatibility matrix.
s is the degree of static indeterminacy.
m is the degree of kinematic indeterminacy.

Structures that have too few constraints to satisfy Maxwell's rule will usually have kinematic mobility, since the structural analysis will not admit a unique solution, and hence finite mechanisms will exist. However, there are exceptional structures that have too few constraints to satisfy Maxwell's rule and yet have first-order stiffness. A number of authors have studied this type of structure (Kötter 1912, Fuller 1975), and Calladine (1978) showed that it is the existence of a state of self-stress in the structure which can have the effect of imparting first-order stiffness to the infinitesimal mechanisms. This class of structure is now commonly referred to as *tensegrity* structures after the work done by Fuller on tensile-integrity structures.

Pellegrino & Calladine (1986, 1991) show how to compute the states of self-stress and the inextensional mechanisms from the *four fundamental vector subspaces* of the equilibrium matrix, and also describe a computational scheme to identify *first-order infinitesimal mechanisms* (involving second-order changes in bar-length) which are stiffened by states of self stress. Work has also been done by Koiter (1984), Pellegrino (1986) and Kuznetsov (1988, 1991) concerning the detection and classification of higher-order infinitesimal mechanisms, which involve third-order (or higher) changes in bar-length. Under this scheme finite mechanisms can be considered as infinite order infinitesimal.

This chapter studies structures which satisfy Maxwell's rule, but in fact allow finite mechanisms which cannot be stiffened by a state of self-stress. Baker, in an appendix to Tarnai (1989), has shown that the existence of a plane reflection symmetry is both a sufficient and necessary condition for such a structure to admit a finite mechanism. In this chapter symmetry arguments are used to block-diagonalise the equilibrium matrix and provide an interesting explanation for the existence of finite mechanisms in symmetric structures.

5.2 Hexagonal Ring with Rotation and Reflection Symmetry

In Section 5.1.1 the existence of special cases which form exceptions to Maxwell's rule was discussed. In this section one of these special cases will be analysed; a structure which satisfies Maxwell's rule but in fact has a finite mechanism.

Tarnai (1980) investigated the structural rigidity of a class of pin-jointed reticulated cylinder structures. These reticulated cylinders consist of congruent rings with n-fold rotational symmetry, and are connected to a rigid foundation; two examples are shown in Figure 5.1. Tarnai showed that while keeping the same topological properties, the state of static and kinematic determinacy of these reticulated cylinders is dependent on the geometry of the structure. The cylinder shown in Figure 5.1(a) satisfies Maxwell's rule and is indeed both statically and kinematically determinate.

However, for a cylinder with the same topological properties but which also has n planes of reflection symmetry, the static and kinematic determinacy of the cylinder is dependent on the size of the n-sided rings; an example is shown in Fig.5.1(b). If n is odd, the cylinder is statically and kinematically determinate. If n is even, the cylinder is statically and kinematically indeterminate, and the degree of indeterminacy is always one, irrespective of the number of rings in the cylinder. Tarnai showed that the single state of self-stress always occurs in the lowest ring,

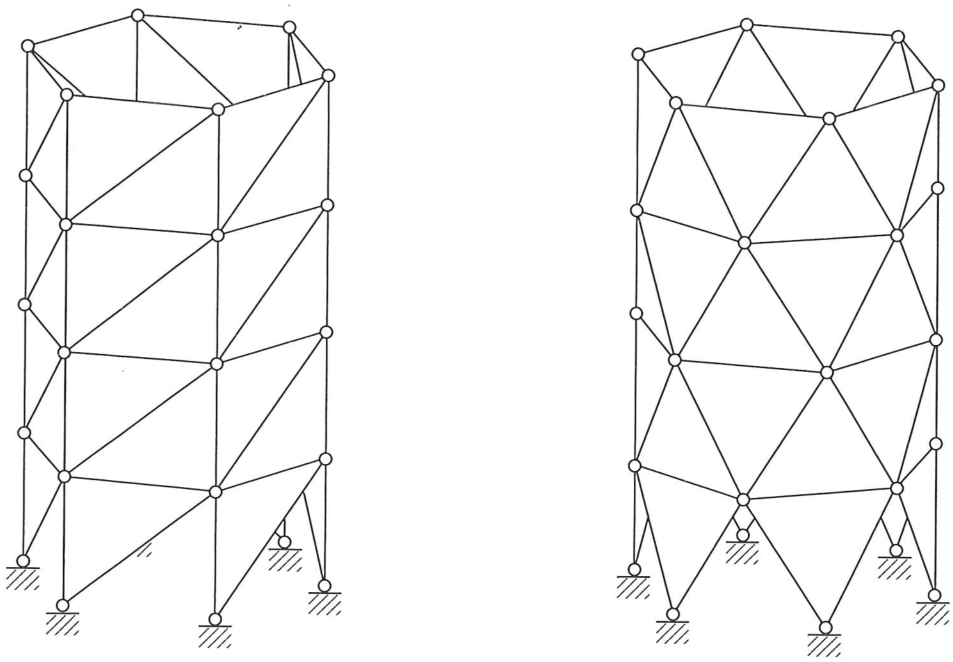

(a) (b)

Figure 5.1: Reticulated cylinders with $\mathbf{C_{6v}}$ symmetry.

while the inextensional mechanism always occurs in the uppermost ring and is a finite mechanism.

In this section, the analysis is limited to a single hexagonal ring with 6-fold rotational symmetry and six planes of reflection symmetry, shown in Figure 5.2. The hexagonal ring consists of $b=18$ bar-elements and $j=6$ pin-joints. Maxwell's rule for a pin-jointed structure connected to a foundation, gives $3j-b=0$. Hence the hexagonal ring should be statically and kinematically determinate according to Maxwell's rule. However, standard structural analysis will show that the (18×18) equilibrium matrix $\mathbf{H}$ has rank 17. Thus, the hexagonal ring contains $s=1$ state of self-stress and $m=1$ inextensional mechanism.

The application of Group Representation Theory to the symmetry properties of the hexagonal ring is used to find *symmetry-adapted coordinate systems* for the external and internal vector spaces. These symmetry-adapted coordinate systems are then used to block-diagonalise the equilibrium matrix $\mathbf{H}$ of the hexagonal ring, into symmetry-adapted equilibrium submatrix blocks $\mathbf{H}^{(\mu)i}$, which considerably simplifies the analysis of the structure and gives valuable insight into the nature of the finite mechanism.

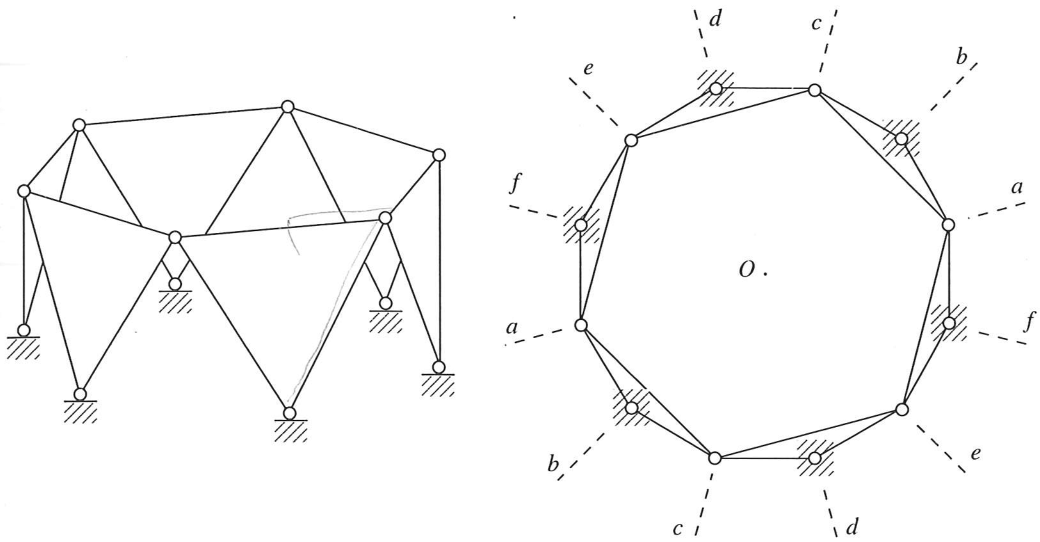

Figure 5.2: Hexagonal ring with $\mathbf{C_{6v}}$ symmetry.

5.2.1 Symmetry-Adapted Coordinate Systems

The external and internal symmetry-adapted coordinate systems of the hexagonal ring are found using the projection operator matrix described in Chapter 3. These symmetry-adapted coordinate systems are made up of vector *symmetry subspaces*, each of which have particular symmetry properties of the hexagonal ring. The calculations required to find these symmetry subspaces are not shown for brevity.

The hexagonal ring is a structure that, when acted on by particular *symmetry operations*, is left in a geometrically and mechanically unaltered configuration, i.e. an *equivalent configuration*. The hexagonal ring is transformed into an equivalent configuration by the following set of symmetry operations:

1. The identity, symmetry operation E.
2. Rotation by 60° about the origin O, symmetry operation C_6.
3. Rotation by 120° about the origin O, symmetry operation C_6^2.
4. Rotation by 180° about the origin O, symmetry operation C_6^3.
5. Rotation by 240° about the origin O, symmetry operation C_6^4.
6. Rotation by 300° about the origin O, symmetry operation C_6^5.
7. Reflection in the vertical plane a, symmetry operation σ_a.
8. Reflection in the vertical plane b, symmetry operation σ_b.

9. Reflection in the vertical plane c, symmetry operation σ_c.

10. Reflection in the vertical plane d, symmetry operation σ_d.

11. Reflection in the vertical plane e, symmetry operation σ_e.

12. Reflection in the vertical plane f, symmetry operation σ_f.

These twelve symmetry operations $\{E,\ C_6,\ C_6^2,\ C_6^3,\ C_6^4,\ C_6^5,\ \sigma_a,\ \sigma_b,\ \sigma_c\ \sigma_d,\ \sigma_e,\ \sigma_f\}$ constitute the symmetry group $\mathbf{C_{6v}}$. The six irreducible matrix representations $\Gamma^{(A_1)}$-$\Gamma^{(E_2)}$, shown in Table 5.1, define the fundamental symmetry properties of symmetry group $\mathbf{C_{6v}}$. In a similar way to that shown in Chapters 3 and 4, these

$\mathbf{C_{6v}}$	E	C_6	C_6^2	C_6^3	C_6^4	C_6^5
$\Gamma^{(A_1)}$	1	1	1	1	1	1
$\Gamma^{(A_2)}$	1	1	1	1	1	1
$\Gamma^{(B_1)}$	1	−1	1	−1	1	−1
$\Gamma^{(B_2)}$	1	−1	1	−1	1	−1
$\Gamma^{(E_1)}$	$\begin{bmatrix}1 & 0\\0 & 1\end{bmatrix}$	$\begin{bmatrix}1/2 & -\sqrt{3}/2\\\sqrt{3}/2 & 1/2\end{bmatrix}$	$\begin{bmatrix}-1/2 & -\sqrt{3}/2\\\sqrt{3}/2 & -1/2\end{bmatrix}$	$\begin{bmatrix}-1 & 0\\0 & -1\end{bmatrix}$	$\begin{bmatrix}-1/2 & \sqrt{3}/2\\-\sqrt{3}/2 & -1/2\end{bmatrix}$	$\begin{bmatrix}1/2 & \sqrt{3}/2\\-\sqrt{3}/2 & 1/2\end{bmatrix}$
$\Gamma^{(E_2)}$	$\begin{bmatrix}1 & 0\\0 & 1\end{bmatrix}$	$\begin{bmatrix}-1/2 & -\sqrt{3}/2\\\sqrt{3}/2 & -1/2\end{bmatrix}$	$\begin{bmatrix}-1/2 & \sqrt{3}/2\\-\sqrt{3}/2 & -1/2\end{bmatrix}$	$\begin{bmatrix}1 & 0\\0 & 1\end{bmatrix}$	$\begin{bmatrix}-1/2 & -\sqrt{3}/2\\\sqrt{3}/2 & -1/2\end{bmatrix}$	$\begin{bmatrix}-1/2 & \sqrt{3}/2\\-\sqrt{3}/2 & -1/2\end{bmatrix}$

σ_a	σ_b	σ_c	σ_d	σ_e	σ_f
1	1	1	1	1	1
−1	−1	−1	−1	−1	−1
1	−1	1	−1	1	−1
−1	1	−1	1	−1	1
$\begin{bmatrix}1 & 0\\0 & -1\end{bmatrix}$	$\begin{bmatrix}1/2 & \sqrt{3}/2\\\sqrt{3}/2 & -1/2\end{bmatrix}$	$\begin{bmatrix}-1/2 & \sqrt{3}/2\\\sqrt{3}/2 & 1/2\end{bmatrix}$	$\begin{bmatrix}-1 & 0\\0 & 1\end{bmatrix}$	$\begin{bmatrix}-1/2 & -\sqrt{3}/2\\-\sqrt{3}/2 & 1/2\end{bmatrix}$	$\begin{bmatrix}1/2 & -\sqrt{3}/2\\-\sqrt{3}/2 & -1/2\end{bmatrix}$
$\begin{bmatrix}1 & 0\\0 & -1\end{bmatrix}$	$\begin{bmatrix}-1/2 & \sqrt{3}/2\\\sqrt{3}/2 & 1/2\end{bmatrix}$	$\begin{bmatrix}-1/2 & -\sqrt{3}/2\\-\sqrt{3}/2 & 1/2\end{bmatrix}$	$\begin{bmatrix}1 & 0\\0 & -1\end{bmatrix}$	$\begin{bmatrix}-1/2 & \sqrt{3}/2\\\sqrt{3}/2 & 1/2\end{bmatrix}$	$\begin{bmatrix}-1/2 & -\sqrt{3}/2\\-\sqrt{3}/2 & 1/2\end{bmatrix}$

Table 5.1: Irreducible matrix representations of symmetry group $\mathbf{C_{6v}}$.

irreducible matrix representations are used to find symmetry-adapted coordinate systems for both the internal vector space $\mathbb{V}_\mathbf{f}$ (e.g. a space suitable for expressing bar-forces and extensions) and the external vector space $\mathbb{V}_\mathbf{p}$ (e.g. a space suitable for expressing loads and displacements).

The symmetry-adapted coordinate systems split the vector spaces into a number of *symmetry subspaces* $\mathbb{V}_\mathbf{p}^{(\mu)i}$ and $\mathbb{V}_\mathbf{f}^{(\mu)i}$, each corresponding to a row i of the irreducible matrix representation $\Gamma^{(\mu)}$, and each having different symmetry properties. For symmetry group $\mathbf{C_{6v}}$ there are eight symmetry subspaces for the internal and external vector spaces, and their symmetry properties are described below.

1. $\mathbb{V}_{\mathbf{p}}^{(A_1)}$ and $\mathbb{V}_{\mathbf{f}}^{(A_1)}$: the full symmetry of symmetry group $\mathbf{C_{6v}}$.
2. $\mathbb{V}_{\mathbf{p}}^{(A_2)}$ and $\mathbb{V}_{\mathbf{f}}^{(A_2)}$: 6-fold rotational symmetry, symmetry group $\mathbf{C_6}$.
3. $\mathbb{V}_{\mathbf{p}}^{(B_1)}$ and $\mathbb{V}_{\mathbf{f}}^{(B_1)}$: 3-fold rotational symmetry and reflection symmetry in planes a, c and e, symmetry group $\mathbf{C_{3v}}$.
4. $\mathbb{V}_{\mathbf{p}}^{(B_2)}$ and $\mathbb{V}_{\mathbf{f}}^{(B_2)}$: 3-fold rotational symmetry and reflection symmetry in planes b, d and f, symmetry group $\mathbf{C_{3v}}$.
5. $\mathbb{V}_{\mathbf{p}}^{(E_1)1}$ and $\mathbb{V}_{\mathbf{f}}^{(E_1)1}$: reflection symmetry in plane a, symmetry group $\mathbf{C_s}$.
6. $\mathbb{V}_{\mathbf{p}}^{(E_1)2}$ and $\mathbb{V}_{\mathbf{f}}^{(E_1)2}$: reflection symmetry in plane d, symmetry group $\mathbf{C_s}$.
7. $\mathbb{V}_{\mathbf{p}}^{(E_2)1}$ and $\mathbb{V}_{\mathbf{f}}^{(E_2)1}$: 2-fold rotational symmetry and reflection symmetry in planes a and d, symmetry group $\mathbf{C_{2v}}$.
8. $\mathbb{V}_{\mathbf{p}}^{(E_2)2}$ and $\mathbb{V}_{\mathbf{f}}^{(E_2)2}$: 2-fold rotational symmetry, symmetry group $\mathbf{C_2}$.

These symmetry properties are defined by the symmetry group and are independent of the topology of the structure in question. Chapters 3 and 4 showed how it is possible to find basis vectors for each of the symmetry subspaces $\mathbb{V}_{\mathbf{p}}^{(\mu)i}$ and $\mathbb{V}_{\mathbf{f}}^{(\mu)i}$. These basis vectors can then be written as columns of a matrix $\mathbf{V_p}^{(\mu)i}$ and $\mathbf{V_f}^{(\mu)i}$. Group Representation Theory shows that together, these basis vectors span the whole space $\mathbb{V}_{\mathbf{p}}$ and $\mathbb{V}_{\mathbf{f}}$.

Hence it is possible to write an orthogonal matrix $\mathbf{V_p}$ which transforms load vectors between the original and the symmetry-adapted coordinate system. For symmetry group $\mathbf{C_{6v}}$ this matrix is:

$$\mathbf{V_p} = \left(\mathbf{V}_{\mathbf{p}}^{(A_1)}|\mathbf{V}_{\mathbf{p}}^{(A_2)}|\mathbf{V}_{\mathbf{p}}^{(B_1)}|\mathbf{V}_{\mathbf{p}}^{(B_2)}|\mathbf{V}_{\mathbf{p}}^{(E_1)1}|\mathbf{V}_{\mathbf{p}}^{(E_1)2}|\mathbf{V}_{\mathbf{p}}^{(E_2)1}|\mathbf{V}_{\mathbf{p}}^{(E_2)2}\right) \tag{5.3}$$

Similarly, the orthogonal matrix $\mathbf{V_f}$ which transforms bar-force vectors between the original and the symmetry-adapted coordinate system with $\mathbf{C_{6v}}$ symmetry is:

$$\mathbf{V_f} = \left(\mathbf{V}_{\mathbf{f}}^{(A_1)}|\mathbf{V}_{\mathbf{f}}^{(A_2)}|\mathbf{V}_{\mathbf{f}}^{(B_1)}|\mathbf{V}_{\mathbf{f}}^{(B_2)}|\mathbf{V}_{\mathbf{f}}^{(E_1)1}|\mathbf{V}_{\mathbf{f}}^{(E_1)2}|\mathbf{V}_{\mathbf{f}}^{(E_2)1}|\mathbf{V}_{\mathbf{f}}^{(E_2)2}\right) \tag{5.4}$$

Figures 5.3 and 5.4 show a set of basis vectors for the first four internal and external symmetry subspaces of the hexagonal ring. The basis vectors for the remaining symmetry subspaces have not been shown in the interests of brevity, and also because they do not participate in the later discussion of the properties of the structure.

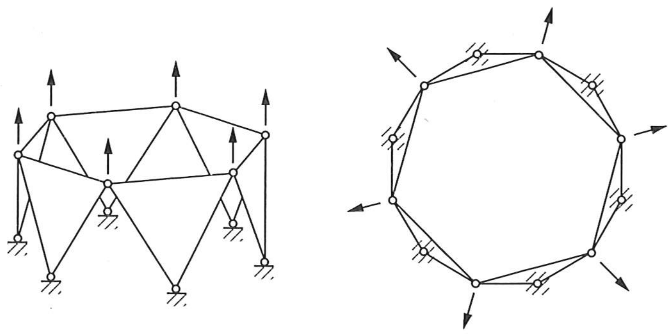

(a) 2-dimensional symmetry subspace $\mathbb{V}_{\mathbf{p}}^{(A_1)}$

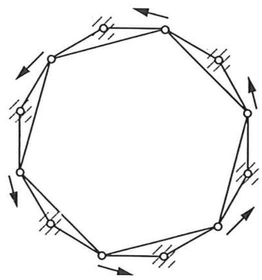

(b) 1-dimensional symmetry subspace $\mathbb{V}_{\mathbf{p}}^{(A_2)}$

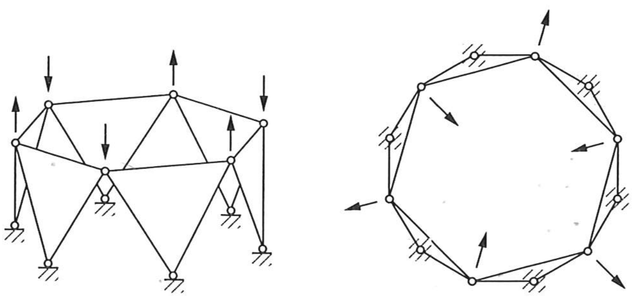

(c) 2-dimensional symmetry subspace $\mathbb{V}_{\mathbf{p}}^{(B_1)}$

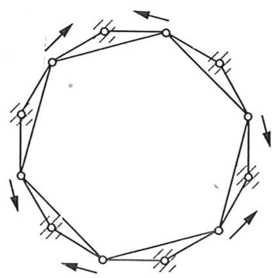

(d) 1-dimensional symmetry subspace $\mathbb{V}_{\mathbf{p}}^{(B_2)}$

Figure 5.3: External symmetry subspaces $\mathbb{V}_{\mathbf{p}}^{(A_1)}$, $\mathbb{V}_{\mathbf{p}}^{(A_2)}$, $\mathbb{V}_{\mathbf{p}}^{(B_1)}$ and $\mathbb{V}_{\mathbf{p}}^{(B_2)}$. Each arrow is of magnitude $1/\sqrt{6}$, to give resultant basis vectors of unit length.

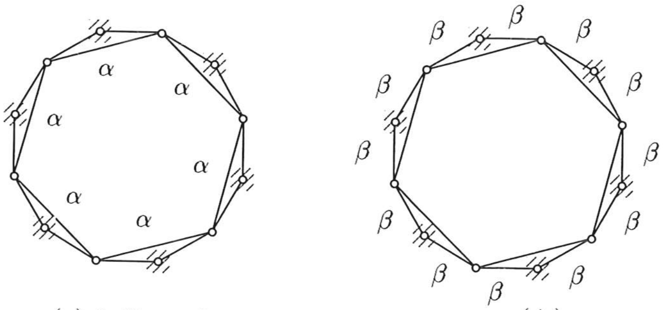

(a) 2-dimensional symmetry subspace $\mathbb{V}_{\mathbf{f}}^{(A_1)}$

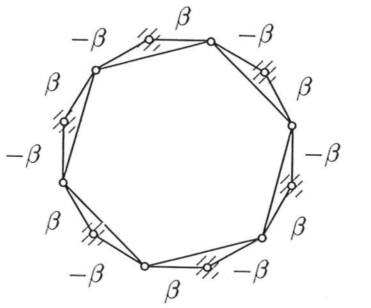

(b) 1-dimensional symmetry subspace $\mathbb{V}_{\mathbf{f}}^{(A_2)}$

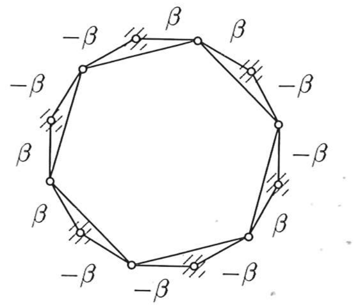

(c) 1-dimensional symmetry subspace $\mathbb{V}_{\mathbf{f}}^{(B_1)}$

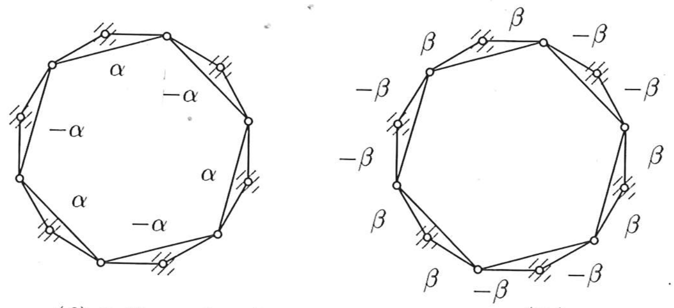

(d) 2-dimensional symmetry subspace $\mathbb{V}_{\mathbf{p}}^{(B_2)}$

Figure 5.4: Internal symmetry subspaces $\mathbb{V}_{\mathbf{f}}^{(A_1)}$, $\mathbb{V}_{\mathbf{f}}^{(A_2)}$, $\mathbb{V}_{\mathbf{f}}^{(B_1)}$ and $\mathbb{V}_{\mathbf{f}}^{(B_2)}$. α and β refer to the magnitude of the force or extension in the corresponding bar. $\alpha = 1/\sqrt{6}$ and $\beta = 1/\sqrt{12}$ give resultant basis vectors of unit length.

5.2.2 Block-Diagonalised Equilibrium Matrix using C_{6v} Symmetry

External loads applied to a structure, which have a particular type of symmetry, will be in equilibrium with internal forces which also have the same symmetry. Therefore, using internal and external symmetry-adapted coordinate systems will block-diagonalise the equilibrium matrix $\mathbf{H}$ into independent equilibrium blocks $\tilde{\mathbf{H}}^{(\mu)i}$.

Chapter 4 showed that to block-diagonalise the equilibrium matrix, the load and bar-force vectors $\mathbf{p}$ and $\boldsymbol{f}$ in some general coordinate system, must be transformed into equivalent load and bar-force vectors $\tilde{\mathbf{p}}$ and $\tilde{\boldsymbol{f}}$ in their symmetry-adapted coordinate systems. Hence, the block-diagonalised equilibrium matrix $\tilde{\mathbf{H}}$ is given by:

$$\tilde{\mathbf{H}} = \mathbf{V}_\mathrm{p}^\mathrm{T}\mathbf{H}\mathbf{V}_\mathrm{f} \tag{5.5}$$

For the hexagonal ring shown in Figure 5.2, the block-diagonalised equilibrium matrix $\tilde{\mathbf{H}}$ has the form shown in Equation 5.6 below. Each of the equilibrium blocks has full rank:

$$\tilde{\mathbf{H}} = \begin{bmatrix} \boxed{\tilde{\mathbf{H}}^{(A_1)}}\,(2\times2) & & & & & & & \\ & \tilde{\mathbf{H}}^{(A_2)}\,(1\times1) & & & & & & \\ & & \tilde{\mathbf{H}}^{(B_1)}\,(2\times1),\ m=1 & & & & & \\ & & & \tilde{\mathbf{H}}^{(B_2)}\,(1\times2),\ s=1 & & & & \\ & & & & \begin{matrix}\tilde{\mathbf{H}}^{(E_1)1}\\(3\times3)\end{matrix} & & & \\ & & & & & \begin{matrix}\tilde{\mathbf{H}}^{(E_1)2}\\(3\times3)\end{matrix} & & \\ & & & & & & \begin{matrix}\tilde{\mathbf{H}}^{(E_2)1}\\(3\times3)\end{matrix} & \\ & & & & & & & \begin{matrix}\tilde{\mathbf{H}}^{(E_2)2}\\(3\times3)\end{matrix} \end{bmatrix} \tag{5.6}$$

The original equilibrium matrix $\mathbf{H}$, has been decomposed into eight independent symmetry-adapted equilibrium blocks $\tilde{\mathbf{H}}^{(\mu)i}$, which give the relationship between symmetry-adapted load and bar-force vectors $\tilde{\mathbf{p}}^{(\mu)i}$ and $\tilde{\mathbf{f}}^{(\mu)i}$ that have particular symmetry properties, as described in Section 5.2.1.

Of particular interest are the first four equilibrium blocks along the diagonal, which are now examined in more detail. Using the load and bar-force symmetry-adapted coordinate systems shown in Figures 5.3 and 5.4 respectively, these equilibrium blocks are:

$$\begin{aligned}
\tilde{\mathbf{H}}^{(A_1)} &= \begin{bmatrix} 0 & -1.21 \\ 1 & 0.1895 \end{bmatrix} \\
\tilde{\mathbf{H}}^{(A_2)} &= \begin{bmatrix} -0.7071 \end{bmatrix} \\
\tilde{\mathbf{H}}^{(B_1)} &= \begin{bmatrix} -1.21 \\ 0.1895 \end{bmatrix} \\
\tilde{\mathbf{H}}^{(B_2)} &= \begin{bmatrix} -1.7321 & -0.7071 \end{bmatrix}
\end{aligned} \tag{5.7}$$

Thus, for example, -0.7071 times the internal bar-forces shown in Figure 5.4(b), are in equilibrium with the external loads shown in Figure 5.3(b).

In general, an equilibrium matrix $\mathbf{H}$ is an $(m \times n)$ matrix of rank r, and from the equilibrium matrix it is possible to find the $(n-r)$ states of self-stress and the $(m-r)$ inextensional mechanisms of a structure (Pellegrino & Calladine 1986). The block-diagonalised equilibrium matrix $\tilde{\mathbf{H}}$ also contains $(m \times n)$ blocks of rank r, and hence the analysis for states of self-stress and the inextensional mechanisms can be carried over to these independent equilibrium submatrix blocks $\tilde{\mathbf{H}}^{(\mu)i}$.

The block-diagonalised equilibrium matrix $\tilde{\mathbf{H}}$ in Equation 5.6 consists of eight independent equilibrium submatrix blocks of which $\tilde{\mathbf{H}}^{(A_1)}$, $\tilde{\mathbf{H}}^{(A_2)}$, $\tilde{\mathbf{H}}^{(E_1)1}$, $\tilde{\mathbf{H}}^{(E_1)2}$, $\tilde{\mathbf{H}}^{(E_2)1}$ and $\tilde{\mathbf{H}}^{(E_2)2}$, are all square matrices of full rank, and hence do not contain any states of self-stress or inextensional mechanisms. The remaining two submatrix blocks, $\tilde{\mathbf{H}}^{(B_1)}$ and $\tilde{\mathbf{H}}^{(B_2)}$, are analysed below.

Mechanism in the Third Equilibrium Submatrix Block

$$\tilde{\mathbf{H}}^{(B_1)} = \begin{bmatrix} -1.21 \\ 0.1895 \end{bmatrix}$$

The (2×1) equilibrium submatrix $\tilde{\mathbf{H}}^{(B_2)}$, corresponding to the irreducible matrix representation $\boldsymbol{\Gamma}^{(B_1)}$, is of rank 1, and hence will have a load vector in the corresponding load vector symmetry subspace $\mathrm{V}_{\mathrm{p}}^{(B_1)}$ which cannot be equilibrated. The inextensional mechanism induced by this load vector is a displacement vector $\tilde{\mathbf{d}}_{\mathbf{m}}^{(B_1)}$, which is compatible with zero bar elongations, and as the compatibility matrix is the transpose of the equilibrium matrix, this can be written:

$$\tilde{\mathbf{C}}^{(B_1)}\tilde{\mathbf{d}}_{\mathbf{m}}^{(B_1)} = \tilde{\mathbf{H}}^{(B_1)\mathbf{T}}\tilde{\mathbf{d}}_{\mathbf{m}}^{(B_1)} = \mathbf{0} \tag{5.8}$$

Thus, the mechanism is given by the nullspace of $\tilde{\mathbf{H}}^{(B_1)\mathbf{T}}$:

$$\tilde{\mathbf{d}}_{\mathbf{m}}^{(B_1)} = \begin{bmatrix} -0.1547 \\ -0.988 \end{bmatrix} \tag{5.9}$$

Because the inextensional mechanism is from the third symmetry subspace $\mathbb{V}_{\mathbf{p}}^{(B_1)}$, it has $\mathbf{C_{3v}}$ symmetry properties, i.e. 3-fold rotational symmetry and reflection symmetry in planes a, c and e. The inextensional mechanism is shown in Figure 5.5.

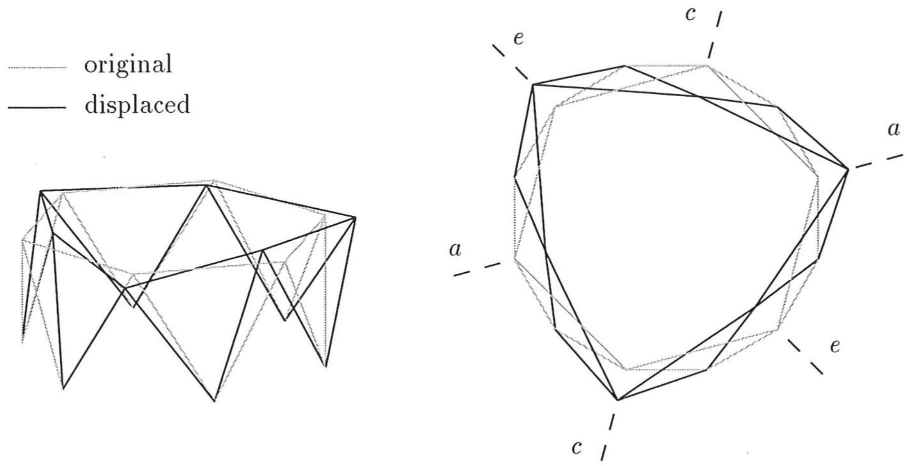

Figure 5.5: Inextensional mechanism in symmetry subspace $\mathbb{V}_{\mathbf{p}}^{(B_1)}$.

State of Self-Stress in the Fourth Equilibrium Submatrix Block

$$\tilde{\mathbf{H}}^{(B_2)} = \begin{bmatrix} -1.7321 & -0.7071 \end{bmatrix}$$

The (1×2) equilibrium submatrix $\tilde{\mathbf{H}}^{(B_2)}$, corresponding to the irreducible matrix representation $\mathbf{\Gamma^{(B_2)}}$, is rank 1 and hence will have a state of self-stress present in the corresponding bar-force vector symmetry subspace $\mathbb{V}_{\mathbf{f}}^{(B_2)}$. The state of self-stress is a bar-force vector $\tilde{\mathbf{f}}_{\mathbf{s}}^{(B_2)}$, in equilibrium with zero load vectors:

$$\tilde{\mathbf{H}}^{(B_2)}\tilde{\mathbf{f}}_{\mathbf{s}}^{(B_2)} = \mathbf{0} \tag{5.10}$$

and is given by the nullspace of $\tilde{\mathbf{H}}^{(B_2)}$:

$$\tilde{\mathbf{f}}_{\mathbf{s}}^{(B_2)} = \begin{bmatrix} -0.378 \\ 0.9258 \end{bmatrix} \tag{5.11}$$

Because the state of self-stress is from the fourth symmetry subspace $\mathbb{V}_{\mathbf{f}}^{(B_2)}$, it also has $\mathbf{C_{3v}}$ symmetry properties, i.e. 3-fold rotational symmetry, but now reflection symmetry is in planes b, d and e. The state of self-stress is shown in Figure 5.6.

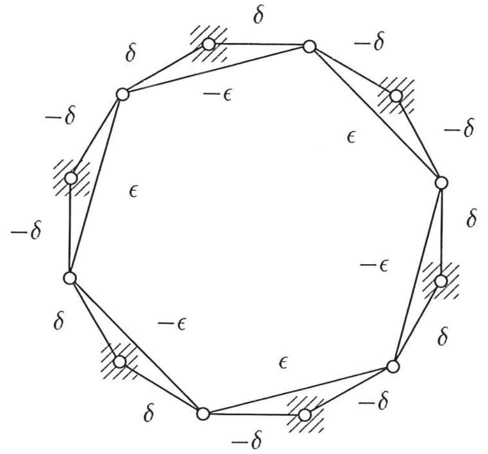

Figure 5.6: State of self-stress in symmetry subspace $\mathbb{V}_{\mathbf{f}}^{(B_2)}$. $\delta = 1/\sqrt{14}$ and $\epsilon = 1/\sqrt{42}$.

5.2.3 Block-Diagonalised Equilibrium Matrix using $\mathbf{C_{3v}}$ Symmetry

The aim of the investigation is to determine whether the inextensional mechanism discovered in Section 5.2.2, is finite or infinitesimal. However, it is clear that the analysis carried out will lose validity as soon as the mechanism is mobilised. The structure will lose its $\mathbf{C_{6v}}$ symmetry and instead will have only $\mathbf{C_{3v}}$ symmetry. Thus, to make further progress, it is necessary to reanalyse the structure using symmetry group $\mathbf{C_{3v}}$.

The following six symmetry operations constitute the symmetry group $\mathbf{C_{3v}}$:

1. The identity, symmetry operation E.
2. Rotation by 120° about the origin O, symmetry operation C_3.
3. Rotation by 240° about the origin O, symmetry operation C_3^2.
4. Reflection in the vertical plane a, symmetry operation σ_a.
5. Reflection in the vertical plane c, symmetry operation σ_c.
6. Reflection in the vertical plane e, symmetry operation σ_e.

For the hexagonal ring in its original configuration, both the load vector space $\mathbb{V}_{\mathbf{p}}$ and the bar-force vector space $\mathbb{V}_{\mathbf{f}}$ are now decomposed into four symmetry subspaces, defined by the three irreducible representations $\{\Gamma^{(A_1)}, \Gamma^{(A_2)}$ and $\Gamma^{(E)}\}$ of symmetry group $\mathbf{C_{3v}}$, shown in Table 3.3. The symmetry properties of these load and bar-force vector symmetry subspaces are described below.

1. $\mathbb{V}_{\mathbf{p}}^{(A_1)}$ and $\mathbb{V}_{\mathbf{f}}^{(A_1)}$: the full symmetry of symmetry group $\mathbf{C_{3v}}$.
2. $\mathbb{V}_{\mathbf{p}}^{(A_2)}$ and $\mathbb{V}_{\mathbf{f}}^{(A_2)}$: 3-fold rotational symmetry, symmetry group $\mathbf{C_3}$.
3. $\mathbb{V}_{\mathbf{p}}^{(E)1}$ and $\mathbb{V}_{\mathbf{f}}^{(E)1}$: reflection symmetry in plane a, symmetry group $\mathbf{C_s}$.
4. $\mathbb{V}_{\mathbf{p}}^{(E)2}$ and $\mathbb{V}_{\mathbf{f}}^{(E)2}$: reflection anti-symmetry in plane a, no symmetry.

Although it may now appear to be necessary to completely reanalyse the structure using symmetry group $\mathbf{C_{3v}}$, it is in fact possible to find the symmetry subspaces using a concept called *subduction*, or the *descent of symmetry*.

Table 5.2 shows one way in which $\mathbf{C_{6v}}$ symmetry subspaces can combine to form the $\mathbf{C_{3v}}$ symmetry subspaces. This descent of symmetry is valid for any

$\mathbf{C_{3v}}$		$\mathbf{C_{6v}}$
$\{\mathbb{V}^{(A_1)}\}$	$\Longleftrightarrow$	$\{\mathbb{V}^{(A_1)}, \mathbb{V}^{(B_1)}\}$
$\{\mathbb{V}^{(A_2)}\}$	$\Longleftrightarrow$	$\{\mathbb{V}^{(A_2)}, \mathbb{V}^{(B_2)}\}$
$\{\mathbb{V}^{(E)1}\}$	$\Longleftrightarrow$	$\{\mathbb{V}^{(E_1)1}, \mathbb{V}^{(E_2)1}\}$
$\{\mathbb{V}^{(E)2}\}$	$\Longleftrightarrow$	$\{\mathbb{V}^{(E_1)2}, \mathbb{V}^{(E_2)2}\}$

Table 5.2: Descent of symmetry from symmetry group $\mathbf{C_{6v}}$ to $\mathbf{C_{3v}}$.

structure with $\mathbf{C_{6v}}$ symmetry, irrespective of its topology. Similar tables can be found for all symmetry groups, and a comprehensive study of symmetry groups and the relationships between the different groups is given by Altmann & Herzig (1994). Now it is only necessary to combine the $\mathbf{C_{6v}}$ symmetry subspaces according to the descent of symmetry shown in Table 5.2, in order to find the $\mathbf{C_{3v}}$ symmetry subspaces. For example, the $\mathbf{C_{3v}}$ vector basis $\mathbf{V_p}^{(A_1)}$ is simply given by the $\mathbf{C_{6v}}$ basis vectors in Figures 5.3(a) and (c). Using the load and bar-force vector symmetry-adapted coordinate systems with $\mathbf{C_{3v}}$ symmetry properties, the block-diagonalised equilibrium matrix $\tilde{\mathbf{H}}$ now has the form:

$$\tilde{\mathbf{H}} = \begin{bmatrix} \boxed{\tilde{\mathbf{H}}^{(A_1)}}\ (4\times3),\ m=1 & & & \\ & \boxed{\tilde{\mathbf{H}}^{(A_2)}}\ (2\times3),\ s=1 & & \\ & & \boxed{\begin{matrix}\tilde{\mathbf{H}}^{(E)1} \\ (6\times6)\end{matrix}} & \\ & & & \boxed{\begin{matrix}\tilde{\mathbf{H}}^{(E)2} \\ (6\times6)\end{matrix}} \end{bmatrix} \tag{5.12}$$

Each of the equilibrium blocks is of full rank. Obviously, the inextensional mechanism and state of self-stress will be identical to those found in the previous analysis, but the mechanism now occurs in the first equilibrium block $\tilde{\mathbf{H}}^{(A_1)}$, with $\mathbf{C_{3v}}$ symmetry, while the state of self-stress occurs in the second equilibrium block $\tilde{\mathbf{H}}^{(A_2)}$, with "lesser" $\mathbf{C_3}$ symmetry.

It is the existence of a mechanism, but no state of self-stress, in the first equilibrium block, which allows us to show that the mechanism must be finite. In Section 5.1.1, it was noted that an equilibrium matrix with more rows than columns, i.e. a structure with too few constraints, would have finite mechanisms. This is true as long as the equilibrium matrix is not rank-deficient, otherwise a state of self-stress exists which may impart first-order stiffness to the mechanisms. This argument carries over to the independent equilibrium blocks $\tilde{\mathbf{H}}^{(\mu)i}$, *as long as the block-form of the equilibrium matrix is not changed when the mechanism of interest is mobilised.* This will be the case if the mechanism is in the first equilibrium block: the block-form depends only on the topology and symmetry of the structure, neither of which is changed by mobilising the mechanism.

Consider displacing the structure by some finite displacement in the direction of the inextensional mechanism. The structure will retain its $\mathbf{C_{3v}}$ symmetry, but because of non-linearities small changes in the length of some bars must be expected. However, these extensions must also have $\mathbf{C_{3v}}$ symmetry, and hence can only be corrected by displacements in the $\mathbb{V}_{\mathbf{p}}^{(A_1)}$ subspace. It is impossible for these extensions to have "lesser" symmetry, e.g. $\mathbf{C_3}$ symmetry, and hence the state of self-stress, which is now situated in symmetry subspace $\mathbb{V}_{\mathbf{f}}^{(A_2)}$ will be unaffected, and cannot stiffen the mechanism. Eventually it will be possible to converge on a new configuration along the path of the finite mechanism with the structure retaining it's $\mathbf{C_{3v}}$ symmetry. Thus, the inextensional mechanism shown in Figure 5.5 is finite.

5.3 Bifurcation Point of the Hexagonal Ring

In the previous section, the hexagonal ring's single degree of kinematic indeterminacy was shown to represent a finite mechanism with $\mathbf{C_{3v}}$ symmetry. If the mobilisation of a finite mechanism leads to a configuration where the degree of kinematic indeterminacy increases, the structure is said to have reached a point of *kinematic bifurcation.* At such points there exists a multi-dimensional vector space of inextensional mechanisms and there is now a possibility of having a number of distinct kinematic paths that admit finite mechanisms.

If the kinematic path of the finite mechanism in Figure 5.5 is followed, the hexagonal ring reaches a configuration shown in Figure 5.7, which is a point of *kinematic bifurcation* (Tarnai 1989). Kumar (1996) analysed the hexagonal ring

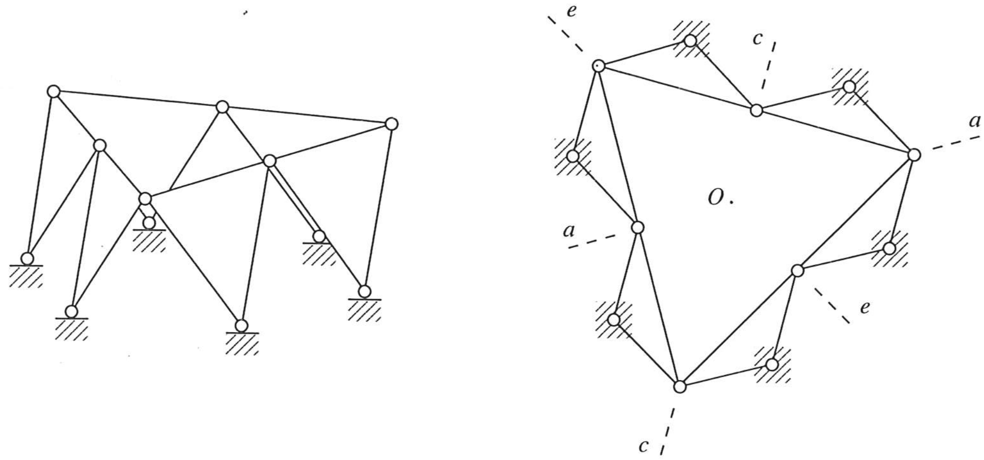

Figure 5.7: Hexagonal ring at the bifurcation point, with $\mathbf{C_{3v}}$ symmetry.

at the point of kinematic bifurcation using singular value decomposition (SVD) techniques to identify the m inextensional mechanisms and the s states of self-stress. The analysis showed that the equilibrium matrix $\mathbf{H}$ now has rank 15, and hence there now exists $s = 3$ states of self-stress and $m = 3$ inextensional mechanisms. Kumar also showed that in this three-dimensional vector space of inextensional mechanisms there exists four distinct kinematic paths that admit finite mechanisms; these are shown in Figure 5.8. Figure 5.8(a) shows the original finite mechanism with $\mathbf{C_{3v}}$ symmetry, Figures 5.8(b), (c) and (d) show three finite mechanisms which only have reflection symmetry in one of the planes a, c or e.

In this section a symmetry analysis is carried out to see if it is possible to identify these four finite mechanisms with the hexagonal ring at the point of kinematic bifurcation. Previously the equilibrium matrix was block-diagonalised using symmetry group $\mathbf{C_{3v}}$, for the hexagonal ring in its original configuration. At the point of kinematic bifurcation the hexagonal ring still has $\mathbf{C_{3v}}$ symmetry, and hence the block-diagonalised equilibrium matrix $\tilde{\mathbf{H}}$ will have the same form shown in Equation 5.12.

As in Section 5.2.3, both equilibrium blocks $\tilde{\mathbf{H}}^{(A_1)}$ and $\tilde{\mathbf{H}}^{(A_2)}$ are of full rank. $\tilde{\mathbf{H}}^{(A_1)}$ contains an inextensional mechanism, and $\tilde{\mathbf{H}}^{(A_2)}$ contains a state of self-stress. Now however, the two (6×6) equilibrium blocks $\tilde{\mathbf{H}}^{(E)1}$ and $\tilde{\mathbf{H}}^{(E)2}$, are of rank 5. Hence, $\tilde{\mathbf{H}}^{(E)1}$ contains a state of self-stress and an inextensional mechanism which have reflection symmetry in plane a, and $\tilde{\mathbf{H}}^{(E)2}$ contains a state of self-stress and an inextensional mechanism which have reflection anti-symmetry in plane a.

From the symmetry analysis it is clear that the original finite mechanism remains in equilibrium block $\tilde{\mathbf{H}}^{(A_1)}$ and hence is not stabilised by any states of self-stress. Now however, it is necessary to see if the remaining three finite mechanisms, which exist in the 3-dimensional vector space of inextensional mechanisms, can be

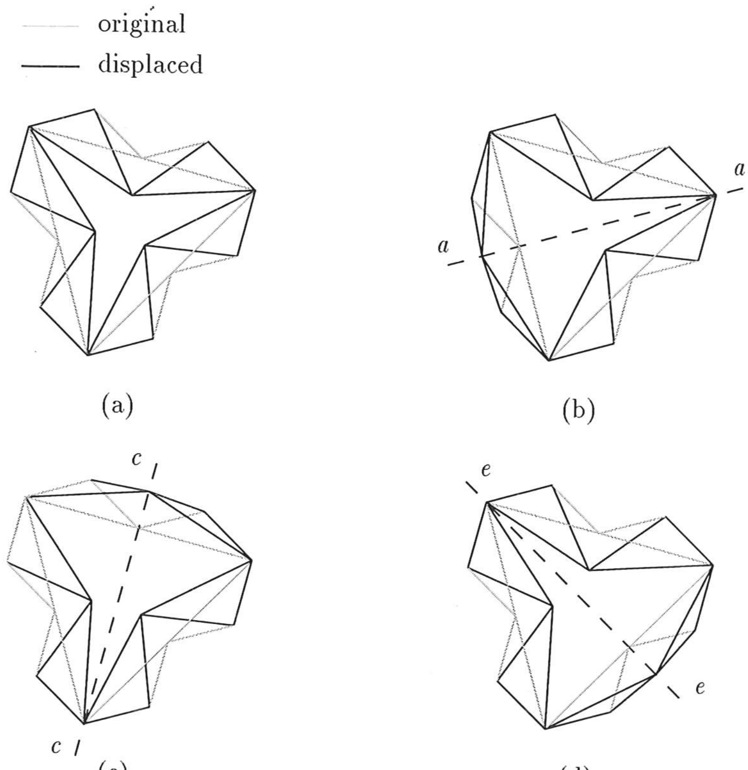

Figure 5.8: Finite mechanisms at the bifurcation point.

identified using symmetry arguments. Kumar's analysis showed that the remaining three finite mechanisms have only reflection symmetry in one of the planes a, c or e. Hence, the following two symmetry operations can be chosen to constitute the symmetry group $\mathbf{C_s}$:

1. The identity, symmetry operation E.

2. Reflection in the vertical plane a, symmetry operation σ_a.

Now the load and bar-force vector spaces $\mathbb{V}_\mathrm{p}$ and $\mathbb{V}_\mathrm{f}$, are each decomposed into two symmetry subspaces, defined by the irreducible representations of symmetry group $\mathbf{C_s}$, shown in Table 5.3. The symmetry subspaces $\mathbb{V}_\mathrm{p}^{(A_1)}$ and $\mathbb{V}_\mathrm{f}^{(A_1)}$ have reflection

$\mathbf{C_s}$	E	σ_a
$\Gamma^{(A_1)}$	1	1
$\Gamma^{(A_2)}$	1	−1

Table 5.3: Irreducible representations of symmetry group $\mathbf{C_s}$.

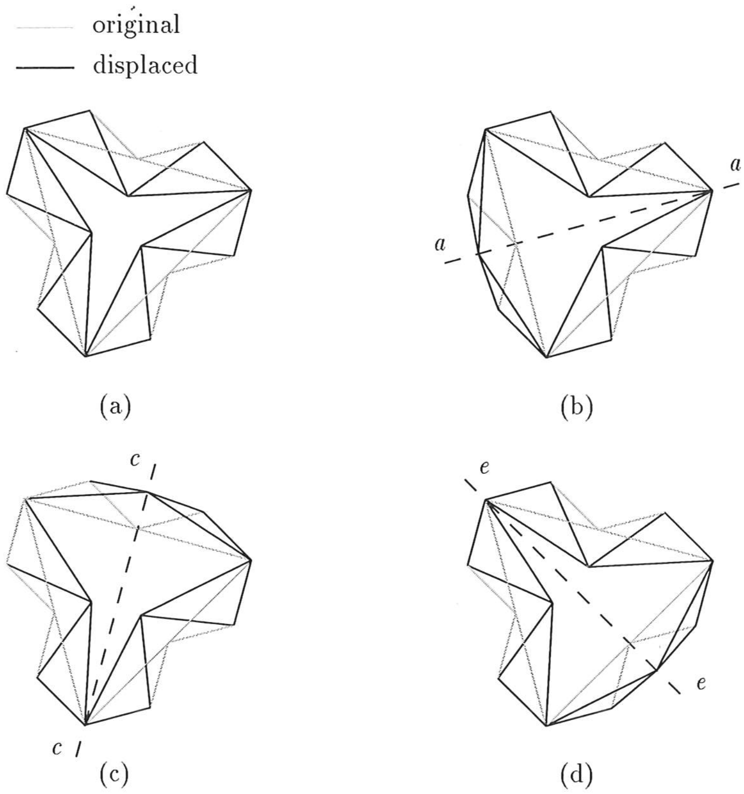

Figure 5.8: Finite mechanisms at the bifurcation point.

identified using symmetry arguments. Kumar's analysis showed that the remaining three finite mechanisms have only reflection symmetry in one of the planes a, c or e. Hence, the following two symmetry operations can be chosen to constitute the symmetry group $\mathbf{C_s}$:

1. The identity, symmetry operation E.

2. Reflection in the vertical plane a, symmetry operation σ_a.

Now the load and bar-force vector spaces $\mathbb{V}_\mathbf{p}$ and $\mathbb{V}_\mathbf{f}$, are each decomposed into two symmetry subspaces, defined by the irreducible representations of symmetry group $\mathbf{C_s}$, shown in Table 5.3. The symmetry subspaces $\mathbb{V}_\mathbf{p}^{(A_1)}$ and $\mathbb{V}_\mathbf{f}^{(A_1)}$ have reflection

$\mathbf{C_s}$	E	σ_a
$\Gamma^{(A_1)}$	1	1
$\Gamma^{(A_2)}$	1	−1

Table 5.3: Irreducible representations of symmetry group $\mathbf{C_s}$.

symmetry in plane a, while the symmetry subspaces $\mathbb{V}_{\mathbf{p}}^{(A_2)}$ and $\mathbb{V}_{\mathbf{f}}^{(A_2)}$ have reflection anti-symmetry in plane a.

Again, it is not necessary to completely reanalyse the structure using symmetry group $\mathbf{C_s}$, Table 5.4 shows how the $\mathbf{C_{3v}}$ symmetry subspaces combine to form the $\mathbf{C_s}$ symmetry subspaces. Using the load and bar-force vector symmetry-adapted coordinate systems with $\mathbf{C_s}$ symmetry properties, the block-diagonalised equilibrium matrix $\tilde{\mathbf{H}}$ now has the form:

$\mathbf{C_s}$		$\mathbf{C_{3v}}$
$\{\mathbb{V}^{(A_1)}\}$	$\Longleftrightarrow$	$\{\mathbb{V}^{(A_1)}, \mathbb{V}^{(E)1}\}$
$\{\mathbb{V}^{(A_2)}\}$	$\Longleftrightarrow$	$\{\mathbb{V}^{(A_2)}, \mathbb{V}^{(E)2}\}$

Table 5.4: Descent of symmetry from symmetry group $\mathbf{C_{3v}}$ to $\mathbf{C_s}$.

$$\tilde{\mathbf{H}} = \begin{bmatrix} \boxed{\begin{matrix} \tilde{\mathbf{H}}^{(A_1)} \\ (10 \times 9) \end{matrix}} & \\ & \boxed{\begin{matrix} \tilde{\mathbf{H}}^{(A_2)} \\ (8 \times 9) \end{matrix}} \end{bmatrix} \tag{5.13}$$

The equilibrium block $\tilde{\mathbf{H}}^{(A_1)}$ is of rank 8 and hence contains a 2-dimensional vector space of inextensional mechanisms and a single state of self-stress, all with reflection symmetry in plane a. The equilibrium block $\tilde{\mathbf{H}}^{(A_2)}$ is of rank 7 and hence contains a single inextensional mechanism and a 2-dimensional vector space of self-stress, all with reflection anti-symmetry in plane a.

In contrast with Section 5.2, symmetry subspace $\mathbb{V}_{\mathbf{f}}^{(A_1)}$ contain a single state of self-stress. Displacing the structure by some finite combination of the two mechanisms in symmetry subspace $\mathbb{V}_{\mathbf{p}}^{(A_1)}$, will cause bar-extensions which have reflection symmetry in plane a. Now however, the state of self-stress may ensure that the only way of correcting these extensions is for the structure to return to its original configuration, thus showing that the combination chosen may not be a finite path.

A way forward appears to be possible because one of the finite mechanisms has already been found. The descent of symmetry from $\mathbf{C_{3v}}$ to $\mathbf{C_s}$ clearly shows that the original finite mechanism shown in Figure 5.8(a), is again in the first symmetry subspace $\mathbb{V}_{\mathbf{p}}^{(A_1)}$. From Kumar's analysis we already know the symmetry properties of the three remaining finite mechanisms and hence the finite mechanism with reflection symmetry in plane a, shown in Figure 5.8(b), must also be contained in $\mathbb{V}_{\mathbf{p}}^{(A_1)}$. However, these two finite mechanisms are in fact not orthogonal, and so this does not help find the second finite path. In this case, finding the other finite paths requires a non-linear analysis.

The remaining two finite mechanisms with reflection symmetry in planes c and e, shown in Figures 5.8(c) and 5.8(d) respectively, are not contained in either $\mathbb{V}_{\mathbf{p}}^{(A_1)}$ or $\mathbb{V}_{\mathbf{p}}^{(A_2)}$. To find symmetry subspaces which contain these finite mechanisms, we must choose the symmetry operations $\{E, \sigma_c\}$ or $\{E, \sigma_e\}$ to constitute the symmetry group $\mathbf{C_s}$. We would then find that the symmetry subspace $\mathbb{V}_{\mathbf{p}}^{(A_1)}$ has reflection symmetry in plane c or e, and hence contain the corresponding finite mechanism.

It should be noted that the $\mathbf{C_{3v}}$ and $\mathbf{C_s}$ symmetry subspaces have combined in this way due to the particular choice of 2-dimensional irreducible representation $\Gamma^{(E)}$, of symmetry group $\mathbf{C_{3v}}$. As explained in Chapter 3, 2-dimensional irreducible representations are not unique (although 1-dimensional irreducible representations are). A different choice could have resulted in symmetry subspaces $\mathbb{V}^{(E)1}$ and $\mathbb{V}^{(E)2}$ having reflection symmetry and anti-symmetry in plane c or e.

5.4 Comments on the Identification of Finite Mechanisms

Section 5.2 has shown that, for some special statically and kinematically indeterminate structures, the identification of a finite mechanism is possible based only on a linear analysis, along with symmetry arguments. However, Section 5.3 has shown that such an analysis cannot always identify all the finite mechanisms in such a structure. This section will identify the conditions under which a finite mechanism can be identified.

The argument put forward in Section 5.2 for the existence of a finite mechanism, is valid when a mechanism exists in symmetry subspace $\mathbb{V}_{\mathbf{p}}^{(A_1)}$, and no states of self-stress exist in the corresponding symmetry subspace $\mathbb{V}_{\mathbf{f}}^{(A_1)}$, i.e. any states of self-stress have "lesser" symmetry properties. In this case, the state of self-stress is always independent of the mechanism and hence can never prevent its motion. The same argument is equally valid for n mechanisms in symmetry subspace $\mathbb{V}_{\mathbf{p}}^{(A_1)}$, and no states of self-stress in symmetry subspace $\mathbb{V}_{\mathbf{f}}^{(A_1)}$. Then these n mechanisms define an n-dimensional space of possible finite mechanisms.

It should be noted that the symmetry analysis does not have to utilise the full symmetry of the structure. Instead, the analysis should be carried out using the symmetry of a mechanism. If this shows that all the states of self-stress in the structure have "lesser" symmetry, then this mechanism will be finite. As shown in Sections 5.2 and 5.3, this analysis can be based on the descent of symmetry, and hence a full reanalysis of the structure is not required.

By contrast, Section 5.3 has shown it is not possible to find *all* the finite mechanisms using a symmetry analysis. If a state of self-stress exists in symmetry subspace $\mathbb{V}_{\mathbf{f}}^{(A_1)}$, then for any particular combination of the inextensional mechanisms in $\mathbb{V}_{\mathbf{p}}^{(A_1)}$, it is not possible to say whether the mechanism would be stiffened by this state of self-stress. In this case, a non-linear analysis is required to find the finite mechanisms.

To summarise, if an analysis is carried out using the symmetry of an inextensional mechanism, and any states of self-stress in the structure have some "lesser" symmetry properties, then this mechanism will be finite.

Chapter 6

Cubic or Higher Symmetry Groups

6.1 Introduction

So far the application of Group Representation Theory has been limited to symmetry groups which are characterised by having only one main axis of symmetry, e.g. symmetry group $\mathbf{C_{3v}}$. However, more complex symmetry groups exist which have more than one main axis of symmetry (These complex symmetry groups are described in Appendix A.2).

If a structure has several n-fold symmetry axes, these must intersect at a point and their spatial arrangement must be such that a rotation C_n about one of the axes results in an interchange of the other axes. This condition severely limits the number of possible symmetry groups which can contain more than one n-fold axis, (Schonland 1965). In fact, these complex symmetry groups define the symmetry of the regular solids, the tetrahedron, cube and icosahedron.

The layout of this chapter is as follows. Section 6.2 analyses a pin-jointed cube with $\mathbf{O_h}$ symmetry properties, to show that Group Representation Theory methods are particularly useful for the analysis of structures with highly complex symmetry. The equilibrium matrix of the pin-jointed cube is block-diagonalised, which greatly simplifies finding and classifying any states of self-stress and inextensional mechanisms present.

The analysis shows that the pin-jointed cube has three internal mechanisms with particular symmetry properties, and Section 6.3 goes on to examine the three internal mechanisms, using the symmetry arguments introduced in Chapter 5, to see if it is possible to identify whether any of the mechanisms are finite.

Chapter 6

Cubic or Higher Symmetry Groups

6.1 Introduction

So far the application of Group Representation Theory has been limited to symmetry groups which are characterised by having only one main axis of symmetry, e.g. symmetry group $\mathbf{C_{3v}}$. However, more complex symmetry groups exist which have more than one main axis of symmetry (These complex symmetry groups are described in Appendix A.2).

If a structure has several n-fold symmetry axes, these must intersect at a point and their spatial arrangement must be such that a rotation C_n about one of the axes results in an interchange of the other axes. This condition severely limits the number of possible symmetry groups which can contain more than one n-fold axis, (Schonland 1965). In fact, these complex symmetry groups define the symmetry of the regular solids, the tetrahedron, cube and icosahedron.

The layout of this chapter is as follows. Section 6.2 analyses a pin-jointed cube with $\mathbf{O_h}$ symmetry properties, to show that Group Representation Theory methods are particularly useful for the analysis of structures with highly complex symmetry. The equilibrium matrix of the pin-jointed cube is block-diagonalised, which greatly simplifies finding and classifying any states of self-stress and inextensional mechanisms present.

The analysis shows that the pin-jointed cube has three internal mechanisms with particular symmetry properties, and Section 6.3 goes on to examine the three internal mechanisms, using the symmetry arguments introduced in Chapter 5, to see if it is possible to identify whether any of the mechanisms are finite.

6.2 Pin-Jointed Cube with O_h Symmetry

A cube is a common and easily recognised structure which has a high degree of symmetry that is often overlooked and rarely fully utilised. In this section a symmetry analysis is carried out on the pin-jointed cube with diagonal supports shown in Figure 6.1, in order to block-diagonalise the equilibrium matrix and classify the different symmetry properties of the cube. This pin-jointed cube consists of $b = 16$

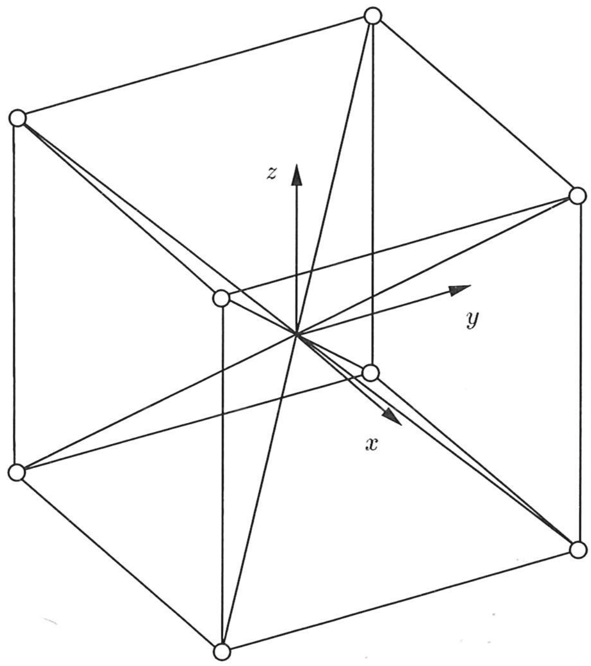

Figure 6.1: Pin-jointed cube with diagonal bars.

bar-elements, $j = 8$ pin-joints and is free to move in 3-dimensional space. The four diagonal bars are not connected at the centre and are free to move adjacent to one another. A real assembly would require these diagonals bars to have small bends around each other. Maxwell's rule for a structure in free space ($b - 3j + 6 = 2$) shows that this pin-jointed cube should require two more bars to be kinematically determinate. However, a previous analysis by Calladine (1978) has shown that it is a tensegrity structure where a single state of self-stress exists which stiffens all the internal inextensional mechanisms present.

A structural analysis shows that the (24×16) equilibrium matrix $\mathbf{H}$ has rank 15. Hence the cube contains $s = 1$ states of self-stress and $m = 9$ inextensional mechanisms. However, this 9-dimensional space of inextensional mechanism must contain the six finite rigid body mechanisms that this unrestrained cube can undergo. Hence, there is only a 3-dimensional space of internal inextensional mechanisms present.

Figure 6.2 shows a cûbe has three 4-fold axes joining the mid-points of opposite faces of the cube; four 3-fold axes along the vertex diagonals; six 2-fold axes joining the mid-points of pairs of opposite edges; six symmetry planes through pairs of opposite edges; three symmetry planes through the centre of the cube parallel to its faces; and a centre of inversion at the centre of the cube.

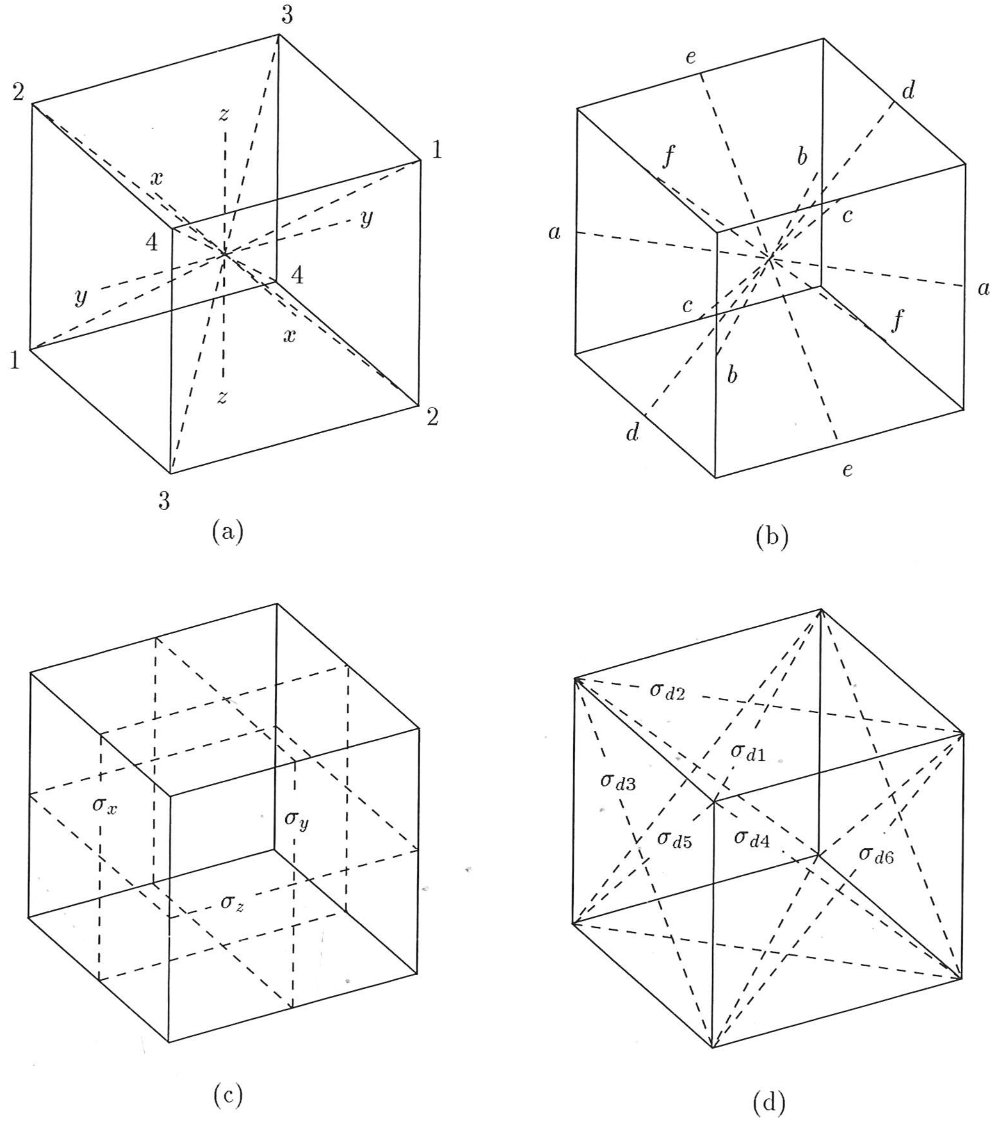

Figure 6.2: Axes and planes of symmetry of a cube, symmetry group $\mathbf{O_h}$: (a) $x \cdots z$ are 4-fold axes of rotation and $1 \cdots 4$ are 3-fold axes of rotation; (b) $a \cdots f$ are 2-fold axes of rotation; (c) $\sigma_x \cdots \sigma_z$ are parallel planes of reflection; (d) $\sigma_{d1} \cdots \sigma_{d6}$ are diagonal planes of reflection.

Hence, a cube can be transformed into an equivalent configuration by the following set of symmetry operations (listed below in their different classes):

1. The identity, symmetry operation E.
2. Rotations by 180° about the x, y and z-axes, symmetry operations $\{C_{2x}, C_{2y}, C_{2z}\}$.
3. Rotations by 90° and 270° about the x, y and z-axes, symmetry operations $\{C_{4x}, C_{4y}, C_{4z}, C_{4x}^3, C_{4y}^3, C_{4z}^3\}$.
4. Rotations by 120° and 240° about the vertex diagonals, symmetry operations $\{C_{31}, C_{32}, C_{33}, C_{34}, C_{31}^2, C_{32}^2, C_{33}^2, C_{34}^2\}$.
5. Rotations by 180° about the edge diagonals, symmetry operations $\{C'_{2a}, C'_{2b}, C'_{2c}, C'_{2d}, C'_{2e}, C'_{2f}\}$.
6. The inversion, symmetry operation i.
7. Improper rotations about the x, y and z-axes, symmetry operations $\{S_{4x}, S_{4y}, S_{4z}, S_{4x}^3, S_{4y}^3, S_{4z}^3\}$.
8. Improper rotations about the vertex diagonals, symmetry operations $\{S_{61}, S_{62}, S_{63}, S_{64}, S_{61}^5, S_{62}^5, S_{63}^5, S_{64}^5\}$.
9. Reflections in planes parallel to the cube faces, symmetry operations $\{\sigma_x, \sigma_y, \sigma_z\}$.
10. Reflections in planes through opposite edges, symmetry operations $\{\sigma_{d1}, \sigma_{d2}, \sigma_{d3}, \sigma_{d4}, \sigma_{d5}, \sigma_{d6}\}$.

These 48 symmetry operations constitute the symmetry group $\mathbf{O_h}$ (the symmetry group of a regular octahedron or cube). There are ten irreducible matrix representations $\{\Gamma^{(A_{1g})}, \Gamma^{(A_{1u})}, \Gamma^{(A_{2g})}, \Gamma^{(A_{2u})}, \Gamma^{(E_g)}, \Gamma^{(E_u)}, \Gamma^{(T_{1g})}, \Gamma^{(T_{1u})}, \Gamma^{(T_{2u})}, \Gamma^{(T_{2u})}\}$ which represent symmetry group $\mathbf{O_h}$; however for clarity only the characters of these irreducible matrix representations are shown in Table 6.1

The characters in Table 6.1 shows that symmetry group $\mathbf{O_h}$ must have a number of 3-dimensional irreducible matrix representations. Symmetry groups which contain more than one main axis of symmetry can have 3-dimensional irreducible matrix representations, which are defined by the symbol T. Appendix B shows how to calculate the actual 2 and 3-dimensional irreducible matrix representations of symmetry group $\mathbf{O_h}$.

Each of the irreducible matrix representations of symmetry group $\mathbf{O_h}$ defines a fundamental aspect of the symmetry of the cube, and can be used to find symmetry-adapted coordinate systems for the external load and internal bar-force vector spaces of the cube. In these symmetry-adapted coordinate systems, both the load and bar-force vector spaces are decomposed into 20 independent symmetry subspaces, each with the particular symmetry properties shown below:

$\mathbf{O_h}$	E	$3C_2$	$8C_3$	$6C_4$	$6C_2'$	i	3σ	$8S_6$	$6S_4$	$6\sigma_d$
A_{1g}	1	1	1	1	1	1	1	1	1	1
A_{2g}	1	1	1	−1	−1	1	1	1	−1	−1
E_g	2	2	−1	0	0	2	2	−1	0	0
T_{1g}	3	−1	0	1	−1	3	−1	0	1	−1
T_{2g}	3	−1	0	−1	1	3	−1	0	−1	1
A_{1u}	1	1	1	1	1	−1	−1	−1	−1	−1
A_{2u}	1	1	1	−1	−1	−1	−1	−1	1	1
E_u	2	2	−1	0	0	−2	−2	1	0	0
T_{1u}	3	−1	0	1	−1	−3	1	0	−1	1
T_{2u}	3	−1	0	−1	1	−3	1	0	1	−1

Table 6.1: Character table of symmetry group $\mathbf{O_h}$.

1. $\mathbb{V}_{\mathbf{p}}^{(A_{1g})}$ and $\mathbb{V}_{\mathbf{f}}^{(A_{1g})}$: symmetry group $\mathbf{O_h}$.

2. $\mathbb{V}_{\mathbf{p}}^{(A_{1u})}$ and $\mathbb{V}_{\mathbf{f}}^{(A_{1u})}$: $\{E, (C_{2x}, C_{2y}, C_{2z}), (C_{4x}, C_{4y}, C_{4z}, C_{4x}^3, C_{4y}^3, C_{4z}^3), (C_{31}, C_{32}, C_{33}, C_{34}, C_{31}^2, C_{32}^2, C_{33}^2, C_{34}^2), (C_{2a}', C_{2b}', C_{2c}', C_{2d}', C_{2e}', C_{2f}')\}$, symmetry group $\mathbf{O}$.

3. $\mathbb{V}_{\mathbf{p}}^{(A_{2g})}$ and $\mathbb{V}_{\mathbf{f}}^{(A_{2g})}$: $\{E, (C_{2x}, C_{2y}, C_{2z}), (C_{31}, C_{32}, C_{33}, C_{34}, C_{31}^2, C_{32}^2, C_{33}^2, C_{34}^2), i, (S_{61}, S_{62}, S_{63}, S_{64}, S_{61}^5, S_{62}^5, S_{63}^5, S_{64}^5), (\sigma_x, \sigma_y, \sigma_z)\}$, symmetry group $\mathbf{T_h}$.

4. $\mathbb{V}_{\mathbf{p}}^{(A_{2u})}$ and $\mathbb{V}_{\mathbf{f}}^{(A_{2u})}$: $\{E, (C_{2x}, C_{2y}, C_{2z}), (C_{31}, C_{32}, C_{33}, C_{34}, C_{31}^2, C_{32}^2, C_{33}^2, C_{34}^2), (S_{4x}, S_{4y}, S_{4z}, S_{4x}^3, S_{4y}^3, S_{4z}^3), (\sigma_{d1}, \sigma_{d2}, \sigma_{d3}, \sigma_{d4}, \sigma_{d5}, \sigma_{d6})\}$, symmetry group $\mathbf{T_d}$.

5. $\mathbb{V}_{\mathbf{p}}^{(E_g)1}$ and $\mathbb{V}_{\mathbf{f}}^{(E_g)1}$: $\{E, C_{2x}, C_{2y}, C_{2z}, i, \sigma_x, \sigma_y, \sigma_z\}$, symmetry group $\mathbf{D_{2h}}$.

6. $\mathbb{V}_{\mathbf{p}}^{(E_g)2}$ and $\mathbb{V}_{\mathbf{f}}^{(E_g)2}$: $\{E, C_{2x}, C_{2y}, C_{2z}, i, \sigma_x, \sigma_y, \sigma_z\}$, symmetry group $\mathbf{D_{2h}}$.

7. $\mathbb{V}_{\mathbf{p}}^{(E_u)1}$ and $\mathbb{V}_{\mathbf{f}}^{(E_u)1}$: $\{E, C_{2x}, C_{2y}, C_{2z}\}$, symmetry group $\mathbf{D_2}$.

8. $\mathbb{V}_{\mathbf{p}}^{(E_u)2}$ and $\mathbb{V}_{\mathbf{f}}^{(E_u)2}$: $\{E, C_{2x}, C_{2y}, C_{2z}\}$, symmetry group $\mathbf{D_2}$.

9. $\mathbb{V}_{\mathbf{p}}^{(T_{1g})1}$ and $\mathbb{V}_{\mathbf{f}}^{(T_{1g})1}$: $\{E, C_{2x}, C_{4x}, C_{4x}^3, i, \sigma_x, S_{4x}, S_{4x}^3\}$, symmetry group $\mathbf{C_{4h}}$.

10. $\mathbb{V}_{\mathbf{p}}^{(T_{1g})2}$ and $\mathbb{V}_{\mathbf{f}}^{(T_{1g})2}$: $\{E, C_{2y}, C_{4y}, C_{4y}^3, i, \sigma_y, S_{4y}, S_{4y}^3\}$, symmetry group $\mathbf{C_{4h}}$.

11. $\mathbb{V}_{\mathbf{p}}^{(T_{1g})3}$ and $\mathbb{V}_{\mathbf{f}}^{(T_{1g})3}$: $\{E, C_{2z}, C_{4z}, C_{4z}^3, i, \sigma_z, S_{4z}, S_{4z}^3\}$, symmetry group $\mathbf{C_{4h}}$.

12. $\mathbb{V}_{\mathbf{p}}^{(T_{1u})1}$ and $\mathbb{V}_{\mathbf{f}}^{(T_{1u})1}$: $\{E, C_{2x}, (C_{4x}, C_{4x}^3), (\sigma_y, \sigma_z), (\sigma_{d4}, \sigma_{d6})\}$, symmetry group $\mathbf{C_{4v}}$.

13. $\mathbb{V}_{\mathbf{p}}^{(T_{1u})2}$ and $\mathbb{V}_{\mathbf{f}}^{(T_{1u})2}$: $\{E,\ C_{2y},\ (C_{4y},\ C_{4y}^3),\ (\sigma_x,\ \sigma_z),\ (\sigma_{d3},\ \sigma_{d5})\}$, symmetry group $\mathbf{C_{4v}}$.
14. $\mathbb{V}_{\mathbf{p}}^{(T_{1u})3}$ and $\mathbb{V}_{\mathbf{f}}^{(T_{1u})3}$: $\{E,\ C_{2z},\ (C_{4z},\ C_{4z}^3),\ (\sigma_x,\ \sigma_y),\ (\sigma_{d1},\ \sigma_{d2})\}$, symmetry group $\mathbf{C_{4v}}$.
15. $\mathbb{V}_{\mathbf{p}}^{(T_{2g})1}$ and $\mathbb{V}_{\mathbf{f}}^{(T_{2g})1}$: $\{E, C_{2x}, C'_{2d}, C'_{2f}, i, \sigma_x, \sigma_{d4}, \sigma_{d6}\}$, symmetry group $\mathbf{D_{2h}}$.
16. $\mathbb{V}_{\mathbf{p}}^{(T_{2g})2}$ and $\mathbb{V}_{\mathbf{f}}^{(T_{2g})2}$: $\{E, C_{2y}, C'_{2c}, C'_{2e}, i, \sigma_y, \sigma_{d3}, \sigma_{d5}\}$, symmetry group $\mathbf{D_{2h}}$.
17. $\mathbb{V}_{\mathbf{p}}^{(T_{2g})3}$ and $\mathbb{V}_{\mathbf{f}}^{(T_{2g})3}$: $\{E, C_{2z}, C'_{2a}, C'_{2b}, i, \sigma_z, \sigma_{d1}, \sigma_{d2}\}$, symmetry group $\mathbf{D_{2h}}$.
18. $\mathbb{V}_{\mathbf{p}}^{(T_{2u})1}$ and $\mathbb{V}_{\mathbf{f}}^{(T_{2u})1}$: $\{E,\ C_{2x},\ (C'_{2d},\ C'_{2f}),\ (\sigma_y,\ \sigma_z),\ (S_{4x},\ S_{4x}^3)\}$, symmetry group $\mathbf{D_{2d}}$.
19. $\mathbb{V}_{\mathbf{p}}^{(T_{2u})2}$ and $\mathbb{V}_{\mathbf{f}}^{(T_{2u})2}$: $\{E,\ C_{2y},\ (C'_{2c},\ C'_{2e}),\ (\sigma_x,\ \sigma_z),\ (S_{4y},\ S_{4y}^3)\}$, symmetry group $\mathbf{D_{2d}}$.
20. $\mathbb{V}_{\mathbf{p}}^{(T_{2u})3}$ and $\mathbb{V}_{\mathbf{f}}^{(T_{2u})3}$: $\{E,\ C_{2z},\ (C'_{2a},\ C'_{2b}),\ (\sigma_x,\ \sigma_y),\ (S_{4z},\ S_{4z}^3)\}$, symmetry group $\mathbf{D_{2d}}$.

The above list shows that the symmetry subspaces corresponding to a particular irreducible representation have the same symmetry properties, that is the symmetry properties of a particular symmetry group, but they are not necessarily defined by the same symmetry operations. For example, symmetry subspaces $\mathbb{V}_{\mathbf{p}}^{(T_{1g})1}$ and $\mathbb{V}_{\mathbf{f}}^{(T_{1g})1}$ have symmetry operations $\{E,\ C_{2x},\ C_{4x},\ C_{4x}^3,\ i,\ \sigma_x,\ S_{4x},\ S_{4x}^3\}$, while symmetry subspaces $\mathbb{V}_{\mathbf{p}}^{(T_{1g})2}$ and $\mathbb{V}_{\mathbf{f}}^{(T_{1g})2}$ have symmetry operations $\{E,\ C_{2y},\ C_{4y},\ C_{4y}^3,\ i,\ \sigma_y,\ S_{4y},\ S_{4y}^3\}$, but both sets of symmetry operations constitute symmetry group $\mathbf{C_{4h}}$. The symmetry properties of the different vector symmetry subspaces are illustrated graphically in the next section.

Note that a different choice of basis vectors for the 2 and 3-dimensional irreducible matrix representations $\{\Gamma^{(E_g)}, \Gamma^{(E_u)}, \Gamma^{(T_{1g})}, \Gamma^{(T_{1u})}, \Gamma^{(T_{2g})}, \Gamma^{(T_{u2})}\}$ (i.e. equivalent irreducible matrix representations) would have resulted in symmetry subspaces with the exactly the same symmetry properties, only with rotation symmetry about different axes and reflection symmetry in different planes. Hence, the block-diagonal form of the equilibrium matrix $\tilde{\mathbf{H}}$ found in the next section, is unaffected by the choice of equivalent irreducible matrix representations.

6.2.1 Block-Diagonalised Equilibrium Matrix using $\mathbf{O_h}$ Symmetry

Using these load and bar-force symmetry-adapted coordinate systems with $\mathbf{O_h}$ symmetry properties, the block-diagonalised equilibrium matrix $\tilde{\mathbf{H}}$ of the pin-jointed cube will have the form:

$$\tilde{\mathbf{H}} = \begin{bmatrix}
\tilde{\mathbf{H}}^{(A_{1g})}\,(1\times 2),\ s=1 \\
\tilde{\mathbf{H}}^{(A_{2u})}\,(1\times 0),\ m=1 \\
\tilde{\mathbf{H}}^{(E_g)1}\,(1\times 1) \\
\tilde{\mathbf{H}}^{(E_u)1}\,(1\times 0),\ m=1 \\
\tilde{\mathbf{H}}^{(E_g)2}\,(1\times 1) \\
\tilde{\mathbf{H}}^{(E_u)2}\,(1\times 0),\ m=1 \\
\tilde{\mathbf{H}}^{(T_{1g})1}\,(1\times 0),\ m=1 \\
\tilde{\mathbf{H}}^{(T_{1u})1}\,(2\times 1),\ m=1 \\
\tilde{\mathbf{H}}^{(T_{1g})2}\,(1\times 0),\ m=1 \\
\tilde{\mathbf{H}}^{(T_{1u})2}\,(2\times 1),\ m=1 \\
\tilde{\mathbf{H}}^{(T_{1g})3}\,(1\times 0),\ m=1 \\
\tilde{\mathbf{H}}^{(T_{1u})3}\,(2\times 1),\ m=1 \\
\tilde{\mathbf{H}}^{(T_{2g})1}\,(2\times 2) \\
\tilde{\mathbf{H}}^{(T_{2u})1}\,(1\times 1) \\
\tilde{\mathbf{H}}^{(T_{2g})2}\,(2\times 2) \\
\tilde{\mathbf{H}}^{(T_{2u})2}\,(1\times 1) \\
\tilde{\mathbf{H}}^{(T_{2g})3}\,(2\times 2) \\
\tilde{\mathbf{H}}^{(T_{2u})3}\,(1\times 1)
\end{bmatrix} \tag{6.1}$$

Each of the equilibrium blocks is of full rank. Equation 6.1 shows that the state of self stress exists in the first block, and an inextensional mechanism exists in each of the next nine blocks. However, the six finite rigid body mechanisms can be identified using standard structural procedures (Pellegrino & Calladine 1986) and are contained in the blocks corresponding to irreducible matrix representations $\Gamma^{(T_{1g})}$ and $\Gamma^{(T_{1u})}$. Hence, it is clear that an internal inextensional mechanism exists in each of the symmetry subspaces $\mathbb{V}_{\mathrm{p}}^{(A_{2u})}$, $\mathbb{V}_{\mathrm{p}}^{(E_u)1}$ and $\mathbb{V}_{\mathrm{p}}^{(E_u)2}$. These internal inextensional mechanisms are investigated further in Section 6.3, to see if it is possible to identify whether they are finite or infinitesimal using symmetry arguments alone. Note that Equation 6.1 does not show blocks $\tilde{\mathbf{H}}^{(A_{1u})}$ and $\tilde{\mathbf{H}}^{(A_{2g})}$ because they are (0×0) blocks, i.e. the load and bar-force vector spaces of this structure do not contain any vectors which have symmetry properties corresponding to either of these blocks.

The high degree of symmetry of the cube is reflected in the block-diagonal form of the equilibrium matrix. Not only has the analysis been reduced to matrix blocks no larger than (2×2), bût it has also greatly simplified finding and classifying both the internal and rigid body mechanism. The block-diagonal equilibrium matrix shows that all nine inextensional mechanisms, internal as well as rigid body, exist independently and have particular symmetry properties.

In order to illustrate the different symmetry properties that the $\mathbf{O_h}$ symmetry subspaces have, Figures 6.3 to 6.10 show the deformed shapes and displacements of the pin-jointed cube from each of the different displacement vector symmetry subspaces $\mathbb{V}_{\mathbf{P}}^{(\mu)i}$. Together, these are all the possible deformations and displacements of the pin-jointed cube due to both extensional and inextensional displacements of some finite length. In all cases the diagonal supports of the pin-jointed cube are not shown for clarity.

Each of the Figures 6.5 to 6.10 show the deformed pin-jointed structure has a number of identical shapes which are orientated about different axes. The different orientations of these identical shapes correspond to the different rows of a particular irreducible representations $\Gamma^{(\mu)}$ of symmetry group $\mathbf{O_h}$. Section 6.2 showed that the different rows of the 2 and 3-dimensional irreducible representations define independent symmetry subspaces with identical symmetry properties; however the particular symmetry operations may occur about different axes and in different planes. Thus, it is possible for the i symmetry subspaces $\mathbb{V}_{\mathbf{P}}^{(\mu)i}$ corresponding to irreducible representation $\Gamma^{(\mu)}$, to contain displacements which deform the structure into an identical shape.

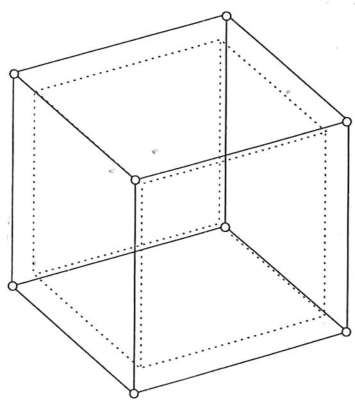

Figure 6.3: Deformed structure with $\mathbf{O_h}$ symmetry, due to the extensional displacement from symmetry subspace $\mathbb{V}_{\mathbf{P}}^{(A_{1g})}$. The dotted lines show the original position of the structure. The cube has been magnified and hence no symmetry has been lost.

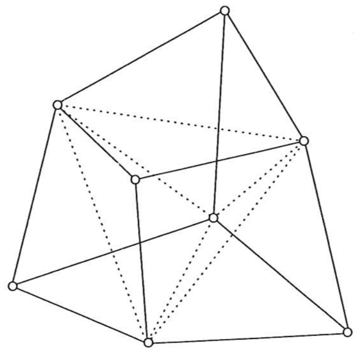

Figure 6.4: Deformed structure with $\mathbf{T_d}$ symmetry, due to the inextensional displacement from symmetry subspace $\mathbb{V}_{\mathbf{P}}^{(A_{2u})}$. The dotted lines represent folds in previously plane faces.

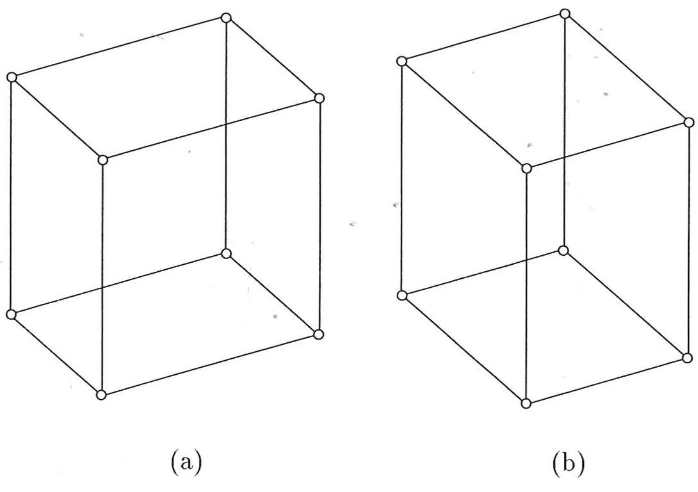

Figure 6.5: Deformed structures with $\mathbf{D_{2h}}$ symmetry $\{E, C_{2x}, C_{2y}, C_{2z}, i, \sigma_x, \sigma_y, \sigma_z\}$, due to the extensional displacement from symmetry subspaces: (a) $\mathbb{V}_{\mathbf{P}}^{(E_g)1}$; (b) $\mathbb{V}_{\mathbf{P}}^{(E_g)2}$.

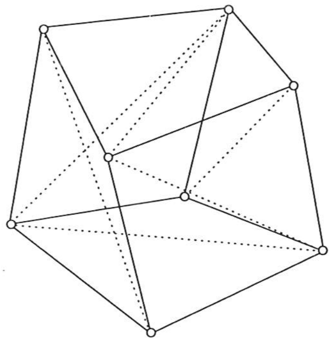

(a) (b)

Figure 6.6: Deformed structures with $\mathbf{D_2}$ symmetry $\{E,\ C_{2x}, C_{2y}, C_{2z}\}$, due to the inextensional displacement from symmetry subspaces: (a) $\mathbb{V}_{\mathbf{P}}^{(E_u)1}$; (b) $\mathbb{V}_{\mathbf{P}}^{(E_u)2}$. The dotted lines represent folds in previously plane faces.

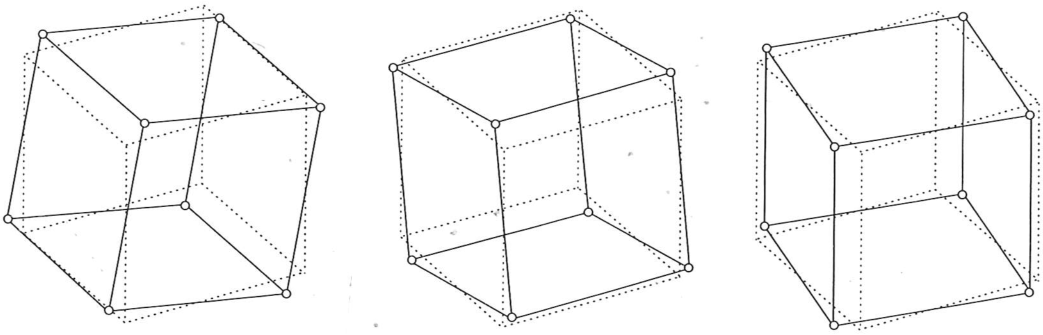

(a) (b) (c)

Figure 6.7: Undeformed structures with $\mathbf{C_{4h}}$ symmetry, due to the inextensional displacement from symmetry subspaces: (a) $\mathbb{V}_{\mathbf{P}}^{(T_{1g})1}$; (b) $\mathbb{V}_{\mathbf{P}}^{(T_{1g})2}$; (c) $\mathbb{V}_{\mathbf{P}}^{(T_{1g})3}$. These inextensional displacements are the three finite rigid body rotations about the x, y and z-axes (the structure is reduced to $\mathbf{C_{4h}}$ symmetry with respect to the original set of axes and planes shown in Figure 6.2). The dotted lines show the original position of the structure.

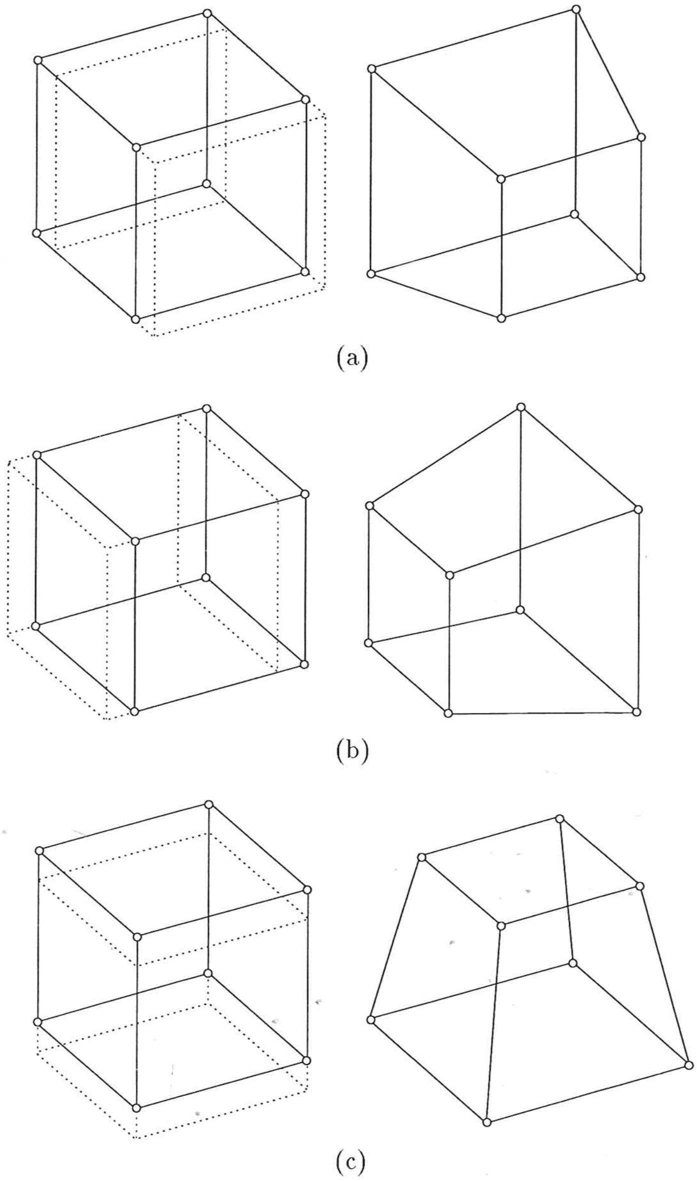

Figure 6.8: (a) Undeformed and deformed structures with $\mathbf{C_{4v}}$ symmetry, due to the inextensional and extensional displacements from symmetry subspaces: (a) $\mathbb{V}_{\mathbf{P}}^{(T_{1u})1}$; (b) $\mathbb{V}_{\mathbf{P}}^{(T_{1u})2}$; (c) $\mathbb{V}_{\mathbf{P}}^{(T_{1u})3}$. These inextensional displacements are the three finite rigid body displacements along the x, y and z-axes (the structure is reduced to $\mathbf{C_{4v}}$ symmetry with respect to the original set of axes and planes shown in Figure 6.2). The dotted lines show the original position of the structure.

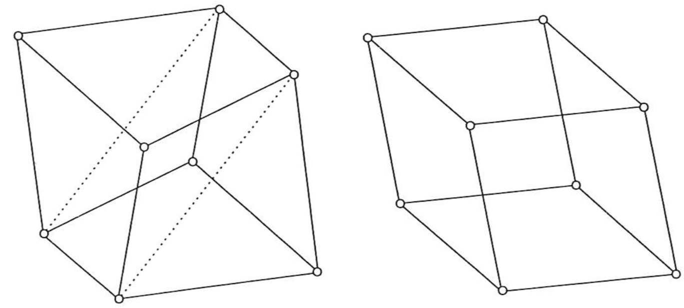

(a)

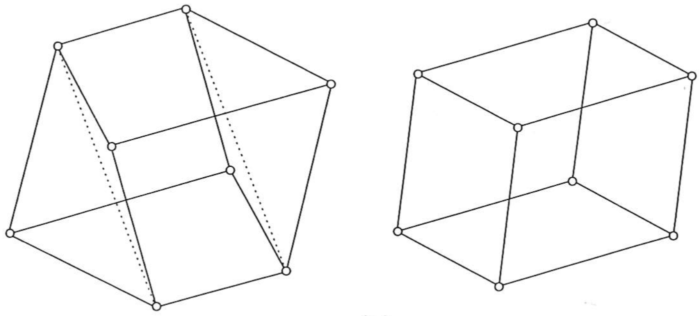

(b)

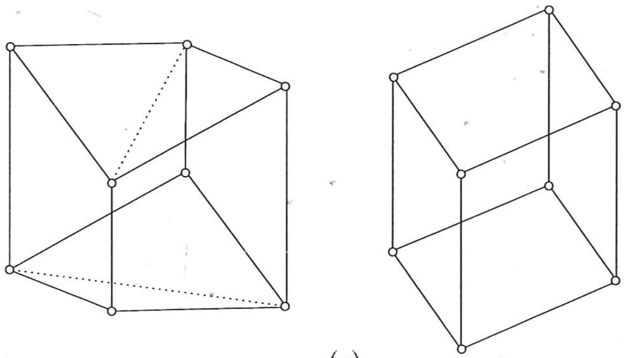

(c)

Figure 6.9: Deformed structures with $\mathbf{D_{2h}}$ symmetry, due to extensional displacements from symmetry subspaces: (a) $\mathbb{V}_{\mathbf{P}}^{(T_{2g})1}$; (b) $\mathbb{V}_{\mathbf{P}}^{(T_{2g})2}$; (c) $\mathbb{V}_{\mathbf{P}}^{(T_{2g})3}$. The dotted lines represent folds in previously plane faces.

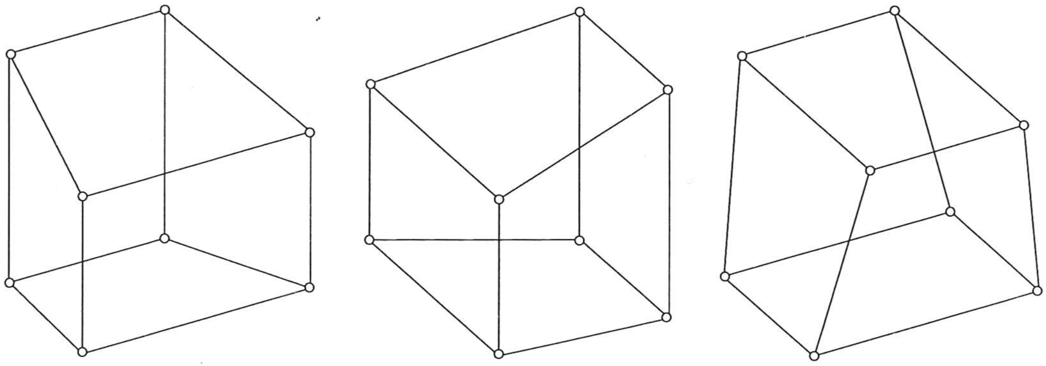

Figure 6.10: Deformed structures with $\mathbf{D_{2d}}$ symmetry, due to extensional displacements from symmetry subspaces: (a) $\mathbb{V}_{\mathbf{P}}^{(T_{2u})1}$; (b) $\mathbb{V}_{\mathbf{P}}^{(T_{2u})2}$; (c) $\mathbb{V}_{\mathbf{P}}^{(T_{2u})3}$.

6.3 Analysis of the Internal Mechanisms

In the previous section the equilibrium matrix of the pin-jointed cube shown in Figure 6.1, was block-diagonalised using $\mathbf{O_h}$ symmetry-adapted coordinate systems. The analysis showed that the pin-jointed cube contains three internal inextensional mechanisms, shown in Figures 6.4 and 6.6, and each of these mechanisms exists independently with particular symmetry properties. Of interest is whether these three mechanisms are finite or infinitesimal. Chapter 5 has shown that in some cases it is possible to identify finite mechanisms using symmetry arguments alone, and in a similar way these three mechanisms will be analysed to see if it is possible to identify any finite mechanisms.

So far the analysis of the pin-jointed cube has been carried out using $\mathbf{O_h}$ symmetry. However once one of the inextensional mechanisms is mobilised the structure will immediately lose its cube shape, i.e. lose its $\mathbf{O_h}$ symmetry, and hence the $\mathbf{O_h}$ symmetry analysis becomes invalid. The structure will instead take on the symmetry properties of the mechanism, thus in order to make further progress it is necessary to reanalyse the structure using the particular symmetry of each of the three mechanisms.

6.3.1 Block-Diagonalised Equilibrium Matrix using $\mathbf{T_d}$ Symmetry

If the mechanism in equilibrium block $\tilde{\mathbf{H}}^{(A_{2u})}$ of Equation 6.1 is mobilised, the structure is immediately reduced to $\mathbf{T_d}$ symmetry properties. These symmetry properties are defined by the irreducible representations of symmetry group $\mathbf{T_d}$, whose characters are shown in Table 6.2. Now the equilibrium matrix must be block-

$\mathbf{T_d}$	E	$3C_2$	$8C_3$	$6S_4$	$6\sigma_d$
A_1	1	1	1	1	1
A_2	1	1	1	−1	−1
E	2	2	−1	0	0
T_1	3	−1	0	1	−1
T_2	3	−1	0	−1	1

Table 6.2: Character table of symmetry group $\mathbf{T_d}$.

diagonalised using $\mathbf{T_d}$ symmetry-adapted coordinate systems. Table 6.3 shows a descent of symmetry from $\mathbf{O_h}$ to $\mathbf{T_d}$ symmetry, from which the ten $\mathbf{T_d}$ symmetry subspaces can be simply constructed. The symmetry properties of these load and

$\mathbf{T_d}$		$\mathbf{O_h}$
$\{\mathbb{V}^{(A_1)}\}$	$\Longleftrightarrow$	$\{\mathbb{V}^{(A_{1g})}, \mathbb{V}^{(A_{2u})}\}$
$\{\mathbb{V}^{(A_2)}\}$	$\Longleftrightarrow$	$\{\mathbb{V}^{(A_{2g})}, \mathbb{V}^{(A_{1u})}\}$
$\{\mathbb{V}^{(E)1}\}$	$\Longleftrightarrow$	$\{\mathbb{V}^{(E_g)1}, \mathbb{V}^{(E_u)2}\}$
$\{\mathbb{V}^{(E)2}\}$	$\Longleftrightarrow$	$\{\mathbb{V}^{(E_g)2}, \mathbb{V}^{(E_u)1}\}$
$\{\mathbb{V}^{(T_1)1}\}$	$\Longleftrightarrow$	$\{\mathbb{V}^{(T_{1g})1}, \mathbb{V}^{(T_{2u})1}\}$
$\{\mathbb{V}^{(T_1)2}\}$	$\Longleftrightarrow$	$\{\mathbb{V}^{(T_{1g})2}, \mathbb{V}^{(T_{2u})2}\}$
$\{\mathbb{V}^{(T_1)3}\}$	$\Longleftrightarrow$	$\{\mathbb{V}^{(T_{1g})3}, \mathbb{V}^{(T_{2u})3}\}$
$\{\mathbb{V}^{(T_2)1}\}$	$\Longleftrightarrow$	$\{\mathbb{V}^{(T_{2g})1}, \mathbb{V}^{(T_{1u})1}\}$
$\{\mathbb{V}^{(T_2)2}\}$	$\Longleftrightarrow$	$\{\mathbb{V}^{(T_{2g})2}, \mathbb{V}^{(T_{1u})2}\}$
$\{\mathbb{V}^{(T_2)3}\}$	$\Longleftrightarrow$	$\{\mathbb{V}^{(T_{2g})3}, \mathbb{V}^{(T_{1u})3}\}$

Table 6.3: Descent of symmetry from symmetry group $\mathbf{O_h}$ to $\mathbf{T_d}$.

bar-force vector symmetry subspaces are described below, with reference to the axes and planes of symmetry defined in Figure 6.2.

1. $\mathbb{V}_{\mathbf{p}}^{(A_1)}$ and $\mathbb{V}_{\mathbf{f}}^{(A_1)}$: 2-fold rotational symmetry about the x, y and z-axes, 3-fold rotational symmetry about the vertex diagonals, improper rotations about the x, y and z-axes and reflection symmetry in the six diagonal planes, symmetry group $\mathbf{T_d}$.

2. $\mathbb{V}_{\mathbf{p}}^{(A_2)}$ and $\mathbb{V}_{\mathbf{f}}^{(A_2)}$: 2-fold rotational symmetry about the x, y and z-axes and 3-fold rotational symmetry about the vertex diagonals, symmetry group $\mathbf{T}$.

3. $\mathbb{V}_{\mathbf{p}}^{(E)1}$ and $\mathbb{V}_{\mathbf{f}}^{(E)1}$: 2-fold rotational symmetry about the x, y and z-axes, symmetry group $\mathbf{D_2}$.

4. $\mathbb{V}_{\mathbf{p}}^{(E)2}$ and $\mathbb{V}_{\mathbf{f}}^{(E)2}$: 2-fold rotational symmetry about the x, y and z-axes, symmetry group $\mathbf{D_2}$.

5. $\mathbb{V}_{\mathbf{p}}^{(T_1)1}$ and $\mathbb{V}_{\mathbf{f}}^{(T_1)1}$: 4-fold improper rotational symmetry about the x-axis, symmetry group $\mathbf{S_4}$.

6. $\mathbb{V}_{\mathbf{p}}^{(T_1)2}$ and $\mathbb{V}_{\mathbf{f}}^{(T_1)2}$: 4-fold improper rotational symmetry about the y-axis, symmetry group $\mathbf{S_4}$.

7. $\mathbb{V}_{\mathbf{p}}^{(T_1)3}$ and $\mathbb{V}_{\mathbf{f}}^{(T_1)3}$: 4-fold improper rotational symmetry about the z-axis, symmetry group $\mathbf{S_4}$.

8. $\mathbb{V}_{\mathbf{p}}^{(T_2)1}$ and $\mathbb{V}_{\mathbf{f}}^{(T_2)1}$: 2-fold rotational symmetry about the x-axis, and reflection symmetry in diagonal planes 4 and 6, symmetry group $\mathbf{C_{2v}}$.

9. $\mathbb{V}_{\mathbf{p}}^{(T_2)2}$ and $\mathbb{V}_{\mathbf{f}}^{(T_2)2}$: 2-fold rotational symmetry about the y-axis, and reflection symmetry in diagonal planes 3 and 5, symmetry group $\mathbf{C_{2v}}$.

10. $\mathbb{V}_{\mathbf{p}}^{(T_2)3}$ and $\mathbb{V}_{\mathbf{f}}^{(T_2)3}$: 2-fold rotational symmetry about the z-axis, and reflection symmetry in diagonal planes 1 and 2, symmetry group $\mathbf{C_{2v}}$.

Thus, using the load and bar-force vector symmetry-adapted coordinate systems with $\mathbf{T_d}$ symmetry properties, the block-diagonalised equilibrium matrix $\tilde{\mathbf{H}}$ now has the form:

$$\tilde{\mathbf{H}} = \begin{bmatrix} \boxed{\tilde{\mathbf{H}}^{(A_1)}\ (2\times2),\ s=1 \text{ and } m=1} & & & & & & & & \\ & \boxed{\tilde{\mathbf{H}}^{(E)1}\ (2\times1),\ m=1} & & & & & & & \\ & & \boxed{\tilde{\mathbf{H}}^{(E)2}\ (2\times1),\ m=1} & & & & & & \\ & & & \boxed{\tilde{\mathbf{H}}^{(T_1)1}\ (2\times1),\ m=1} & & & & & \\ & & & & \boxed{\tilde{\mathbf{H}}^{(T_1)2}\ (2\times1),\ m=1} & & & & \\ & & & & & \boxed{\tilde{\mathbf{H}}^{(T_1)3}\ (2\times1),\ m=1} & & & \\ & & & & & & \boxed{\begin{matrix}\tilde{\mathbf{H}}^{(T_2)1}\\ (4\times3)\\ m=1\end{matrix}} & & \\ & & & & & & & \boxed{\begin{matrix}\tilde{\mathbf{H}}^{(T_2)2}\\ (4\times3)\\ m=1\end{matrix}} & \\ & & & & & & & & \boxed{\begin{matrix}\tilde{\mathbf{H}}^{(T_2)3}\\ (4\times3)\\ m=1\end{matrix}} \end{bmatrix} \tag{6.2}$$

Equation 6.2 shows that the mechanism with $\mathbf{T_d}$ symmetry now exists in the first equilibrium block with the state of self-stress, and it is not possible to say using symmetry arguments alone whether the mechanism would be stiffened by this state of self stress. However, a *product-force* vector analysis (Pellegrino & Calladine 1986) shows that this mechanism is in fact first-order infinitesimal, i.e. the state of self-stress imparts first-order stiffness when the mechanism is displaced. Note that Equation 6.2 does not show block $\tilde{\mathbf{H}}^{(A_2)}$ because it is a (0×0) block.

Figure 6.11 shows a linear displacement of the pin-jointed structure in the direction of this mechanism. The diagonal supports are not shown for clarity and the dotted lines represent folds in the previously plane faces. The $\mathbf{T_d}$ symmetry of the structure is clearly distinguishable from the $\mathbf{O_h}$ symmetry of the structure in Figure 6.1.

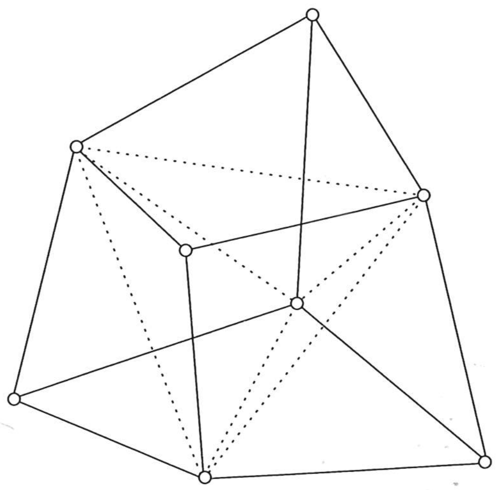

Figure 6.11: Pin-jointed structure with $\mathbf{T_d}$ symmetry, the diagonal supports are not shown.

6.3.2 Block-Diagonalised Equilibrium Matrix using $\mathbf{D_2}$ Symmetry

If the mechanism in either equilibrium block $\tilde{\mathbf{H}}^{(E_u)1}$ or $\tilde{\mathbf{H}}^{(E_u)2}$ of Equation 6.1 is mobilised the structure is immediately reduced to $\mathbf{D_2}$ symmetry properties in both cases. These symmetry properties are defined by the irreducible matrix representations of symmetry group $\mathbf{D_2}$, shown in Table 6.4.

Now the equilibrium matrix must be block-diagonalised using $\mathbf{D_2}$ symmetry-adapted coordinate systems. Table 6.5 shows a descent of symmetry from $\mathbf{O_h}$ to $\mathbf{D_2}$ symmetry, from which the four $\mathbf{D_2}$ symmetry subspaces can be simply constructed.

$\mathbf{D_2}$	E	C_{2x}	C_{2y}	C_{2z}
$\Gamma^{(A)}$	1	1	1	1
$\Gamma^{(B_1)}$	1	−1	−1	1
$\Gamma^{(B_2)}$	1	−1	1	−1
$\Gamma^{(B_3)}$	1	1	−1	−1

Table 6.4: Irreducible matrix representations of symmetry group $\mathbf{T_d}$.

$\mathbf{D_2}$		$\mathbf{O_h}$
$\{\mathbb{V}^{(A)}\}$	$\Longleftrightarrow$	$\left\{ \begin{array}{c} \mathbb{V}^{(A_{1g})}, \mathbb{V}^{(A_{1u})}, \mathbb{V}^{(A_{2g})}, \mathbb{V}^{(A_{2u})}, \\ \mathbb{V}^{(E_g)1}, \mathbb{V}^{(E_g)2}, \mathbb{V}^{(E_u)1}, \mathbb{V}^{(E_u)2} \end{array} \right\}$
$\{\mathbb{V}^{(B_1)}\}$	$\Longleftrightarrow$	$\{\mathbb{V}^{(T_{1g})3}, \mathbb{V}^{(T_{2g})3}, \mathbb{V}^{(T_{1u})3}, \mathbb{V}^{(T_{2u})3}\}$
$\{\mathbb{V}^{(B_2)}\}$	$\Longleftrightarrow$	$\{\mathbb{V}^{(T_{1g})2}, \mathbb{V}^{(T_{2g})2}, \mathbb{V}^{(T_{1u})2}, \mathbb{V}^{(T_{2u})2}\}$
$\{\mathbb{V}^{(B_3)}\}$	$\Longleftrightarrow$	$\{\mathbb{V}^{(T_{1g})1}, \mathbb{V}^{(T_{2g})1}, \mathbb{V}^{(T_{1u})1}, \mathbb{V}^{(T_{2u})1}\}$

Table 6.5: Descent of symmetry from symmetry group $\mathbf{O_h}$ to $\mathbf{D_2}$.

The symmetry properties of these load and bar-force vector symmetry subspaces are described below, with reference to the axes and planes of symmetry defined in Figure 6.2.

1. $\mathbb{V}_{\mathbf{p}}^{(A)}$ and $\mathbb{V}_{\mathbf{f}}^{(A)}$: 2-fold rotational symmetry about the x, y and z-axes, symmetry group $\mathbf{D_2}$.
2. $\mathbb{V}_{\mathbf{p}}^{(B_1)}$ and $\mathbb{V}_{\mathbf{f}}^{(B_1)}$: 2-fold rotational symmetry about the z-axis, symmetry group $\mathbf{C_2}$.
3. $\mathbb{V}_{\mathbf{p}}^{(B_2)}$ and $\mathbb{V}_{\mathbf{f}}^{(B_2)}$: 2-fold rotational symmetry about the y-axis, symmetry group $\mathbf{C_2}$.
4. $\mathbb{V}_{\mathbf{p}}^{(B_3)}$ and $\mathbb{V}_{\mathbf{f}}^{(B_3)}$: 2-fold rotational symmetry about the x-axis, symmetry group $\mathbf{C_2}$.

Thus, using the load and bar-force vector symmetry-adapted coordinate systems with $\mathbf{D_2}$ symmetry properties, the block-diagonalised equilibrium matrix $\tilde{\mathbf{H}}$ now has the form shown in Equation 6.3. The two mechanisms with $\mathbf{D_2}$ symmetry now exist in the first equilibrium block with the state of self-stress, and it is not possible to say using symmetry arguments alone whether either mechanism would be stiffened by this state of self stress. However, a *product-force* vector analysis (Pellegrino & Calladine 1986) shows that both mechanisms are in fact first-order infinitesimal. Note that the mechanism with $\mathbf{T_d}$ symmetry also exists in the first equilibrium block, this can be seen from either Equation 6.3 or the descent of symmetry in Table 6.5.

$$\tilde{\mathbf{H}} = \begin{bmatrix} \boxed{\begin{matrix}\tilde{\mathbf{H}}^{(A)}\\(6\times4)\\s=1\\m=3\end{matrix}} & & & \\ & \boxed{\begin{matrix}\tilde{\mathbf{H}}^{(B_1)}\\(6\times4)\\m=2\end{matrix}} & & \\ & & \boxed{\begin{matrix}\tilde{\mathbf{H}}^{(B_2)}\\(6\times4)\\m=2\end{matrix}} & \\ & & & \boxed{\begin{matrix}\tilde{\mathbf{H}}^{(B_3)}\\(6\times4)\\m=2\end{matrix}} \end{bmatrix} \tag{6.3}$$

Figure 6.12(a) and (b) show linear displacements of the pin-jointed structure in the direction of the two mechanisms from blocks $\tilde{\mathbf{H}}^{(E_u)1}$ and $\tilde{\mathbf{H}}^{(E_u)2}$ of Equation 6.1. The diagonal supports are not shown for clarity and the dotted lines represent folds in the previously plane faces. The $\mathbf{D_2}$ symmetry of the structure is clearly distinguishable from both the $\mathbf{T_d}$ symmetry of the structure in Figure 6.11 and the $\mathbf{O_h}$ symmetry of the structure in Figure 6.1.

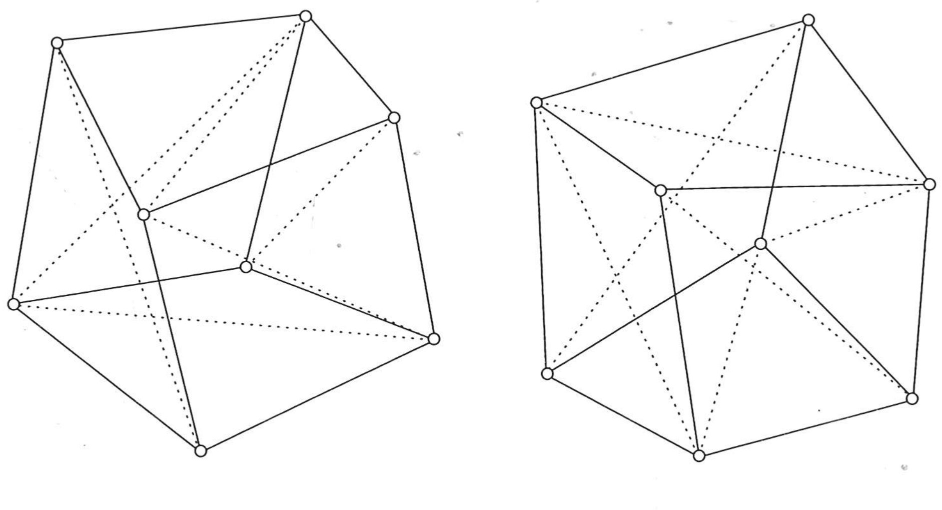

(a) (b)

Figure 6.12: Pin-jointed structure with $\mathbf{D_2}$ symmetry, the diagonal supports are not shown.

Chapter 7

Frame Structures

7.1 Introduction

The pin-jointed examples that have been analysed so far can only carry axial forces, referred to as the "bar-forces". The same ideas can be easily extended to more general *beam-elements*, which can also carry shear forces and bending moments. The techniques used to analyse the equilibrium, compatibility and flexibility equations for pin-jointed structures are equally suited to the analysis of frames made up of these beam-elements.

In this chapter, the analysis of symmetric structures using Group Representation Theory is extended to included frames made up of beam-elements, and connected by *rigid joints*, i.e. moment-resisting joints instead of pin-joints. These frames are also subject to both external loads and couples applied at the joints. The rest of this section gives an introduction to the analysis of these frames. In Section 7.2 a symmetry analysis of a simple frame is carried out to show how more general loads and forces can also be decomposed into components with particular symmetry properties, hence block-diagonalising the equilibrium matrix of the frame. Then Section 7.3 analyses two statically and kinematically indeterminate frames with interesting behaviour, and uses symmetry arguments to show that both frames contain finite mechanisms.

For a 3-dimensional frame, a moment-resisting joint between any two beam-elements is capable of transmitting the following forces and moments:

- axial force.
- shear forces along the two principal axes.
- torsional moment.
- bending moments about the two principal axes.

In order to carry out the symmetry analysis, internal and external vector spaces must be defined for the rigid frame. A typical straight beam-element in 3-dimensional space is shown in Figure 7.1. The beam has six degrees of freedom at each end

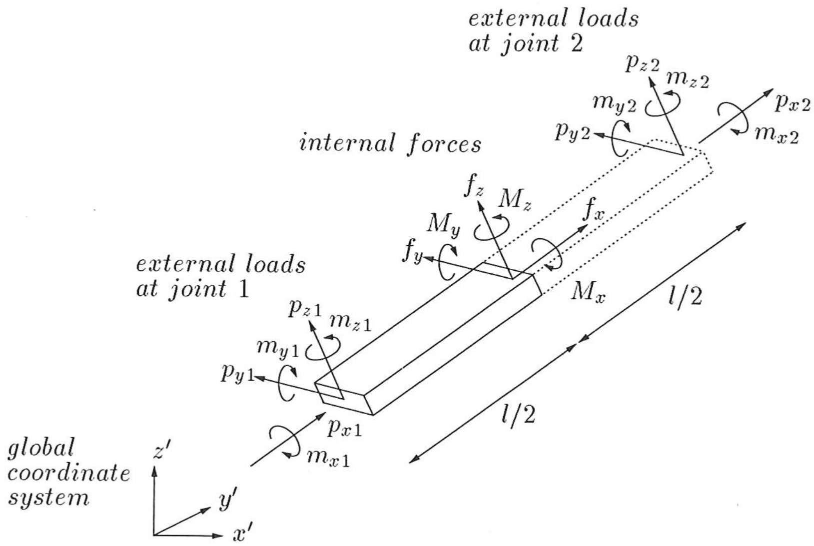

Figure 7.1: Beam-element in 3-dimensional space, with coordinate systems for the internal force and external load vector spaces.

joint, consisting of three linear displacements and three rotations. Thus, in order to ensure elemental equilibrium, external load vectors are required which define the loads p and couples m associated with particular degrees of freedom. A local coordinate system for the external loads and couples acting on a beam-element is shown in Figure 7.1, and hence the external load vector acting on joint i can be defined in this coordinate system as:

$$\mathbf{p}_i = [p_{xi}\ p_{yi}\ p_{zi}\ m_{xi}\ m_{yi}\ m_{zi}]^T \tag{7.1}$$

The corresponding displacement vector at joint i occupies the same local coordinate system as the load vector, and defines the joint displacements d and joint rotations θ:

$$\mathbf{d}_i = [d_{xi}\ d_{yi}\ d_{zi}\ \theta_{xi}\ \theta_{yi}\ \theta_{zi}]^T \tag{7.2}$$

Together, the load or displacement vectors acting at each joint define the external vector space $\mathbb{V}_\mathrm{p}$ of the frame.

Also shown in Figure 7.1 is a local coordinate system for the internal force vector, which defines the beam-forces f and bending moments M acting at the centre of each beam-element. Hence, the internal force vector of beam-element i is:

$$\mathbf{f}_i = [f_{xi}\ f_{yi}\ f_{zi}\ M_{xi}\ M_{yi}\ M_{zi}]^T \tag{7.3}$$

The corresponding deformation vector of beam-element i occupies the same coordinate system as the force vector, and defines the beam-elongations e and the relative rotations ϕ between the two end joints:

$$\mathbf{e}_i = [e_{xi}\ e_{yi}\ e_{zi}\ \phi_{xi}\ \phi_{yi}\ \phi_{zi}]^T \tag{7.4}$$

Livesley (1975) shows that with the internal coordinate system defined at the centre of the beam-element, the flexibility matrix $\mathbf{R}_i$ is conveniently simplified to give direct relationships between components of the force and deformation vectors $\mathbf{f}_i$ and $\mathbf{e}_i$ (see Equations 7.7 and 7.8). Hence, it is clear that e_{xi}, e_{xi} and e_{xi} are components of relative displacement between the two end joints of beam-element i. Similarly, it is clear that ϕ_{xi} is a component of relative twist, while ϕ_{yi} and ϕ_{zi} are components of relative rotation between the two end joints of beam-element i.

Together, the force or deformation vectors for each beam-element define the internal vector space $\mathbb{V}_\mathbf{f}$ of the frame.

In the local external and internal coordinate systems shown in Figure 7.1, the equilibrium matrix $\mathbf{h}$ for a beam-element is:

$$\mathbf{h} = \begin{bmatrix} -1 & 0 & 0 & 0 & 0 & 0 \\ 0 & -1 & 0 & 0 & 0 & 0 \\ 0 & 0 & -1 & 0 & 0 & 0 \\ 0 & 0 & 0 & -1 & 0 & 0 \\ 0 & 0 & l/2 & 0 & -1 & 0 \\ 0 & -l/2 & 0 & 0 & 0 & -1 \\ 1 & 0 & 0 & 0 & 0 & 0 \\ 0 & 1 & 0 & 0 & 0 & 0 \\ 0 & 0 & 1 & 0 & 0 & 0 \\ 0 & 0 & 0 & 1 & 0 & 0 \\ 0 & 0 & l/2 & 0 & 1 & 0 \\ 0 & -l/2 & 0 & 0 & 0 & 1 \end{bmatrix} \tag{7.5}$$

The corresponding compatibility matrix $\mathbf{c}$ for a beam-element in the local external and internal coordinate systems is simply given by $\mathbf{c} = \mathbf{h}^\mathbf{T}$.

In order to assemble the full equilibrium matrix $\mathbf{H}$ for a complete frame, the external load vectors of each beam-element must be transformed into a global coordinate system, for example the $x'y'z'$ Cartesian coordinate system shown in Figure 7.1. Thus, an equilibrium matrix $\mathbf{H}_i$ for beam-element i of a frame, defined in the global coordinate system is given by:

$$\mathbf{H}_i = \mathbf{T}_i\mathbf{h} \tag{7.6}$$

where $\mathbf{T}_i$ is the required transformation matrix.

The full equilibrium matrix **H** (or compatibility matrix **C**) for a complete frame, can then be generated from the global beam-element equilibrium matrices $\mathbf{H}_i$ using standard assembly techniques (Livesley 1975, McGuire & Gallagher 1979).

In the local internal coordinate system shown in Figure 7.1, the flexibility matrix **r** for a beam-element is:

$$\mathbf{r} = \begin{bmatrix} l/EA & 0 & 0 & 0 & 0 & 0 \\ 0 & l^3/12EI_z & 0 & 0 & 0 & 0 \\ 0 & 0 & l^3/12EI_y & 0 & 0 & 0 \\ 0 & 0 & 0 & l/GJ & 0 & 0 \\ 0 & 0 & 0 & 0 & l/EI_y & 0 \\ 0 & 0 & 0 & 0 & 0 & l/EI_z \end{bmatrix} \tag{7.7}$$

where E is Young's Modulus, A is the cross-sectional area, G is the shear modulus, I is the second moment of area and J is the polar second moment of area.

In order to assemble the full flexibility matrix **R** for a complete frame, no transformation is required for the internal force or deformation vectors. Together the local internal coordinate systems of the beam-elements define the a natural coordinate system for the complete frame. Hence a flexibility matrix $\mathbf{R}_i$ for beam-element i of a frame is simply:

$$\mathbf{R}_i = \mathbf{r} \tag{7.8}$$

The full flexibility matrix **R** for a frame is then easily assembled, it is simply a block-diagonal matrix with the beam-element flexibility matrices $\mathbf{R}_i$ arranged along its diagonal.

7.2 Simple Frame with $\mathrm{C_{3v}}$ Symmetry

The simple 2-dimensional rigid frame shown in Figure 7.2, is analysed to show how more general loads and forces can also be decomposed into components with particular symmetry properties, thus simplifying the analysis of more general structures with symmetry. The frame consists of three beam-elements connected together by a rigid joint, and is fully restrained by its foundations.

The load and couple vectors shown in Figure 7.2 define a 3-dimensional external load and displacement vector space $\mathbb{V}_\mathbf{p}$ for the frame, where a load or displacement vector is:

$$\mathbf{p} = [p_{x1}\ p_{y1}\ m_{z1}]^T \tag{7.9}$$

$$\mathbf{d} = [d_{x1}\ d_{y1}\ \theta_{z1}]^T \tag{7.10}$$

In order to define an internal force and deformation vector space $\mathbb{V}_\mathbf{f}$, the internal coordinate system shown in Figure 7.1 is attached to each of the three beam-

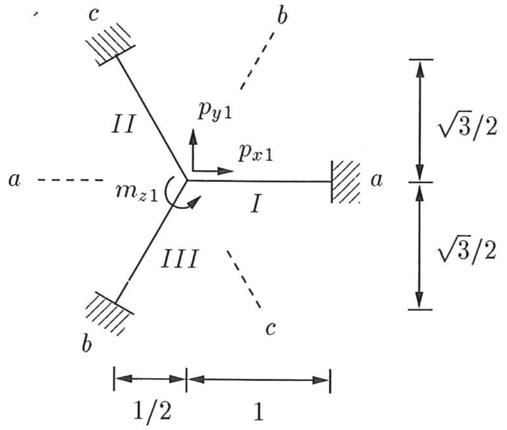

Figure 7.2: Simple 2-dimensional rigid frame with $\mathbf{C_{3v}}$ symmetry, An external coordinate system is attached for the external loads and couples.

elements. However, this is only a 2-dimensional analysis, and hence each beam-element has the following non-zero internal force and deformation vectors:

$$\mathbf{f}_i = [f_{xi}\ f_{yi}\ M_{zi}]^T \tag{7.11}$$

$$\mathbf{e}_i = [e_{xi}\ e_{yi}\ \phi_{zi}]^T \tag{7.12}$$

Together, these three internal coordinate systems define a 9-dimensional internal force and deformation vector space $\mathbb{V}_{\mathbf{f}}$, where a force or deformation vector for the frame is:

$$\mathbf{f} = [f_{x1}\ f_{y1}\ M_{z1}\ f_{x2}\ f_{y2}\ M_{z2}\ f_{x3}\ f_{y3}\ M_{z3}]^T \tag{7.13}$$

$$\mathbf{e} = [e_{x1}\ e_{y1}\ \phi_{z1}\ e_{x2}\ e_{y2}\ \phi_{z2}\ e_{x3}\ e_{y3}\ \phi_{z3}]^T \tag{7.14}$$

A structural analysis gives the following equilibrium matrix $\mathbf{H}$, written in the external and internal coordinate systems defined above:

$$\mathbf{H} = \begin{bmatrix} -1 & 0 & 0 & 1/2 & \sqrt{3}/2 & 0 & 1/2 & -\sqrt{3}/2 & 0 \\ 0 & -1 & 0 & -\sqrt{3}/2 & 1/2 & 0 & \sqrt{3}/2 & 1/2 & 0 \\ 0 & -1/2 & -1 & 0 & -1/2 & -1 & 0 & -1/2 & -1 \end{bmatrix} \tag{7.15}$$

This (3×9) equilibrium matrix is of rank 3, and hence there must exist six states of self-stress. These states of self-stress are now examined further utilising the symmetry properties of the frame.

The frame in Figure 7.2 has 3-fold rotation symmetry and reflection symmetry in planes a, b and c. Hence, this frame can be transformed into an equivalent configuration by symmetry operations $\{E,\ C_3,\ C_3^2,\ \sigma_a,\ \sigma_b,\ \sigma_c\}$, which constitute the symmetry group $\mathbf{C_{3v}}$ (see Chapter 3 for a description of symmetry group $\mathbf{C_{3v}}$). The three irreducible matrix representations $\{\Gamma^{(A_1)},\ \Gamma^{(A_2)}$ and $\Gamma^{(E)}\}$ which define the fundamental symmetry properties of symmetry group $\mathbf{C_{3v}}$ are shown in

Table 3.3, and are used to find the following symmetry-adapted coordinate systems for the external load and internal force vector spaces $\mathbb{V}_\mathbf{p}$ and $\mathbb{V}_\mathbf{f}$:

$$\mathbf{V_p} = \left(\mathbf{V_p}^{(A_1)} | \mathbf{V_p}^{(A_2)} | \mathbf{V_p}^{(E)1} | \mathbf{V_p}^{(E)2}\right) \tag{7.16}$$

$$\mathbf{V_p}^{(A_1)} = [\,]\ \mathbf{V_p}^{(A_2)} = \begin{bmatrix} 0 \\ 0 \\ 1 \end{bmatrix}\ \mathbf{V_p}^{(E)1} = \begin{bmatrix} 1 \\ 0 \\ 0 \end{bmatrix}\ \mathbf{V_p}^{(E)2} = \begin{bmatrix} 0 \\ -1 \\ 0 \end{bmatrix}$$

$$\mathbf{V_f} = \left(\mathbf{V_f}^{(A_1)} | \mathbf{V_f}^{(A_2)} | \mathbf{V_f}^{(E)1} | \mathbf{V_f}^{(E)2}\right) \tag{7.17}$$

$$\mathbf{V_f}^{(A_1)} = \begin{bmatrix} 1/\sqrt{3} \\ 0 \\ 0 \\ 1/\sqrt{3} \\ 0 \\ 0 \\ 1/\sqrt{3} \\ 0 \\ 0 \end{bmatrix} \qquad \mathbf{V_f}^{(A_2)} = \begin{bmatrix} 0 & 0 \\ 1/\sqrt{3} & 0 \\ 0 & 1/\sqrt{3} \\ 0 & 0 \\ 1/\sqrt{3} & 0 \\ 0 & 1/\sqrt{3} \\ 0 & 0 \\ 1/\sqrt{3} & 0 \\ 0 & 1/\sqrt{3} \end{bmatrix}$$

$$\mathbf{V_f}^{(E)1} = \begin{bmatrix} \sqrt{2/3} & 0 & 0 \\ 0 & 0 & 0 \\ 0 & 0 & 0 \\ -1/\sqrt{6} & 0 & 0 \\ 0 & 1/\sqrt{2} & 0 \\ 0 & 0 & 1/\sqrt{2} \\ -1/\sqrt{6} & 0 & 0 \\ 0 & -1/\sqrt{2} & 0 \\ 0 & 0 & -1/\sqrt{2} \end{bmatrix} \quad \mathbf{V_f}^{(E)2} = \begin{bmatrix} 0 & 0 & 0 \\ 0 & -\sqrt{2/3} & 0 \\ 0 & 0 & -\sqrt{2/3} \\ -1/\sqrt{2} & 0 & 0 \\ 0 & 1/\sqrt{6} & 0 \\ 0 & 0 & 1/\sqrt{6} \\ 1/\sqrt{2} & 0 & 0 \\ 0 & 1/\sqrt{6} & 0 \\ 0 & 0 & 1/\sqrt{6} \end{bmatrix}$$

The basis vectors for the external load and internal force symmetry subspaces $\mathbb{V}_\mathbf{p}^{(\mu)i}$ and $\mathbb{V}_\mathbf{f}^{(\mu)i}$, are shown in Figures 7.3 and 7.4.

Using Equation 4.8 to transform from the original external and internal co-ordinate systems to the $\mathbf{C_{3v}}$ symmetry-adapted coordinate systems, the block-diagonalised equilibrium matrix $\tilde{\mathbf{H}}$ is:

$$\tilde{\mathbf{H}} = \begin{bmatrix} \boxed{0} & \boxed{-\sqrt{3}/2 \;\; \sqrt{3}} & 0 & 0 & 0 & 0 & 0 & 0 \\ 0 & 0 & 0 & \boxed{\sqrt{3}/2 \;\; \sqrt{3}/2 \;\; 0} & & 0 & 0 & 0 \\ 0 & 0 & 0 & 0 & 0 & 0 & \boxed{\sqrt{3}/2 \;\; \sqrt{3}/2 \;\; 0} & \end{bmatrix} \tag{7.18}$$

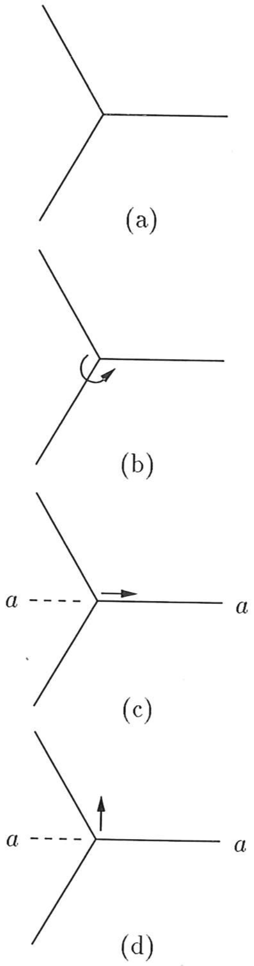

Figure 7.3: External load vector symmetry subspaces: (a) $\mathbb{V}_{\mathbf{p}}^{(A_1)}$ has $\mathbf{C_{3v}}$ symmetry; (b) $\mathbb{V}_{\mathbf{p}}^{(A_2)}$ has $\mathbf{C_3}$ symmetry; (c) $\mathbb{V}_{\mathbf{p}}^{(E)1}$ has reflection symmetry in plane a, symmetry group $\mathbf{C_s}$; (d) $\mathbb{V}_{\mathbf{p}}^{(E)2}$ has reflection anti-symmetry in plane a, no symmetry group.

Equation 7.18 shows that the block-diagonalised equilibrium matrix $\tilde{\mathbf{H}}$ has the form:

$$\tilde{\mathbf{H}} = \left[\begin{array}{llll} \tilde{\mathbf{H}}^{(A_1)}\ (0\times 1),\ s=1 & & & \\ & \boxed{\tilde{\mathbf{H}}^{(A_2)}}\ (1\times 2),\ s=1 & & \\ & & \boxed{\tilde{\mathbf{H}}^{(E)1}}\ (1\times 3),\ s=2 & \\ & & & \boxed{\tilde{\mathbf{H}}^{(E)2}}\ (1\times 3),\ s=2 \end{array}\right] \tag{7.19}$$

Of particular interest is the (0×1) *empty* equilibrium block $\tilde{\mathbf{H}}^{(A_1)}$, from which it is immediately clear that the single internal force vector given by $\mathbb{V}_{\mathbf{f}}^{(A_1)}$ is in equilibrium with zero load vectors. Thus, it is a state of self-stress, and the symmetry

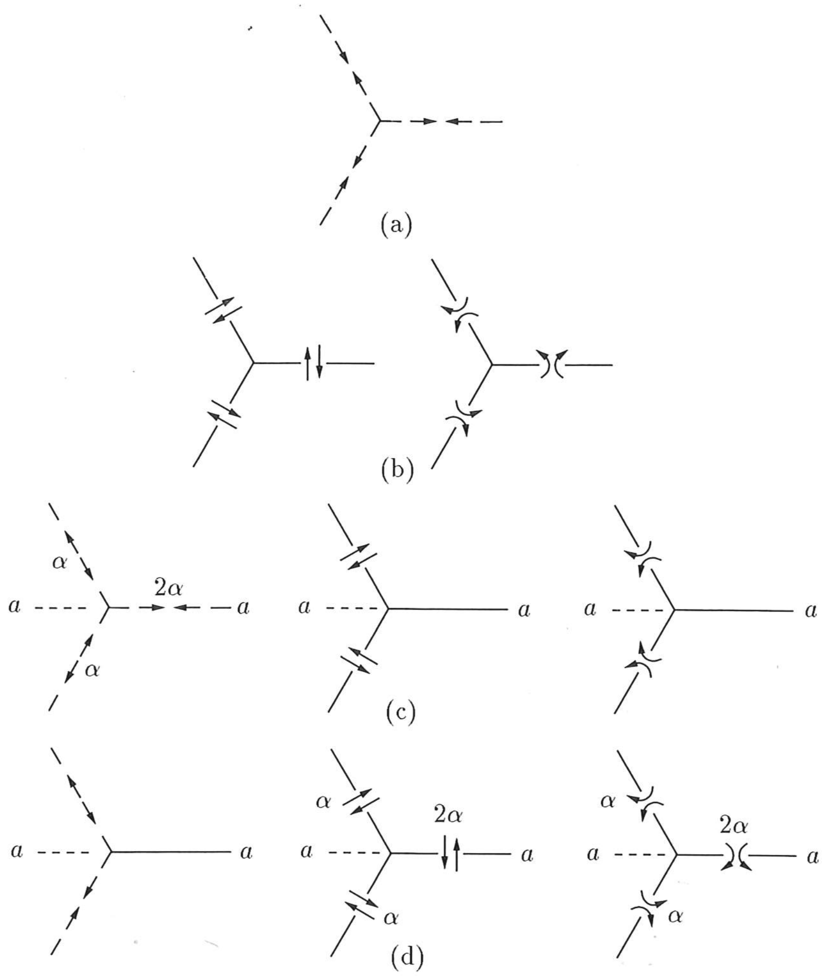

Figure 7.4: Internal force vector symmetry subspaces: (a) $\mathbb{V}_{\mathbf{f}}^{(A_1)}$ has $\mathbf{C_{3v}}$ symmetry; (b) $\mathbb{V}_{\mathbf{f}}^{(A_2)}$ has $\mathbf{C_3}$ symmetry; (c) $\mathbb{V}_{\mathbf{f}}^{(E)1}$ has reflection symmetry in plane a, symmetry group $\mathbf{C_s}$; (d) $\mathbb{V}_{\mathbf{f}}^{(E)2}$ has reflection anti-symmetry in plane a, no symmetry. α is an arbitrary constant.

analysis shows that it has the full $\mathbf{C_{3v}}$ symmetry properties of the frame. This state of self-stress is shown in Figure 7.5.

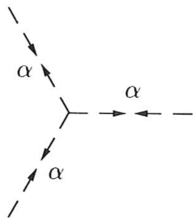

Figure 7.5: State of self-stress in $\mathbb{V}_{\mathbf{f}}^{(A_1)}$. $\alpha = 1/\sqrt{3}$.

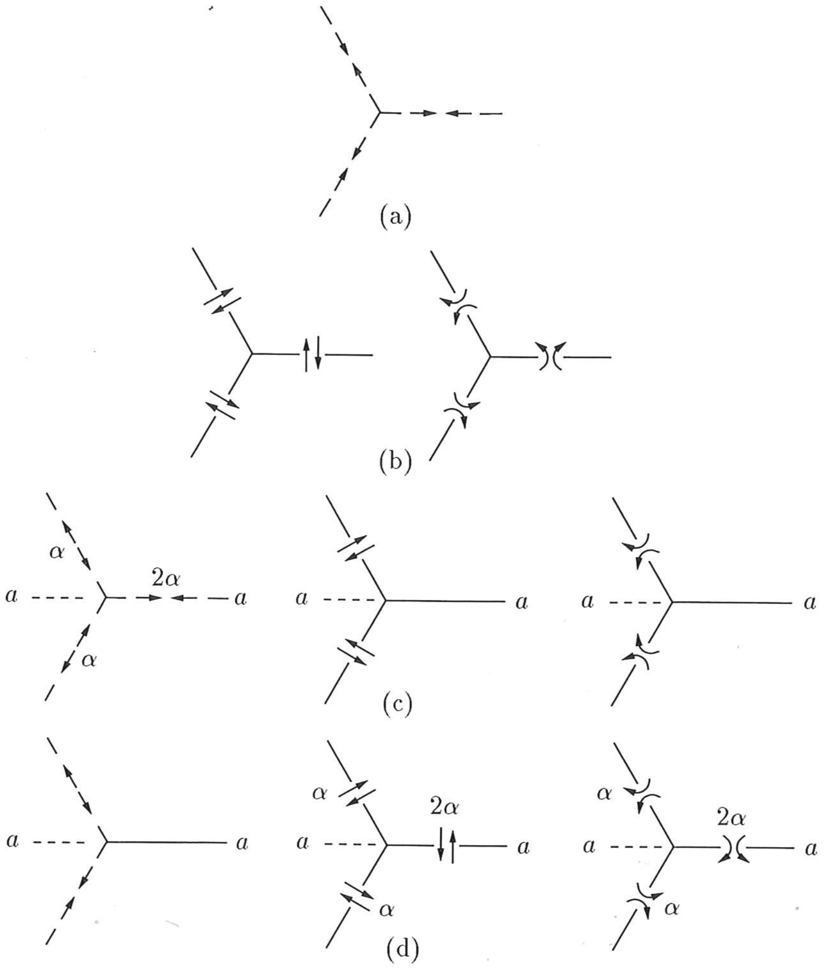

Figure 7.4: Internal force vector symmetry subspaces: (a) $\mathbb{V}_{\mathbf{f}}^{(A_1)}$ has $\mathbf{C_{3v}}$ symmetry; (b) $\mathbb{V}_{\mathbf{f}}^{(A_2)}$ has $\mathbf{C_3}$ symmetry; (c) $\mathbb{V}_{\mathbf{f}}^{(E)1}$ has reflection symmetry in plane a, symmetry group $\mathbf{C_s}$; (d) $\mathbb{V}_{\mathbf{f}}^{(E)2}$ has reflection anti-symmetry in plane a, no symmetry. α is an arbitrary constant.

analysis shows that it has the full $\mathbf{C_{3v}}$ symmetry properties of the frame. This state of self-stress is shown in Figure 7.5.

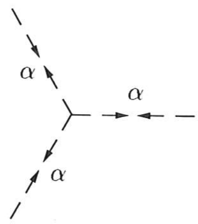

Figure 7.5: State of self-stress in $\mathbb{V}_{\mathbf{f}}^{(A_1)}$. $\alpha = 1/\sqrt{3}$.

The (1×2) equilibrium block $\tilde{\mathbf{H}}^{(A_2)}$ is of rank 1 and hence, $\mathbb{V}_{\mathbf{f}}^{(A_2)}$ contain a single state of self-stress which has only 3-fold rotation symmetry:

$$\mathbf{f}_{\mathrm{s}}^{(A_2)} = \begin{bmatrix} 0 \\ -2/\sqrt{15} \\ 1/\sqrt{15} \\ 0 \\ -2/\sqrt{15} \\ 1/\sqrt{15} \\ 0 \\ -2/\sqrt{15} \\ 1/\sqrt{15} \end{bmatrix} \tag{7.20}$$

This state of self-stress in $\mathbb{V}_{\mathbf{f}}^{(A_2)}$, is shown in Figure 7.6.

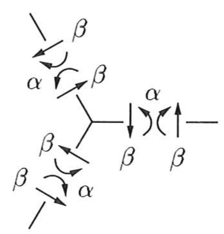

Figure 7.6: State of self-stress in $\mathbb{V}_{\mathbf{f}}^{(A_2)}$. $\alpha = 1/\sqrt{15}$ and $\beta = 2/\sqrt{15}$.

The two (1×3) equilibrium blocks $\tilde{\mathbf{H}}^{(E)1}$ and $\tilde{\mathbf{H}}^{(E)2}$ are also of rank 1, and hence $\mathbb{V}_{\mathbf{f}}^{(E)1}$ and $\mathbb{V}_{\mathbf{f}}^{(E)2}$ each contain a 2-dimensional state of self-stress:

$$\mathbf{f}_{\mathrm{s}}^{(E)1} = \begin{bmatrix} -1/\sqrt{3} & 0 \\ 0 & 0 \\ 0 & 0 \\ 1/\sqrt{12} & 0 \\ -1/2 & 0 \\ 0 & 1/\sqrt{2} \\ 1/\sqrt{12} & 0 \\ 1/2 & 0 \\ 0 & -1/\sqrt{2} \end{bmatrix} \quad \mathbf{f}_{\mathrm{s}}^{(E)2} = \begin{bmatrix} 0 & 0 \\ -1/\sqrt{3} & 0 \\ 0 & -\sqrt{2/3} \\ 1/2 & 0 \\ 1/\sqrt{12} & 0 \\ 0 & 1/\sqrt{6} \\ -1/2 & 0 \\ 1/\sqrt{12} & 0 \\ 0 & 1/\sqrt{6} \end{bmatrix} \tag{7.21}$$

The states of self-stress in $\mathbb{V}_{\mathbf{f}}^{(E)1}$ have only reflection symmetry in plane a, and are shown in Figure 7.7.

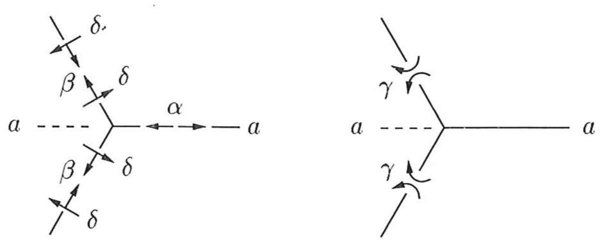

Figure 7.7: States of self-stress in $\mathbb{V}_{\mathbf{f}}^{(E)1}$. $\alpha = 1/\sqrt{3}$, $\beta = 1/\sqrt{12}$, $\delta = 1/2$ and $\epsilon = 1/\sqrt{2}$.

The states of self-stress in $\mathbb{V}_{\mathbf{f}}^{(E)2}$ have only reflection anti-symmetry in plane a, and are shown in Figure 7.8.

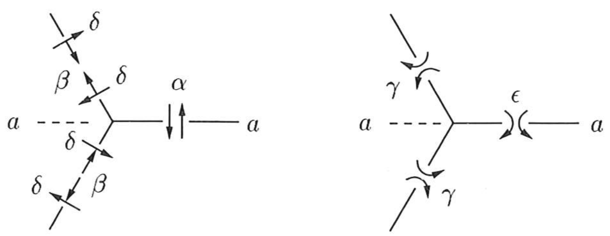

Figure 7.8: States of self-stress in $\mathbb{V}_{\mathbf{f}}^{(E)2}$. $\alpha = 1/\sqrt{3}$, $\beta = 1/2$, $\delta = 1/\sqrt{12}$, $\epsilon = \sqrt{2/3}$ and $\gamma = 1/\sqrt{6}$.

7.3 Frames with Finite Mechanisms

This section investigates two frames which satisfy a criterion for determinacy and yet contain finite mechanisms. Both frames are linkage structures containing six revolute joints. Structures such as these are often studied by *kinematicians*, who describe them as "overconstrained mechanisms", since in general a linkage requires seven revolute joints before it has a finite mechanism. A good description of overconstrained mechanisms is contained in Hunt (1978).

7.3.1 Frame with C_{2v} Symmetry

A similar symmetry analysis to that carried out for pin-jointed structures can be used to investigate statically and kinematically indeterminate frames. Of interest is whether it is possible to find finite mechanisms in frames which have some degree of freedom in their joints.

Figure 7.9 shows an unrestrained frame in 3-dimensional space, and is constructed from six "right-angle" beam-elements connected together using six joints with rotational hinges which allow torsional freedom only.

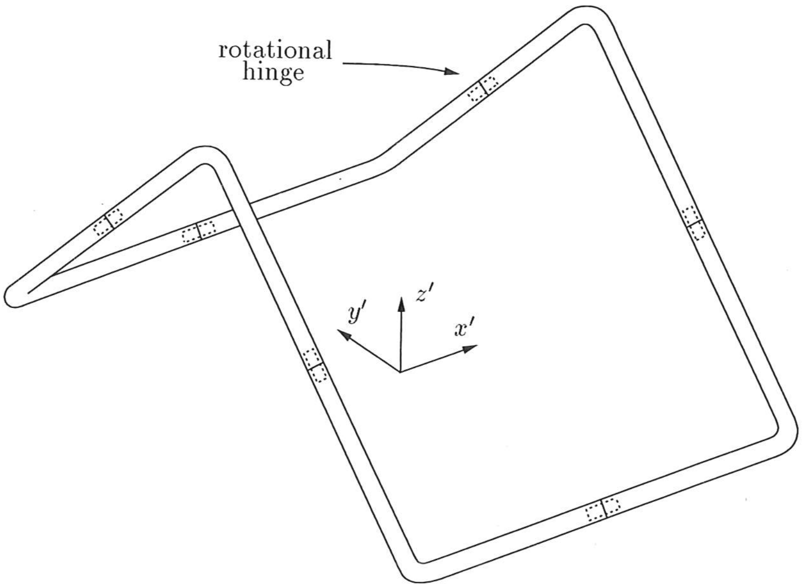

Figure 7.9: Frame with $\mathbf{C_{2v}}$ symmetry, each joint allows torsional freedom only. A global Cartesian coordinate system is shown.

In order to analyse this frame, coordinate systems for the internal and external vector spaces $\mathbb{V}_\mathbf{f}$ and $\mathbb{V}_\mathbf{p}$ must be defined. In Figure 7.10 the frame is modelled as having 12 joints numbered 1-12, and 12 straight beam-elements numbered *I-XII*. Every odd numbered joint has a rotational hinge which allows torsional freedom between connecting beams. At these odd numbered joints the local x-axes are defined along the axis of torsional freedom, hence two independent couples m_{xi1} and m_{xi2} must be defined at each of these joints to allow independent torsional rotations θ_{xi1} and θ_{xi2} of the two connecting beams. Thus, the required external load and displacement vectors at the odd numbered joints are:

$$\mathbf{p}_i = [p_{xi}\ p_{yi}\ p_{zi}\ m_{xi1}\ m_{xi2}\ m_{yi}\ m_{zi}]^T \tag{7.22}$$

$$\mathbf{d}_i = [d_{xi}\ d_{yi}\ d_{zi}\ \theta_{xi1}\ \theta_{xi2}\ \theta_{yi}\ \theta_{zi}]^T \tag{7.23}$$

where: $i = 1, 3, 5, 7, 9, 11$.

The even numbered joints are the fully rigid corner joints, and hence have load and displacement vectors defined by Equations 7.1 and 7.2.

Only the external loads and couples acting on joints 1 and 2 are shown in Figure 7.10 for clarity; similar loads and couples act on the remaining joints and hence

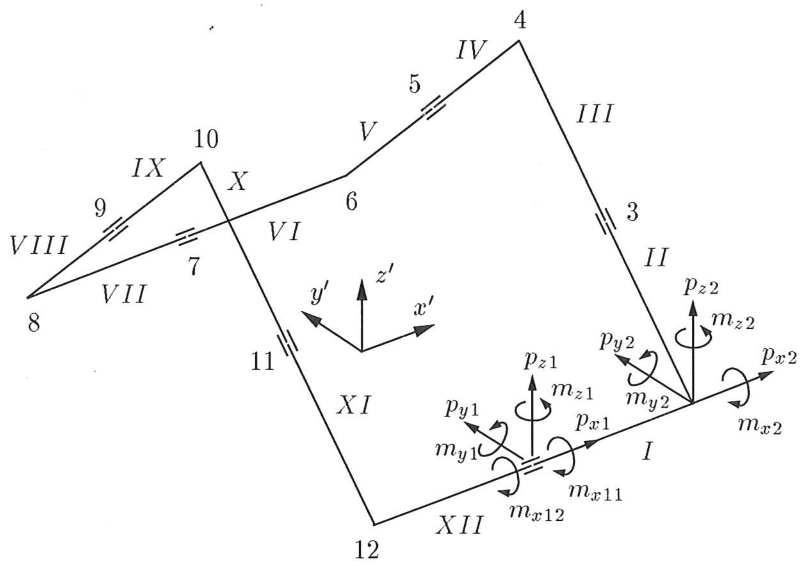

Figure 7.10: $\mathbf{C_{2v}}$ frame, modelled with 12 joints and 12 straight beam elements. Only the loads and couples acting on joints 1 and 2 are shown for clarity (the corresponding displacement vectors occupy the same vector basis). Similar external coordinate systems are attached to the remaining joints. The internal coordinate system defined in Figure 7.1 is also attached to each beam-element.

coordinate systems can be attached to these joints, thus defining a 78-dimensional external load and displacement vector space $\mathbb{V}_\mathbf{p}$ for the frame, where a load or displacement vector is:

$$\mathbf{p} = \begin{bmatrix} \mathbf{p}_1 \\ \mathbf{p}_2 \\ \mathbf{p}_3 \\ \mathbf{p}_4 \\ \mathbf{p}_5 \\ \mathbf{p}_6 \\ \mathbf{p}_7 \\ \mathbf{p}_8 \\ \mathbf{p}_9 \\ \mathbf{p}_{10} \\ \mathbf{p}_{11} \\ \mathbf{p}_{12} \end{bmatrix}, \qquad \mathbf{d} = \begin{bmatrix} \mathbf{d}_1 \\ \mathbf{d}_2 \\ \mathbf{d}_3 \\ \mathbf{d}_4 \\ \mathbf{d}_5 \\ \mathbf{d}_6 \\ \mathbf{d}_7 \\ \mathbf{d}_8 \\ \mathbf{d}_9 \\ \mathbf{d}_{10} \\ \mathbf{d}_{11} \\ \mathbf{d}_{12} \end{bmatrix} \tag{7.24}$$

In order to define an internal force and deformation vector space $\mathbb{V}_\mathbf{f}$, the internal coordinate system shown in Figure 7.1 is attached to each of the 12 beam-elements. Hence, each beam-element has the internal force and deformation vectors $\mathbf{f}_i$ and $\mathbf{e}_i$, defined by Equations 7.3 and 7.4. Together, these 12 internal coordinate systems define a 72-dimensional internal force and deformation vector space $\mathbb{V}_\mathbf{f}$ for the frame, and a force or deformation vector is:

$$\mathbf{f} = \begin{bmatrix} \mathbf{f}_1 \\ \mathbf{f}_2 \\ \mathbf{f}_3 \\ \mathbf{f}_4 \\ \mathbf{f}_5 \\ \mathbf{f}_6 \\ \mathbf{f}_7 \\ \mathbf{f}_8 \\ \mathbf{f}_9 \\ \mathbf{f}_{10} \\ \mathbf{f}_{11} \\ \mathbf{f}_{12} \end{bmatrix}, \qquad \mathbf{e} = \begin{bmatrix} \mathbf{e}_1 \\ \mathbf{e}_2 \\ \mathbf{e}_3 \\ \mathbf{e}_4 \\ \mathbf{e}_5 \\ \mathbf{e}_6 \\ \mathbf{e}_7 \\ \mathbf{e}_8 \\ \mathbf{e}_9 \\ \mathbf{e}_{10} \\ \mathbf{e}_{11} \\ \mathbf{e}_{12} \end{bmatrix} \tag{7.25}$$

The static and kinematic determinacy of rigid frames can be investigated with methods similar to those used for pin-jointed structures. For an unrestrained rigid frame in 3-dimensional space, a criterion for determinacy (an adaptation of Maxwell's rule for frames), relates the number of unknown internal forces to the number of independent equilibrium equations:

$$6b = 6j + s - 6 \tag{7.26}$$

where: b is the number of beam-elements.
j is the number of rigid joints.
s is the number of special releases, such as hinges.

In this case $b = 6$, $j = 6$ and $s = 6$, hence this frame should be structurally stiff. However, this topological condition is not sufficient to determine whether this frame is actually stiff; a complete structural analysis will show that the (78×72) equilibrium matrix $\mathbf{H}$ is of rank 71, hence there exists seven inextensional mechanisms and a single state of self-stress. Since this frame is unrestrained, it can be displaced by the six rigid body mechanisms. This accounts for six of these inextensional mechanisms, and leaves only one unknown internal mechanism. This internal mechanism is now examined further by utilising the symmetry properties of the frame.

The frame in Figure 7.10 has 2-fold rotation symmetry about the z'-axis and reflection symmetry in the x'-z' and y'-z' vertical planes. Hence, this frame can be transformed into an equivalent configuration by the following set of symmetry operations:

1. The identity, symmetry operation E.

2. Rotation by 180° about the z'-axis, symmetry operation C_2.

3. Reflection in the $x'z'$-plane, symmetry operation σ_x.

4. Reflection in the $y'z'$-plane, symmetry operation σ_y.

These four symmetry operations constitute the symmetry group $\mathbf{C_{2v}}$. The four irreducible matrix representations $\{\Gamma^{(A_1)}, \Gamma^{(A_2)}, \Gamma^{(A_3)}$ and $\Gamma^{(A_3)}\}$ which represent symmetry group $\mathbf{C_{2v}}$ are shown in Table 7.1. Each of the irreducible matrix

$\mathbf{C_{2v}}$	E	C_2	σ_x	σ_y
$\Gamma^{(A_1)}$	1	1	1	1
$\Gamma^{(A_2)}$	1	1	−1	−1
$\Gamma^{(A_3)}$	1	−1	1	−1
$\Gamma^{(A_4)}$	1	−1	−1	1

Table 7.1: Irreducible matrix representations of symmetry group $\mathbf{C_{2v}}$.

representations in Table 7.1 defines fundamental symmetry properties of the frame, and can be used to find symmetry-adapted coordinate systems for the load and force vector spaces (they are not shown here due to their size). In these symmetry-adapted coordinate systems both the load and force vector spaces are decomposed into four independent symmetry subspaces, each with the particular symmetry properties shown below:

1. $\mathbb{V}_\mathbf{p}^{(A_1)}$ and $\mathbb{V}_\mathbf{f}^{(A_1)}$: full symmetry of the frame, symmetry group $\mathbf{C_{2v}}$.

2. $\mathbb{V}_\mathbf{p}^{(A_2)}$ and $\mathbb{V}_\mathbf{f}^{(A_2)}$: 2-fold rotational symmetry about the z'-axis, symmetry group $\mathbf{C_2}$.

3. $\mathbb{V}_\mathbf{p}^{(A_3)}$ and $\mathbb{V}_\mathbf{f}^{(A_3)}$: reflection symmetry in the $x'z'$-plane, symmetry group $\mathbf{C_s}$.

4. $\mathbb{V}_\mathbf{p}^{(A_4)}$ and $\mathbb{V}_\mathbf{f}^{(A_4)}$: reflection symmetry in the $y'z'$-plane, symmetry group $\mathbf{C_s}$.

In order to block-diagonalise an equilibrium matrix, load vectors $\mathbf{p}$ and force vectors $\mathbf{f}$ in the original coordinate systems, must be transformed into equivalent load vectors $\tilde{\mathbf{p}}$ and force vectors $\tilde{\mathbf{f}}$ in the symmetry-adapted coordinate systems. In these symmetry-adapted coordinate systems with $\mathbf{C_{2v}}$ symmetry properties, the block-diagonalised equilibrium matrix $\tilde{\mathbf{H}}$ has the form shown in Equation 7.27.

Equilibrium blocks $\tilde{\mathbf{H}}^{(A_1)}$, $\tilde{\mathbf{H}}^{(A_2)}$ and $\tilde{\mathbf{H}}^{(A_3)}$ are of full rank, while the (19×18) equilibrium block $\tilde{\mathbf{H}}^{(A_4)}$ is of rank 17 and hence contains the single state of self-stress.

$$\tilde{\mathbf{H}} = \begin{bmatrix} \boxed{\begin{array}{l} \tilde{\mathbf{H}}^{(A_1)} \\ (19\times 18) \\ m=1 \end{array}} & & & \\ & \boxed{\begin{array}{l} \tilde{\mathbf{H}}^{(A_2)} \\ (20\times 18) \\ m=2 \end{array}} & & \\ & & \boxed{\begin{array}{l} \tilde{\mathbf{H}}^{(A_3)} \\ (20\times 18) \\ m=2 \end{array}} & \\ & & & \boxed{\begin{array}{l} \tilde{\mathbf{H}}^{(A_4)} \\ (19\times 18) \\ s=1 \\ m=2 \end{array}} \end{bmatrix} \tag{7.27}$$

The six finite rigid body mechanisms can be identified and exist in the following symmetry subspaces:

1. Symmetry subspace $\mathbb{V}_{\mathbf{P}}^{(A_1)}$ contains the rigid body translation in the y'-direction.
2. Symmetry subspace $\mathbb{V}_{\mathbf{P}}^{(A_2)}$ contains the rigid body rotation about the z'-axis.
3. Symmetry subspace $\mathbb{V}_{\mathbf{P}}^{(A_3)}$ contains the rigid body translation in the x'-direction and the rigid body rotation about the y'-axis.
4. Symmetry subspace $\mathbb{V}_{\mathbf{P}}^{(A_4)}$ contains the rigid body translation in the z'-direction and the rigid body rotation about the x'-axis.

Hence, the one remaining inextensional mechanism exists in symmetry subspace $\mathbb{V}_{\mathbf{P}}^{(A_2)}$. Figure 7.11 shows a linear displacement of the frame in the direction of this mechanism. It is clear that once the inextensional mechanism is displaced the frame has only the $\mathbf{C_2}$ symmetry properties corresponding to irreducible representation $\Gamma^{(A_2)}$. This inextensional mechanism is now investigated further.

Block-Diagonalisation of the Equilibrium Matrix using $\mathbf{C_2}$ Symmetry

The analysis has shown that the frame with $\mathbf{C_{2v}}$ symmetry contains an internal mechanism with only $\mathbf{C_2}$ symmetry. Thus, in order to determine whether this mechanism is finite or infinitesimal, a reduced symmetry analysis of the frame

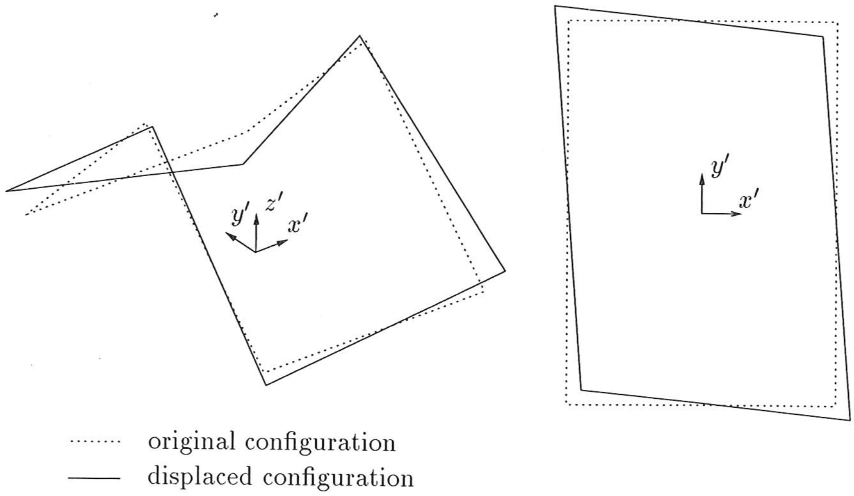

Figure 7.11: Frame with $\mathbf{C_2}$ symmetry, after a linear displacement in the direction of the internal finite mechanism.

$\mathbf{C_2}$	E	C_2
$\Gamma^{(A_1)}$	1	1
$\Gamma^{(A_2)}$	1	-1

Table 7.2: Irreducible matrix representations of symmetry group $\mathbf{C_2}$.

must be carried out using symmetry group $\mathbf{C_2}$. The irreducible matrix representations of symmetry group $\mathbf{C_2}$ are shown in Table 7.2. The two irreducible matrix representations in Table 7.2 now decompose both the load and force vector spaces into two independent symmetry subspaces with the following symmetry properties:

1. $\mathbb{V}_{\mathbf{p}}^{(A_1)}$ and $\mathbb{V}_{\mathbf{f}}^{(A_1)}$: full symmetry of the frame, symmetry group $\mathbf{C_s}$.
2. $\mathbb{V}_{\mathbf{p}}^{(A_2)}$ and $\mathbb{V}_{\mathbf{f}}^{(A_2)}$: no symmetry.

Table 7.3 shows a descent of symmetry from $\mathbf{C_{2v}}$ to $\mathbf{C_2}$ symmetry, from which the two $\mathbf{C_2}$ symmetry subspaces can be constructed. These symmetry subspaces

$\mathbf{C_2}$		$\mathbf{C_{2v}}$
$\{\mathbb{V}^{(A_1)}\}$	$\Longleftrightarrow$	$\{\mathbb{V}^{(A_1)}, \mathbb{V}^{(A_2)}\}$
$\{\mathbb{V}^{(A_2)}\}$	$\Longleftrightarrow$	$\{\mathbb{V}^{(A_3)}, \mathbb{V}^{(A_4)}\}$

Table 7.3: Descent of symmetry from symmetry group $\mathbf{C_{2v}}$ to $\mathbf{C_2}$.

give the new load and force vector symmetry-adapted coordinate systems with $\mathbf{C_2}$

symmetry properties, and the block-diagonalised equilibrium matrix $\tilde{\mathbf{H}}$ now has the form:

$$\tilde{\mathbf{H}} = \begin{bmatrix} \boxed{\begin{array}{l} \tilde{\mathbf{H}}^{(A_1)} \\ (39\times 36) \\ m=3 \end{array}} & \\ & \boxed{\begin{array}{l} \tilde{\mathbf{H}}^{(A_2)} \\ (39\times 36) \\ s=1 \\ m=4 \end{array}} \end{bmatrix} \tag{7.28}$$

Equation 7.28 shows that the internal inextensional mechanism with $\mathbf{C_2}$ symmetry now exists in the first equilibrium block $\tilde{\mathbf{H}}^{(A_1)}$ (with two of the rigid body mechanisms), while the state of self-stress exists in the second equilibrium block $\tilde{\mathbf{H}}^{(A_2)}$ (with the other four rigid body mechanisms) and has no symmetry.

Hence, the symmetry analysis shows that the internal mechanism in Figure 7.11, must be a finite mechanism, since no state of self-stress exists in the first equilibrium block which can stiffen the frame when it is displaced along this finite path. Figure 7.12(a) and (b) shows two displaced configurations of the frame as it follows the path of the finite mechanism. In both configurations the frame has $\mathbf{C_{2v}}$ sym-

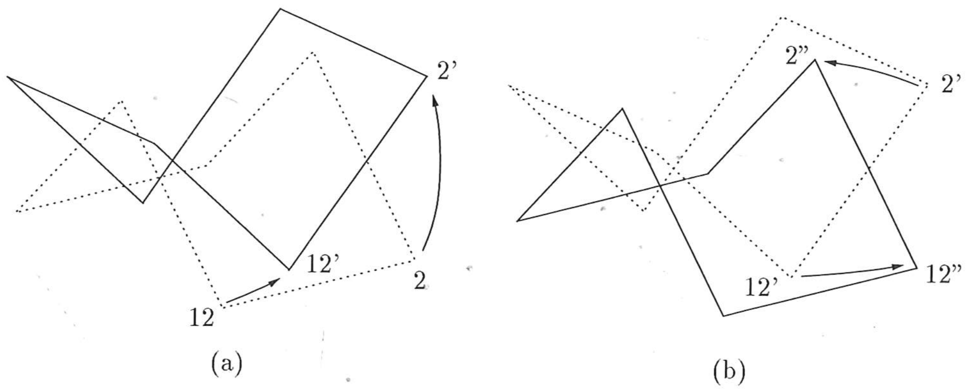

Figure 7.12: (a) and (b) show two different configurations of the frame as it follows the path of the finite mechanism. In particular, the displaced positions of joints 2 and 12 are shown. In both configurations along this path the frame has $\mathbf{C_{2v}}$ symmetry.

metry and hence, the block-diagonalised equilibrium matrix $\tilde{\mathbf{H}}$ will have the block form shown in Equation 7.27. In any intermediate configuration the frame has $\mathbf{C_2}$ symmetry only and hence, the block-diagonalised equilibrium matrix $\tilde{\mathbf{H}}$ will have the block form shown in Equation 7.28.

7.3.2 Frame with $\mathbf{C_{3v}}$ Symmetry

Another example of a statically and kinematically indeterminate frame which contains an internal finite mechanism is shown in Figure 7.13. This planar frame is

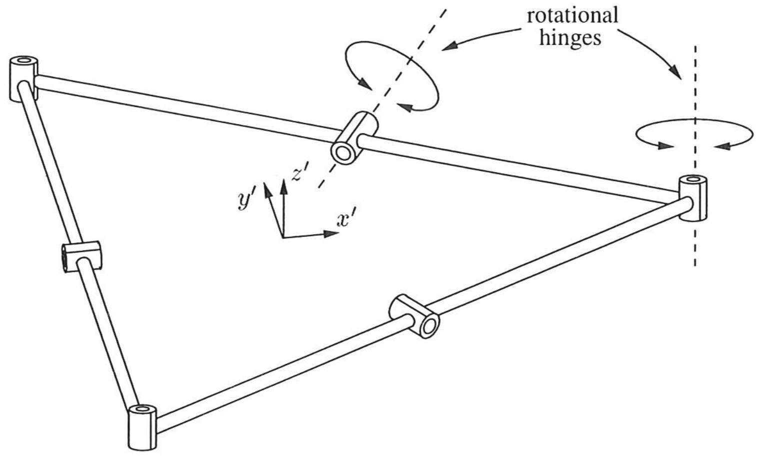

Figure 7.13: Frame with $\mathbf{C_{3v}}$ symmetry. Each joint allows rotational freedom in a single direction only.

unrestrained in 3-dimensional space and is made up of six beam-elements connected together using six joints which allow rotational freedom in a single direction only.

In Figure 7.14 the planar frame is modelled as having six joints numbered 1-6, and six beam-elements numbered *I*-*VI*. A coordinate system is also attached for the external load and displacement vectors acting at each joint. The odd numbered joints all have hinges which allow rotational freedom about their local z-axes only. Hence two independent couples m_{zi1} and m_{zi2} are required at each of the odd numbered joints to allow independent rotations θ_{zi1} and θ_{zi2} of the two connecting beams. The required external load and displacement vectors at the odd numbered joints are therefore:

$$\mathbf{p}_i = [p_{xi}\ p_{yi}\ p_{zi}\ m_{xi}\ m_{yi}\ m_{zi1}\ m_{zi2}]^T \tag{7.29}$$

$$\mathbf{d}_i = [d_{xi}\ d_{yi}\ d_{zi}\ \theta_{xi}\ \theta_{yi}\ \theta_{zi1}\ \theta_{zi2}]^T \tag{7.30}$$

where: $i = 1, 3, 5$.

The even numbered joints all have hinges which allow rotational freedom about their local y-axes only. Hence two independent couples m_{yi1} and m_{yi2} are required at each of the even numbered joints to allow independent rotations θ_{yi1} and θ_{yi2} of the two connecting beams. The required external load and displacement vectors at the even numbered joints are therefore:

$$\mathbf{p}_i = [p_{xi}\ p_{yi}\ p_{zi}\ m_{xi}\ m_{yi1}\ m_{yi2}\ m_{zi}]^T \tag{7.31}$$

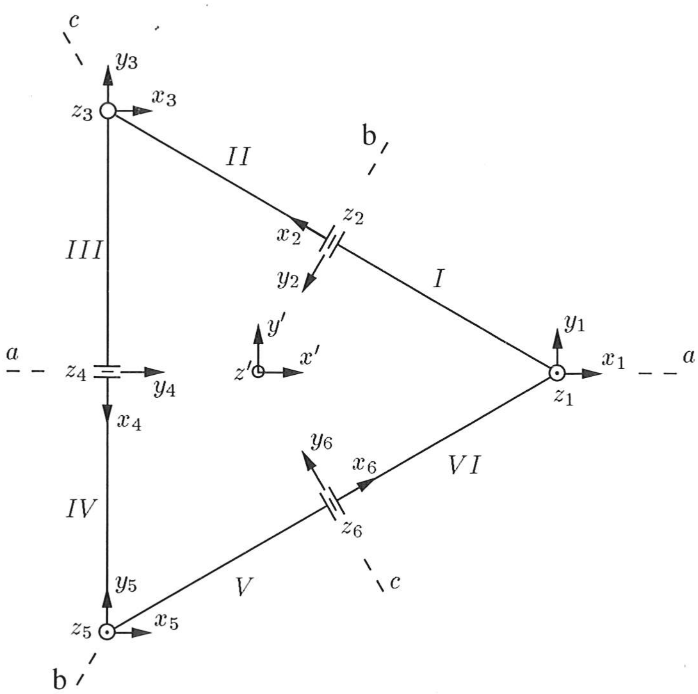

Figure 7.14: Frame with $\mathbf{C_{3v}}$ symmetry, modelled with an attached coordinate system for the external load and displacement vectors.

$$\mathbf{d}_i = [d_{xi}\ d_{yi}\ d_{zi}\ \theta_{xi}\ \theta_{yi1}\ \theta_{yi2}\ \theta_{zi}]^T \tag{7.32}$$

where: $i = 2, 4, 6$.

Thus, Equations 7.29-7.32 define a 42-dimensional external load and displacement vector space $\mathbb{V}_\mathbf{p}$ for the frame, where a load or displacement vector is:

$$\mathbf{p} = \begin{bmatrix} \mathbf{p}_1 \\ \mathbf{p}_2 \\ \mathbf{p}_3 \\ \mathbf{p}_4 \\ \mathbf{p}_5 \\ \mathbf{p}_6 \end{bmatrix}, \quad \mathbf{d} = \begin{bmatrix} \mathbf{d}_1 \\ \mathbf{d}_2 \\ \mathbf{d}_3 \\ \mathbf{d}_4 \\ \mathbf{d}_5 \\ \mathbf{d}_6 \end{bmatrix} \tag{7.33}$$

In order to define the internal vector space $\mathbb{V}_\mathbf{f}$, the internal coordinate system shown in Figure 7.1 is attached to each of the six beam-elements. Hence, each beam-element has the internal force and deformation vectors $\mathbf{f}_i$ and vectors $\mathbf{e}_i$ defined by Equations 7.3 and 7.4. Together, these six internal coordinate systems define a 36-dimensional internal force and deformation vector space $\mathbb{V}_\mathbf{f}$ for the frame, and a force or deformation vector is:

$$\mathbf{f} = \begin{bmatrix} \mathrm{f}_1 \\ \mathrm{f}_2 \\ \mathrm{f}_3 \\ \mathrm{f}_4 \\ \mathrm{f}_5 \\ \mathrm{f}_6 \end{bmatrix}, \qquad \mathbf{e} = \begin{bmatrix} \mathrm{e}_1 \\ \mathrm{e}_2 \\ \mathrm{e}_3 \\ \mathrm{e}_4 \\ \mathrm{e}_5 \\ \mathrm{e}_6 \end{bmatrix} \tag{7.34}$$

This frame also satisfies the criterion for determinacy expressed by Equation 7.26, and hence should be structurally stiff. However, a structural analysis shows that the (42×36) equilibrium matrix $\mathbf{H}$ is of rank 35, hence there exists seven inextensional mechanisms and a single state of self-stress. Since this frame is unrestrained, six of these inextensional mechanisms are accounted for by the six rigid body mechanism that the frame can undergo; this leaves only one remaining internal inextensional mechanism to investigate.

The frame in Figure 7.14 has 3-fold rotation symmetry about the z'-axis and reflection symmetry in vertical planes a, b and c. Hence, this frame can be transformed into an equivalent configuration by the following set of symmetry operations:

1. The identity, symmetry operation E.
2. Rotation by 120° about the z'-axis, symmetry operation C_3.
3. Rotation by 240° about the z'-axis, symmetry operation C_3^2.
4. Reflection in plane a, symmetry operation σ_a.
5. Reflection in plane b, symmetry operation σ_b.
6. Reflection in plane c, symmetry operation σ_c.

Note, planes a, b and c are all perpendicular to the $x'y'$-plane.

These six symmetry operations constitute the symmetry group $\mathbf{C_{3v}}$. The three irreducible matrix representations $\{\Gamma^{(A_1)}$, $\Gamma^{(A_2)}$ and $\Gamma^{(E)}\}$ which define the fundamental symmetry properties of symmetry group $\mathbf{C_{3v}}$ are shown in Table 3.3, and are used to find symmetry-adapted coordinate systems for the load and force vector spaces (they are not shown here due to their size).

In these symmetry-adapted coordinate systems both the load and force vector spaces are decomposed into four independent symmetry subspaces, each with the particular symmetry properties shown below:

1. $\mathbb{V}_{\mathbf{p}}^{(A_1)}$ and $\mathbb{V}_{\mathbf{f}}^{(A_1)}$: full symmetry of the frame, symmetry group $\mathbf{C_{3v}}$.

2. $\mathbb{V}_{\mathbf{p}}^{(A_2)}$ and $\mathbb{V}_{\mathbf{f}}^{(A_2)}$: 3-fold rotational symmetry about the z'-axis, symmetry group $\mathbf{C_3}$.

3. $\mathbb{V}_{\mathbf{p}}^{(E)1}$ and $\mathbb{V}_{\mathbf{f}}^{(E)1}$: reflection symmetry in plane a, symmetry group $\mathbf{C_s}$.

4. $\mathbb{V}_{\mathbf{p}}^{(E)2}$ and $\mathbb{V}_{\mathbf{f}}^{(E)2}$: reflection anti-symmetry in plane a, no symmetry.

In these symmetry-adapted coordinate systems with $\mathbf{C_{3v}}$ symmetry properties, the block-diagonalised equilibrium matrix $\tilde{\mathbf{H}}$ has the form:

$$\tilde{\mathbf{H}} = \begin{bmatrix} \boxed{\tilde{\mathbf{H}}^{(A_1)}}\ (8\times 6),\ m=2 & & & \\ & \boxed{\tilde{\mathbf{H}}^{(A_2)}}\ (6\times 6),\ s=1 \text{ and } m=1 & & \\ & & \boxed{\begin{array}{c}\tilde{\mathbf{H}}^{(E)1}\\ (14\times 12)\\ m=2\end{array}} & \\ & & & \boxed{\begin{array}{c}\tilde{\mathbf{H}}^{(E)2}\\ (14\times 12)\\ m=2\end{array}} \end{bmatrix} \tag{7.35}$$

Equation 7.35 shows that equilibrium blocks $\tilde{\mathbf{H}}^{(A_1)}$, $\tilde{\mathbf{H}}^{(E)1}$ and $\tilde{\mathbf{H}}^{(E)2}$ are of full rank, while the (6×6) equilibrium block $\tilde{\mathbf{H}}^{(A_2)}$ is of rank 5 and hence contains the state of self-stress. The six finite rigid body mechanisms can be identified and exist in the following symmetry subspaces:

1. Symmetry subspace $\mathbb{V}_{\mathbf{p}}^{(A_1)}$ contains the rigid body translation in the z'-direction.

2. Symmetry subspace $\mathbb{V}_{\mathbf{p}}^{(A_2)}$ contains the rigid body rotation about the z'-axis.

3. Symmetry subspace $\mathbb{V}_{\mathbf{p}}^{(E)1}$ contains the rigid body translation in the x'-direction and the rigid body rotation about the y'-axis.

4. Symmetry subspace $\mathbb{V}_{\mathbf{p}}^{(E)2}$ contains the rigid body translation in the y'-direction and the rigid body rotation about the x'-axis.

Hence, the one remaining inextensional mechanism exists in symmetry subspace $\mathbb{V}_{\mathbf{p}}^{(A_1)}$. Figure 7.15 shows a linear displacement of the frame in the direction of this mechanism. It is clear that the frame keeps its $\mathbf{C_{3v}}$ symmetry properties when the inextensional mechanism is displaced, and hence the form of the block-diagonalised

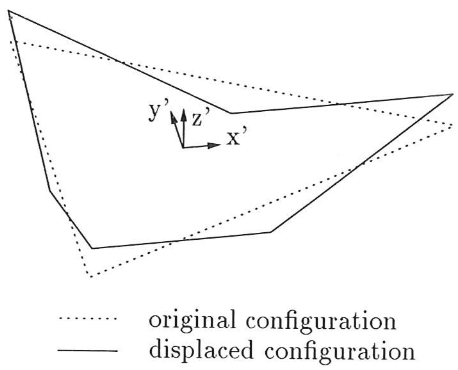

Figure 7.15: Frame with $\mathbf{C_{3v}}$ symmetry, after a linear displacement in the direction of the internal finite mechanism.

equilibrium matrix in Equation 7.35 does not change. Thus, no further analysis is required in order to determine whether this mechanism is finite or infinitesimal.

The block-diagonalised equilibrium matrix in Equation 7.35 shows that the state of self-stress exists in the second block $\tilde{\mathbf{H}}^{(A_2)}$ and is therefore unaffected when the mechanism in the first block $\tilde{\mathbf{H}}^{(A_1)}$ is displaced, i.e. this mechanism must be finite since it cannot be stiffened by the state of self-stress.

Figure 7.16(a)-(d) shows the frame in different configurations as it follows the actual path of this internal finite mechanism. At each configuration the block-diagonalised equilibrium matrix will have the same block form as shown in Equation 7.35, since the frame always has $\mathbf{C_{3v}}$ symmetry. Only the contents of the blocks change as the frame is displaced along the finite path; the symmetry properties of the blocks remain the same.

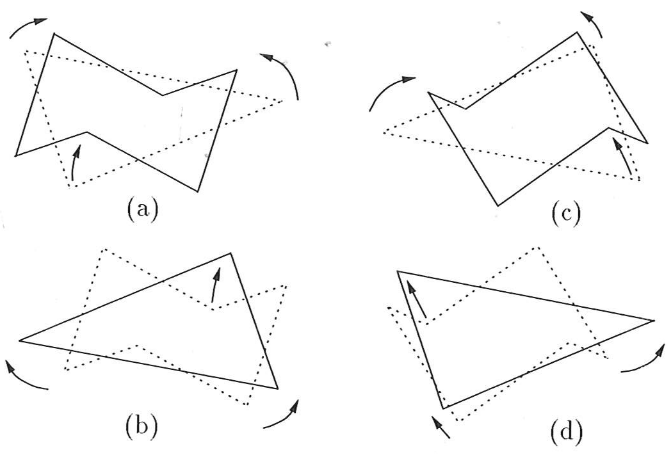

Figure 7.16: (a)-(d) show different configurations of the frame as it follows the path of the finite mechanism. In all configurations along this path the frame has $\mathbf{C_{3v}}$ symmetry.

Chapter 8

Conclusions and Future Work

8.1 Conclusions

This dissertation provides an introduction to the analysis of symmetric structures, in particular showing that simple procedures based on Group Representation Theory can reduce the complexity of the analysis and provide great savings in the computational effort required to analyse any symmetric structure. It is hoped that these ideas will become more widely known and used by the structural engineering community.

A large linear structural analysis consists of the construction and solution of a system of linear equations, and even with the assistance of modern computers any reduction in computational effort is of great value. Hence, finding ways to achieve computational efficiency are of interest. Large structures are often composed of a number of identical elements and hence have particular symmetry properties. This dissertation has shown that utilising these symmetry properties allows a very efficient method of analysis.

The methods developed in this dissertation utilise Group Representation Theory, which is the mathematical language best suited to describing the symmetry properties of a structure. In Chapters 1 and 2 the exploitation of simple bilateral symmetry and purely rotational symmetry using a Fourier transformation were discussed. In contrast with these methods, this dissertation has shown that the application of Group Representation Theory fully utilises the symmetry properties of the structure to simplify the analysis of the governing system of simultaneous equations. Thus, Group Representation Theory provides a systematic approach to the analysis of symmetric structures, with the result that the symmetry properties of any structure are fully exploited. Furthermore, it is clear that Group Representation Theory is indispensable for any structure which has symmetry properties that are more complex than simple bilateral or purely rotational symmetry.

Although the mathematical background of Group Theory is both complex and abstract, the application of Group Representation Theory and the calculations required to find symmetry-adapted coordinate systems are quite simple. These symmetry-adapted coordinate systems consist of independent symmetry subspaces which have particular symmetry properties, and this dissertation showed that by transforming into these symmetry-adapted coordinate systems the stiffness or equilibrium matrix of a pin-jointed structure was block-diagonalised into independent submatrices with particular symmetry properties. The solution for each of these submatrices requires fewer computational operations, hence reducing the complexity of the analysis and increasing the efficiency.

However, Chapters 4 to 7 showed that applying Group Representation Theory to block-diagonalise the equilibrium matrix not only simplified the analysis of a structure in terms of the computational effort required, but also provided valuable insight into the physical behaviour of a structure. In the symmetry-adapted coordinate systems each equilibrium submatrix block relates applied external loads with particular symmetry properties to internal forces of the structure with the same symmetry properties. Hence, any states of self-stress or inextensional mechanism present in a particular equilibrium submatrix block will necessarily have these symmetry properties. Chapter 6 for example, showed that a symmetry analysis of the equilibrium matrix was extremely useful for structures with highly complex symmetry, such as a pin-jointed cube with $\mathbf{O_h}$ symmetry.

A symmetry analysis proved particularly useful for investigating the physical behaviour of statically and kinematically indeterminate structures. The analysis not only showed that states of self-stress and inextensional mechanisms with particular symmetry properties were systematically identified, but it was also possible in some cases to identify when a symmetric structure contains a finite mechanism. This was done by showing that a state of self-stress with particular symmetry properties could not stiffen an inextensional mechanism with different symmetry properties and hence, the mechanism was free to follow a finite path.

This dissertation also showed that these symmetry techniques can be systematically applied to all types of structures with symmetry. More general structures with rigid or partially rigid joints were investigated in Chapter 7, using the same Group Representation Theory techniques but necessarily applied to more complex systems of simultaneous equations. However, it was clear that the underlying results of these more general structures have the same characteristics as less complex pin-jointed structures with the same symmetry properties.

8.2 Future Work

In this dissertation Group Theory methods have been used to simplify the static analysis of pin-jointed structures and frames with rigid or partially rigid joints.

However these methods could be similarly applied to any other type of structure which has symmetry, e.g. solid surface structures, and to different areas of structural analysis, such as analysing buckling and bifurcations problems, or finding natural frequencies and modes of vibrations of symmetric structures. Hence, the purpose of this dissertation was two-fold, the first was to provide a systematic methodology for the application of symmetry arguments to the fundamentals of structural analysis, and the second was, rather than concentrating on the mathematical basis of the required Group Representation Theory, to emphasise the implications that the application of symmetry arguments has on the analysis of symmetric structures.

One of the limitations imposed in this dissertation is that the example structures were limited to those which had both geometrical and mechanical symmetry have only been considered. Hence, an interesting possible extension of this work could be to investigate structures which have geometric symmetry but less or no mechanical symmetry. These structures would still have equilibrium and compatibility matrices which can be block-diagonalised using symmetry arguments. However the effects of the missing mechanical symmetry on both the stiffness and flexibility matrices would have to be examined.

In Chapters 3 and 4 the symmetry analysis was carried using the stiffness or equilibrium matrix of the rotational symmetry sub-structure. However if the symmetry of a structure is more complex, e.g. a symmetric structure often also has reflection symmetry as well as rotation symmetry, then there may exist a smaller symmetry sub-structure which would increase the efficiency of the analysis further. Hence, in a similar way to that for a rotational symmetry sub-structure, the symmetry analysis could be carried using the smallest symmetry sub-structure possible.

Another limitation of the work in this dissertation is the use of only symmetry point groups. Further work could be done to utilise for example, translational and magnification symmetry properties present in many large structures. These types of structure can be treated in a similar way to structures with rotation symmetry; however the end boundary conditions must be satisfied, i.e. the system of simultaneous equations must take into account the first and last symmetry sub-structure which do not have translational or magnification symmetry. Similar problems occur with structure which have only partial symmetry, that is structures which are "almost" symmetric in that they do have a lot of repetition, but are not truly symmetric in accordance with the definition of a symmetry operations or equivalent configurations. So of interest is whether this partial symmetry can be exploited to simplify the analysis of these types of structure using similar methods to those described in this dissertation. Some initial work has been carried out on these types of structure by Bossavit (1988), who takes into account the areas where true symmetry does not exist.

In Chapters 5-7 work was done to show how a symmetry analysis could be carried out on structures which have been displaced in the direction of an inextensional mechanism. Once the structure has been displaced it immediately takes on the symmetry properties of the mechanism. It was shown that a further analysis using these new symmetry properties can sometimes show whether the mechanism is in fact finite rather than infinitesimal. Similar work could also be carried out for structures which exhibit large deflections or elastic buckling under applied external loads and hence, take on new configurations with particular symmetry properties. In these cases further analysis may also show some interesting symmetry implications.

Finally, from a more abstract point of view, it is of interest how different choices of equivalent 2 or 3-dimensional irreducible matrix representations define symmetry subspaces with different basis vectors but with the same symmetry properties. Furthermore, the same block-diagonalised stiffness or equilibrium matrix can be found, irrespective of the axes of rotation or the planes of reflection defined by a 2 or 3-dimensional irreducible matrix representation and whether they coincide with the axes of rotation and planes of reflection of the structure. A remarkable characteristic of the symmetry subspaces corresponding to a 2 or 3-dimensional irreducible matrix representation, is that the basis vectors can always be arranged such that the corresponding stiffness or equilibrium blocks are identical, for example blocks $\tilde{\mathbf{H}}^{(E)1}$ and $\tilde{\mathbf{H}}^{(E)2}$ in Equation 4.23. Further investigation is required to determine whether this could provide additional insight into the characteristics of symmetric structures.

Appendix A

Group Representation Theory

Although the basic mathematical ideas of Group Theory are abstract, the actual techniques required to apply the theory are relatively simple. For the purpose of analysing symmetric structures, Group Theory must be applied to vectors in a vector space; this gives rise to *Group Representation Theory.* This appendix introduces some background and key concepts of Group Representation Theory, that are used in this dissertation. For a more detailed description of Group Representation Theory, see Schonland (1965) or Bishop (1973).

A.1 Symmetry Operations

A *symmetry operation*, such as a rotation about an axis or a reflection in a plane, brings a structure into a new position which coincides exactly with the original position, such that the structure is left in a geometrically and mechanically identical configuration. This is called an *equivalent configuration.* Described below are the five different types of symmetry operation that can be applied to symmetric structures:

1. The identity operation: the structure is left in its original configuration, this can occur when structure is rotated by 0° or an integer multiple of 360° about an axis of symmetry. The identity operation is denoted by the symbol E.

2. A rotation about an axis of symmetry: this operation is also called a proper rotation. A rotation about an axis of symmetry that brings the structure into an equivalent configuration is denoted by the symbol C_n. The corresponding axis of rotation is said to be an axis of n-fold symmetry.

   This rotation, which brings the structure into an equivalent configuration, is through an angle α about an axis of symmetry, where positive α corresponds to an anti-clockwise rotation. Further rotations about the same axis through angle α will also bring the structure into an equivalent configuration. If α is taken as the smallest angle of rotation that gives rise to an equivalent configuration, then n is given by:

$$n = 2\pi/\alpha$$

The results of applying rotation C_n n times is to bring the structure back to its original configuration after a rotation of 360° about the axis of symmetry. This equivalent to applying the identity operation E:

$$C_n^n = E$$

3. A reflection in a plane of symmetry: the operation of reflecting a structure in a plane of symmetry is denoted by the symbol σ. Reflecting the structure twice in the same plane brings it back to its original configuration:

$$\sigma^2 = E$$

4. A rotary reflection or improper rotation: this is the combination of a rotation through an angle of $2\pi/n$ about some axis and a reflection in a plane perpendicular to this axis. The order of these operations does not matter and the combined operation is denoted by the symbol S_n:

$$S_n = \sigma_h C_n = C_n \sigma_h$$

where σ_h denotes a reflection in the plane perpendicular to the axis of symmetry.

5. Inversion in the centre of symmetry: this operation is denoted by the symbol i and the effect is to move any point of the structure to a position the same distance away directly through the centre of symmetry. Thus i is simply the special case of an improper rotation when the angle rotation is 180°:

$$S_n = i = S_2 = \sigma_h C_2$$

A.2 Symmetry Groups

For any structure it is possible to write down all the symmetry operations that can be performed to bring it into an equivalent configuration. This set of symmetry operations forms the *symmetry group* of the structure, and are called the elements of the symmetry group. For example, the six symmetry operations $\{E, C_3, C_3^2, \sigma_a, \sigma_b, \sigma_c\}$ form the symmetry group $\mathbf{C_{3v}}$ of the example structure in Figure 3.1.

Any set of elements that forms a symmetry group must satisfy the following multiplication properties:

1. The product of two elements in a set, P and Q say, is also an element of the set:

$$R = PQ$$

This product PQ is the result of first applying element Q to the structure, then applying element P. The order of the elements is important because in general any two elements are not commutative. For example, the products of the two symmetry operations C_3 and σ_a:

$$C_3\sigma_a = \sigma_c$$

$$\sigma_a C_3 = \sigma_b$$

2. The product of two elements is associative:

$$R(PQ) = (RP)Q$$

For example, the product of the three symmetry operations C_3, σ_a and σ_b:

$$C_3(\sigma_a\sigma_b) = C_3C_3 = C_3^2 = \sigma_c\sigma_b = (C_3\sigma_a)\sigma_b$$

3. The set contains an identity element E with the property:

$$E = EP = PE$$

where P is any element of the set.

4. Each element of the set has an inverse which is also an element of the set:

$$PP^{-1} = P^{-1}P = E$$

For example, the inverse symmetry operation of C_3 is C_3^2:

$$C_3C_3^2 = E$$

Alternatively, the symmetry operations can form a multiplication table which completely defines the symmetry group, e.g. the multiplication table of symmetry group $\mathbf{C_{3v}}$, shown in Table 3.1.

Hence, it follows that Group Representation Theory is not concerned with the nature of the elements; it deals only with the formal structure of the symmetry group defined by the multiplication properties. The multiplication properties of a symmetry group depend only on the relationship between its elements, and these relationships are completely determined by the spatial relationships between the axes and planes of symmetry. Any two structures, no matter how different in form or complexity, which have the same system of axes and planes of symmetry will also have the same symmetry group. This is one of the reasons for the power and generality of Group Representation Theory applied to symmetric structures; for although the number of different imaginable structures is unbounded, this is not true of their possible systems of axes and planes of symmetry. They are severely restricted by geometrical considerations and it is possible to write down a list of all the symmetry groups and their properties that can exist in Euclidean space. To apply Group Representation Theory to a particular structure, all that is necessary is to identify the symmetry group of the structure and then apply standard methods to extract the desired information from the known symmetry properties of the symmetry group.

A.2.1 Classes of Conjugate Elements

An important concept in Group Representation Theory is the division of the elements into classes of conjugate elements. Two elements of a symmetry group P and Q are said to be conjugate to each other if there is some other element S of the symmetry group such that:

$$P = S^{-1}QS \tag{A.1}$$

It follows from Equation A.1 that if elements P and Q are both conjugate to an element W, then they are also conjugate to each other:

$$P = S^{-1}WS \text{ and } Q = TWT^{-1} \tag{A.2}$$

where T is also an element of the symmetry group.

Thus, $W = T^{-1}QT$ and substituting back into Equation A.2 gives:

$$P = S^{-1}(T^{-1}QT)S = (S^{-1}T^{-1})Q(TS) = (TS)^{-1}Q(TS) \tag{A.3}$$

where by multiplication property (1), (TS) must be some element of the symmetry group, and hence P is conjugate to Q.

Thus given any particular element W of a symmetry group, a subset of elements can be found which are conjugate to W and therefore to each other, by forming all the possible products $R^{-1}WR$, where R runs over all the elements of the symmetry group. This subset is called a *class of conjugate elements*, and the elements of any symmetry group can be divided into a number of mutually exclusive classes in this way.

For example, if a symmetry group contains an element Q which commutes with every other element R, then $R^{-1}QR = Q$ for every R, and hence Q is in a class by itself. Thus, in every symmetry group the identity operation E is in a class by itself. Furthermore, if every element in a symmetry group commutes with every other element, each element is in a class by itself. However, in general a symmetry group will contain some non-commuting elements and some of its classes will contain more than one element.

This division of a symmetry group into classes of conjugate elements based on the rather abstract definition of a class given above, can be thought of more naturally as a division of the elements into sets of geometrically similar operations. For example, the classes of symmetry group $\mathbf{C_{3v}}$ are the identity operation $\{E\}$, the three reflections $\{\sigma_a, \sigma_b, \sigma_c\}$, and the two rotations $\{C_3, C_3^2\}$. Schonland (1965) provides simple rules based on geometrically similar operations, for dividing the elements of a symmetry group into its classes.

This concept of classes of conjugate elements is used later to help determine the irreducible matrix representations of a symmetry group.

A.2.2 Point Groups

The symmetry groups discussed above are all formed from symmetry operation pertaining to a physical structure. These symmetry operations all leave a fixed point in space, i.e. the structure has an axis or plane of symmetry, and the fixed point must lie on this axis or plane. From this it follows that all the axes and planes that a structure may possess must intersect at one common point, which remains fixed under all the symmetry operations. Such symmetry groups are called *point groups*. (Alternatively, for a structure of infinite size it is possible to have symmetry operations that leave no point fixed in space, e.g. translations; these give rise to *space groups*.)

Point groups can be classified into three broad classes using Schoenflies notation (Schonland 1965). The first class consists of the two simple non-axial groups. A structure may possess just one plane of symmetry so that its only symmetry operations are the identity E and the reflection σ in the plane of symmetry; this symmetry group is denoted $\mathbf{C_s}$. Alternatively a structure may possess just a centre of symmetry, so that its only symmetry operations are the identity E and the inversion i (an improper rotation through an angle of 180°); this symmetry group is denoted $\mathbf{C_i}$.

The second class consists of groups which are distinguished by possessing a single main n-fold axis of symmetry. If a structure possesses one main n-fold axis of symmetry all its symmetry operations must leave the axis of symmetry unaltered or reversed in direction. The symmetry operations which satisfy this class are:

(a) Rotations about the main axis, denoted C_n^i.

(b) Improper rotations about the main axis, denoted S_n^i.

(c) Reflections in a plane perpendicular to the main axis, such a plane is called a *horizontal* plane and the operation is denoted σ_h.

(d) Reflections in a plane containing the main axis, such a plane is called a *vertical* plane and the operation is denoted σ_v.

(e) A rotation through 180° about a 2-fold axis perpendicular to the main axis, denoted C'_2.

These operations may be combined in various way to form the following symmetry groups with one main symmetry axis:

(a) Symmetry group $\mathbf{C_n}$, which has the single n-fold symmetry axis and the elements of the group are the rotations C^i_n.

(b) Symmetry group $\mathbf{S_{2n}}$, which has the single axis of *even* order $2n$ and the elements of the group are the improper rotations S^i_{2n}.

(c) Symmetry group $\mathbf{C_{nh}}$, which is obtained by adding a horizontal symmetry plane perpendicular to the single n-fold symmetry axis and the elements of the group are the rotations C^i_n and the improper rotations S^i_n.

(d) Symmetry group $\mathbf{C_{nv}}$, which is obtained by adding n vertical symmetry planes containing the single n-fold symmetry axis and the elements of the group are the rotations C^i_n and the n reflections σ_v.

(e) Symmetry group $\mathbf{D_n}$, which is obtained by adding n 2-fold axes perpendicular to the main axis and the elements of the group are the rotations C^i_n and the n rotations C'_2 about these 2-fold axes.

(f) Symmetry group $\mathbf{D_{nh}}$, which is obtained if the horizontal plane containing the 2-fold axes of symmetry group $\mathbf{D_n}$ is also a symmetry plane, then the elements of the group are the rotations C^i_n; the n rotations C'_2 about these 2-fold axes, n reflections σ_v and the improper rotations S^i_n.

(g) Symmetry group $\mathbf{D_{nd}}$, which is obtained by adding n vertical symmetry planes containing the main axis and bisecting the angles between adjacent 2-fold axes. The elements of the group are the rotations C^i_n, the n rotations C'_2 about these 2-fold axes, n reflections σ_v and improper rotations of the form S^{2i+1}_{2n}, where $i = 0$ to $n - 1$.

The third class consists of symmetry groups with more than one main n-fold symmetry axis, and these are related to the symmetry of the regular solids, the tetrahedron, cube and icosahedron. If a structure has several n-fold symmetry axes, these axes must intersect at a point and their spatial arrangement must be such that a rotation C^i_n about one of the axes results in an interchange of the other axes. This condition severely limits the number of possible groups containing more than one n-fold axis.

These symmetry groups are discussed below in order of increasing values of n:

(a) $n = 2$, Symmetry groups $\mathbf{D_2}$, $\mathbf{D_{2h}}$ and $\mathbf{D_{2d}}$. If there is a set of intersecting 2-fold axes, there must be three of them, mutually perpendicular to each other. This is the set of axes of symmetry group $\mathbf{D_2}$. There are only two different ways of adding planes of reflection symmetry to this set of axes; these give rise to the symmetry groups $\mathbf{D_{2h}}$ and $\mathbf{D_{2d}}$.

(b) $n = 3$, Symmetry groups $\mathbf{T}$, $\mathbf{T_d}$ and $\mathbf{T_h}$. If there is a set of intersecting 3-fold axes, there must be four such axes whose directions are those of the body diagonals of a cube. However, the existence of the four 3-fold axes necessarily implies the existence of three mutually perpendicular 2-fold axes. This set of 3-fold and 2-fold axes form symmetry group $\mathbf{T}$. There are only two different ways of adding planes of reflection symmetry to this set of axes; these give rise to the symmetry groups $\mathbf{T_d}$ and $\mathbf{T_h}$. These are the symmetry groups related to a tetrahedron.

(c) $n = 4$, Symmetry groups $\mathbf{O}$ and $\mathbf{O_h}$. If there is a set of intersecting 4-fold axes, there must be three such axes, mutually perpendicular to each other. The existence of the four 3-fold axes necessarily implies the existence of four 3-fold axes, like those of symmetry group $\mathbf{T}$, and the existence of six 2-fold axes. This set of 4-fold, 3-fold and 2-fold axes form symmetry group $\mathbf{O}$. There is only one way of adding planes of reflection symmetry to this set of axes, to give symmetry group $\mathbf{O_h}$. This is the symmetry group of a cube or regular octahedron.

(d) $n = 5$, Symmetry groups $\mathbf{S}$ and $\mathbf{S_h}$. These symmetry groups contain twelve 5-fold, twenty 3-fold and fifteen 2-fold axes. They are related to the symmetry of the icosahedron.

There are no point groups with intersecting axes for which n is greater than five. Further detailed description of these symmetry groups can be obtained in most Group Theory books.

A.3 Reducible and Irreducible Matrix Representations

In Chapters 3 and 4 two different matrix representations were found for the operations of a symmetry group. It is possible to classify and characterise all the possible representations of a symmetry group. It is this classification of representations that results in the main applications of Group Representation Theory to symmetric structures.

The classification of the representations of a symmetry group may initially seem an infinite task since vector spaces of any dimension can be considered and the choice of vector basis for a given vector space is arbitrary. However, all the representations which arise from a given vector space are essentially equivalent and it is possible to show that any representation can be described in terms of a small number of fundamental irreducible representations.

Hence, this section will show that the key concepts of Group Representation Theory are those of equivalent representations, the character of a representation, and the reduction of a representation into its irreducible components.

A.3.1 Equivalent Representations

To find a matrix representation it is necessary to choose a vector basis for the given vector space and then calculate the effects each of the operations have on each basis vector. A different choice of vector basis will produce a numerically different matrix representation, and since the choice of vector basis is arbitrary, there can be many matrix representations of a symmetry group in a given vector space. However all these representations are essentially equivalent since they contain exactly the same information, namely the effects the operations have on a general vector in the vector space. Hence, it is necessary to show how these equivalent representations are related to each other.

For a given vector space, two matrix representations $\mathbf{P}$ and $\mathbf{Q}$ of a symmetry group are *equivalent* if there is some non-singular matrix $\mathbf{A}$ (i.e. matrix $\mathbf{A}$ has an inverse $\mathbf{A^{-1}}$) such that:

$$\mathbf{PA} = \mathbf{AQ} \qquad or \qquad \mathbf{P} = \mathbf{AQA^{-1}} \tag{A.4}$$

for every operation of the symmetry group.

Equation A.4 shows that any one matrix representation can be obtained from another by using the appropriate similarity transformation matrix $\mathbf{A}$.

A.3.2 Character of a Representation

Of interest is a quantity of a representation that describes the representation in general, without referring to some specific vector basis, i.e. a quantity which is the same for all equivalent representations and is different for all non-equivalent representations. This invariant quantity associated with the matrices in a representation is the *trace* $Tr[\mathbf{M}]$ of a matrix $\mathbf{M}$. The trace of a matrix is defined to be the sum of the diagonal components; for an $(n \times n)$ matrix $\mathbf{M}$ with components d_{ij}:

$$Tr(\mathbf{M}) = \sum_{i=1}^{n} d_{ii} \tag{A.5}$$

It is possible to show that the trace of any matrix in a representation remains invariant under a change of vector basis, i.e. the trace of corresponding matrices $\mathbf{P}(\alpha)$ and $\mathbf{Q}(\alpha)$ in two equivalent representations $\mathbf{P}$ and $\mathbf{Q}$, is the same:

$$Tr[\mathbf{P}(\alpha)] = Tr[\mathbf{Q}(\alpha)] \tag{A.6}$$

Hence, the trace of the matrices in a representation gives a set of numbers which is characteristic of the representation in the sense that all equivalent representations have the same set of numbers, while non-equivalent representations have different sets. Thus, the trace of a matrix in a representation is called the *character* $\chi[\mathbf{R}(\alpha)]$ of the corresponding operation in the symmetry group.

$$\chi[\mathbf{R}(\alpha)] = Tr[\mathbf{R}(\alpha)] \tag{A.7}$$

The complete set of characters, one for each operation in the symmetry group, is called the *character of the representation*, and hence it is possible to say that *two representations are equivalent if they have the same character.*

A.3.3 Reducible and Irreducible Matrix Representations

So far this section has shown how a change of vector basis will give an equivalent matrix representation and how to characterise all non-equivalent matrix representations. Now it is possible to introduce reducible and irreducible matrix representations; these are concepts that lead directly to the application of Group Representation Theory to symmetric structures.

For a symmetry group and a given vector space, it is possible to find a vector basis for the matrix representation that is particularly simple. There exists a vector basis such that the matrices of a representation appear in a *reduced form* as direct sums of matrices belonging to *irreducible matrix representations.*

If there is a representation $\mathbf{R}$ such that a vector basis can be found which splits the vector space $\mathbb{V}$ into two subspaces $\mathbb{V}'$ and $\mathbb{V}''$, where any vector in either subspace, is transformed into another vector in the *same* subspace under all of the symmetry operations, then $\mathbb{V}'$ and $\mathbb{V}''$ are *invariant subspaces* of vector space $\mathbb{V}$ and $\mathbf{R}$ is a *reducible matrix representation.* $\mathbf{R}$ now appears in a reduced form with representations $\mathbf{R}'$ and $\mathbf{R}''$ along the diagonal. The relationship between the original representation and representations $\mathbf{R}'$ and $\mathbf{R}''$ is written:

$$\mathbf{R} = \mathbf{R}' \oplus \mathbf{R}'' \tag{A.8}$$

where $\oplus$ is a direct sum. If no such vector basis exists then $\mathbf{R}$ is an *irreducible matrix representation.*

This procedure can be continued to consider whether the representations $\mathbf{R}'$ and $\mathbf{R}''$ are themselves reducible. The invariant subspaces $\mathbb{V}'$ and $\mathbb{V}''$ may also contain invariant subspaces such that $\mathbf{R}'$ and $\mathbf{R}''$ can be reduced by a suitable change of vector basis for $\mathbb{V}'$ and $\mathbb{V}''$. Then $\mathbf{R}'$ and $\mathbf{R}''$ are also expressed as direct sums of representations with smaller dimensions. This reduction process can be continued until the original vector space $\mathbb{V}$ has been decomposed into a number of invariant subspaces, each of which gives rise independently to a representation and none of which can be further divided into invariant subspaces of smaller dimension. At this point all the matrices of the representation have been transformed into a *block-diagonal* form:

$$\tilde{\mathbf{R}} = \begin{bmatrix} \boxed{\Gamma^{(1)}} & & & \mathbf{0} \\ & \boxed{\Gamma^{(2)}} & & \\ & & \boxed{\Gamma^{(3)}} & \\ \mathbf{0} & & & \ddots \quad \boxed{\Gamma^{(p)}} \end{bmatrix} \tag{A.9}$$

This fully reduced representation is denoted $\tilde{\mathbf{R}}$, and contains the irreducible matrix representations along its diagonal, i.e. the original matrix representation has been decomposed into its component irreducible matrix representations, which are denoted by the symbol $\Gamma^{(\mu)}$:

$$\tilde{\mathbf{R}} = \Gamma^{(1)} \oplus \Gamma^{(2)} \oplus \Gamma^{(3)} \oplus \cdots \oplus \Gamma^{(p)} \tag{A.10}$$

A.3.4 Properties of Irreducible Matrix Representations

Equation A.10 does not fully define a reduced representation $\tilde{\mathbf{R}}$, i.e. it does not identify which irreducible representations appear in the reduced representation. However, the irreducible matrix representations of a symmetry group possess a number of remarkable properties. These properties allow all the possible irreducible matrix representations of a symmetry group to be enumerated and classified, and any reducible matrix representations to be decomposed into its irreducible components. The properties of irreducible matrix representations, that are of interest in this dissertation, are stated below.

If a symmetry group $\mathbf{G}$ contains g symmetry operations, which can be divided into k different classes of mutually conjugate symmetry operations, as described in Section A.2. Then it is possible to prove that,

Theorem 1 *The symmetry group* $\mathbf{G}$ *possess exactly* k *different (i.e. non-equivalent) irreducible matrix representations* $\{\Gamma^{(1)}, \Gamma^{(2)}, \cdots, \Gamma^{(k)}\}$ *whose dimensions* $\{n_1, n_2, \cdots, n_k\}$

satisfy the equation:

$$n_1^2 + n_2^2 + \cdots + n_k^2 = g \tag{A.11}$$

All symmetry groups have a g and a k which are such that there is only one possible set of k integers, the sum of whose squares is equal to g. Hence, Theorem 1 gives both the number of irreducible representations possessed by a given symmetry group and also what dimensions they are.

A property of the k classes of symmetry operations is that in each class all the symmetry operations will have the same character. The k different classes of symmetry group $\mathbf{G}$ can be denoted $\{K_1, K_1, \cdots, K_k\}$, where each class contains $\{g_1, g_2, \cdots, g_k\}$ symmetry operations respectively. Furthermore, in irreducible representation $\Gamma^{(\mu)}$, the character of all the symmetry operations in class K_i, is denoted by $\chi_i^{(\mu)}$. Then the next theorem is,

Theorem 2 *The characters $\chi_i^{(\mu)}$ of the different irreducible representations satisfy the relationship:*

$$\sum_{i=1}^{k} g_i \chi_i^{(\mu)*} \chi_i^{(\nu)} = g\delta_{\mu\nu} \tag{A.12}$$

where $\chi_i^{(\mu)*}$ is the complex conjugate of $\chi_i^{(\mu)}$.

The consequence of Theorem 2 is that the sets of characters $\chi_i^{(\mu)}$ belonging to the different irreducible representations must be different. Thus, characters may be used to classify irreducible representations and distinguish them from each other. This classification is conveniently shown in the form of a *character table*, e.g. Table 6.1.

The final property of irreducible representations that is required to fully reduce a representation into its irreducible components is, which of the irreducible representations of a symmetry group appear in a reduced representation; that is, to write down the appropriate form of Equation A.10.

The same irreducible representation may occur more than once in the reduction of a representation; equally, not every irreducible representation will necessarily appear. Using Theorem 2 it is possible to show that the number of times irreducible representation $\Gamma^{(\mu)}$ occurs in the reduction of a representation $\mathbf{R}$ is:

$$a_\mu = \frac{1}{g} \sum_{i=1}^{k} g_i \chi_i^{(\mu)*} \chi_i^{(K)}[\mathbf{R}] \tag{A.13}$$

where in representation $\mathbf{R}$, $\chi_i^{(K)}[\mathbf{R}]$ is the character of all the symmetry operations belonging to class K_i.

Hence, a reduced representation $\tilde{\mathbf{R}}$ is fully defined by:

$$\tilde{\mathbf{R}} = a_1\Gamma^{(1)} \oplus \cdots \oplus a_\mu\Gamma^{(\mu)} \oplus \cdots \oplus a_k\Gamma^{(k)} = \sum_{\mu=1}^{k} a_\mu\Gamma^{(\mu)} \qquad \text{(A.14)}$$

Now however, the more difficult problem is to find the vector basis for the vector space in which the representation appears in its reduced form. This problem requires the Great Orthogonality Theorem and is addressed in the next two sections.

A.3.5 Notation for Irreducible Representations

Mulliken symbols are commonly used to denote the irreducible representations of a symmetry group, and are used in this dissertation. A brief description is given below, a more detailed description can be found in Schonland (1965).

None of the symmetry groups used in this dissertation have irreducible representations with dimensions greater than three. Also the characters of an irreducible representation are mostly real numbers; certain 1-dimensional irreducible representations have complex characters.

The 1-dimensional irreducible representations with real characters are defined by the symbols A or B, the 2-dimensional irreducible representations are defined by the symbol E, and the 3-dimensional irreducible representations are defined by the symbols T or F.

Suffixes $1, 2, 3, \ldots$ are used where necessary, to distinguish between different irreducible representations with the same dimensions. For certain symmetry groups, the Mulliken symbols may also have suffixes g or u attached, or they may appear with primes or double primes. (The significance of these additions are not described here).

For example, symmetry group $\mathbf{C_{3v}}$ has the irreducible matrix representations $\{\Gamma^{(A_1)}, \Gamma^{(A_2)}, \Gamma^{(E)}\}$; these are shown in Table 3.3.

A symmetry group which has a 1-dimensional irreducible representation with complex characters, denoted $\Gamma^{(c)}$, will always have its complex conjugate pair $\Gamma^{(c)*}$. In Mulliken notation these pairs of representations are bracketed together and given the symbol E appropriate to a 2-dimensional irreducible representation. For example, symmetry group $\mathbf{C_3}$ has the irreducible matrix representations $\{\Gamma^{(A)}, \Gamma^{(E)}\}$; these are shown in Table 3.5.

A.4 Great Orthogonality Theorem

The results of the previous section show which of the irreducible matrix representations $\Gamma^{(\mu)}$ of a symmetry group are contained in a reducible matrix representation

R. In order to solve the more difficult problem of finding a vector basis in which the matrices of the reducible matrix representation **R** have the completely reduced form of Equation 3.4, the Great Orthogonality Theorem is required and states:

Theorem 3 *The components of any two irreducible matrix representations $\Gamma^{(\mu)}$ and $\Gamma^{(\nu)}$ which belong to the same symmetry group, satisfy the relationship:*

$$\sum_R \Gamma_{ij}^{(\mu)*}\Gamma_{pq}^{(\nu)} = \frac{g}{n_\mu}\delta_{\mu\nu}\delta_{ip}\delta_{jq} \tag{A.15}$$

where: subscripts (ij) and (pq) identify particular components of the two irreducible matrix representations $\Gamma^{(\mu)}$ and $\Gamma^{(\nu)}$,
g is the number of elements in the symmetry group and the summation is over all the elements,
n_μ is the dimension of $\Gamma^{(\mu)}$,
$\Gamma^{(\mu)*}$ is the complex conjugate of $\Gamma^{(\mu)}$,
δ_{mn} is the "Kronecker delta" defined by,

$$\delta_{mn} = \begin{cases} 1 \; if \; m = n, \\ 0 \; if \; m \neq n. \end{cases} \tag{A.16}$$

Equation A.15 covers three different cases.

(a) If $\Gamma^{(\mu)}$ and $\Gamma^{(\nu)}$ are different irreducible matrix representations, so that $\mu \neq \nu$ and hence $\delta_{\mu\nu} = 0$, then:

$$\sum_R \Gamma_{ij}^{(\mu)*}\Gamma_{pq}^{(\nu)} = 0 \tag{A.17}$$

(b) If $\Gamma^{(\mu)}$ and $\Gamma^{(\nu)}$ are the same ($\mu = \nu$, $\delta_{\mu\nu} = 1$), but $i \neq p$ and/or $j \neq q$, so that $\delta_{ip} = 0$ and/or $\delta_{jq} = 0$, then:

$$\sum_R \Gamma_{ij}^{(\mu)*}\Gamma_{pq}^{(\mu)} = 0 \tag{A.18}$$

(c) If $\mu = \nu$ and at the same time $i = p$ and $j = q$, so that $\delta_{ip} = \delta_{jq} = 1$, then:

$$\sum_R \Gamma_{ij}^{(\mu)*}\Gamma_{ij}^{(\mu)} = \sum_R \left|\Gamma_{ij}^{(\mu)}\right|^2 = \frac{g}{n_\mu} \tag{A.19}$$

For example, using the irreducible matrix representations $\{\Gamma^{(A_1)}, \Gamma^{(A_2)}, \Gamma^{(E)}\}$ of symmetry group $\mathbf{C_{3v}}$ shown in Table 3.3.

(a) $\mu = A_1$ and $\nu = A_2$:

$$\begin{aligned}\sum_R \Gamma_{ij}^{(\mu)*}\Gamma_{pq}^{(\nu)} &= \sum_R \Gamma_{11}^{(A_1)*}\Gamma_{11}^{(A_2)} \\ &= (1 \times 1) + (1 \times 1) + (1 \times 1) + \\ &\quad (1 \times -1) + (1 \times -1) + (1 \times -1) \\ &= 0 \end{aligned} \tag{A.20}$$

(b) $\mu = \nu = E$, $ij = 11$ and $pq = 22$:

$$\begin{aligned}\sum_R \Gamma_{ij}^{(\mu)*}\Gamma_{pq}^{(\nu)} &= \sum_R \Gamma_{11}^{(E)*}\Gamma_{22}^{(E)} \\ &= (1 \times 1) + (-1/2 \times -1/2) + (-1/2 \times -1/2) + \\ &\quad (-1 \times 1) + (1/2 \times -1/2) + (1/2 \times -1/2) \\ &= 0 \end{aligned} \tag{A.21}$$

(c) $\mu = \nu = E$ and $ij = pq = 12$:

$$\begin{aligned}\sum_R \Gamma_{ij}^{(\mu)*}\Gamma_{pq}^{(\nu)} &= \sum_R \Gamma_{12}^{(E)*}\Gamma_{12}^{(E)} \\ &= (0 \times 0) + (-\sqrt{3}/2 \times -\sqrt{3}/2) + (\sqrt{3}/2 \times \sqrt{3}/2) + \\ &\quad (0 \times 0) + (-\sqrt{3}/2 \times -\sqrt{3}/2) + (\sqrt{3}/2 \times \sqrt{3}/2) \\ &= 3 \end{aligned} \tag{A.22}$$

The Great Orthogonality Theorem is the *key* theorem of Group Representation Theory and can be used to solve the problem of finding symmetry-adapted coordinate systems for any vector space of a symmetric structure. The next section shows how the great Orthogonality Theorem is used to find orthonormal basis vectors for any symmetry subspaces $\mathbb{V}^{(\mu)i}$ corresponding to row i of irreducible matrix representation $\Gamma^{(\mu)}$.

A.5 Projection Operator Theory

In Section A.3 irreducible matrix representations $\Gamma^{(\mu)}$ were described which operate on irreducible invariant subspaces $\mathbb{V}^{(\nu)}$. The following orthonormal vector basis can be defined for an irreducible invariant subspace $\mathbb{V}^{(\nu)}$:

$$\mathbf{V}^{(\nu)} = \left(\mathbf{v}_1^{(\nu)}, \mathbf{v}_2^{(\nu)}, \cdots, \mathbf{v}_{n_\nu}^{(\nu)}\right) \tag{A.23}$$

where n_ν is the dimension of the irreducible matrix representation $\Gamma^{(\mu)}$.

Hence, the irreducible matrix representation $\Gamma^{(\mu)}$ can be defined as a representation which transforms the basis vectors of an irreducible invariant subspaces $\mathbb{V}^{(\nu)}$ amongst themselves.

If one of the orthonormal basis vectors $\mathbf{v}_q^{(\nu)}$ is operated on by a reducible matrix representation $\mathbf{R}$, then by the definition of an irreducible invariant subspace, this basis vector must be transformed into a new vector in the same irreducible invariant subspace. This new vector is a combination of the orthonormal basis vectors shown in Equation A.23, according to the components of the corresponding irreducible matrix representation $\Gamma^{(\mu)}$:

$$\mathbf{R}\mathbf{v}_q^{(\nu)} = \sum_{p=1}^{n_\nu} \Gamma_{pq}^{(\nu)} \mathbf{v}_p^{(\nu)} \tag{A.24}$$

Equation A.24 can be multiplied by $\Gamma_{ij}^{(\mu)*}$ and summed over all the operations in $\mathbf{R}$, to obtain:

$$\sum_R \Gamma_{ij}^{(\mu)*} \mathbf{R}\mathbf{v}_q^{(\nu)} = \sum_{p=1}^{n_\nu} \sum_R \Gamma_{ij}^{(\mu)*} \Gamma_{pq}^{(\nu)} \mathbf{v}_p^{(\nu)} \tag{A.25}$$

Then by the Great Orthogonality Theorem, the right-hand side of Equation A.25 is equal to:

$$\sum_{p=1}^{n_\nu} \frac{g}{n_\mu} \delta_{\mu\nu} \delta_{ip} \delta_{jq} \mathbf{v}_p^{(\nu)} \tag{A.26}$$

The only non-zero term in the summation over p is the one for which $p = i$, hence Equation A.25 becomes:

$$\sum_R \Gamma_{ij}^{(\mu)*} \mathbf{R}\mathbf{v}_q^{(\nu)} = \frac{g}{n_\mu} \delta_{\mu\nu} \delta_{jq} \mathbf{v}_i^{(\nu)} \tag{A.27}$$

Equation A.27 can be rewritten as:

$$\mathbf{O}_{ij}^{(\mu)} \mathbf{v}_q^{(\nu)} = \frac{g}{n_\mu} \delta_{\mu\nu} \delta_{jq} \mathbf{v}_i^{(\nu)} \tag{A.28}$$

where:

$$\mathbf{O}_{ij}^{(\mu)} = \sum_R \Gamma_{ij}^{(\mu)*} \mathbf{R} \tag{A.29}$$

$\mathbf{O}_{ij}^{(\mu)}$ is the *projection operator matrix*, which is a linear combination of the operations in $\mathbf{R}$ with coefficients that depend on the matrix components of the irreducible matrix representations $\Gamma^{(\mu)}$.

Consider the application of the projection operator matrix to the basis vector $\mathbf{v}_q^{(\nu)}$, Equation A.28 covers three cases.

(a) If $\mu \neq \nu$:

$$\mathbf{O}_{ij}^{(\mu)}\mathbf{v}_q^{(\nu)} = 0 \tag{A.30}$$

(b) If $\mu = \nu$ but $q \neq j$:

$$\mathbf{O}_{ij}^{(\mu)}\mathbf{v}_q^{(\mu)} = 0 \tag{A.31}$$

(c) If $\mu = \nu$ and $q = j$:

$$\mathbf{O}_{ij}^{(\mu)}\mathbf{v}_j^{(\mu)} = \frac{g}{n_\mu}\mathbf{v}_i^{(\mu)} \tag{A.32}$$

Cases (a)-(c) show that the projection operator matrix $\mathbf{O}_{ij}^{(\mu)}$, corresponding to row i of irreducible matrix representations $\Gamma^{(\mu)}$, projects out (with factor g/n_μ) any basis vectors $\mathbf{v}_i^{(\mu)}$. That is, the column space of projection operator matrix $\mathbf{O}_{ij}^{(\mu)}$ gives a vector basis for *symmetry subspace* $\mathbb{V}^{(\mu)i}$, corresponding to row i of irreducible matrix representations $\Gamma^{(\mu)}$.

If an irreducible matrix representations $\Gamma^{(\mu)}$ occurs a_μ times in the equivalent block-diagonalised matrix representation $\tilde{\mathbf{R}}$, then symmetry subspace $\mathbb{V}^{(\mu)i}$ will have a_μ basis vectors, i.e. the column space of projection operator matrix $\mathbf{O}_{ij}^{(\mu)}$ will be a_μ-dimensional.

Furthermore, it is clear that for any n_μ-dimensional irreducible matrix representation, the projection operator matrix finds n_μ different symmetry subspaces $\mathbb{V}^{(\mu)i}$, each corresponding to a different row i of the irreducible matrix representations $\Gamma^{(\mu)}$.

For all (1×1) irreducible matrix representations $\Gamma^{(\mu)}$, the corresponding symmetry subspace may be denoted $\mathbb{V}^{(\mu)}$, i.e. the superscript $i = 1$ is omitted.

For a $(n_\mu \times n_\mu)$ irreducible matrix representation, where $n_\mu > 1$, only matrix components from the different rows of the $(n_\mu \times n_\mu)$ irreducible matrix representation $\Gamma^{(\mu)}$ will give different symmetry subspaces $\mathbb{V}^{(\mu)i}$. For example, the column space of the following projection operator matrices $\{\mathbf{O}_{11}^{(\mu)}, \mathbf{O}_{12}^{(\mu)}\}$, both of which correspond to matrix components from the first row of a (2×2) irreducible matrix representation $\Gamma^{(\mu)}$, will give the same symmetry subspaces $\mathbb{V}^{(\mu)1}$.

Together, all the symmetry subspaces $\mathbb{V}^{(\mu)i}$ make up the full vector space $\mathbb{V}$.

Appendix B

Calculating Irreducible Matrix Representations

In general, most textbooks on Group Representation Theory only give the character tables of the different symmetry point groups, since the character of each irreducible representation often gives all the information that is required by, for example, a chemist. However, this dissertation has shown that the coefficients of the 2 and 3-dimensional irreducible matrix representations also provide valuable information for the analysis of symmetric structures. Hence it is necessary to have a systematic method for calculating the irreducible matrix representations of any symmetry group. This appendix shows how it is possible with the use of example symmetry group $\mathbf{O_h}$.

In Chapter 4 an analysis of a pin-jointed cube with $\mathbf{O_h}$ symmetry was carried out. There are ten irreducible matrix representations $\{\Gamma^{(A_{1g})}, \Gamma^{(A_{1u})}, \Gamma^{(A_{2g})}, \Gamma^{(A_{2u})}, \Gamma^{(E_g)}, \Gamma^{(E_u)}, \Gamma^{(T_{1g})}, \Gamma^{(T_{1u})}, \Gamma^{(T_{2g})}, \Gamma^{(T_{2u})}\}$ which represent the different symmetry properties of symmetry group $\mathbf{O_h}$, and Table 6.1 gives the characters of these irreducible matrix representations.

The irreducible matrix representations $\Gamma^{(A_{1g})}$, $\Gamma^{(A_{1u})}$, $\Gamma^{(A_{2g})}$ and $\Gamma^{(A_{2u})}$ are all 1-dimensional representations, and hence are identical to their characters in Table 6.1. For the non-trivial 2 and 3-dimensional irreducible matrix representations however, the required matrices must be found.

It is fairly straight forward to find a single 2 or 3-dimensional irreducible matrix representation, which this appendix will refer to as the *initial irreducible matrix representation*. However, some of the complex symmetry groups can have more than one 2 or 3-dimensional irreducible matrix representation, hence a procedure is also required to calculate these remaining irreducible matrix representations once the initial irreducible matrix representation has been generated. This is done by observing the difference between the remaining irreducible matrix representations and the initial irreducible matrix representation, given by the character table of the particular symmetry group.

B.1 Calculating the Initial Irreducible Matrix Representations

For any given symmetry group with 2-dimensional irreducible matrix representations, the initial irreducible matrix representation is found by carrying out all the operations in the symmetry group on a 2-dimensional set of orthogonal vectors (say u and v), acting at a single point in space. For example, the matrix operation C_3 rotates the u and v vectors 120° anti-clockwise to their new positions u' and v':

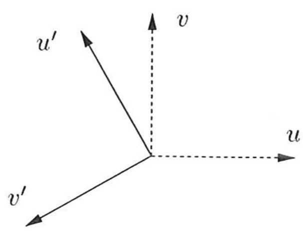

$$\begin{aligned} u' &= -1/2u - \sqrt{3}/2v \\ v' &= \sqrt{3}/2u - 1/2v \end{aligned}, \quad C_3 = \begin{bmatrix} -1/2 & -\sqrt{3}/2 \\ \sqrt{3}/2 & -1/2 \end{bmatrix} \tag{B.1}$$

For symmetry group $\mathbf{O_h}$, the full set of matrix operations for the initial irreducible matrix representation $\Gamma^{(E_u)}$, are shown in Table B.1.

Note that, for any irreducible matrix representation, once a few of the matrix operations (at least one from each of the different classes) have been found, the multiplication table can be used to quickly generate the rest of the matrix operations.

The multiplication table for symmetry group $\mathbf{O_h}$ (see Altmann & Herzig 1994), can also be used to check that this set of matrix operations actually constitutes a representation. It is also straight forward to check that the characters of this set of matrix operations identify it as the initial irreducible matrix representation $\Gamma^{(E_u)}$, defined in Table 6.1.

Similarly, for any given symmetry group with 3-dimensional irreducible matrix representations, the initial irreducible matrix representation is found by carrying out all the operations in the symmetry group on a 3-dimensional set of orthogonal vectors, (say x, y and z), acting at a single point in space. For example, the matrix operation C_{2x} rotates the y and z vectors 180° anti-clockwise about the x-axis:

$$E = C_{2x} = C_{2y} = C_{2z} = \begin{bmatrix} 1 & 0 \\ 0 & 1 \end{bmatrix}$$

$$C_{31} = C_{32} = C_{33} = C_{34} = \begin{bmatrix} -1/2 & -\sqrt{3}/2 \\ \sqrt{3}/2 & -1/2 \end{bmatrix}$$

$$C_{31}^2 = C_{32}^2 = C_{33}^2 = C_{34}^2 = \begin{bmatrix} -1/2 & \sqrt{3}/2 \\ -\sqrt{3}/2 & -1/2 \end{bmatrix}$$

$$C_{4x} = C_{4x}^3 = C'_{2d} = C'_{2f} = \begin{bmatrix} \sqrt{3}/2 & -1/2 \\ -1/2 & -\sqrt{3}/2 \end{bmatrix}$$

$$C_{4y} = C_{4y}^3 = C'_{2c} = C'_{2e} = \begin{bmatrix} -\sqrt{3}/2 & -1/2 \\ -1/2 & \sqrt{3}/2 \end{bmatrix}$$

$$C_{4z} = C_{4z}^3 = C'_{2a} = C'_{2b} = \begin{bmatrix} 0 & 1 \\ 1 & 0 \end{bmatrix}$$

$$i = \sigma_x = \sigma_y = \sigma_z = \begin{bmatrix} -1 & 0 \\ 0 & -1 \end{bmatrix}$$

$$S_{4x} = S_{4x}^3 = \sigma_{d4} = \sigma_{d6} = \begin{bmatrix} -\sqrt{3}/2 & 1/2 \\ 1/2 & \sqrt{3}/2 \end{bmatrix}$$

$$S_{4y} = S_{4y}^3 = \sigma_{d3} = \sigma_{d5} = \begin{bmatrix} \sqrt{3}/2 & 1/2 \\ 1/2 & -\sqrt{3}/2 \end{bmatrix}$$

$$S_{4z} = S_{4z}^3 = \sigma_{d1} = \sigma_{d2} = \begin{bmatrix} 0 & -1 \\ -1 & 0 \end{bmatrix}$$

$$S_{61} = S_{62} = S_{63} = S_{64} = \begin{bmatrix} 1/2 & -\sqrt{3} \\ \sqrt{3}/2 & 1/2 \end{bmatrix}$$

$$S_{61}^5 = S_{62}^5 = S_{63}^5 = S_{64}^5 = \begin{bmatrix} 1/2 & \sqrt{3} \\ -\sqrt{3}/2 & 1/2 \end{bmatrix}$$

Table B.1: 48 matrix operations of initial irreducible matrix representation $\Gamma^{(E_u)}$, symmetry group $\mathbf{O_h}$.

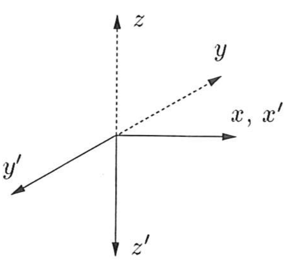

$$\begin{aligned} x' &= x \\ y' &= -y\,, \\ z' &= -z \end{aligned} \qquad C_{2x} = \begin{bmatrix} 1 & 0 & 0 \\ 0 & -1 & 0 \\ 0 & 0 & -1 \end{bmatrix} \tag{B.2}$$

For symmetry group $\mathbf{O_h}$, the full set of matrix operations for the initial irreducible matrix representations $\Gamma^{(T_{1u})}$, are not shown here for brevity but can be found in Altmann & Herzig (1994).

B.2 Calculating the Remaining Irreducible Matrix Representations

For any given symmetry group, once an initial irreducible matrix representation has been generated, the remaining irreducible matrix representations can be calculated by observing the difference between them and the initial irreducible matrix representation, shown by the corresponding character table.

The character table of symmetry group $\mathbf{O_h}$ shows that some matrix operations in irreducible matrix representation $\Gamma^{(E_g)}$ have characters which are simply the opposite sign of the characters for the matrix operations in the initial irreducible matrix representation $\Gamma^{(E_u)}$. Hence, it is clear that the simplest way to generate the remaining 2-dimensional irreducible matrix representation $\Gamma^{(E_g)}$ is to multiply the required matrix operations by $[-1]$. For example, matrix operation σ_x has characters $[2]$ and $[-2]$ for $\Gamma^{(E_u)}$ and $\Gamma^{(E_g)}$ respectively, thus for irreducible matrix representation $\Gamma^{(E_g)}$:

$$\sigma_x = -1 \times \begin{bmatrix} -1 & 0 \\ 0 & -1 \end{bmatrix} = \begin{bmatrix} 1 & 0 \\ 0 & 1 \end{bmatrix} \tag{B.3}$$

The full set of matrix operations for irreducible matrix representation $\Gamma^{(E_g)}$, are shown in Table B.2.

Both 2-dimensional irreducible matrix representations $\Gamma^{(E_u)}$ and $\Gamma^{(E_g)}$ now satisfy the multiplication table for symmetry group $\mathbf{O_h}$, i.e. satisfy the four multiplication properties of a symmetry group given in Appendix A, and as shown by the character table, are non-equivalent irreducible matrix representations.

Similarly, for the remaining 3-dimensional irreducible matrix representations $\Gamma^{(T_{1g})}$, $\Gamma^{(T_{2u})}$ and $\Gamma^{(T_{2g})}$, the character table of symmetry group $\mathbf{O_h}$ again shows that some of their matrix operations have characters which are simply the opposite sign of the characters for matrix operations in the initial irreducible matrix representation $\Gamma^{(T_{1u})}$. Thus, the remaining 3-dimensional irreducible matrix representations $\Gamma^{(T_{1g})}$, $\Gamma^{(T_{2u})}$ and $\Gamma^{(T_{2g})}$, can be generated by multiplying the required matrix operations by $[-1]$. For example, matrix operation S_{4z} has characters $[-1]$ and $[1]$ for $\Gamma^{(T_{1u})}$ and $\Gamma^{(T_{1g})}$ respectively, thus for irreducible matrix representation $\Gamma^{(T_{1g})}$:

$$S_{4z} = -1 \times \begin{bmatrix} 0 & -1 & 0 \\ 1 & 0 & 0 \\ 0 & 0 & -1 \end{bmatrix} = \begin{bmatrix} 0 & 1 & 0 \\ -1 & 0 & 0 \\ 0 & 0 & 1 \end{bmatrix} \tag{B.4}$$

$$E = C_{2x} = C_{2y} = C_{2z} = i = \sigma_x = \sigma_y = \sigma_z = \begin{bmatrix} 1 & 0 \\ 0 & 1 \end{bmatrix}$$

$$C_{31} = C_{32} = C_{33} = C_{34} = S_{61}^5 = S_{62}^5 = S_{63}^5 = S_{64}^5 = \begin{bmatrix} -1/2 & -\sqrt{3}/2 \\ \sqrt{3}/2 & -1/2 \end{bmatrix}$$

$$C_{31}^2 = C_{32}^2 = C_{33}^2 = C_{34}^2 = S_{61} = S_{62} = S_{63} = S_{64} = \begin{bmatrix} -1/2 & \sqrt{3}/2 \\ -\sqrt{3}/2 & -1/2 \end{bmatrix}$$

$$C_{4x} = C_{4x}^3 = C_{2d}' = C_{2f}' = S_{4x} = S_{4x}^3 = \sigma_{d4} = \sigma_{d6} = \begin{bmatrix} \sqrt{3}/2 & -1/2 \\ -1/2 & -\sqrt{3}/2 \end{bmatrix}$$

$$C_{4y} = C_{4y}^3 = C_{2c}' = C_{2e}' = S_{4y} = S_{4y}^3 = \sigma_{d3} = \sigma_{d5} = \begin{bmatrix} -\sqrt{3}/2 & -1/2 \\ -1/2 & \sqrt{3}/2 \end{bmatrix}$$

$$C_{4z} = C_{4z}^3 = C_{2a}' = C_{2b}' = S_{4z} = S_{4z}^3 = \sigma_{d1} = \sigma_{d2} = \begin{bmatrix} 0 & 1 \\ 1 & 0 \end{bmatrix}$$

Table B.2: 48 matrix operations of irreducible matrix representation $\Gamma^{(E_g)}$, symmetry group $\mathbf{O_h}$.

See Altmann & Herzig (1994) for the full set of matrix operations for irreducible matrix representations $\Gamma^{(T_{1g})}$, $\Gamma^{(T_{2u})}$ and $\Gamma^{(T_{2g})}$.

Note that, there is an infinite choice of equivalent representations for any 2 or 3-dimensional irreducible matrix representations. These equivalent irreducible matrix representations are given by different choices of basis vectors (The effects of different basis vectors for irreducible matrix representation $\Gamma^{(E)}$ of symmetry group $\mathbf{C_{3v}}$, are discussed in Chapter 3).

Bibliography

Altmann, S. & Herzig, P. (1994), *Point-Group Theory Tables*, Clarendon Press, Oxford.

Bishop, D. (1973), *Group Theory and Chemistry*, Clarendon Press, Oxford.

Bossavit, A. (1986), 'Symmetry, groups and boundary value problems, a progressive introduction to noncommutative harmonic analysis of partial differential equations in domains with geometrical symmetry', *Computer Methods in Applied Mechanics and Engineering* **56**, 167–215.

Bossavit, A. (1988), 'On the exploitation of geometrical symmetry in structural computations of space power stations', *Space Power* **7**(2), 199–210.

Bossavit, A. (1993), 'On the computation of strains and stresses in symmetrical articulated structures', *Lectures in Applied Mathematics, American Mathematical Society* **29**, 111–123.

Calladine, C. (1978), 'Buckminster Fuller's "Tensegrity" structures and Clerk Maxwell's rules for the construction of stiff frames', *International Journal of Solids and Structures* **14**, 161–172.

Chang, P. & Healey, T. (1988), 'Computation of symmetry modes and exact reduction in nonlinear structural analysis', *Computers and Structures* **28**(2), 135–142.

Charlton, T. (1969), *Principles of Structural Analysis*, Longmans Green and Co., Ltd.

Cotton, F. (1971), *Chemical Applications of Group Theory*, Wiley-Interscience.

Crandall, S., Dahl, N. & Landner, T. (1978), *An Introduction to the Mechanics of Solids*, McGraw-Hill Book Co., Inc.

Dinkevich, S. (1984), 'The spectral method of calculation of symmetric structures of finite size', *Transactions of the Canadian Society of Mechanical Engineering* **8**(4), 167–215.

Dinkevich, S. (1991), 'Finite symmetric systems and their analysis', *International Journal of Solids and Structures* **27**(10), 1215–1253.

Föppl, A. (1912), *Vorlesungen über Technische Mechanik*, Vol. 2, Teubner, Leipzig and Berlin.

Fortescue, C. (1918), 'Method of symmetrical co-ordinates applied to the solution of polyphase networks', *Transactions AIEE* **37**(2), 1027–1140.

Fuller, R. (1975), *Synergetics: Explorations in the Geometry of Thinking*, Macmillan Publishing Co., New York.

Geiger, D., Cambell, D., Chen, D., Gossen, P., Hamilton, K. & Houg, G. (1988), Design details of an elliptical cable dome and a large span cable dome (210m) under construction in the united states, *in* 'Proc. International Symposium on Innovative Applications of Shells and Spatial Forms', Oxford & IBH Publishing Co.

Glockner, P. (1973), 'Symmetry in structural mechanics', *Journal of the Structural Division, ASCE* **99**, 71–89.

Golubitsky, M., Stewart, I. & Schaeffer, D. (1988), Singularities and groups in bifurcation theory, *in* 'Applied Mathematical Sciences', Vol. 69, Springer-Verlag.

Hammermesh, M. (1962), *Group Theory and its Applications to Physical Problems*, Addison-Wesley Publishing Co.

Hargittai, I. & Hargittai, M. (1994), *Symmetry: A Unifying Concept*, Shelter Publications, Inc.

Healey, T. (1988), 'A group-theoretic approach to computational bifurcation problems with symmetry', *Computer Methods in Applied Mechanics and Engineering* **67**, 257–295.

Healey, T. & Treacy, J. (1991), 'Exact block diagonalization of large eigenvalue problems for structures with symmetry', *International Journal for Numerical Methods in Engineering* **31**, 265–285.

Hibbitt, Karlsson and Sorensen, Inc. (1993), *ABAQUS Verification and Example Problems Manual.* Version 5.3.

Hunt, K. (1978), *Kinematic Geometry of Mechanisms*, Clarendon Press, Oxford.

Hussey, M. (1967), 'General theory of cyclically symmetric frames', *ASCE Journal of Structural Division* **93**(No. ST2, Paper 5182), 163–176.

Ikeda, K., Ario, I. & Torii, K. (1992), 'Block-diagonalisation analysis of symmetric plates', *International Journal of Solids and Structures* **29**(22), 2779–2793.

Ikeda, K. & Murota, K. (1991), 'Bifurcation analysis of symmetric structures using block-diagonalisation', *Computer Methods in Applied Mechanics Engineering* **86**(2), 215–243.

Koiter, W. (1984), On Tarnai's conjecture with reference to both statically and kinematically indeterminate structures, Technical Report 788, Laboratory for EngineeringMechanics, Delft.

Kötter, E. (1912), 'Über die möglichkeit, n puckte in der ebene oder im raume durch weinger als $2n-3$ oder $3n-6$ stäbe von ganz unveränderlicher länge unverschielblich miteinander zu verbinden', *Festschrift Heinrich Muller-Breslau* pp. 61–80. Cited by Pellegrino and Calladine (1991).

Kron, G. (1935), 'The application of tensors to electrical engineering problems', *General Electrical Review* **38**.

Kumar, P. (1996), Kinematic Bifurcations and Deployment Simulations of Foldable Space Structures, PhD thesis, University of Cambridge.

Kuznetsov, E. (1988), 'Underconstrained structural systems', *International Journal of Solids Structures* **24**, 153–163.

Kuznetsov, E. (1991), 'Systems with infinitesimal mobility', *Journal of Applied Mechanics* **58**, 513–526.

Leech, J. & Newman, D. (1969), *How to use Groups*, Methuen & Co.

Livesley, R. (1975), *Matrix Methods of Structural Analysis*, Permagon Press.

Mackay, G. (1980), 'Harmonic analysis as the exploitation of symmetry - a historical survey', *Bulletin of the American Mathematical Society* **3**(1), 543–696.

MacNeal, R., Harder, R. & Mason, J. (1977), NASTRAN cyclic symmetry capability, *in* 'NASTRAN Users Experience - 3rd Colloquium', Langley Research Centre, Virginia, U.S.A., pp. 395–421. NASA TM X-2893.

Maxwell, J. (1864), 'On the calculation of the equilibrium and stiffness of frames', *Phil. Mag.* **27**(4th series), 294–299. (Reprinted in Niven W.D. (1980). *The Scientifc Papers of J.C. Maxwell*, Vol. 2, 598-604, Cambridge University Press).

McGuire, W. & Gallagher, R. (1979), *Matrix Structural Analysis*, John Wiley & Sons.

Miller, A. (1981), 'application of group representation theory to symmetric structures', *Applied Mathematical Modelling* **5**, 290–294.

Mohr, O. (1885), 'Beitrag zur theorie des fachwerkes', *Der Civilingenieur* **31**, 289–310. Cited by Pellegrino and Calladine (1991).

Pellegrino, S. (1986), Mechanics of kinematically indeterminate structures, PhD thesis, University of Cambridge.

Pellegrino, S. (1992), 'A class of tensegrity domes', *International Journal of Space Structures* **7**, 127–142.

Pellegrino, S. & Calladine, C. (1986), 'Matrix analysis of statically and kinematically indeterminate frameworks', *International Journal of Solids and Structures* **22**, 409–428.

Pellegrino, S. & Calladine, C. (1991), 'First-order infinitesimal mechanisms', *International Journal of Solids and Structures* **27**, 505–515.

Pipes, L. (1966), 'Circulant matrices and the theory of symmetrical components', *The Matrix and Tensor Quarterly* **17**(2), 35–50.

Renton, J. (1964), 'On the stability analysis of symmetrical frameworks', *Quarterly Journal of Mechanics and Applied Mathematics* **17**(2), 175–197.

Samartin, A. (1988), Analysis of spatially periodic structures - application to shell and spatial structures, *in* 'Proc. International Symposium on Innovative Applications of Shells and Spatial Forms', Vol. 2, Oxford & IBH Publishing Co., pp. 205–221.

Sattinger, D. (1979), *Group Theoretic Methods in Bifurcation Theory*, Springer, New York.

Schonland, D. (1965), *Molecular Symmetry, an Introduction to Group Theory and its uses in Chemistry*, D.Van Nostrand Company Ltd.

Serre, J.-P. (1977), *Linear Representations of Finite Groups*, Springer-Verlag.

Strang, G. (1986), *Introduction to Applied Mathematics*, Wellesley-Cambridge Press.

Swanson Analysis Systems, Inc. (1992), *ANSYS Users Manual.* Revision 5.0.

Tarnai, T. (1980), 'Simultaneous static and kinematic indeterminacy of space trusses with cyclic symmetry', *International Journal of Solids and Structures* **16**, 347–359.

Tarnai, T. (1989), 'Finite mechanisms and the timber octagon of ely cathedral', *Structural Topology* **14**, 9–20.

The MathWorks, Inc. (1996), *The Language of Technical Computing. Using MATLAB.* Version 5.

Thomas, D. (1979), 'Dynamics of rotationally periodic structures', *International Journal for Numerical Methods in Engineering* **14**, 81–102.

Weyl, H. (1946), *The Classical Groups, their Invariants and Representations*, Princeton University Press.

Williams, F. (1986*a*), 'An algorithm for exact eigenvalue calculations for rotationally periodic structures', *International Journal for Numerical Methods in Engineering* **23**, 609–622.

Williams, F. (1986*b*), 'Exact eigenvalue calculations for structures with rotationally periodic sub-structures', *International Journal for Numerical Methods in Engineering* **23**, 695–706.

Wilson, E., Decius, J. & Cross, P. (1955), *Molecular Vibrations. The Theory of Infrared and Raman Vibrational Spectra*, McGraw-Hill Book Company, Inc.

Wohlever, J. (1993), A Group Theoretic Approach to the Nonlinear Bifurcation Analysis of Shells of Revolution, PhD thesis, Cornell University.

Zhong, W. & Qiu, C. (1983), 'Analysis of symmetric or partially symmetric structures', *Computer Methods in Applied Mechanics and Engineering* **38**, 1–18.

Zlokovic, G. (1973), *Group Theory in G-Vector Spaces in Vibrations, Stability and Statics of Structures*, ICS, Beograd.

Zlokovic, G. (1989), *Group Theory and G-Vector Spaces in Structural Analysis, Vibration, Stability and Statics*, Ellis Horwood Ltd.